



Ph.D. Thesis

**Development and characterization of a
self-bioluminescent heavy
metal cyanobacterial bioreporter strain**

Keila Martín Betancor

2017

UAM

Ph.D. Thesis

DEVELOPMENT AND CHARACTERIZATION OF A SELF-BIOLUMINESCENT HEAVY METAL CYANOBACTERIAL BIOREPORTER STRAIN

Keila Martin Betancor

Madrid, 14/06/2017

Programa de Doctorado de Microbiología

Dirigida por:

Dr. Francisca Fernández Piñas
Departamento de Biología
Facultad de Ciencias
Universidad Autónoma de Madrid

Dr. Ismael Rodea Palomares
Departamento de Biología
Facultad de Ciencias
Universidad Autónoma de Madrid

Memoria presentada para optar al título de Doctor por la Universidad Autónoma de Madrid.

La presente memoria ha sido realizada cumpliendo los requisitos para optar a la Mención de Doctorado Internacional

FUNDING

The thesis was supported by the Spanish government (projects MICIN CGL2010-15675 and MINECO CTM2013-45775-C2-2-R) and the Dirección General de Universidades e Investigación de la Comunidad de Madrid, Research Network (Comunidad de Madrid S-2009/AMB/1511)

Abbreviations

(AA) Allen and Arnon culture medium	(ICP/MS) Mass spectrometry
(ANOVA) Analyses of variance	(IPTG) Isopropyl- β -D-thio-galactoside
(ATP) Adenosine 5'-triphosphate	(LL.4) Four parameter log-logistic model
(Atz) Atrazine	(LOD) Limit of detection
(BG11) Blue-Green culture medium	(LOEC) Lowest observed effect concentration
(BIFs) Bioluminescence induction factors	(<i>m</i>) Slope of the dose-response curve
(BLM) Biotic ligand model	(M _d) Metal dissolved
(CA) Concentration addition	(MOA) Mode of Action
(CI) Combination Index	(MOF _f) MOF filtrates
(CI _w) Weighted Combination Index	(MOFs) Metal Organic Frameworks
(D) Doses	(MOF _s) MOF suspensions
(DCP) 3,5 dichlorophenol	(MOPS) 3-(N-morpholino)propanesulfonic acid
(ddH ₂ O) Double distilled water	(MPC) Maximum permissible concentration
(D _m) Median doses	(NMs) Nanomaterials
(DNA) Deoxyribonucleic acid	(NOEC) No observed effect concentration
(E) Effect	(OD) Optical density
(EC) European Community	(<i>p</i>) Fractional effects
(EC _x) Effective Concentration	(R) Linear correlation coefficient
(ED) Effective dose	(RLU) Relative luminescence units
(ED _p) Fractional effective doses	(SIM) Substituted Imidazolate Material
(EDTA) Ethylenediaminetetraacetic acid	(TAP-) Tris-minimal phosphate medium
(E _{max}) Maximum level of effect	(TAZ) Triazole
(E _p) Fractional effect scale	(TU) Toxic Unit
(EPA) Environmental Protection Agency	(UMT) Urogen III methyltransferase
(<i>fa</i>) Fraction affected	(WHAM) Windermere Humic Aqueous Model
(FIAAS) Flow injection atomic absorption	(WWTP) Wastewater treatment plant
(FIM) Free ion model	(X-Gal) bromo-chloro-indolyl-galactopyranoside
(<i>fu</i>) Fraction unaffected	(ZIF) Zeolite imidazolate frameworks
(GFP) Green fluorescent protein	(β -Gal) β -galactosidase
(IA) Independent action	
(ICP/AES) Inductively coupled plasma atomic electron spectrometry	

CONTENTS

RESUMEN	1
SUMMARY	11
CHAPTER I: General introduction.....	21
1 Heavy metals in the environment	23
2 Microbial bioreporters	26
3 Reporter genes.....	28
3.1 <i>Colored-protein based bioreporters</i>	28
3.2 <i>Photoprotein bioreporters</i>	28
3.3 <i>Fluorescent bioreporters</i>	29
3.4 <i>Bioluminescent bioreporters.....</i>	30
4 Microorganisms metal-resistance proteins and gene regulation	31
4.1 <i>ArsR/SmtB family:.....</i>	34
4.2 <i>MerR family:</i>	35
4.3 <i>CsoR/RcnR family:.....</i>	36
4.4 <i>DtxR, Fur, and NikR family</i>	37
5 Heavy metals bioluminescent microorganism-based bioreporters and applications	38
5.1 <i>Bacterial bioreporters:</i>	39
5.2 <i>Eukaryotic bioreporters:.....</i>	40
6 Cyanobacteria and their applications in environmental monitoring.....	44
6.1 <i>Global toxicity cyanobacterial bioreporters.....</i>	46
6.2 <i>Cyanobacterial bioreporters responsive to heavy metals.....</i>	47
7 Turn-off vs. Turn-on bioreporters dose-response curves	48
8 Theoretical models of chemical mixture effects	50
8.1 <i>Independent Action (IA):.....</i>	51
8.2 <i>Concentration Addition (CA):.....</i>	51

9	Current approach to study mixtures in inducible systems	55
10	Other potential applications of the heavy metals bioreporters	57
11	Preservation methods	59
	OBJECTIVES.....	75
	CHAPTER II: Construction of a self-luminescent cyanobacterial bioreporter that detects abroad range of bioavailable heavy metals in aquatic environments.....	81
	Supplementary material.....	95
	CHAPTER III: Defining an additivity framework for mixture research in inducible whole-cell biosensors	105
	Supplementary material.....	121
	CHAPTER IV: Co, Zn and Ag-MOFS evaluation as biocidal materials towards photosynthetic organisms	155
	Supplementary material.....	167
	CHAPTER V: High-throughput freeze-dried cyanobacterial bioassay for freshwaters environmental monitoring.....	177
	Supplementary material.....	193
	GENERAL DISCUSSION.....	201
	CONCLUSIONS / CONCLUSIONES.....	217

**R
E
S
U
M
E
N**

RESUMEN

El control de la calidad del agua y de los suelos requiere el desarrollo de técnicas combinadas para obtener información global sobre la composición química de la muestra y la evaluación de los efectos biológicos. En este sentido, los bioensayos de toxicidad se ha convertido en una herramienta muy útil ya que permiten obtener información sobre los efectos biológicos de un contaminante discriminando la fracción biodisponible y / o la toxicidad de los mismos. Otra aplicación de los bioensayos de toxicidad es el desarrollo y construcción de organismos reporteros o “bioreporters” para aplicaciones ambientales. Un bioreporter es una célula viva, intacta, que ha sido genéticamente modificada para producir una señal medible (gen reportero) en respuesta a un agente químico o físico específico en el medio ambiente. El uso de células enteras tiene una ventaja fundamental por el hecho de que reacciones complejas sólo pueden existir en una célula intacta, metabólicamente activa; De esta manera, pueden evaluarse parámetros globales tales como la biodisponibilidad de los contaminantes o la toxicidad. Los bioreporters constituidos por células enteras pueden ser básicamente de dos tipos: (turn-off) que se reprimen en presencia de una muestra tóxica (portan fusiones de promotores constitutivos con los genes reportero) y aquellas que se inducen (turn-on) en presencia de un contaminante o un grupo de contaminantes concreto (portan fusiones de promotores inducibles frente a determinados compuestos y los genes reportero).

Los metales pesados son uno de los contaminantes que generan mayor preocupación dada su persistencia en el medio ambiente y su alta toxicidad para todos los organismos. Dado que la toxicidad de los metales pesados viene determinada por su biodisponibilidad, la combinación de métodos químicos y bioreportes para detectarlos y cuantificarlos constituye una mejora en la realización de una evaluación ambiental.

El objetivo principal de esta tesis fue la construcción de un bioreporter cianobacteriano turn-on (lights-on, dado que el sistema génico reportero utilizado fue la luciferasa bacteriana) para detectar metales pesados biodisponibles en sistemas acuáticos. Esta nueva cepa bioreporter se basa en una cianobacteria unicelular de agua dulce, *Synechococcus elongatus* PCC 7942, denominada *Synechococcus elongatus* PCC 7942 pBG2120 que lleva una fusión transcripcional de la región promotora del locus cianobacteriano *smt* que codifica una metalotioneína cianobacteriana (SmtA) y un represor de su expresión (SmtB) a los genes *luxCDABE* de la bacteria luminescente terrestre *Photorhabdus luminescens*. Esta cepa bioreporter se ha utilizado para detectar

diferentes metales pesados tanto en medios de cultivo como en diferentes matrices ambientales en las que se incluye la detección de metales pesados procedentes de nanomateriales biocidas. Por otra parte, dado que los metales pesados están presentes como mezclas en el medio ambiente, se ha desarrollado e implementado un modelo matemático predictivo para analizar la respuesta del bioreporter a mezclas de metales pesados. Finalmente, dado que el mantenimiento a largo plazo es la principal limitación en la generalización del uso de estos sistemas biológicos en monitorización ambiental, se han desarrollado protocolos de liofilización para bioreporters basados en cianobacterias.

CAPÍTULO I: Introducción general

En este capítulo se presenta el estado actual de los siguientes temas: En *Heavy metals in the environment*, se introducen las principales razones de la presencia de metales pesados en el medio ambiente y las leyes actuales que regulan su aparición en los ambientes acuáticos. Además, se han detallado los métodos clásicos utilizados para detectar y cuantificar los metales pesados en el medio ambiente, así como los nuevos métodos basados en la detección de su fracción biodisponible. En *Microbial bioreporters*, se define el concepto de bioreporter microbiano, así como los diferentes tipos de bioreporters microbianos basado en su especificidad. En *Reporter genes*, se han detallado los principales sistemas utilizados como genes reporteros en la construcción de bioreporters microbianos y sus principales características. El epígrafe *Microbial metal-resistance proteins and gene regulation*, se ha dedicado a explicar en profundidad los distintos mecanismos que poseen los microorganismos para detectar y responder a flujos variables de metales en el medio ambiente, ya que estos genes de resistencia a metales pesados pueden ser potencialmente utilizados como el elemento sensor en el desarrollo de bioreporters capaces de detectar metales pesados en el medio ambiente. *Heavy metals bioluminescent microorganisms-based bioreporters and applications* recoge los bioreporters luminiscentes, tanto bacterianos como eucariotas, que existen actualmente para detectar metales pesados, indicando los genes de resistencia que se han utilizado como elemento sensor así como sus aplicaciones principales. En *Cyanobacteria and their applications in environmental monitoring*, las principales características de las cianobacterias son detalladas enfocándose en sus habilidades particulares para ser elegidas como organismos modelo para la evaluación ambiental, especialmente como bioreporters de contaminación ambiental en ecosistemas acuáticos. Dentro de esta

sección, se pueden encontrar los bioreporters luminiscentes basados en cianobacterias que existen hasta la fecha para determinar la toxicidad global de una muestra (*Global toxicity cyanobacterial bioreporters*) y para la detección específica de metales pesados (*Cyanobacterial bioreporters responsive to heavy metals*). La sección *Turn-off vs. turn-on bioreporter dose-response curves* sirve para indicar las principales diferencias en la respuesta de un bioreporter tipo turn-off (que se reprimen) y de uno tipo turn-on (que se inducen) y establece las bases para una mejor comprensión de las siguientes secciones, *Theoretical models of chemical mixture effects* y *Current approach to study mixture in inducible systems*. En la primera sección, se describen los dos métodos principales utilizados para estudiar los efectos de las mezclas, mientras que el último se centra en los métodos disponibles para estudiar el efecto de las mezclas en sistemas inducibles (turn-on). En *Other potential application of the heavy metals bioreporters* se describen otros usos de los bioreporters de metales pesados, específicamente, su uso para estudiar el efecto de los iones metálicos liberados de nanomateriales metálicos. Por último, en *Preservation methods*, se describen los principales métodos utilizados para mantener a los bioreporters viables y activos durante largos períodos de tiempo.

CAPÍTULO II:

Este capítulo está integrado por el manuscrito:

- ***Construction of a self-luminescent cyanobacterial bioreporter that detects a broad range of bioavailable heavy metals in aquatic environments.*** Keila Martín-Betancor, Ismael Rodea-Palomares, M.A. Muñoz-Martin, Francisco Leganés, Francisca Fernández-Piñas. **Frontiers in Microbiology. 6: Article 186. (2015).**

Keila Martín Betancor participó en este estudio desarrollando el diseño experimental, planificando y realizando los experimentos, procesando y analizando los datos y elaborando el material gráfico. La redacción y discusión del trabajo se realizó con la colaboración de todos los autores.

Los metales pesados son contaminantes muy persistentes en el medio ambiente, por lo tanto, el control de la concentración de éstos en el medio ambiente es de gran importancia para asegurar que no produzcan un efecto tóxico sobre los organismos. Existen varios métodos químicos para determinar la concentración total de metales pesados, sin embargo, su toxicidad está estrechamente relacionada con su especiación en el medio

ambiente y por lo tanto con su biodisponibilidad. En este contexto, el uso de sistemas biológicos (bioreporters de células enteras) ofrece muchas ventajas, ya que la respuesta que muestran estos organismos es el resultado de la interacción directa con estos contaminantes y, por lo tanto, proporciona datos reales sobre la biodisponibilidad.

En este manuscrito, se construyó una cepa bioreporter auto-luminiscente basada en la cianobacteria unicelular *Synechococcus* sp. PCC 7942 para detectar metales pesados biodisponibles y fue posteriormente utilizada para detectar diferentes metales pesados en medio de cultivo y en muestras ambientales con diferentes complejidades, concretamente se utilizaron dos muestras de río y una muestra obtenida del efluente de una depuradora de aguas. La optimización del bioreporter se realizó midiendo la luminiscencia emitida a diferentes densidades ópticas y diferentes tiempos de exposición a metales pesados. Además, dada la importancia de la especiación de metales pesados en las diferentes matrices, se utilizó un modelo químico para vincular la respuesta del bioreporter con la especiación y la biodisponibilidad del metal. Los resultados de este trabajo revelaron que el bioreporter respondió linealmente a los cationes divalentes de Zn, Cd, Cu, Co, Hg y monovalente de Ag con diferentes límites de detección (LOD) y diferentes niveles de inducción. Los experimentos de muestras ambientales validaron el uso de este bioreporter para la detección de metales pesados biodisponibles en ambientes acuáticos.

CAPÍTULO III:

Este capítulo está integrado por el manuscrito:

- ***Defining an additivity framework for mixture research in inducible whole-cell biosensors.*** Keila Martín-Betancor, Christian Ritz, Francisca Fernández-Piñas. Francisco Leganés and Ismael Rodea-Palomares. **Scientific Reports. 5: 17200 (2015).**

Este trabajo fue desarrollado en colaboración con el Dr. Christian Ritz del departamento de Nutrición, Ejercicio y Deportes de la Universidad de Copenhague (Dinamarca).

Keila Martín Betancor participó en este estudio desarrollando el diseño experimental, planificando y realizando los experimentos, procesando y analizando los datos y elaborando el material gráfico. Christian Ritz se encargó de programar el modelo desarrollado en el paquete *drc* del software R. La redacción y discusión del trabajo se realizó con la colaboración de todos los autores.

Los compuestos químicos están presentes en mezclas en el medio ambiente, por lo que se requieren métodos y modelos para analizar y predecir el efecto de estas mezclas con el fin de mejorar la evaluación de riesgo ambiental. Existen varios modelos disponibles para estudiar el efecto de las mezclas químicas (principalmente, *Independent action* y *Concentration addition*), aplicable en el campo de la toxicología global (por ejemplo, en bioreporters de tipo turn-off); Sin embargo, los métodos para estudiar el efecto de las mezclas en sistemas inducibles (bioreporters de tipo turn-on) son prácticamente inexistentes.

En este manuscrito, se desarrolló un nuevo modelo matemático basado en la aditividad para estudiar el efecto de las mezclas en el contexto de bioreporters de células enteras de tipo inducible (turn-on). Además, este modelo fue implementado en R, un software libre para el uso de métodos estadísticos. Este método propone una extensión multivariada de la *dosis efectiva (EDp)* que permite tener en cuenta la aparición de efectos máximos diferentes y curvas dosis-respuesta bifásicas (típicas de sistemas inducibles) lo cual es una mejora de los métodos actuales para poder predecir y estudiar la interacción de mezclas de contaminantes a través de la respuesta de un sistema inducible. Este método se ilustró estudiando la respuesta del bioreporter cianobacteriano *Synechococcus elongatus* PCC 7942 pBG2120 (construido y caracterizado previamente) a mezclas binarias de seis metales pesados (Zn, Cd, Cu, Co, Hg y Ag). Los resultados destacados de este manuscrito fueron la posibilidad, por primera vez, de predecir las respuestas de los sistemas inducibles a las mezclas de compuestos utilizando la información experimental de los compuestos cuando están presentes de forma individual y la posibilidad de investigar las desviaciones de la aditividad (sinergia y antagonismo). La respuesta del bioreporter *Synechococcus* PCC 7942 pBG2120 a las mezclas binarias de metales pesados se pudo considerar aditiva excepto cuando Hg, Co y en menor medida, Ag estaban presentes en las mezclas lo que dio lugar a importantes desviaciones de la aditividad.

CAPÍTULO IV:

Este capítulo está integrado por el manuscrito:

- ***Co, Zn and Ag-MOFs evaluation as biocidal materials towards photosynthetic organisms.*** Keila Martín-Betancor, Sonia Aguado, Ismael Rodea-Palomares, Miguel Tamayo-

Belda, Francisco Leganés, Roberto Rosal and Francisca Fernández-Piñas. **Science of the total environment**. 595: 547-555 (2017).

Este trabajo fue desarrollado en colaboración con el grupo de investigación del Dr. Roberto Rosal del departamento de Ingeniería Química de la Universidad de Alcalá. Madrid, España).

Keila Martín Betancor participó en este estudio desarrollando el diseño experimental, planificando y realizando los experimentos, procesando y analizando los datos y elaborando el material gráfico. Sonia Aguado llevó a cabo la síntesis de los MOF utilizados en este estudio. La redacción y discusión del trabajo se realizó con la colaboración de todos los autores.

Los nanomateriales metálicos son una de las últimas aplicaciones de metales pesados. Estos nanomateriales son ampliamente utilizados debido a sus propiedades biocidas. Entre estos nanomateriales metálicos, los *Metal Organic Frameworks* (MOFs) son uno de los últimos desarrollos en nanotecnología y ofrecen múltiples ventajas como materiales biocidas ya que son materiales de naturaleza inorgánica-orgánica construidos directamente con el metal deseado unido por enlaces covalentes. Dada su estructura, permiten una liberación más controlada de los iones metálicos en comparación con otros materiales metálicos.

En el presente trabajo se ha evaluado, por primera vez, la actividad biocida de tres MOFs diferentes basados en Co (Co-SIM1), Zn (Zn-SIM1) y Ag (Ag-TAZ), frente a organismos fotosintéticos, concretamente, un alga verde, *Chlamydomonas reinhardtii* y dos cepas diferentes de cianobacterias, una filamentosa, *Anabaena* sp. PCC 7120 y una unicelular, *Synechococcus* sp. PCC 7942. Además, como resaltan algunos autores, es importante comprender el mecanismo de acción de los compuestos antimicrobianos antes de su aplicación a gran escala. Como se indicó anteriormente, uno de los principales aspectos que determinan la toxicidad de los metales pesados es su especiación y por lo tanto su biodisponibilidad. Por lo tanto, el metal liberado de estos MOFs y la biodisponibilidad de estos metales se estudiaron usando ICP-MS, el programa de especiación química, Visual MINTEQ y el bioreporter de metales pesados construido en esta tesis *Synechococcus* sp. PCC 7942 pBG2120. A través de este estudio, se encontró que ambas cianobacterias presentaban una gran sensibilidad a los tres MOFs diferentes, mientras que el alga mostró una gran sensibilidad a Ag-TAZ, pero fue mucho más resistente a los MOFs basados en Co y Zn. Estas diferencias se deben probablemente a las diferencias en la composición de

la pared celular de estos organismos. Además, mediante el uso del bioreporter basado en *Synechococcus*, se determinó que la actividad biocida presentada por estos MOFs se debe principalmente a la concentración de iones metálicos liberados de estos MOFs.

CAPÍTULO V:

Este capítulo está integrado por el manuscrito:

High-throughput freeze-dried cyanobacterial bioassay for fresh-waters environmental monitoring Keila Martín-Betancor, Marie-José Durand, Gérald Thouand, Francisco-Leganés, Francisca Fernández-Piñas, Ismael Rodea-Palomares (**No publicado**).

Este trabajo fue desarrollado en colaboración con el grupo de investigación del Dr. Gerald Thouand y la Dra. Marie-Josée Durand de la Universidad de Nantes, Francia.

Keila Martín Betancor participó en este estudio desarrollando el diseño experimental, planificando y realizando los experimentos, procesando y analizando los datos y elaborando el material gráfico. El protocolo de liofilización se desarrolló bajo la guía del Dr. Gerald Thouand y la Dra. Marie-Josée Durand. La redacción y discusión del trabajo se realizó con la colaboración de todos los autores.

La mayor limitación para generalizar el uso de los bioreporters (tanto turn-on como turn-off) en la monitorización ambiental es la falta de métodos que permitan mantener la viabilidad y la actividad de los bioreporters a lo largo del tiempo, con el objetivo final de desarrollar un dispositivo celular autónomo o biosensor. Esta carencia es de gran importancia en el caso de los bioreporters cianobacterianos ya que no se han probado muchos métodos para mantenerlos viables y activos a lo largo del tiempo. En el presente manuscrito, se aplicó por primera vez un método de liofilización a un bioreporter cianobacteriano, especialmente, al bioreporter bioluminiscente constitutivo *Anabaena* CPB4337. Esta cianobacteria lleva en su cromosoma un derivado tn5 con los genes *luxCDABE*. Con el fin de seleccionar el protocolo óptimo de liofilización, se evaluó el efecto de diferentes fases de crecimiento celular, crioprotectores, protocolos de congelación, soluciones de rehidratación y condiciones de incubación. Como conclusión de este estudio, se definió el protocolo óptimo para la liofilización de este bioreporter cianobacteriano. Esta cianobacteria liofilizada fue, en general, más sensible a los metales pesados (Cu, Zn y Cd) y a los productos químicos orgánicos (atrazina y fenol) que los

ensayos estándar. La viabilidad de las células permaneció durante tres años, aunque después de 1 y 3 años de almacenamiento, la bioluminiscencia basal de las células disminuyó un orden de magnitud. Los metales pesados se utilizaron para evaluar la sensibilidad del bioreporter a lo largo del tiempo, concluyendo que la sensibilidad a los metales pesados permaneció prácticamente constante, excepto en el caso de Cu después de 1 año ($p < 0,1$) y 3 años ($p < 0,05$) y Zn después de 3 años ($p < 0,05$) cuya sensibilidad aumentó significativamente.

**S
U
M
M
A
R
Y**

SUMMARY

The control of the quality of water and soils requires the development of combined techniques to obtain global information on the chemical composition of the sample and the evaluation of biological effects. In this sense, toxicity bioassays have become a very useful tool since they allow obtaining information on the biological effects of a pollutant by discriminating the bioavailable fraction and / or toxicity of the same. A further progress of toxicity bioassays is the development and construction of bioreporters for environmental applications. A bioreporter is an intact, living cell, which has generally been genetically engineered to produce a measurable signal (reporter gene) in response to a specific chemical or physical agent in the environment. The use of whole cells has a fundamental advantage for the fact that a series of complex reactions can exist only in an intact, metabolically active cell; in this way, global parameters such as the bioavailability of the contaminants or the toxicity can be evaluated. Whole-cell bioreporters can basically be of two types: turn-off bioreporters, in which reporter signal decreases in the presence of a toxic sample (they carry fusions of constitutive promoters with the reporter genes) and turn-on bioreporters in which reporter signal increases in the presence of a particular pollutant or group of contaminants (carry fusions of inducible promoters against certain compounds with reporter genes).

Heavy metals are one of the pollutants that generate greater concern in the environment given their persistence and their high toxicity for all organisms. Since the toxicity of heavy metals is determined by their bioavailability in the environment, the combination of chemical methods and bioreporters to detect and quantify them is an improvement to perform an environmental assessment.

The aim of the present study was to construct a cyanobacterial turn-on (lights-on, because the reporter system used was luciferase) bioreporter strain for detecting bioavailable heavy metals in aquatic systems. This new bioreporter strain is based on a freshwater unicellular cyanobacterium, *Synechococcus elongatus* PCC 7942, derivative strain named *Synechococcus elongatus* PCC 7942 pBG2120 which carries a transcriptional fusion of the promoter region of the *smt* cyanobacterial locus encoding a cyanobacterial metallothionein (SmtA) and a repressor of its expression (SmtB) to the *luxCDABE* genes of the terrestrial luminescent bacteria *Photobacterium luminescens*. This bioreporter strain has been used to detect different heavy metals both in culture media and in different

environmental matrices including biocidal nanomaterials. Furthermore, as heavy metals are present as mixtures in the environment, a predictive mathematical model has been developed and implemented to analyse the response of the bioreporter to heavy metal mixtures. Finally, as long-term maintenance is the main limitation in the generalization of the use of these biological systems in environmental monitoring, freeze-dried protocols for cyanobacterial bioreporters have been performed.

CHAPTER I: General introduction

In this chapter, a state of the art is presented on the following topics: *Heavy metals in the environment*, the main reasons for the occurrence of heavy metals in the environment and current laws regulating their appearance in the aquatic environments have been introduced. In addition, the classical methods used to detect and quantify them in the environment as well as new methods based on the detection of their bioavailability have been detailed. In *Microbial bioreporters*, the concept of microbial bioreporter has been defined as well as the different types of microbial bioreporters based on their specificity. In *Reporter genes*, the main systems used as reporter genes in the construction of microbial bioreporters and their main characteristics have been itemised. *Microbial metal-resistance proteins and gene regulation*, is dedicated to explain in depth the microorganism mechanisms to sense and respond to variable fluxes of metals in the environment since they are the potential genes that could be used as the sensor element in the development of bioreporters capable of detecting heavy metals in the environment. *Heavy metals bioluminescent microorganisms-based bioreporters and applications* section collects the luminescent bioreporters, both bacterial and eukaryotic, to detect heavy metals that currently exist and the promoters of the resistance genes that have been used for their construction as well as their main applications have been indicated. In *Cyanobacteria and their applications in environmental monitoring*, the main characteristics of cyanobacteria are reviewed focusing on their particular skills to be chosen as model organisms for environmental application, especially as bioreporters of environmental pollution in aquatic ecosystems. Within this section, the luminescent cyanobacteria-based bioreporters that exist to date both to determine the overall toxicity of a sample (*Global toxicity cyanobacterial bioreporters*) and for the specific detection of heavy metals (*Cyanobacterial bioreporters responsive to heavy metals*) can be found. *Turn-off vs. turn-on bioreporter dose-response curves* section serves to indicate the main

differences of a turn-off and turn-on bioreporter output and establishes the basis for a better understanding of the following sections, the *Theoretical models of chemical mixture effects* and the *Current approach to study mixture in inducible systems*. In the former, the two main methods used to study mixtures effects are described while the latter is focused on the methods available to study the effect of mixtures on inducible systems (turn-on). In *Other potential application of the heavy metals bioreporters* are described other uses of the heavy metals bioreporters, specifically, the use of them to study the effect of metal ion released from metal nanomaterials. And finally, in *preservation methods*, the main methods used to keep bioreporters viable and active for long periods of time are described.

CHAPTER II:

This chapter is integrated by the manuscript:

- ***Construction of a self-luminescent cyanobacterial bioreporter that detects a broad range of bioavailable heavy metals in aquatic environments.*** Keila Martín-Betancor, Ismael Rodea-Palomares, M.A. Muñoz-Martin, Francisco Leganés, Francisca Fernández-Piñas. **Frontiers in Microbiology. 6: Article 186. (2015).**

Keila Martín Betancor participated in this study developing the experimental design, planning and performing the experiments, processing and analyzing the data and preparing the graphical material. The writing and discussion of the paper was carried out with the collaboration of all authors.

Heavy metals are very persistent pollutants in the environment, thus, the control of the concentration of these in the environment is of great importance to ensure that they do not produce a toxic effect on organisms. Several chemical methods are available to determine the total concentration of heavy metals, however, their toxicity is closely related to their speciation in the environment and therefore with their bioavailability. In this context, the use of biological systems (whole-cell bioreporters) provides many advantages since the response displayed by these organisms is a result of direct interaction with these pollutants and therefore provides real data on bioavailability.

In this manuscript, the construction of the self-luminescent bioreporter strain of the unicellular cyanobacterium *Synechococcus* sp. PCC 7942 for bioavailable heavy metals detection was constructed and applied to detect different heavy metals in culture medium

and in real environmental samples with different water matrix complexity, specifically, two river samples and one wastewater effluent sample. The optimization of the bioreporter was carried out by measuring the luminescence emitted at different optical densities and different times of heavy metals exposure. Furthermore, given the importance of heavy metals speciation in the different matrices, a chemical model was used to link the bioreporter response with metal speciation and bioavailability. Results of this work revealed that the bioreporter responded linearly to divalent Zn, Cd, Cu, Co, Hg and monovalent Ag with different limits of detection (LODs) and different induction levels. The real environments samples experiments validated the use of this bioreporter for free heavy metals cations bioavailability detection in aquatic environments.

CHAPTER III:

This chapter is integrated by the manuscript:

- **Defining an additivity framework for mixture research in inducible whole-cell biosensors.** Keila Martín-Betancor, Christian Ritz, Francisca Fernández-Piñas. Francisco Leganés and Ismael Rodea-Palomares. *Scientific Reports*. **5: 17200 (2015)**.

This work was developed in collaboration with Dr. Christian Ritz from the department of Nutrition, Exercise and Sports of the University of Copenhagen (Denmark).

Keila Martín Betancor participated in this study developing the experimental design, planning and performing the experiments, processing and analyzing the data and preparing the graphical material. Christian Ritz was in charge of programming the model developed in the *drc* package of R software. The writing and discussion of the paper was carried out with the collaboration of all authors.

Chemicals in the environment are present in mixtures, thus, methods and models are required to analyse and predict the effect of mixtures in order to improve risk assessment. There are several models available for studying the effect of chemical mixtures (mainly *Independent action* and *Concentration addition*), applicable in the field of global toxicology (e.g., turn-off bioreporters); however, methods for studying the effect of mixtures on inducible systems (turn-on bioreporters) are practically non-existent.

In this manuscript, a novel additivity framework for mixture effect modelling in the context of whole-cell inducible biosensors has been mathematically developed and

implemented in R, a free software for statistical methods. This method proposes a multivariate extension of the *effective dose (EDp)* to take into account the occurrence of differential maximal effects and biphasic-dose response curves (typical of inducible systems) which is an improvement of the current methods to be able to predict and study the interaction of pollutants mixtures through the output of an inducible system. This method was illustrated studying the response of the cyanobacterial bioreporter *Synechococcus elongatus* PCC 7942 pBG2120 (previously constructed and characterized) to binary mixtures of six heavy metals (Zn, Cd, Cu, Co, Hg and Ag). The results highlighted in this manuscript are the possibility, for the first time, of predicting inducible whole-cell systems responses to mixtures using single chemical experimental information only and the possibility of investigating departures from additivity (synergism and antagonism). The response of *Synechococcus* PCC 7942 pBG2120 to the heavy metal binary mixtures can be considered nearly additive except when Hg, Co and to lesser extent Ag were present in the mixtures which resulted in important departures from additivity.

CHAPTER IV:

This chapter is integrated by the manuscript:

- **Co, Zn and Ag-MOFs evaluation as biocidal materials towards photosynthetic organisms.** Keila Martín-Betancor, Sonia Aguado, Ismael Rodea-Palomares, Miguel Tamayo-Belda, Francisco Leganés, Roberto Rosal and Francisca Fernández-Piñas. *Science of the total environment*. **595: 547-555 (2017)**.

This work was developed in collaboration with the research group of Dr. Roberto Rosal from the department of Chemical Engineering of the Universidad de Alcalá. Madrid (Spain).

Keila Martín Betancor participated in this study developing the experimental design, planning and performing the experiments, processing and analyzing the data and preparing the graphical material. Sonia Aguado carried out the synthesis of MOFs used in this study. The writing and discussion of the paper was carried out with the collaboration of all authors.

Metallic-nanomaterials are one of the latest applications of heavy metals. These nanomaterials are widely used due to their biocidal properties. Among these metal-

nanomaterials, Metal Organic Frameworks (MOFs) are one of the latest development in nanotechnology and provide multiple advantages as biocidal materials since they are inorganic-organic materials constructed directly with the desired metal linked by covalent bonds. Given their structure a more controlled release of metal ions are found in comparison with other metal-containing materials.

In the present manuscript, the biocidal activity of three different MOFs based on Co (Co-SIM1), Zn (Zn-SIM1) and Ag (Ag-TAZ) have been evaluated, for the first time, to photosynthetic organisms, especially, towards one green alga, *Chlamydomonas reinhardtii* and two different cyanobacterial strains, one filamentous, *Anabaena* sp. PCC 7120 and one unicellular, *Synechococcus* sp. PCC 7942. Furthermore, as highlighted by some authors, it is important to understand the key mechanism of action of potential antimicrobial compounds *prior* to their large-scale application. As indicated before, one of the main aspects that determines the toxicity of heavy metals is their speciation and therefore their bioavailability. Thus, metal released from these MOFs and bioavailability of these metals were studied using ICP-MS, the chemical speciation program, Visual MINTEQ and the heavy metal bioreporter constructed in this thesis *Synechococcus* sp. PCC 7942 pBG2120. Through this study, we found that both cyanobacteria presented high sensitivity to the three different MOFs while the green alga was very sensitivity to Ag-TAZ but much more resistant to Co and Zn-based MOFs most likely due to differences in the composition of the cell wall. Moreover, by the use of the *Synechococcus*-based bioreporter, we elucidated that the biocidal activity presented by these MOFs was mainly due to the concentration of free metal ion released from these MOFs.

CHAPTER V:

This chapter is integrated by the manuscript:

- ***High-throughput freeze-dried cyanobacterial bioassay for fresh-waters environmental monitoring*** Keila Martín-Betancor, Marie-José Durand, Gérald Thouand, Francisco-Leganés, Francisca Fernández-Piñas, Ismael Rodea-Palomares (**Unpublished**).

This work was developed in collaboration with the research group of Dr. GERAL Thouand and Dr. Marie-José Durand from the University of Nantes, France.

Keila Martín Betancor participated in this study developing the experimental design, planning and performing the experiments, processing and analyzing the data and preparing the graphical material. The freeze-drying protocol was developed under the guidance of Dr. Gerald Thouand and Dr. Marie-Jose Durand. The writing and discussion of the paper was carried out with the collaboration of all authors.

The greatest limitation to generalize the use of the bioreporters (both turn-off and turn-on) in environmental monitoring is the lack of methods that allow maintaining the viability and the activity of the bioreporters for a long time, and as the ultimate goal to develop an autonomous cell-device or biosensor. This lack is of great importance in the case of cyanobacterial-based bioreporters since not many methods to keep them viable and active over time have been tested. In the present manuscript, a freeze-dried method was applied for the first time to a cyanobacterial-based bioreporter, especially, to the constitutively bioluminescent bioreporter *Anabaena* CPB4337. This cyanobacterium bears in its chromosome a *tn5* derivative with *luxCDABE* genes. In order to select the optimal freeze-drying protocol, the effect of different cell growth phases, cryoprotectants, freezing protocols, rehydration solution and incubations conditions methods were evaluated. As a conclusion of this study, we defined the optimal protocol for freeze-drying this cyanobacterial-based bioreporter. This freeze-dried cyanobacterium was, in general, more sensitive to heavy metals (Cu, Zn and Cd) and to organic chemicals (atrazine and phenol) than standard assays. The viability of the cells remained for three years, although after 1 year or 3 years of storage, the basal bioluminescence of the cells decreased one order of magnitude. Heavy metals were used to assess the sensitivity of the bioreporter over time, concluding that the sensitivity to heavy metals remained practically constant except for the case of Cu after 1 year ($p < 0.1$) and 3 years ($p < 0.05$) and Zn after 3 years ($p < 0.05$) whose sensitivity increased significantly.

General introduction

C

H

A

P

T

E

R

I

GENERAL INTRODUCTION

1 Heavy metals in the environment

Heavy metals are naturally occurring elements that have a high atomic weight and a relative high density compared to water (equal to or greater than 5 g cm^{-3} , when they are in elemental form). Their presence in the earth's crust is less than 0.1% and almost always less than 0.01%. They are also considered as trace elements because of their presence in trace concentrations ($\mu\text{g L}^{-1}$ range to less than 10 mg L^{-1}) in various environmental matrices (Kabata-Pendias and Pendias, 2001).

Some metals such as cobalt (Co), copper (Cu), iron (Fe), magnesium (Mg), manganese (Mn), molybdenum (Mo), nickel (Ni), selenium (Se) and zinc (Zn) are essential nutrients that are required for various biochemical and physiological functions (Rengel, 1999; Tchounwou et al., 2012). Approximately half of all known proteins are predicted to incorporate metal atoms in their structure and to be involved in key cellular processes such as respiration or photosynthesis. These metals are essential for the biochemistry of life in all organisms; however, high concentrations of these metals can induce toxicity in the organisms (Tchounwou et al., 2012). On the other hand, other metals such as silver (Ag), cadmium (Cd), mercury (Hg), nickel (Ni) or lead (Pb) and metalloids (chemical elements with properties that resemble those of both metals and non-metal elements) such as arsenic (As) have no established biological functions and are considered as non-essential metals (Tchounwou et al., 2012). These metals are toxic for most organisms in very low concentrations.

Although heavy metals are naturally occurring elements, anthropogenic activities such as mining and smelting operations, industrial production and use, and domestic and agricultural use of metals and metal-containing compounds has dramatically increased their presence in the natural environment (Nel et al., 2006). In fact, metal-containing compounds have been used as antimicrobial agents since ancient times, especially in the case of non-essential metals, due to their potent toxicity to bacteria and yeast (Ivask et al., 2012). Nowadays, the properties of heavy metals have been used in the development of nanotechnology and nanomaterials (NMs), which has been growing exponentially during the last years. Metallic-based NMs have been widely applied, especially Ag-based NMs, in products such as wound dressings, textiles, air filters, personal care products, baby products, water disinfection and microbial control (Duran et al., 2016). Because of

their use, heavy metals reach the environment indirectly or directly, especially to aquatic environments through the wastewater treatment plants. A key challenge to environmental safety will be to ensure that consequences to human health and to ecosystems are prevented or minimized while permitting the advantages of the technology to be fully developed.

In this sense, more protective legislations have been developed in the last 20 years (2000/60/EC; 2006/1907/EC). In the case of aquatic ecosystems, the objective is to protect not only the physicochemical water quality but also ecological status for water bodies, from marine to freshwater environments. In Europe, Water Framework Directive (2000/60/EC) was implemented with the objective of *establishing a framework for the protection of inland surface waters, coastal waters and ground waters* based on three basic objectives, a) prevents further deterioration and to enhance the status of aquatic ecosystems, b) to promote sustainable water use based on long-term protection of available water resources and c) to enhance protection and improvement of the aquatic environment through specific measures for the progressive reduction of discharges of priority substances and the cessation of emissions of priority hazardous substances. Within the European community the eleven metals or metalloids of highest concern are As, Cd, Co, Cr, Cu, Hg, Mn, Ni, Pb, Sn, and Tl (EC/1272/2008; EC/105/2008). Although environmental regulations for aquatic ecosystems are based predominantly on assessment carried out on individual substances, it is widely recognized that these substances normally appear as mixtures or as a part of complex mixture of different chemicals (Heys et al., 2016; Meyer et al., 2015). In fact, the empirical evidences that the mixture effects are uncovered by the individual chemical-by-chemical investigation have forced regulatory authorities to incorporate mixture risk assessment in regulatory frameworks (EC/2011). However, there is no specific regulation of heavy metal mixtures. To our knowledge, currently, Australia and New Zealand are the only two countries that consider metal mixtures in their environmental regulations (*Australian and New Zealand Guidelines for Fresh and Marine Water Quality*, 2000).

One of the most important aspects when studying the presence of heavy metals in the environment is their chemical fate (partition, speciation, etc.). Once in the aquatic environment, the toxicity of heavy metals is determined by their speciation and therefore their bioavailability in the environment. Speciation is defined as the identification and

quantification of the different, defined chemical species forms, or phases, in which a metal occurs, while bioavailability is the portion of the total amount of a metal in an environment that is available for uptake by living organisms in their direct surroundings. Speciation of metal and its bioavailability determines the physiological and toxic effects of a metal on living organisms (Merrington et al., 2016).

Several traditional analytical methods such as inductively coupled plasma atomic electron spectrometry (ICP/AES) or mass spectrometry (ICP/MS), flow injection atomic absorption (FIAAS) or electrochemical methods have been largely used to determine the metal concentration in the environmental samples (Helaluddin et al., 2016). Although these techniques are very powerful, accurate and sensitive, the environmental samples need to be digested to free the metal ions in solution as a prerequisite; they are costly and require specialized equipment. In addition, they fail to provide data on the bioavailability of a pollutant. The total amount of metal detected by these methods may not always be related to the toxicity of the samples, hence, the use of total metal concentration to evaluate heavy metal risk to aquatic organisms is well known to be inaccurate (Allen and Hansen, 1996).

Several studies have demonstrated the importance of water chemistry on the degree of bioavailability of metals, and therefore, on their toxicity. The way in which these water quality parameters interact with metals to influence metal bioavailability have been widely studied leading to the development of models such as the Biotic Ligand Model (BLM) (Di Toro et al., 2001). BLMs is an adaptation of the gill surface interaction model (Pagenkopf, 1983; Pagenkopf et al., 1974) and the free ion activity model (FIM) (Campbell, 1995). The model is based on the hypothesis that toxicity is not simply related to the total aqueous metal concentration but that the aqueous speciation of the metal, metal-biotic ligand complexation and metal interaction with competing cations at the site of action of toxicity need to be considered. Unlike the gill surface interaction model, the BLM considers other biotics sites (biotic ligands) that may potentially interact with heavy metals, being applicable to other aquatic organisms. This model is limited as it is a predictive tool, but it has useful applications in aquatic toxicology and is now routinely used in setting metal quality standards (currently the US Environmental Protection Agency (EPA) use the BLM to perform the Ambient Water Quality Criteria for Cu content in freshwaters).

Other methods to quantify the bioavailable fraction out of the total concentration of the studied chemicals have also been proposed. These include physical/chemical extraction techniques, some of them attempting to mimic human exposure (Intawongse and Dean, 2006; Oomen et al., 2004; Rodriguez et al., 1999; Ruby et al., 1996; Ruby et al., 1999; Schroder et al., 2003) or plant uptake (Chojnacka et al., 2005; Dayton et al., 2006; Zhang et al., 2001) as well as an array of bioassays. The latter group includes methodologies based on molecular approaches, cell cultures, isolated tissues and organs, and whole-organisms approaches (Casteel et al., 2006; Darling and Thomas, 2005; Marschner et al., 2006; Sijm et al., 2000; Van Straalen et al., 2005). Among the whole-organism assays, the whole-cell microorganisms-based bioreporters are one of the most advantageous method proposed. This, generally, consists of genetically engineered microorganisms able to respond to the presence of the target compound or to the global toxicity of a sample by a readily quantifiable signal (Belkin, 2003; Ron, 2007; Sorensen et al., 2006; Yagi, 2007). For this response to occur, the compound has to enter into the cellular interior, thus providing a true measure of bioavailability. The use of microorganisms for environmental sensing offers several advantages over higher organisms, including large population, short generation times, facility of maintenance and storage, low costs and rapid responses.

2 Microbial bioreporters

Microbial bioreporters, in general, are intact, living microbial cells that have been genetically engineered to produce a measurable signal in response to a specific chemical or physical agent in their environment (Harms et al., 2006; Van der Meer and Belkin, 2010). Bioreporters were originally developed for basic research on factors affecting gene expression (Fernandez-Pinas et al., 2000; Waidmann et al., 2011) and were early applied for detecting environmental contaminants, in medical diagnostics or food safety control (Griffiths, 2000; Harms et al., 2006; Van der Meer and Belkin, 2010). The genetic modification consists in the introduction of a reporter system fused to a promoter sequence in the organism via a genetic vector. The vectors can be replicative plasmids or integrative plasmids, which carry a fusion of a gene promoter sequence and a reporter gene. The reporter gene typically codes for a reporter protein that ultimately generates a detectable signal. There are three types of microbial bioreporters depending on the gene

promoter selected for their development: non-specific, semi-specific and specific bioreporters (Belkin, 2003; Van der Meer and Belkin, 2010) (Figure 1).

In the field of toxicology, non-specific or ecotoxicity bioreporters, also known as global toxicity bioreporters, provide data on the toxicity of a sample but do not detect specific pollutants. This type of bioreporters usually consist of a reporter element fused to a constitutive promoter so that the reporter product is continuously produced but in the presence of a toxin that impairs metabolism, the bioreporter response is reduced or even fully inhibited; in other words, the reporter response is turned off, so these strains may be denoted as turn-off bioreporters. The semi-specific bioreporters report on pollutants/stressors that cause cellular responses to stresses such as oxidative stress, genotoxicity (DNA damage) or membrane damage; the promoters are activated in response to global changes in the cell. These bioreporters harbour a fusion between the reporter element and stress responsive gene promoters; since in this case, the bioreporter response is induced (turned-on), these strains may be denoted as turn-on bioreporters. The specific bioreporters are able to detect a specific pollutant or group of related pollutants as they have a fusion between a pollutant-responsive gene(s) promoter and the promoterless reporter system; they are usually called turn-on strains. In some cases, given that some promoters responsive to nutrient deficiency are used to develop bioreporters of nutrient bioavailability, they could be also turn-off strains (Belkin, 2003; Sorensen et al., 2006; Van der Meer and Belkin, 2010).

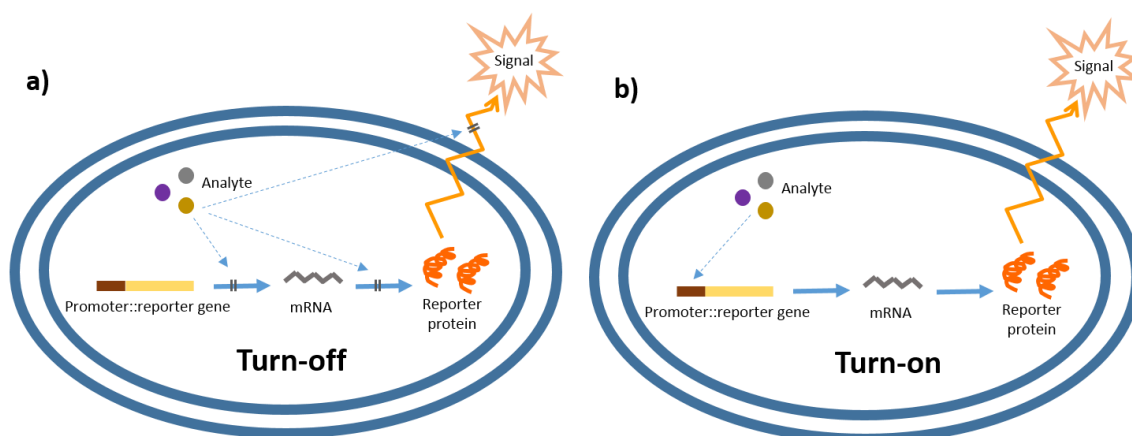


Fig. 1 Types of microbial bioreporters. a) Turn-off bioreporters, which produce the signal constitutively and the sample toxicity is estimated from the degree of inhibition of this signal. Such inhibition can occur along any stage of the reaction's development or in any site affecting cellular viability. b) In turn-on bioreporters, the reporter gene is fused to a specific gene promoters, which are activated by the target chemical(s).

3 Reporter genes

The chosen promoter determines the specificity of a bioreporter, however, the decision of the reporter gene can be critical in some cases. A reporter gene has to be readily detectable and easily measured. With some reporter genes, an exogenously added substrate/prosthetic group is needed to be added to the bioassay so that the signal can be generated (i.e.; *Luc* and aequorin). For other bioreporters, the signal must be activated by an external light source (GFP and UMT), and for a selected few bioreporters, the signal is completely self-induced, with no exogenous substrate or external activation being required (i.e. *luxCDABE*, when the five genes are cloned within the bioreporter organism) (Belkin, 2003; Daunert et al., 2000; Kohler et al., 2000; Sorensen et al., 2006; Van der Meer and Belkin, 2010; Van der Meer et al., 2004; Yagi, 2007). The reporter genes that in general present more advantages are:

3.1 Colored-protein based bioreporters

LacZ encodes β -galactosidase (β -Gal), an intracellular enzyme that cleaves the disaccharide lactose into glucose and galactose. Isopropyl- β -D-thio-galactoside (IPTG) binds the *lactose repressor* and makes the expression of *lacZ* dependent only on its own promoter. By using some lactose analogues such as X-gal (bromo-chloro-indolyl-galactopyranoside) the activity of β -Gal produces a blue residue. In gene cloning, X-gal is used in a technique called blue/white screening, and it has been used also to generate bioreporters by fusing a gene promoter of interest to *lacZ* (Van der Meer and Belkin, 2010). *CrtA* gene is responsible for carotenoid synthesis in purple bacteria; *CrtA* in these bacteria is responsible for changing the colour of the cultures from yellow to red due to O-methylation of spheroidene to spheroidenone (Fujimoto et al., 2006). Due to the inexpensiveness of the detection technique (it can be identified “*de visu*” or quantitatively by spectrophotometry) these reporter genes have been successfully used to develop several kinds of microbial bioreporters including arsenic bioreporters for wide-range screening applications in developing countries (Harms et al., 2006).

3.2 Photoprotein bioreporters

Aequorin is a Ca^{2+} -binding photoprotein isolated from the jellyfish *Aequorea victoria*. Upon addition of calcium ions (Ca^{2+}) and its prosthetic group, coelenterazine, a reaction

occurs where the coelenterazine is oxidized to coelenteramide and blue light is emitted in the 460 - 470 nm range. Aequorin has been incorporated into human B cell lines for the detection of pathogenic bacteria and viruses in the CANARY assay (Cellular Analysis and Notification of Antigen Risks and Yields) (Rider et al., 2003). The B cells are genetically engineered to produce aequorin. Upon exposure to antigens of different pathogens, the recombinant B cells emit light as a result of the activation of an intracellular signalling cascade that releases calcium ions inside the cell. Aequorin has also been cloned in many organisms including plant, animal fungi and bacteria (Knight et al., 1991; Kudla et al., 2010), and it has also been used by our group to record specific calcium signatures induced by different stresses and pollutants in a recombinant aequorin-bioreporter cyanobacterial strain (Barran-Berdon et al., 2011; Leganes et al., 2009; Torrecilla et al., 2000; Torrecilla et al., 2001).

3.3 *Fluorescent bioreporters*

Green fluorescent protein (GFP) was also originally isolated and cloned from the jellyfish *Aequorea victoria*, it forms a dual system with the photoprotein aequorin in this organism (Stepanenko et al., 2008). Variants of GFP have also been isolated from the sea pansy *Renilla reniformis*. GFP emits green light when exposed to blue light. GFP does not need exogenous cofactors but it requires oxygen for formation and stabilization of the fluor. This ability to fluoresce makes GFP highly useful in biosensing assays since it can be used on-line and in real-time to monitor intact, living cells. Additionally, the ability to mutate the *gfp* gene to code for GFPs with emissions other than blue (i.e., cyan, red, and yellow) allows it to be used as a multianalyte detector (Stepanenko, 2008). Consequently, GFP has been used extensively in bioreporter constructs within bacterial, yeast, plant, and mammalian hosts (Palmer et al., 2011; Sorensen et al., 2006; Van der Meer and Belkin, 2010; Yagi, 2007). Uroporphyrinogen (urogen) III methyltransferase (UMT) catalyzes a reaction that yields two fluorescent products which produce red-orange fluorescence in the 590 - 770 nm range when illuminated with ultraviolet light (Feliciano et al., 2006; Ripp, 2005). Therefore, as in the case of GFP, no addition of exogenous substrates is required. UMT has been used as a bioreporter for the selection of recombinant plasmids, as a marker for gene transcription in bacterial, yeast, and mammalian cells, and for the detection of toxic salts such as arsenite and antimonite (Roessner and Scott, 1995; Wildt and Deuschle, 1999)

3.4 *Bioluminescent bioreporters*

Bioluminescent bioreporters include those based on luciferases which is a generic name for an enzyme that catalyzes a light-emitting reaction and can be found in bacteria, algae, fungi, jellyfish, insects, shrimp, and squid (Fernandez-Pinas et al., 2000; Fernandez-Pinas and Wolk, 1994; Greer and Szalay, 2002; Van der Meer and Belkin, 2010). Firefly luciferase (*luc* genes) catalyzes a reaction that produces visible light in the 550 – 575 nm range. A click-beetle luciferase is also available that produces light at a peak closer to 595 nm. Both luciferases require the addition of an exogenous substrate (luciferin) for the light reaction to occur. In bacteria, the genes responsible for the light-emitting reaction (the *lux* genes) have been isolated and used extensively in the construction of bioreporters that emit a blue-green light with a maximum intensity at 490 nm. Among all reporter genes, the bacterial bioluminescence is probably the most widely used for its high sensitivity and fast response (Ron, 2007; Van der Meer and Belkin, 2010). The *lux* genetic system consists of several genes, five of them are *luxA*, *luxB*, *luxC*, *luxD*, and *luxE* (Meighen, 1991). *LuxAB* encode bacterial luciferase which catalyzes the oxidation of a long chain aliphatic aldehyde and FMNH₂, producing light at 490 nm (Prosser et al., 1996). In naturally luminescent bacteria, the aldehyde substrate of luciferase (tetradecanal) is synthesized by the reductase, transferase and synthetase genes encoded by *luxC*, *D*, *E*.



bacterial luciferase

Depending on the combination of these genes, two types of bioluminescent bioreporters can be constructed: *luxAB* bioreporters and *luxCDABE* bioreporters (Fernandez-Pinas et al., 2000; Fernandez-Pinas and Wolk, 1994). In the first configuration, as in *luc* bioreporters, to fully complete the light-emitting reaction, a substrate must be supplied to the cell. Typically, this occurs through the addition of the chemical decanal at some point during the bioassay procedure. In the other hand, instead of containing only the *luxAB*, bioreporters can contain the five *lux* genes, thereby allowing for a completely independent light generating system that requires neither exogenous additions of substrate nor any excitation by an external light source. In this case, the bioreporter is simply exposed to a target analyte and a quantitative increase or decrease in bioluminescence results, often

within less than one hour. Its quickness and ease of use, along with the reproducibility of the bioassay in real-time and on-line recordings, make *luxCDABE* bioreporters extremely attractive. In practice, bacterial luciferase (*lux* operon) is the most versatile choice for bacteria-based bioreporters, whereas bioreporters constructed using insect luciferase (*luc* genes) are best for detecting systems based on eukaryotic cells.

When *lux* genes are used to construct a turn-off bioreporter, these bioreporters are commonly called lights-off bioreporters. The lights-off bioreporters are based on the fact that the light-emitting enzyme (luciferase) is highly dependent on cellular energy levels. Any change in the physiological state of the bioreporter cells that impacts ATP or reduced cofactors levels as a consequence of a sample exposure will thus produce a decrease in the level of luminescence emitted. On the contrary, the luminescent turn-on bioreporters are called lights-on bioreporters and the induction of the luminescence level result from the gene reporter activation and the ATP and enzyme cofactors present within the cell.

For developing bioreporters able to sense the presence of heavy metals in the environment the use of promoters of genes involved in microorganisms' metal-resistance mechanisms provides a wide variety of sensing elements. The sensing ability of the transcription factor determines bioreporter specificity (which metals are detected) and sensitivity (which range of concentrations is detectable). In case of metal bioreporters the sensor element usually consists of a transcriptional factor gene and the respective DNA operator area fused to a promoterless reporter gene. The potential metal sensing element that could be used in the metal-bioreporters constructions and bioreporters examples already available for heavy metals detection are detailed in the following sections.

4 Microorganisms metal-resistance proteins and gene regulation

During evolution, microorganisms have developed mechanisms to sense and respond to variable fluxes of metals in the environment (Bruins et al., 2000; Lemire et al., 2013; Ma et al., 2009). These mechanisms try to keep a beneficial intracellular concentration of the essential metals to meet the requirements of the metalloproteins and to detoxify the nonessential ones. The precise control of cytoplasmic metal ion concentrations is termed *metal homeostasis*; the three main mechanisms responsible of maintaining the metal

homeostasis are the regulation of the expression of active transport mechanisms to export metals (efflux proteins), the intracellular metal sequestration by proteins (e.g. metallothioneins) and the regulation of the metal ion uptake process (uptake proteins).

Efflux proteins: Active transport or efflux systems represent the largest category of metal resistance systems. Efflux system can be chromosomal or plasmid-encoded and they are usually induced in cases of excess of intracellular metal ions (Bruins et al., 2000). This mechanism is an organism's attempt to protect metal-sensitive cellular components by exporting toxic metals from their cytoplasm. These efflux systems can be non-ATPase or ATPase-linked and they are, usually, high specific for the metal ion they export. Export of excess metal ions is largely carried out by cation diffusion facilitator proteins and P-type ATPases (Kolaj-Robin et al., 2015; Nies, 2003). Several efflux pumps are described, for instance, Mn(II) (Huang et al., 2017; Waters et al., 2011), Zn(II) (Hantke, 2001) and Cu(I) efflux proteins have been well defined (Rensing and Grass, 2003), and recent work in *Bacillus subtilis* has revealed the role of P- type ATPases in Fe(II) efflux (Guan et al., 2015).

Intracellular sequestering proteins: Intracellular sequestration is the accumulation of metals within the cytoplasm to prevent exposure to essential cellular components. The main sequestering proteins are the metallothioneins and in the case of Fe homeostasis, the bacterioferritins. Metallothioneins are ubiquitous, low-molecular weight and cysteine-rich metal-binding protein, as their sulphur content is very high, they are the proteins with the overall highest metal ion binding capacity. The criteria that define a protein as a metallothionein are: (I) low molecular weight (<10 kDa), (II) high metal and sulfur content (>10%), (III) spectroscopic features typical of M-S bonds and (IV) absence or scarcity of aromatic amino acids (Blindauer, 2011; Blindauer and Leszczyszyn, 2010; Fowler et al., 1987). Metallothioneins can, in principle, bind a variety of metals ions, but the most important *in vivo* binding partners are Zn (II), Cu (II) and Cd (II). On the other hand, metallochaperones that are specialized proteins in charge of trafficking metals within a particular cellular compartment, e.g. the periplasm or cytosol, and function to “hold” the metal until it reaches the appropriate acceptor protein, are also involved in metal homeostasis (Ma et al., 2009; Tottey et al., 2005).

Uptake proteins: Trimeric β -barrel proteins called porins embedded in the outer membrane allow for nonselective passive diffusion of metal ions across the membrane.

However, in order to meet cellular metal demands, the cytosol must effectively *concentrate* metal ions. As a result, high-affinity active transport systems in the outer membrane or embedded in the plasma or inner membranes function to transport and release metal ions into the cytosol. Inner membrane transport systems are driven either by the hydrolysis of ATP on the cytoplasmic side of the membrane, e.g., by ATP binding cassette (ABC) transporters or by coupling to an energetically favourable transfer of protons or other ions across the bilayer, e.g., by Nramp proteins (Ma et al., 2009; Nevo and Nelson, 2006). When the cytosolic concentration of a metal ion becomes too high, genes encoding for these transporters are repressed in an effort to decrease the cytosolic uptake of that metal ion (Ma et al., 2009).

The expression of genes encoding these proteins is controlled by a panel of specialized transcriptional regulators known as metalloregulatory proteins, or “metal sensor” proteins. These metal sensors have at least one DNA-binding site or domain, responsible for recognition and binding of the operator DNA and an effector binding domain, responsible of interacting with the metal ion. Binding of the cognate metal to the metalloregulator activates or inhibits protein-DNA operator binding, thus, these transcriptional regulators can act as transcriptional repressors or activators, which results in the transcriptional regulation of genes responsible for metal homeostasis.

These transcriptional regulators specifically sense one or a small number of metal ions and are classified into seven major families based on their structural homology (Ma et al., 2009; Waldron et al., 2009), or into two groups according to their controlled genes function. Functionally speaking, these metal sensors can be classified into those that control gene expression linked to metal-ion efflux or/and sequestration proteins which normally regulate these genes via a transcriptional de-repression or an activation mechanism; and those that control the expression of genes required for metal ion uptake that always function as co-repressors, i.e. excessive ion concentration cause metal binding and the consequently repression of the genes that allow for metal ion uptake.

In general, when there is a metal excess in the cytoplasm, de-repression of the genes encoding for metal efflux or detoxification proteins, and associate repression of genes encoding metal uptake systems, will restore the metal cytoplasm homeostasis. Within the first group (metal efflux or detoxification proteins), three main metal sensors families

based on their structural homology can be distinguished: ArsR/SmtB, MerR family and CsoR/RcnR family.

4.1 *ArsR/SmtB* family:

Ars/SmtB family is the most extensively studied and likely the largest and most functionally diverse metalloregulatory protein family (Busenlehner et al., 2003; Osman and Cavet, 2010). The ArsR/SmtB family is named for its founding members, *Escherichia coli* As²⁺/Sb³⁺ sensor ArsR and *Synechococcus* PCC 7942 Zn²⁺ sensor SmtB. The ArsR/SmtB family includes proteins responsible for sensing a wide range variety of metal ions, both essential metal ions such as Zn²⁺ and Ni²⁺ and toxic metal pollutants such as As²⁺, Cd²⁺ and Pb²⁺. Genes regulated by ArsR/SmtB family proteins are usually responsible for effluxion, scavenging or detoxifying excess metal ions found in the cytosol. As transcriptional repressor, apo ArsR/SmtB proteins bind to a DNA operator that physically overlaps the promoter where they repress transcription of downstream genes. Metal binding induces a low-affinity conformation that mediates dissociation from the DNA and thus drives transcriptional de-repression.

The Zn-sensor SmtB from *Synechococcus* PCC 7942 was cloned and characterized in 1993 (Huckle et al., 1993). Apo-SmtB binds to the operator-promoter region of the *smtA* gene, encoding a class II metallothionein (SmtA) as a homodimer to inhibit *smtA* transcription (Huckle et al., 1993; Morby et al., 1993). This metallothionein is involved in sequestering excess of Zn²⁺. Although it also senses Cd²⁺ and Co²⁺ but with less affinity. The SmtB DNA-binding site contains an imperfect 12-2-12 inverted repeat within the *smt* operator-promoter region. Similar repeat sequences are also present in the DNA-binding site of other ArsR/SmtB representatives such as ZiaR, NmtR and CzrA. This generates a consensus sequence that allows predicting the target genes of related sensors (Harvie et al., 2006). Zn-SmtB has a weak affinity for DNA, therefore, when the cellular interior level of Zn increased, the SmtB occupancy decreased causing de-repression of *smtA* gene. A close homolog of *Synechococcus* SmtB is ZiaR from *Synechocystis* PCC 6803. ZiaR shares ~ 50 % sequence identity with SmtB and regulates the expression of the divergent *zia* operon, which encodes ZiaR and ZiaA, a P-type ATPase metal efflux pump. ZiaR appears to be a highly Zn²⁺-specific sensor (Thelwell et al., 1998). The other founding member of this family is the plasmid or chromosomally encode ArsR that acts as the arsenic/ antimony-responsive repressor of the *ars* operon in

E. coli and other bacteria (Busenlehner et al., 2003; Osman and Cavet, 2010). The *ars* operon from most bacteria encodes an arsenate reductase, as well as proteins required for metal ion extrusion. ArsR-mediated repression can be alleviated by +3 oxidation state oxyanions of As, Sb and Bi, rather than Zn. CadC was shown to repress the expression of *cadA*, encoding a Cd efflux ATPase, with CadC-mediated repression alleviated by Cd, Pb and Zn. Other ArsR/SmtB family member include proteins with additional metal-specificities including Co and Zn (CzrA), Ni and Co (NmtR and KmtR), Cd and Pb (CmtR), or Cu, Ag, Zn and Cd (BmxR). Genes encoding ArsR/SmtB sensors are known to be widespread, with the majority of sequenced bacterial genomes possessing at least one representative (Osman and Cavet, 2010).

4.2 MerR family:

MerR family proteins are unique in the mechanism of transcription activation among all the metalloregulatory proteins (Brown et al., 2003; Hobman et al., 2005). The main representative of this family is MerR, a transcriptional factor presents in Gram- and Gram+ bacteria, which bind to Hg and regulates the expression of the Hg resistance operon, *mer*. This Hg-ion resistance regulator was first studied in transposons Tn501 from *Pseudomonas aeruginosa* and Tn21 from *Shigella flexneri*. The *mer* operon is composed by the *merTP(C/F)AD(E)* genes, which encode the transporter MerT, a peroplasmic protein MerP, additional transporters MerC (in Tn21) or MerF (in Pmer327/419) and Tn5053), the Hg reductase enzyme MerA, a co-repressor MerD and a possible further transporter MerE. The DNA sequences that recognize MerR proteins have one common feature: a long 19 or 20bp spacer between the -35 and -10 promoter elements, which results in poor RNA polymerase binding affinity and transcription initiation efficiency (Brown et al., 2003). As originally determined for MerR itself, both the apo- and effector-bound forms are capable of binding to their cognate operator DNA sequences with similar affinities. However, only the effector-bound form can significantly unwind and distort the DNA helix, bringing the -35 and -10 elements to the same side of the DNA helix in a position optimized for RNA polymerase binding and ultimately transcriptional activation. Thus, only when the effector binds to the transcriptional factor, the transcription of the genes regulated by MerR transcriptional factor family can start. MerR proteins are characterized by a very similar N-terminal helix-turn-helix DNA binding region and a quite divergent C-terminal effector binding domain. The structural diversity in C-terminal region makes it possible for individual MerR family proteins to sense not only other metal

ions such as Zn^{2+} by ZntR (regulator of the ZntA Zn/Cd/Pb ATPase) (Beard et al., 1997), Cu^+ by CueR (regulator of the Cu/Ag ATPase, CopA) (Outten et al., 2000), Cd^{2+} by CadR (regulates expression of CadA, a Cd efflux ATPase) (Lee et al., 2001) and Pb^{2+} by PbrR (regulates expression of a CPx P-type ATPase and several other genes involved in Pb resistance) (Borremans et al., 2001), but also oxidative stress by SoxR (Demple, 1996) and small molecule drugs by BmrR (Heldwein and Brennan, 2001) or MtaN (Godsey et al., 2001).

4.3 *CsoR/RcnR family:*

The CsoR/RcnR family is the last metalloregulatory protein class structurally described. *Mycobacterium tuberculosis* CsoR is representative of a subfamily of Cu^+ sensors (Liu et al., 2007), while *E. coli* RcnR is representative of a subset of Ni^{2+}/Co^{2+} sensors (Iwig et al., 2008). Although described firstly in *M. tuberculosis*, genes encoding CsoRs are widely distributed through most major bacterial species (Liu et al., 2007). CsoR is the transcriptional repressor of the *cso* (Cu-sensitive operon) which encodes CsoR itself and a Cu^+ -effluxing P-type ATPase CtpV. Apo-CsoR binds to the operator-promoter region upstream of the *csoR* gene, Cu^+ binding negatively regulates the binding of CsoR to a DNA fragment encompassing the operator-promoter region of the *cso* operon; resulting in a de-repression of transcription. The crystallographic structure reveals a homodimeric antiparallel four-helix bundle and a short C-terminal helix, different from the classical DNA binding motif such as the winged helix-turn-helix domain found in other metalloregulatory proteins. Other CsoR homologue have been described such as CsoR from *B. subtilis*, also involved in Cu^+ homeostasis (Smaldone and Helmann, 2007). *E. coli* RcnR regulates the expression of the Ni^{2+} and Co^{2+} exporter, RcnA and an associated periplasmic protein, RcnB (Iwig et al., 2006). RcnR coordinates a variety of metal ions but only the binding of Ni^{2+} and Co^{2+} results in conformational changes that allosterically negatively regulate DNA binding interactions (Higgins and Giedroc, 2014).

Unlike ArsR and MerR families, which are related with metal resistance or detoxification proteins, the second group, metal sensors who regulate the expression of genes required for metal ion uptake, are in charge of maintaining optimum concentration of essential metals. Three families of transcriptional repressors have a key role in this process, DtxR, Fur, and NikR family. These transcriptional regulators, since they are activated in the

absence of metal, are not as widely used as sensing element in construction of heavy metal detection bioreporters.

4.4 DtxR, Fur, and NikR family:

The DtxR family of metalloregulatory proteins includes two major subfamilies, Fe²⁺ and Mn²⁺ sensors. *Corynebacterium diphtheriae* DtxR is the founding member of the first subgroup and named for its function in regulating diphtheria toxin expression, which is strongly tied to the Fe status of the cell (Andrews et al., 2003). DtrR family regulates genes that encode for proteins that mediate Fe uptake and storage. These genes are constitutively expressed under Fe limiting conditions, while elevated cytosolic concentration results in repression mediated by DtxR. The second subgroup is represented by the transcriptional regulator MntR of *Bacillus subtilis* (Que and Helmann, 2000). MntR regulates the transcription of the high-affinity manganese uptake systems encode by the *mntABCD* and *mntH* genes. As in the case before, when the cytosolic Mn²⁺ concentration is high, MntR represses the expression of these genes (Schmitt, 2002). The Fe uptake repressor Fur of *E. coli* represents the Fur family (Andrews et al., 2003). This family is constituted generally by transcriptional repressors, which represses the expression of the genes when bound to their cognate metal ion effectors, although some transcriptional activators can be found within the family (Delany et al., 2004; Troxell and Hassan, 2013). Other relevant members of Fur family include Mur, Nur and Zur, which respond to manganese, Ni and Zn, respectively (Troxell and Hassan, 2013). The third family, NikR family, comprises a set of homologous proteins for Ni homeostasis, generally known as NikR proteins. The first regulator of this family characterized was *E. coli* NikR, which regulates the transcription of the *nik* operon (*nikABCDE*) which encodes a Ni specificity high affinity ABC transporter (Schreiter et al., 2003; West et al., 2010). Ni²⁺ bound to NikR binds to the *nik* operator-promoter DNA with high affinity and thus represses transcription under Ni²⁺ replete conditions.

This detailed control of the heavy metal homeostasis provides a wide range of possibilities to using genetic engineering and in the last two decades, microbial resistance mechanisms against various metals and metalloid cations have been used to construct living whole-cell bioreporters that detect heavy metals in the environment (Fernandez-Lopez et al., 2015).

The understanding of metal-responsive transcriptional control is thus exceptionally well advanced in prokaryotes compared with eukaryotes (Rutherford and Bird, 2004; Waldron et al., 2009), for which only a relative small number of metal-sensing transcriptional regulators are known, mostly in yeast and only few bioreporters based on eukaryotic transcriptional factors for heavy metal detection have been developed (Jarque et al., 2016).

As described before, the binding capacity (metal species and sensed concentration) of the transcription factor used in the sensing element influences sensitivity and specificity, however, these factors also depend greatly on microbial metal homeostasis systems. Different bacterial species have very different transport/resistance systems. Some bacteria may contain several mechanisms for the same metal, whereas others may completely lack resistance to the same metal. Moreover, the mechanisms by which metal ions enter the cell may also differ between bacterial species and consequently the intracellular metal concentration will be different. All these factors may influence the sensing ability of the bioreporter and as a result, the same sensing element may respond in a different way to the same metal/group of metals in different bacterial bioreporters. Furthermore, due to the limited possibilities to coordinate binding between proteins and metal ions, metal activated transcription factors usually sense several different heavy metal ions with similar properties (Reyes-Caballero et al., 2011). Thus, it is generally not possible in practice to construct a bioreporter that senses only one metal. However, because binding affinities vary between metals, different metals are sensed at different concentrations.

5 Heavy metals bioluminescent microorganism-based bioreporters and applications

Given the large number of bacterial bioreporters for the detection of heavy metals and since the vast majority use luminescence as a reporter system, in this section we will focus on luminescent bioreporters of heavy metals. Table 1 summarizes all the heavy metals bioluminescent bioreporters described in the following sections.

5.1 *Bacterial bioreporters:*

Because its metal resistance systems are well studied and it is easy to genetically manipulate, *E. coli* has been the most favoured host for whole-cell heavy metal bioreporter applications. Hg sensing bioreporter strains were among the first heavy metal responsive systems to be developed. Selifonova et al. (1993) cloned the Hg resistance operon of transposon 21 (Tn21 *mer*) upstream from a promoterless *lux* operon (*luxCDABE*) from *Aliivibrio fischeri* and Virta et al. (1995) fused the same operon to the firefly luciferase from *Photinus pyralis*. Both reported that the bioreporter strains were very sensitive to Hg although they found differences in the sensitivity between both possibly due to the different reporter genes used. Virta et al. (1995) tested also the bioreporter strain toward other heavy metals finding a slight induction by Cd. In addition, to these sensors, more have also been developed based on the *mer* operon (Hakkila et al., 2004; Ivask et al., 2002) but also for the detection of metalloids such as As using the As resistance gene *arsR* of *E. coli* (Hakkila et al., 2004; Stocker et al., 2003; Tauriainen et al., 1999; Trang et al., 2005) and Cu using the Cu P-type ATPase efflux pump gene, *copA*, able to response to Cu but also to Ag (Hakkila et al., 2004; Riether et al., 2001). Also *E. coli* based bioreporters have been developed using *zntA* gene responsible for encoding an integral membrane protein of the CPx-type ATPase family, described able to be induced by Zn, but also by Cd, Pb, Co, Ni, SbO_2^- , CrO_4^{2-} and $\text{Cr}_2\text{O}_7^{2-}$ due to a weak affinity to the transcriptional repressor ZntR responsible of regulating the *zntA* transcription (Riether et al., 2001). Charrier et al. (2011) developed a set of three heavy metal detection bioreporters using the heavy metal-inducible promoters, *zntA*, *copA* and *arsR* fused to the *A. fischeri lux* operon, given place to *E. coli* Zntlux, *E. coli* Coplux, and *E. coli* Arslux strains, respectively and a strain that constitutively expresses the *A. fischeri* bioluminescence *lux* operon, *E. coli pBfilux*. Moreover, a bioreporter for Hg detection was also constructed using the *merR* promoter, giving rise to the bioreporter, *E. coli* Merlux (Jouanneau et al., 2011). Like most bioreporters, these strains were not specific to only one metal but rather to a range of metals.

Other bacteria largely used in heavy metal detection is the natural resistant to heavy metals, *Cupriavidus metallidurans*, (previously named as *Ralstonia eutropha* or *Alcaligenes eutrophus*). This bacterium has been genetically modified to detect heavy metals such as Cr using *chrB* or *chrAB* as inducible promoters (Corbisier et al., 1999; Ivask et al., 2002), Co and Ni (*cnxXYH* promoter), Cu (*copSRA*) or Pb (*pbrR*) (Corbisier

et al., 1999; Tibazarwa et al., 2001). Moreover, a few studies have been developed using other bacteria as host strain. Petanen et al. (2001) have cloned the *arsR* gene from *E. coli* in *P. fluorescens* and the *merR* operon from the same bacteria. Tauriainen et al. (1997) used the promoter *arsR* fused to the *lucFF* genes and expressed it in *S. aureus*. In addition, these authors used the *cadC* promoter from *S. aureus* to express it in *B. subtilis* also using the genes *lucFF* as reporter genes (Tauriainen et al., 1998). In the former, the reporter strain responded to Cd and Sb while in the last case the strain was inducible by Cd, Pb, Sb, Sn and Zn.

5.2 *Eukaryotic bioreporters:*

Eukaryotic cells have not been widely used as hosts for metal bioreporters. Approximately 15% of total heavy metal bioreporters have been developed using eukaryotic cells (Gutierrez et al., 2015). Roda et al. (2011) constructed the unique bioluminescent heavy metal bioreporter based on *Saccharomyces cerevisiae*. They use the ability of the transcriptional activator protein Ace1 present in *S. cerevisiae* to control the expression of the luciferase firefly for detecting Cu^{2+} . For a greater knowledge of the bioreporters based on *S. cerevisiae* to detect heavy metals with other reporter genes systems or the detection of other environmental pollutants, see the recent review of Jarque et al. (2016). Some studies based on eukaryotic cells require special attention since they are based on the protozoon *Tetrahymena thermophila*. These ciliate-based bioreporters present some advantages over other eukaryotic-based bioreporters. Firstly, this organism lacks cell wall in its vegetative stage, hence making it highly sensitive towards any chemicals. On the other hand, it has similar metabolic pathways as in human cells with respect to yeast or bacterial cells. Hence, it can be used as a model for the study of impact of heavy metals towards human cells. Amaro et al. (2011) developed two whole-cell bioreporters based on this ciliate using the promoters of the genes *MTT1* and *MTT5*, which codify for two metallothioneins preferably overexpressed under Cd^{2+} or Pb^{2+} , respectively, though there are also induced by other metals, using the luciferase genes (*lucFF*) as reporter protein (Amaro et al., 2011). More recently, they generated a second bioreporter using the gene promoter of *MTT1* fused to GFP as the reporter molecule (Amaro et al., 2014). These transformed strains were used to detect heavy metals in artificial and natural (soil and aquatic) samples.

Table 1. Heavy metals bioluminescent bioreporters

Promoter (origin)*	Element	Reporter gene	Host	Linear response** (µM)	Assay Time	Reference
Bacteria						
<i>arsB</i>	As	<i>luxAB</i> (<i>A. fischeri</i>)	<i>E. coli</i>	0.01-1	120 min	Cai and Dubow (1997)
<i>arsR</i>	As	<i>lucFF</i> (Firefly)	<i>E. coli</i>	0.01-1	8 h	Hakkila et al. (2002)
	As	<i>luxCDABE</i> (<i>A. fischeri</i>)				
	As ³⁺	<i>lucFF</i> (Firefly)	<i>E. coli</i>	0.033-1	90 min	Taurianien et al. (1999)
	As ⁵⁺			33-33000		
	Cd			10-1000		
	Sb			0.1-100		
	As	<i>luxAB</i> (<i>A. fischeri</i>)	<i>E. coli</i>	0.1-0.8	60 min	Stocker et al. (2003)
	As	<i>luxAB</i> (<i>A. fischeri</i>)	<i>E. coli</i>	0.1-0.4		Trang et al. (2005)
<i>arsR</i>	As ³⁺	<i>luxCDABE</i> (<i>A. fischeri</i>)	<i>E. coli</i>	0.256	60 min	Charrier et al. (2011)
	As ⁵⁺			0.3		
	Cd			5.9		
	Pb			4.16		
<i>arsR</i> (<i>E. coli</i>)	As	<i>lucGR</i> (<i>P. plagiophthalmus</i>)	<i>P. fluorescens</i>	0.1-10	120 min	Petanen et al. (2001)
<i>arsR</i>	Cd	<i>lucFF</i> (Firefly)	<i>S. aureus</i>	0.5-5	120 min	Taurianien (1997)
<i>cadC</i> (<i>S. aureus</i>)	Cd	<i>lucFF</i> (Firefly)	<i>B. subtilis</i>	0.003-0.1	180 min	Taurianien (1998)
	Pb			1-10		
	Sb			0.033-3.3		
	Sn			33-1000		
	Zn			1-33		
<i>chrB</i>	Cr ³⁺	<i>luxCDABE</i>	<i>C. metallidurans</i>	5-80	90 min	Corbisier et al. (1999)
<i>chrAB</i>	Cr ⁶⁺			2.5-40		
	Cr ³⁺	<i>lucFF</i> (Firefly)	<i>C. metallidurans</i>	2-100	120 min	Ivas et al. (2002)
	Cr ⁶⁺			0.04-1		
<i>cnrXYH</i>	Co	<i>luxCDABE</i> (<i>A. fischeri</i>)	<i>C. metallidurans</i>	9-400	16 h	Tibazarwa et al. (2001)
	Ni			0.1-60		
<i>copA</i>	Ag	<i>luxCDABE</i> (<i>A. fischeri</i>)	<i>E. coli</i>	0.3-3	80 min	Riether et al. (2001)
	Cu			3-30		
	Ag	<i>lucFF</i> (Firefly)	<i>E. coli</i>	0.003-0.3	120 min	Hakkila et al. (2004)
	Cu			0.3-300		
	Cu	<i>luxCDABE</i>		90.5	60 min	Charrier et al. (2011)
	Ag			2.75		
	Cu	<i>lucFF</i> (Firefly)	<i>E. coli</i>	0.15		Roda et al. (2011)
<i>copBC</i>	Cu	<i>luxAB</i> (<i>A. fischeri</i>)	<i>P. fluorescens</i>	1-100	180 min	Tom-Petersen et al. (2001)

Promoter (origin)*	Element	Reporter gene	Host	Linear response** (µM)	Assay Time	Reference	
<i>copSRA</i>	Cu	<i>luxCDABE</i> (<i>A. fischeri</i>)	<i>C. metallidurans</i>	1-200	90 min	Corbisier et al. (1999)	
<i>katG</i>	Cd	<i>luxCDABE</i> (<i>A. fischeri</i>)	<i>E. coli</i>	2-35	90 min	Ben-israel et al. (1998)	
<i>merR</i> (<i>S. flexneri</i>)	Cd	<i>lucFF</i> (Firefly)	<i>E. coli</i>	1-100	60 min	Virta et al. (1995)	
<i>merR</i>	Hg	<i>lucFF</i> (Firefly)	<i>E. coli</i>	10 ⁻⁹ -0.01	8 h	Hakkila et al. (2002)	
	Hg			0.005-0.1			
<i>merRB</i>	Hg	<i>luxCDABE</i> (<i>A. fischeri</i>)	<i>E. coli</i>	0.0001-0.1	120 min	Jouanneau et al. (2011)	
	Cd			<i>lucFF</i>			1-10
	Hg			<i>luxCDABE</i> (<i>A. fischeri</i>)			10 ⁻⁵ -0.1
	Hg						10 ⁻⁷
	Cd						0.011
<i>merRB</i>	As ³⁺	<i>lucFF</i>	<i>E. coli</i>	15.6	120 min	Ivask et al. (2002)	
	As ⁵⁺			12.65			
	Zn			2.3			
<i>merRB</i>	Cd	<i>lucFF</i>	<i>E. coli</i>	0.27-80	120 min	Ivask et al. (2001)	
	Hg			0.1-15			
	Zn			1380-4000			
<i>merRT</i>	Hg	<i>luxCDABE</i> (<i>A. fischeri</i>)	<i>E. coli</i>	0.0002-0.01	120 min	Selifonova et al. (1993)	
	Hg			0.005-0.5	40 min		
<i>pbrR</i>	Pb	<i>luxCDABE</i> (<i>A. fischeri</i>)	<i>C. metallidurans</i>	500-5000	180 min	Corbisier et al. (1999)	
<i>zntA</i>	Cd	<i>luxCDABE</i> (<i>A. fischeri</i>)	<i>E. coli</i>	0.01-0.33	60 min	Charrier et al. (2011)	
	Zn			3-30			
	Cr ⁶⁺			30-300			
	Hg			1-30			
	Pb			0.03-1			
	Zn			1.7			
	Cd			0.0045			
	Hg			0.01			
	As ³⁺			28.52			
	As ⁵⁺			9.32			
	Cu			16.92			
	Pb			2.2			
	Sn			12.95			
	Ni			4.4			
	Co			0.22			
Cr ⁶⁺	597.2						
<i>zntR</i>	Fe	<i>lucFF</i> (Firefly)	<i>E. coli</i>	4.34	60 min	Ivask et al. (2002)	
	Cd			0.05-30			
	Hg			0.01-1			
<i>zntR</i>	Zn	<i>lucFF</i> (Firefly)	<i>E. coli</i>	40-15000	120 min	Roda et al. (2011)	
	Zn			40-15000			
Eucaryote							
<i>CUP1</i>	Cu	<i>lucFF</i> (Firefly) (red-emitting mutant)	<i>S. cerevisiae</i>	0.5	120 min	Roda et al. (2011)	

Promoter (origin)*	Element	Reporter gene	Host	Linear response** (μM)	Assay Time	Reference
<i>MTT1</i>	Cd	<i>lucFF</i>	<i>T. thermophila</i>	0.025	120 min	Amaro et al. (2011)
	Cu			2.5		
	Zn			0.5		
	Pb			0.5		
	As			0.05		
	Hg			0.025		
<i>MTT2</i>	Cd	<i>lucFF</i>	<i>T. thermophila</i>	0.005	120 min	Amaro et al. (2011)
	Cu			1.5		
	Zn			1.5		
	Pb			0.05		
	As			0.025		
	Hg			0.025		
Cyanobacteria						
<i>smtA</i>	Zn	<i>luxCDABE</i> (<i>A. fischeri</i>)	<i>Synechococcus</i>	0.5-4	60 min	Erbe et al. (1993)
	Cd			0.5-1.5		
	Cu			2-15		
<i>coaT</i>	Co	<i>luxAB</i> (<i>V. harveyi</i>)	<i>Synechocystis</i>	0.3-6	210 min	Peca et al. (2008)
	Zn			1-3		
<i>nrsBACD</i>	Ni	<i>luxAB</i> (<i>V. harveyi</i>)	<i>Synechocystis</i>	0.2-6	210 min	Peca et al. (2008)
<i>isiAB</i>	Fe	<i>luxAB</i> (<i>V. harveyi</i>)	<i>Synechococcus</i>	10^{-15} - 10^{-14}	12 h	Durham et al. (2002)
<i>isiAB</i>	Fe	<i>luxAB</i> (<i>V. harveyi</i>)	<i>Synechococcus</i>	10^{-15} - 10^{-13}	12 h	Boyanapalli et al. (2007)
<i>alr0397</i>	Fe	<i>luxAB</i> (<i>A. fischeri</i>)	<i>Anabaena</i>	10^{-15} - 10^{-13}	12 h	Zha et al. (2012)

*The origin strain of the promoter is indicated when it is different from the host strain

**When not available, the LOD is indicated

The development of bioreporters based on different organisms is essential to have a wider range of detection of different metals. Since the mechanisms of homeostasis differ between different bacteria, specificity and sensitivity may vary among bioreporters. Another very important aspect is the use of organisms of different trophic levels. As previously described, until now most bioreporters (~ 85% of total heavy metals bioreporters) are based on bacteria and more specifically in *E. coli*, an enterobacteria. It has been widely used to determine heavy metals in both soils and aquatic systems. In this sense, more ecologically relevant bacteria are desirable to increase the relevance in environmental monitoring.

Cyanobacteria are among the most relevant organisms ubiquitous in the aquatic environment. They are a group of Gram- photosynthetic bacteria, responsible, along with

the algae, of the primary production in the aquatic systems. Further characteristic of this group of bacteria are detailed in the next section.

6 Cyanobacteria and their applications in environmental monitoring

Cyanobacteria, also known as blue-green algae or Cyanophyta, are a diverse group of Gram- photosynthetic bacteria (Whitton, 1992). They originated during the Precambrian era (2.8×10^9 years ago), and as a group are known to survive a wide spectrum of environmental stresses (Knoll, 2008). The ability of cyanobacteria to perform oxygenic photosynthesis is thought to have converted the early reducing atmosphere into an oxidizing one (Knoll, 2008), which dramatically changed the composition of life forms on Earth by stimulating biodiversity and leading to the near-extinction of oxygen-intolerant organisms. According to the endosymbiotic theory, cyanobacteria are the ancestors of chloroplasts in plants and eukaryotic algae, which evolved from them via endosymbiosis. Cyanobacteria are organisms with a wide ecological distribution and present a variety of strategies that allow them to adapt and alter their physical environment (Whitton, 1992): they can be found in freshwater, marine and soil environments. They can even be found in extreme ecosystems such as deserts, hypersaline waters or thermal springs (Garcia-Pichel and Wojciechowski, 2009; McGregor and Rasmussen, 2008; Yannarell et al., 2006). A few are endosymbionts in lichens, plants, various protists, or sponges (Bergman et al., 2008; Wilkinson and Fay, 1979). The only condition in which cyanobacteria are not usually found is in acidic environments (pHs below 5) (Whitton, 1992).

Cyanobacteria show a prokaryotic cellular organization. They have a Gram- type cell envelope with plasma membrane and outer membrane separated by a periplasmic space. However, their cell envelope share some similarities with that of Gram+ bacteria, such as the kind and proportion of lipid components, the thickness of the peptidoglycan layer and the degree of crosslinking between the peptidoglycan chains (Hoiczuk and Hansel, 2000). Some of them can also present an external surface layer and mucilaginous sheet (Smarda et al., 2002). They present a multicopy circular chromosome and a variable number of plasmids of different length (Schneider et al., 2007), and as prokaryotic organisms do not present organelles; however, they have a complex system of inner membranes called thylakoid membranes where the different components of the photosynthetic apparatus are

located. The thylakoid membrane hosts both respiratory and photosynthetic electron transport (DeRuyter and Fromme, 2008) while their plasma membrane contains only components of the respiratory chain. Attached to thylakoid membrane, phycobilisomes act as light harvesting antennae complexes for the photosystems. As in plants and algae, the oxygenic photosynthesis is accomplished by coupling the activity of two light harvesting systems: photosystem (PS) II and I (Z-scheme). The most usual photosynthetic pigments present in cyanobacteria are chlorophyll a, phycoerythrin, phycocyanin and allophycocyanin; unlike plants, the majority of cyanobacteria lack chlorophyll b. A few genera of cyanobacteria, however, lack phycobilisomes and have chlorophyll b instead (*Prochloron*, *Prochlorococcus*, *Prochlorothrix*). Thus, the cyanobacteria could be defined as organisms characterized by a prokaryotic cell organization, and a photosynthetic apparatus similar to eukaryotic chloroplasts (DeRuyter and Fromme, 2008). Cyanobacteria include unicellular and filamentous species. Some filamentous strains show the ability to differentiate into several different cell types: vegetative cells, the normal, photosynthetic cells that are formed under favourable growing conditions; akinetes, draught-resistant spore-like cells, can be formed when environmental conditions become harsh; hormogonia which are gliding filaments which serve as propagation forms, and thick-walled heterocysts, which contain the enzyme nitrogenase, can be differentiated in poor nitrogen environmental conditions (Flores and Herrero, 2010; Meeks et al., 2002; Whitton, 1992).

Cyanobacterial taxonomy is an issue of controversy. The most accepted classification for cyanobacteria is that developed by Komareck (2016). In the study, Komareck (2016) classified the cyanobacteria into nine sections: Nostocales, Chroococciidiopsidales, Rubidibacter/Halothece, Spirulinales, Pleurocapsales, Chroococcales, Oscillatoriales, Synechococcales and Gloeobacterales.

Cyanobacteria have a long history of adaptation in the planet and have developed strategies to respond and to adapt to almost any environmental change (Garcia-Pichel and Wojciechowski, 2009; McGregor and Rasmussen, 2008; Whitton, 1992; Yannarell et al., 2006) and have been found to respond to a large number of both organic pollutants (different types of pesticides) and heavy metals (Bachmann, 2003; Rawson et al., 1989). As primary producers with a key role in the N and C cycles, they are a dominant component of marine and freshwater phytoplankton and any detrimental effect on this

group may have a negative impact in nutrient availability to organisms of higher trophic level; for this, cyanobacteria are well suited to be used in environmental toxicity testing and environmental monitoring (Fernandez-Piñas et al., 1991; Perona et al., 1998). Many cyanobacteria are amenable to genetic manipulation and at least 100 cyanobacterial genomes have been sequenced (<http://genome.microbebd.jp/cyanobase>) (Shih et al., 2013), this greatly facilitates the genetic engineering of strains. As in environmental monitoring, cyanobacteria have already been applied in the field of microbial bioreporters but in a marginal way compared to other microorganisms of less ecological relevance (Bachmann, 2003).

6.1 Global toxicity cyanobacterial bioreporters

Only two cyanobacterial global toxicity bioreporters have been described up to date; both are lights-off bioreporters. One is based in the unicellular *Synechocystis* strain PCC 6803 (Shao et al., 2002). This cyanobacterial chromosome was doubled tagged with both *luc* (from firefly *Photinus pyralis*) and *luxAB* genes (from marine bacterium *A. fischeri*) under the control of the *tac* promoter. As aldehyde (substrate for bacterial luciferase) addition was toxic to the culture, Shao and coworkers measured the luminescence of the *luc* genes. They tested the toxicity of four herbicides with different modes of action, two heavy metals (Cu and Zn) and the organic 3,5 dichlorophenol (DCP). The *Synechocystis* bioreporter was not self-luminescent and the luciferin substrate had to be added at each time point for measurement excluding its use for continuous monitoring; besides it does not appear to have been tested with environmental samples. The other cyanobacterial lights-off bioreporter was developed in our group. This bioreporter is based on the filamentous heterocystous cyanobacterium *Anabaena* sp. PCC 7120 denoted *Anabaena* CPB4347. This is a self-luminescent bioreporter, which bears in its chromosome a *tn5* derivative with *luxCDABE* from the luminescent terrestrial bacterium *Photorhabdus luminescens*. This strain shows a high constitutive luminescence and does not need the addition of exogenous aldehyde. This strain of cyanobacterium was successfully tested as general toxicity bioreporter against single and combined heavy metals (Rodea-Palomares et al., 2009), single and mixtures of priority and emerging pollutants (Gonzalez-Pleiter et al., 2013; Rodea-Palomares et al., 2015b; Rodea-Palomares et al., 2010; Rosal et al., 2010a; Rosal et al., 2010b) and nanomaterials (Martín-de-Lucía et al.,

2017; Rodea-Palomares et al., 2011). It has been also tested in environmental matrices of different complexity (Rodea-Palomares et al., 2010; Rosal et al., 2010a).

6.2 *Cyanobacterial bioreporters responsive to heavy metals*

To our knowledge the first cyanobacterial bioreporter able to detect heavy metals was constructed by Erbe et al. (1996). It was based on the *smt* locus of the unicellular *Synechococcus* sp. PCC 7942; this locus consists of the cyanobacterial metallothionein gene *smtA* and *smtB* a divergently transcribed gene encoding the transcriptional repressor of *smtA* (see 4.1 *ArsR/SmtB* family). These authors fused part of the *smt* locus including the *smtB*, the *smt* operator/promoter region and the first codon of *smtA* to *luxCDABE* of *A. fischeri*. The strain, although self-luminescent, did not generate enough endogenous aldehyde and dodecanal was added at each sample before measurement. This strain was able to detect Zn^{2+} , Cu^{2+} and Cd^{2+} . Peca et al. (2008) constructed a self-luminescent novel cyanobacterial bioreporters able to detect Ni, Co and Zn. They fused the *coaT* promoter which is inducible by Co and Zn and the *nrsBACD* Ni responsive promoter to *luxAB* from *Vibrio harveyi*; the constructions were transformed into a *Synechocystis* sp. PCC 6803 strain harbouring the fatty acid reductase complex genes *luxCD,E* from *V. harveyi*. From the tested metals, only Zn and Co significantly induced the bioluminescence of the *coaLux* strain while the *nrsLux* strain was specific to Ni. Most cyanobacterial bioreporters constructed to detect Fe, an essential nutrient, have been made based on the Fe-responsive *isiAB* promoter, which is in part regulated by Fur (ferric uptake regulator). When cells are depleted of iron, the *isiAB* promoter is induced; when increasing concentrations of iron are supplied to the cells, the *isiAB* promoter is down-regulated in a dose-response manner; so that these bioreporters are considered as lights-off bioreporters. There are some strains based on *Synechococcus* (Boyanapalli et al., 2007; Durham et al., 2002) but also in *Anabaena* (Zha et al., 2012). All these bioreporters were successfully used in environmental samples for Fe detection.

In addition to Fe, cyanobacterial bioreporters have been also constructed to detect other nutrients such as phosphate and nitrogen, which are essential for primary producers and usually limiting in certain aquatic environment such as the ocean of large lakes. On the other hand, an excess of P and/or N may lead to eutrophication of water bodies and developments of algal blooms which may lead to toxin production by cyanobacteria (Dodds, 2006). In our group, *Anabaena* sp. PCC 7120 derivative strains have been

constructed which are self-luminescent *luxCDABE* marked bioreporters able to respond to different nutrient bioavailability such as phosphate and nitrates (Munoz-Martin et al., 2011; Munoz-Martin et al., 2014). Since it is not the objective of this thesis to enter in depth in this matter, the extensive and comprehensive review on the use of cyanobacterial bioreporters as sensor nutrient availability reported by Bullerjahn and coworkers (Bullerjahn et al., 2010) and Mateo and coworkers (Mateo et al., 2015) are highly recommended.

A bioreporter is a very useful tool in the detection of different compounds in the environment, however, understanding and analyzing their response is essential to be able to draw conclusions from the environmental analysis.

7 Turn-off vs. Turn-on bioreporters dose-response curves

The dose-response relationship is a fundamental and essential concept in toxicology and pharmacology. It quantitatively defines the role of the dose of a chemical in evoking a biological response. The classical dose-response curve in toxicology as well as in turn-off (lights-off) or global toxicity bioreporters output is generally characterized by a monotonic dose-response curve. This type of curve is defined by a concentration dependent inhibition of a vital function of an organism (such as respiration, feeding rate, mobility, etc.), or, as in the present case, to the inhibition of the signal emitted by the reporter gene. This is usually represented as the inhibition percentage of the signal with respect to the control signal. When there is not toxicity or there is a non-toxic amount of pollutant for the organism, the signal emitted by the reporter gene stays at its maximum (100 %), in other words, the % of the signal inhibition is equal to zero. The point at which toxicity first appears is known as the threshold dose level or the lowest observed effect concentration (LOEC). The no observed effect concentration (NOEC) is the tested concentration immediately below the LOEC which, when compared with the control, has no statistically significant effect, within a given exposure time. From the LOEC, the percentage of signal inhibition increases in a dose-dependent manner when increasing the concentration of the pollutant until it reaches the maximum toxicity, i.e. the 100% of signal inhibition (**Figure 2a**). Dose-response curves are used to derive dose estimates of chemical substances. A common dose estimate is the effective dose that exhibit the 50 %

of the effect, in this case, the effective dose that causes the 50 % of signal inhibition (ED_{50}). However, other effective doses such as ED_{10} , ED_{20} or ED_{90} can also be calculated. Knowledge of the shape and slope of the dose-response curve is extremely important in predicting the toxicity of a substance at specific dose levels.

Different from the turn-off whole-cell bioreporters output, the inducible or turn-on (lights-on) whole cell bioreporters produce a biphasic dose-response curve. Contrary to the previous case, this is usually represented as the induction percentage of the signal with respect to the control. This curve is characterized by a background signal when the effector concentration is too low to activate the sensor element. When it reaches the threshold concentration, which is the limit of detection (LOD), the signal increases linearly with increasing concentrations of the effector, allowing the calculation of the concentration using a linear regression. At a certain concentration of the effector, the bioreporter is maximally induced (Maximum permissive concentration, MPC) and no further increase in the signal can be observed. Above this concentration, the pollutant usually exerts a cytotoxic effect and the signal rapidly drops to zero (**Figure 2b**).

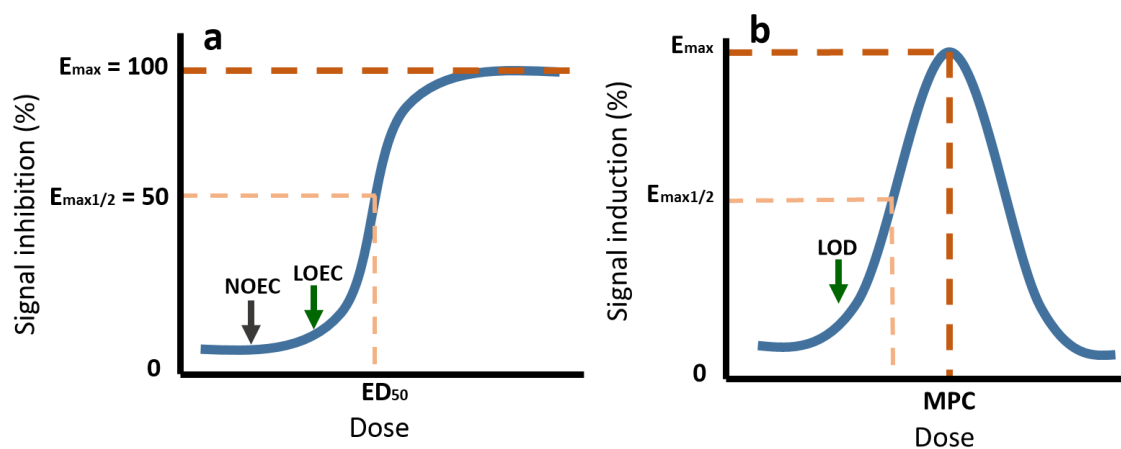


Fig. 2. Typical dose-response profiles for a) classical monotonic dose-response curves and b) biphasic dose-response curves.

Furthermore, since the level of response exhibited by the bioreporter is dependent on the metal sensor affinity for the effector, different effectors can generate different levels of induction of the reporter protein, giving rise to different maximum effects (**Figure 3a**). Moreover, the effector concentration that induce the maximum effect may vary between different effectors, giving rise to different maxima in terms of induction but also in terms of dose (**Figure 3b**).

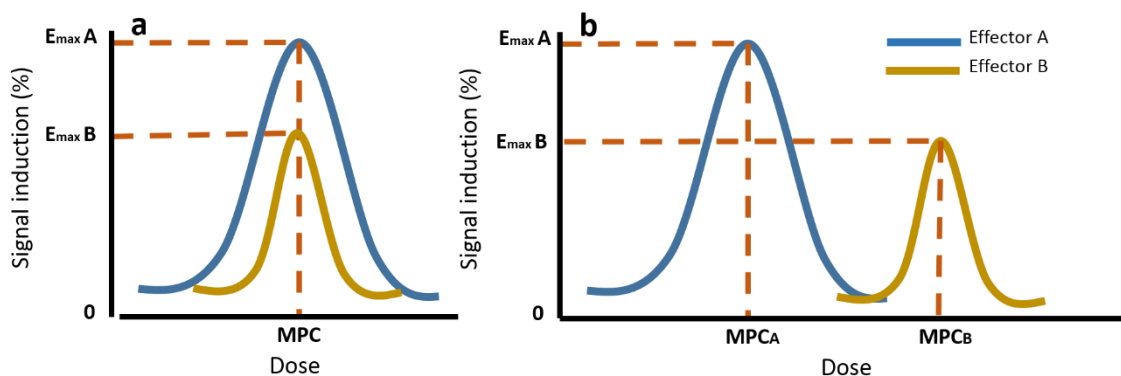


Fig. 3. Biphasic dose-response curves by two effectors, a) both effectors have the same MPC but they induced different maximal effects; b) both effectors have different MPCs and they induced different maximal effects.

In summary, the turn-on bioreporters' output could be defined as a biphasic dose-response curve with different effectors causing different maximal responses. In addition to turn-on biosensors output, these biphasic dose-response patterns are commonly observed in other areas such as hormetic effects, hormone agonist/antagonist research, AhR agonist/antagonist activity research and in endocrine disruptors activity research (Calabrese, 2008; Hecker et al., 2006; Scholze et al., 2014; Silva et al., 2007)

8 Theoretical models of chemical mixture effects

As explained before the chemicals are found as part of complex mixtures in the environment. Methods and models are required to analyse and predict the effect of mixtures in order to improve risk assessment. Study of mixtures intends to predict the combined effect of a mixture of chemicals based on the information of the effect of the individual components. Its ultimate goal is to be able to predict the combined effect of any environmental mixture based on the information and conclusions obtained by studying a limited number of mixtures. The most used methods to study mixtures effects in human toxicology and ecotoxicology are fractional additivity methods named Independent action (IA) and Concentration addition (CA) (Chou, 2006; Kortenkamp et al., 2009). These methods are based on two different additivity definitions, respectively: *Bliss additivity* (IA) (Bliss, 1939) and *Loewe additivity* (CA) (Loewe, 1953). Additivity methods are based on the basic idea that the expected effect of a mixture of chemicals can be predicted based on the sum of the exposure levels or the effects of the individual

components. The term “effect” generally refers to the measured response, while the term “sum” is different according to the method use, it may be a conditional sum (see IA) or a weighted sum (see CA).

8.1 *Independent Action (IA):*

IA assumes that chemicals under consideration have dissimilar mode of actions (MOAs). The toxic response of each chemical is thought of as a biologically and statistically independent event. As the name indicate, the components of the mixture are acting independently and so they do not affect the toxicity of each other. In the IA, the total mixture effect is predicted based on the probabilities of response of the individual chemicals, i.e. the fractional responses of the individual chemicals are multiplied to obtain the joint effect. As IA is based on effects, a relevant difference with the CA model is that a mixture component used in a concentration below its NOEC will not contribute to the total effect of the mixture. The mathematical form is as follows:

$$E_{(c_{mix})} = 1 - \prod_{i=1}^n (1 - E_{(c_i)}) \quad (1)$$

Where, $E_{(c_i)}$ denotes the corresponding effects of the individual components and $E_{(c_{mix})}$ the total effect of the mixture. E are expressed as fractions (x %) of a maximum possible effect.

8.2 *Concentration Addition (CA):*

Contrary to the IA, the CA model assumes that the chemicals present in the mixture have the same MOAs i.e. they behave as if they are simple dilutions of one another. The joint effect of such kind of chemicals is therefore expected to be equal to the effect of the sum of the chemicals, taking into account the shape of the dose-effect curves of the individual chemicals. So that, even if all components are at a level below the toxicity threshold, the overall mixture would have toxicity due to the additivity effect. For a mixture of “n” components, the CA concept can be expressed as follows:

$$\frac{\sum_{i=1}^n d_i}{D_{x,mix}} = \frac{C_{mix}}{D_{x,mix}} = \sum_{i=1}^n \frac{d_i}{D_{x,i}} \quad (2)$$

where d_i is the dose for chemical “i” in the mixture, $D_{x,i}$ the concentration of the “i” component that causes “x” effect for a given endpoint when individually exposed, c_{mix} the total concentration of the mixture, and $D_{x,mix}$ the mixture concentration causing the same effect “x”. As $c_{mix} = D_{x,mix}$ the well-known form for CA arises:

$$\sum_{i=1}^n \frac{d_i}{D_{x,i}} = 1 \quad (3)$$

In some cases, a mixture effect can result in a departure from additivity; i.e. the toxicity of a mixture differs from that expected using the assumptions of concentration addition or independent action. In these cases, mixture components influence each other to result in the overall effect of the mixture. These interactions can be defined as “Synergism” or “more than additive” when the mixture effect is greater than expected or “Antagonism” or “less than additive” when the mixture effect is lesser than expected. For a deeper understanding of the most commonly models used to analyse mixture in ecotoxicology see Rodea-Palomares et al. (2015a).

These two basic models have been used, adapted, reviewed, and discussed during the twentieth century and discussion continues in the twenty-first century, both from theoretical and practical viewpoints (Berenbaum, 1985; Berenbaum, 1989; Chou, 2006; Chou and Talalay, 1984; Faust et al., 2003; Greco et al., 1995; Junghans et al., 2006). Both of them are extensively accepted although CA has been largely used in risk assessment probably due to its more conservative character being defined as the goal standard for additivity in ecotoxicology. In fact, this is the method recommended by the EU (EU Commission 2011) when the MOAs of the mixture chemicals are not known.

Several methods have been developed to analyze chemical mixtures based on CA. The most commonly methods used include: Toxic Units (TU), Toxic Equivalency Factors (TEFs) and the Hazard Index (HI) (Heys et al., 2016). Among them, TU approach is the most direct and commonly application of the CA model and it is extensively used in environment risk assessment. It represent the ratio between the concentration of a component in a mixture and its toxic endpoint definer such as the ED₅₀ (the dose at which a 50 % effect is exhibited when that chemical is individually used) converting the concentration of each compound into a TU scale. The overall TU of the mixture is calculated by the summation of the individuals TUs. The TU concept can be used to

quantify the toxicity of a mixture on the basis of its composition, e.g. based on the ED₅₀, if the TUs of a mixture is equal to 10, it means that a dilution of 10 % of the mixture would produce 50 % of a function or signal inhibition. Furthermore, if the toxic effect (e.g. the 50 % of signal inhibition) is observed when the sum of the TUs is equal to one, then the mixture toxicity is classified as strictly additive. If the effect is observed when the sum of TUs is greater than one, then the effect of the mixture is antagonistic or less than additive, and if it is observed when the sum of TUs is less than one, then the mixture has an synergistic effect or greater than additive (Norwood et al., 2003).

A *Loewe additivity* based method to study departures from additivity that require special attention is the Isobologram-Combination index (CI) developed by Chou and Talalay (1984). This method, originated in the field of pharmacology, is based on the median-effect principle (mass-action law) (Chou, 1976) that demonstrates that there is a univocal relationship between dose and effect independently of the number of substrates or products and of the mechanism of action or inhibition. This method involved plotting the dose-effect curves for each compound and their combinations in multiple diluted concentrations by using the median-effect equation:

$$\frac{fa}{fu} = \left(\frac{D}{D_m}\right)^m \quad (4)$$

Where D is the dose of a drug, fa is the fraction affected by D (i.e. percentage inhibition /100), fu is the unaffected fraction (therefore, $fu = 1 - fa$). D_m is the median-effect dose (ED₅₀) that inhibit the system under study by 50 %, and m is the slope of the dose-response curve which depicts the shape of the curve ($m = 1$, $m > 1$, and $m < 1$ indicate hyperbolic, sigmoidal, and negative sigmoidal dose-response curve, respectively). Therefore, the method takes into account both the potency (D_m) and shape (m) parameters. If Eq. (4) is rearranged, then:

$$D = D_m \cdot [fa/(1 - fa)]^{1/m} \quad (5)$$

The D_m and m values for each drug are easily determined by the median-effect plot: $x = \log(D)$ versus $y = \log(fa/fu)$ which is based on the logarithmic form of Equation (5). The conformity of the data to the median-effect principle can be readily manifested by the linear correlation coefficient (R) of the data to the logarithmic form of Equation (5). The median-effect equation for a single drug can be extended to multiple drugs. Based on this

general median-effect equation, Chou and Talalay (Chou and Talalay, 1983; Chou and Talalay, 1984) developed the Combination Index (CI) equation for the quantification of synergism or antagonism for n -drug combination at $x\%$ inhibition:

$${}^n(CI)_x = \sum_{j=1}^n \frac{(D)_j}{(D_x)_j} = \sum_{j=1}^n \frac{(D_x)_{1-n} \left\{ [D]_j / \sum_1^n [D] \right\}}{(D_m)_j \left\{ (f_{ax})_j / [1 - (f_{ax})_j] \right\}^{1/m_j}} \quad (6)$$

where ${}^n(CI)_x$ is the combination index for n drugs at $x\%$ inhibition; $(D_x)_{1-n}$ is the sum of the dose of n chemicals that exerts $x\%$ inhibition in combination, $[D]_j / \sum_1^n [D]$ is the proportionality of the dose of each of n chemicals that exerts $x\%$ inhibition in combination; and $(D_m)_j \{ (f_{ax})_j / [1 - (f_{ax})_j] \}^{1/m_j}$ is the dose of each drug alone that exerts $x\%$ inhibition. From Equation (6) $CI < 1$, $CI = 1$, and $CI > 1$ indicates synergism, additive effect, and antagonism, respectively. This method allows computerized quantitation of several parameters such as dose-effect curve parameters, CI values or fa -CI plots (plot representing CI versus fa , the fraction affected by a particular dose) through the software CompuSyn (Chou and Martin, 2005)(Combosyn Inc., Paramus, NJ, USA).

A schematic representation of a fa -CI plot can be seen below:

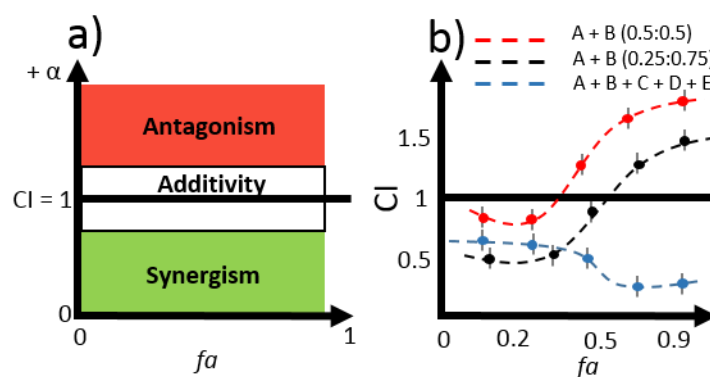


Fig. 4. a) Schematic representation of a fa -CI plot. fa -CI plot is an effect-oriented plot (see x -axis). The additivity line is $CI = 1$; $CI < 1$ indicates synergism and $CI > 1$ indicates antagonism. The type of combined effect between any combinations of compounds (from 2 to n) are shown for the entire range of fractional effect levels (from 0 to 1). **b)** schematic representation of three theoretical mixtures, in the same graphic, the effect-dependent type of interaction of compounds A + B can be visualized for the same mixture (A +

B) at two different mixture ratios (0.5:0.5) and (0.25:0.75). In addition, the effect-dependent interaction of a hypothetical complex mixture compound of (A+B+C+D+E) can be similarly visualized.

Different to the TU previous described, CI can be applied to the all effect levels (fa) simultaneously and it takes into account both the potency (Dm) and the shape (m) of the curve, which as reported by other authors is essential to increase the validity of the model used when studying mixtures interactions.

The CI method originated and extensively used in pharmacology, was first applied in ecotoxicology by our group (Gonzalez-Pleiter et al., 2013; Rodea-Palomares et al., 2010), to study the interactions of priority and emerging pollutants. Given the importance of heavy metals as priority pollutants, the first study was carried out to assess the individual and combined toxicity of heavy metals by the constitutively bioluminescent bioreporter, *Anabaena* CPB4347 (previously described, light-off bioreporter). The main conclusion of this study was to prove the suitability of the CI for toxicity assessment of metal interaction using this cyanobacterial bioreporter.

9 Current approach to study mixtures in inducible systems

The crucial prerequisite for the applicability of any additivity model is to fulfil certain mathematical assumptions (Scholze et al., 2014). As we have seen throughout the previous epigraphs, the basic mathematical feature of *Loewe additivity* is that the effect of mixture components could be formulated in terms of a common effective dose (ED).

This requisite is trivially met when all individual mixture components present identical maximal effect, as generally found in turn-off bioreporters output (**Figure 2a**). An important complication occurs with mixtures of chemicals that show differential maximal effects, which is likely to occur in turn-on bioreporters (**Figure 3a**). When this happens, additivity hypothesis can only be formulated up to the effect levels achieved by the less potent compound present in the mixture due to the inherent mathematical features of the additivity definition (Scholze et al., 2014). An additional challenge for formulating the additivity hypothesis occurs when the studied response is susceptible to result in non-monotonic dose-response curve (**Figure 2a**). For instance, in biphasic dose-response curves, two different concentrations can result in the same fractional effect, before and after the MPC. In fact, studies of inducible bioreporters that respond to mixtures have been focused on the induction part of the curve, neglecting the information that is obtained

from the signal inhibition part (Kong, 2014). These problems have hampered the applicability of additivity models in important areas where differential maximal effects and biphasic dose-response patterns are commonly observed. Thus, some authors have suggested the need for a formal mathematical expansion of the additivity formulation that may allow working with differential maximal effects (Belz et al., 2008; Ohlsson et al., 2010).

Until now, only few studies have focused on this fact. Scholze et al. (2014) highlighted the difficulty to assess mixture effect predictions when mixtures are composed of agonist substances. These authors proposed a pragmatic numerical approximation based on a TU method extrapolation to solve the problems of the differential maximal effects. This method consisted in extrapolating the dose-response curves of partial agonist to higher effects level beyond their levelling-off range, giving this compound a toxic unit fixed value between a minimum and a maximum toxic unit assumption. Although they found that the maximal toxic unit assumption predicted better the combination effects with the experimentally data, this method, as reported by the authors, continue to have some limitations, the most significant is the selection of an appropriate slope for extrapolating the dose-response curve. Furthermore, they do not deal with biphasic curves.

In the biphasic-dose response curves context, some approaches have been made in the hormesis field. Hormesis is a biphasic dose response phenomenon characterized by a low dose stimulation and a high dose inhibition. These phenomena have been widely described for a range of substances and in a range of organisms through the literature (Calabrese and Blain, 2011). Belt et al. (2008) proposed a modified CA model based on two separate modules, where the maximum stimulatory response is predicted using a linear model and the inhibitory part (below 100%) is predicted using the standard CA model. The linearity model well described the data while mostly no interaction occurred between the compounds; however, significant deviation of this model was observed when mixtures compounds interact at dose level. An extension of the linearity model has been recently made (Belz and Piepho, 2017) to overcome this limitation. Although this new approach seems to improve the prediction in these cases, as reported by the authors, future research is necessary to prove the relevance of the model proposed.

To our knowledge, no mixture-effect prediction models have been proposed in the inducible bioreporter output-like biphasic dose-response context. Only Kong (2014)

performed the evaluation of effects of binary inducers mixtures using a bioluminescent inducible bioreporter throughout a simply mathematical model based on the theory of probabilities (IA based-approach), however, this study was not based on effective doses which may result in deviations when applying the definition of additivity. On the other hand, no biphasic dose-response curves study was performed.

Hence, the development of a mathematical model that allows predicting the effects of mixtures within the biphasic dose-response framework and when different maximum effects occur is of great interest for a wide range of applications.

10 Other potential applications of the heavy metals bioreporters

As described before, the properties of heavy metals have been used in the field of nanotechnology and specifically in developing of nanomaterials (NMs), which has been growing since the last years. Several NMs such a nanoscale Ag, metal oxides such as CuO, ZnO and TiO₂, Fe⁰ and chitosan-based nanocomposites are already widely used due to their biocidal properties (Ivask et al., 2012; Li et al., 2008). We find these materials, especially Ag-based NMs, in products such as wound dressings, textiles, air filters, care products, baby products, water disinfection technologies and microbial control. Due to their toxic properties, metal-containing NMs are good candidates for novel antimicrobial consumer and patent-care products. In this context, Metal Organic Frameworks (MOFs) are one of the latest developments in nanotechnology (Ferey, 2008; McKinlay et al., 2010). These are porous inorganic-organic hybrid materials constructed by crystallization through joining metal-containing units with multifunctional organic ligands. Different from others metal-based materials, MOFs are constructed directly with the desired metal linked by covalent bonds. Thus, the structures of MOFs can be designed at the atomic scale by an appropriate choice of metal and organic ligand, which will define their antimicrobial activity. Given this structure, the main advantage of MOFs versus nanoparticles or other metal-containing materials is the more controlled release of metal ions.

Recently, the use of some MOFs as biocidal material in water treatment and biomedical applications have been evaluated. In most cases, these MOFs have been tested towards heterotrophic organisms such as *Pseudomonas putida*, *E. coli*, *S. cerevisiae*, or *Staphylococcus aureus* and to the marine bacterium *Cobetia marina* (Aguado et al., 2014;

Arpa Sancet et al., 2013; Wang et al., 2015; Wojciechowska et al., 2012; Zhuang et al., 2012). However, until now, nothing is known about the applications of MOFs to photosynthetic organisms such as cyanobacteria or algae.

On the other hand, the study of the antimicrobial mechanism of nanomaterials has been of great interest to the scientific community. As reported by Ivask et al. (2012), it is of utmost importance to understand the key mechanisms of action of already applied or potential antimicrobial compounds *prior* to their large-scale application. As highlighted by these authors, the early studies on metal-containing nanomaterials did not explain the mechanisms of action of these materials and only after 2007 major efforts have been made to link the toxicological and antimicrobial potency of NMs to their physicochemical properties. Among these physicochemical properties, metal ion dissolution from the metal-containing materials may be considered as one of the most important key factors in their toxicity.

Several methods have been proposed to study the effect of metal ion released from the NMs. One of the most used is the complexation of the free ions through adding chelating compounds such as sulphur-containing molecules (cysteine), sulphides anions (SO_4^{2-} , S^{2-}) or EDTA (ethylenediaminetetraacetic acid). However, this method only offers a qualitative proof of the presence of dissolved ions, since the addition of a chelator may not result in a decrease of the toxicity exhibited by the NM. Moreover, greater than the amount of the total metal dissolved the speciation of these dissolved metal ions is important in determining the origin of toxicity since not all metal complexes formed in aqueous systems are equally toxic. As reported by a myriad of articles, the free-ion metal is the most available and, therefore, toxic form of the metals.

Speciation chemical models such as WHAM (Windermere Humic Aqueous Model) or Visual Minteq can be very useful in determining the potential toxicity of metallic nanomaterials, however, their use so far has not been widespread in the field of nano-safety. Additionally, in recent years, the use of bioreporters of heavy metals has been proposed to directly determine the bioavailable metals released from NMs (Ivask et al., 2012; Kahru et al., 2008) and few studies have employed this novel approach (Kahru et al., 2008). The combination of both chemical speciation methods and the specific heavy metals bioreporters can give a very complete idea about the origin of the toxicity of the

metallic nanomaterials and serve as an analytical tool of the mechanics of action of these materials.

11 Preservation methods

As highlighted previously, the ability of the microorganisms to sense their environment surrounding can be used to measure the bioavailability and/or toxicity of the pollutants. As described before, there are a number of bioreporters capable of sensing global toxicity or detecting a specific analyte in a sample. One of the most important things to employ these systems is to maintain their viability and sensitivity along time and as the ultimate goal to develop an autonomous cell-device or biosensor. In the strict sense, a biosensor is an analytical device, where the biological sensing element and the transducer of the signal are directly in contact. However, since the immobilization of cells is, in most cases, a fundamental requirement for the further development of the biosensor, it is very common that in the literature immobilized bioreporters are also designated as biosensors. This broader definition of biosensor is the one we are going to use in this section. If the biosensor is also attached to the transducer, it will be specified.

To keep cells viable and active is a non-trivial issue, since most bioreporters are developed in rapidly growing species such as *E. coli*. The most used way to keep a bioreporter active and ready to be used in environmental assessment is through continuous cultivation (Bjerketorp et al., 2006; Roggo and van der Meer, 2017). Although this technique allows to keep the bioreporters active and fresh, it displays a great number of inconveniences. First, it is very laborious and time-consuming; it needs someone to take care of renewing the cultures and keeping them in the best metabolic state for their later use. On the other hand, with the continuous cultivation, organisms are at risk of genetic mutations or contamination with other microorganisms. Despite these drawbacks, several authors have successfully developed systems for continuous or semi-continuous toxicity monitoring using fresh recombinant *E. coli* cells (Gu et al., 1999; Kim and Gu, 2005; van der Meer, 2016) However, techniques to keep these microorganisms along time without the need to be continually cultivating them brings many advantages in the development of whole-cell devices or biosensors. In fact, it has been the main limitation in the use of biosensors for environmental monitoring.

Improved methods for maintaining bioreporters cells in an active physiological state have been described (Bjerketorp et al., 2006; Roggo and van der Meer, 2017). One of the most used is immobilization. The main immobilization strategy include organic (e.g. hydrogels such agar) and inorganic (e.g. sol-gel) encapsulation. Although encapsulation in these polymers confers physical shielding, isolation and allows solute diffusion, it is very difficult to maintain the stability of the immobilized organisms due to cellular growth (Jouanneau et al., 2015; Michelini and Roda, 2012). In addition, encapsulation in organic polymers may hamper optical signal detection because of opacity (Bjerketorp et al., 2006; Michelini and Roda, 2012) when using optical bioreporters. The other method most used is freeze-drying or lyophilisation. Freeze-drying of cultures is a process that removes water from frozen cultures by sublimation under reduced pressure giving rise to a structurally intact and easily reconstituted end product. In this strategy the bioreporter cells are first cultured, washed and pre-treated with cryoprotecting agents, aliquoted and freeze-dried, and then kept under specific storage conditions to optimally retain cellular survival and activity. The assay is started by rehydrating the dried bioreporters to revival the cells, which are subsequently incubated during the time required to produce the reporter signal. Different from immobilization, if the freeze-dried cells are protected from humidity, they can be stored for a long period without changes (Jouanneau et al., 2015). These advantages make freeze-drying the most used industrial standard method for preserving microbes.

There are several commercially freeze-dried toxicity kits based on naturally bioluminescent bacteria commercially available commonly used to assess the toxicity of water samples, for instance, Microtox based on *A. fischeri* (Johnson, 2005) or ToxScreen test with *Photobacterium leiognathi* (Ulitzur et al., 2002). Both strains correspond to naturally luminescent marine bacteria widely used in environmental assessment to evaluate heavy metals, organic compounds, mixtures of pollutants, etc. However, a number of drawbacks have been described when measuring turbid or highly coloured solutions. In addition, these marine bacteria operate at salt concentrations of around 2%, which limits the solubility of some compounds and can alter heavy metal speciation (Deheyn et al., 2004; Newman and McCloskey, 1996). These problems raise the question of the ecological relevance of this bioassay and thus, many researchers doubt that the use of these bioluminescent marine organisms is justified for toxicity tests in continental environments (freshwater and soil).

On the other hand, the freeze-dried method has also successfully demonstrated to maintain bioreporters cells in the optimal state for environmental monitoring. Most of them are based on *E. coli* (Choi and Gu, 2002; Gu et al., 2001; Jouanneau et al., 2011) but also in widespread microorganisms like *Pseudomonas*, from which bioluminescent strains have been used, mostly for soil ecotoxicity assessment (de las Heras and de Lorenzo, 2011; Ko and Kong, 2017). However, biosensors based on freshwater ecologically relevant organisms are still lacking. Cyanobacteria that live in marine and fresh water could offer a solution for the construction of novel biosensors.

Wild-type cyanobacteria were among the first organisms to be used for developing whole-cell biosensors for environmental monitoring (Brayner et al., 2011). The first cyanobacteria biosensors were based on the sensitivity of these organisms to heavy metals and herbicides that inhibit the photosynthetic activity. Rawson et al. (1989) developed an amperometric biosensor, based on *Synechococcus* using alginate as an immobilization matrix. Although the biosensor was able to detect a wide range of herbicides with sites of action on the photosynthetic electron transport chain, the self-life of the biosensor was up to 7 days and there was a decrease in the sensitivity of the biosensor with respect to fresh cells due to the matrix barrier. Croisetiére et al. (2001) also developed an electrochemical devices based on a cyanobacteria but it was not enough sensitive. Some authors have immobilized *Anabaena* in poli (2-hydroxyethyl methacrylate) (pHEMA), a type of synthetic hydrophilic polymer that can retain up to 70% of water (w/w), membranes for detecting heavy metals (Tay et al., 2003; Tay et al., 2009) using an electrochemical transducer. Response was measured in the form of inhibition of photosynthetic activity of the immobilized cyanobacteria through assessment of oxygen concentration changes. In both case, the cyanobacteria showed high sensitivity to heavy metals. In addition, Shing et al. (2013) developed a whole-cell fluorescence biosensor of *Anabaena torulosa* entrapped on a cellulose membrane for heavy metals and pesticides detection. Later, the method was improved adding a layer of pHEMA. As reported by these authors, the use of pHEMA increased the reproducibility and storage stability. However, a gradual reduction of the biosensor response was observed after 25 days of storage. In addition, although the biosensor was enough sensitive, the use of pHEMA increased the limit of detection compared with the immobilization without pHEMA.

Schreiter et al. (2001) and Mbeunkui et al. (2002) have developed two immobilized bioluminescent cyanobacterial bioreporter strains for nutrients monitoring in aquatic ecosystems denominated CyanoSensors. Both CyanoSensors were successfully immobilized in 24-well plates using agar as a matrix. However, as in the cases before, the stability along time is very limited, remaining stable up to only one month of storage.

The long-term maintenance of both viability and stability of the cyanobacteria bioreporters is the main limitation in the generalized use of these as biosensors for environmental monitoring. The improvement of these ecologically relevant biosensors would bring many advantages in environmental monitoring, especially in aquatic systems.

References

- Aguado, S., Quirós, J., Canivet, J., Farrusseng, D., Boltes, K., Rosal, R., 2014. Antimicrobial activity of cobalt imidazolate metal–organic frameworks. *Chemosphere*. 113, 188-192.
- Allen, H.E., Hansen, D.J., 1996. The Importance of Trace Metal Speciation to Water Quality Criteria. *Water Environment Research*. 68, 42-54.
- Amaro, F., Turkewitz, A.P., Martin-Gonzalez, A., Gutierrez, J.C., 2011. Whole-cell biosensors for detection of heavy metal ions in environmental samples based on metallothionein promoters from *Tetrahymena thermophila*. *Microb Biotechnol*. 4, 513-522.
- Amaro, F., Turkewitz, A.P., Martin-Gonzalez, A., Gutierrez, J.C., 2014. Functional GFP-metallothionein fusion protein from *Tetrahymena thermophila*: a potential whole-cell biosensor for monitoring heavy metal pollution and a cell model to study metallothionein overproduction effects. *Biometals*. 27, 195-205.
- Andrews, S.C., Robinson, A.K., Rodriguez-Quinones, F., 2003. Bacterial iron homeostasis. *FEMS Microbiol Rev*. 27, 215-237.
- Arpa Sancet, M.P., Hanke, M., Wang, Z., Bauer, S., Azucena, C., Arslan, H.K., et al., 2013. Surface anchored metal-organic frameworks as stimulus responsive antifouling coatings. *Biointerphases*. 8, 29.
- Australian. and New Zealand Environment and Conservation Council and Agriculture and Resource Management Council of Australia and New Zealand. 2000. *Australian and New Zealand Guidelines for Fresh and Marine Water Quality*, Vol 2: Aquatic Ecosystems—Rationale and Background Information. Australian Water Association, Artarmon, New South Wales, Australia; and the New Zealand Water & Wastes Association.
- Bachmann, T., 2003. Transforming cyanobacteria into bioreporters of biological relevance. *Trends Biotechnol*. 21, 247-249.
- Barran-Berdon, A.L., Rodea-Palomares, I., Leganes, F., Fernandez-Pinas, F., 2011. Free Ca²⁺ as an early intracellular biomarker of exposure of cyanobacteria to environmental pollution. *Anal Bioanal Chem*. 400, 1015-1029.
- Beard, S.J., Hashim, R., Membrillo-Hernandez, J., Hughes, M.N., Poole, R.K., 1997. Zinc(II) tolerance in *Escherichia coli* K-12: evidence that the *zntA* gene (*o732*) encodes a cation transport ATPase. *Mol Microbiol*. 25, 883-891.
- Belkin, S., 2003. Microbial whole-cell sensing systems of environmental pollutants. *Current Opinion in Microbiology*. 6, 206-212.
- Belz, R.G., Cedergreen, N., Sørensen, H., 2008. Hormesis in mixtures — Can it be predicted? *Science of The Total Environment*. 404, 77-87.
- Belz, R.G., Piepho, H.-P., 2017. Predicting biphasic responses in binary mixtures: Pelargonic acid versus glyphosate. *Chemosphere*. 178, 88-98.
- Berenbaum, M.C., 1985. The expected effect of a combination of agents: the general solution. *J Theor Biol*. 114, 413-431.
- Berenbaum, M.C., 1989. What is synergy? *Pharmacol Rev*. 41, 93-141.
- Bergman, B., Ran, L., Adams, D.G. Cyanobacterial-plant Symbioses: Signaling and Development. In *The Cyanobacteria: Molecular Biology, Genomics And Evolution*. Norfolk, U.K.: Caister Academic Press, 2008.
- Bjerketorp, J., Hakansson, S., Belkin, S., Jansson, J.K., 2006. Advances in preservation methods: keeping biosensor microorganisms alive and active. *Curr Opin Biotechnol*. 17, 43-49.
- Blindauer, C.A., 2011. Bacterial metallothioneins: past, present, and questions for the future. *JBIC Journal of Biological Inorganic Chemistry*. 16, 1011-1024.
- Blindauer, C.A., Leszczyszyn, O.I., 2010. Metallothioneins: unparalleled diversity in structures and functions for metal ion homeostasis and more. *Nat Prod Rep*. 27, 720-741.
- Bliss, C.I., 1939. THE TOXICITY OF POISONS APPLIED JOINTLY1. *Annals of Applied Biology*. 26, 585-615.
- Borremans, B., Hobman, J.L., Provoost, A., Brown, N.L., van Der Lelie, D., 2001. Cloning and functional analysis of the *pbr* lead resistance determinant of *Ralstonia metallidurans* CH34. *J Bacteriol*. 183, 5651-5658.
- Boyanapalli, R., Bullerjahn, G.S., Pohl, C., Croot, P.L., Boyd, P.W., McKay, R.M., 2007. Luminescent whole-cell cyanobacterial bioreporter for measuring Fe availability in diverse marine environments. *Appl Environ Microbiol*. 73, 1019-1024.
- Brayner, R., Coute, A., Livage, J., Perrette, C., Sicard, C., 2011. Micro-algal biosensors. *Anal Bioanal Chem*. 401, 581-597.

- Brown, N.L., Stoyanov, J.V., Kidd, S.P., Hobman, J.L., 2003. The MerR family of transcriptional regulators. *FEMS Microbiology Reviews*. 27, 145-163.
- Bruins, M.R., Kapil, S., Oehme, F.W., 2000. Microbial resistance to metals in the environment. *Ecotoxicol Environ Saf*. 45, 198-207.
- Bullerjahn, G.S., Boyanapalli, R., Rozmarynowycz, M.J., McKay, R.M., 2010. Cyanobacterial bioreporters as sensors of nutrient availability. *Adv Biochem Eng Biotechnol*. 118, 165-188.
- Busenlehner, L.S., Pennella, M.A., Giedroc, D.P., 2003. The SmtB/ArsR family of metalloregulatory transcriptional repressors: structural insights into prokaryotic metal resistance. *FEMS Microbiology Reviews*. 27, 131-143.
- Calabrese, E.J., 2008. Hormesis: why it is important to toxicology and toxicologists. *Environ Toxicol Chem*. 27, 1451-1474.
- Calabrese, E.J., Blain, R.B., 2011. The hormesis database: the occurrence of hormetic dose responses in the toxicological literature. *Regul Toxicol Pharmacol*. 61, 73-81.
- Campbell, P. Interactions between trace metals and aquatic organisms: A critique of the free-ion activity model. Vol Metal Speciation and Bioavailability in Aquatic Systems. New York, NY, USA, 1995.
- Casteel, S.W., Weis, C.P., Henningsen, G.M., Brattin, W.J., 2006. Estimation of relative bioavailability of lead in soil and soil-like materials using young Swine. *Environ Health Perspect*. 114, 1162-1171.
- Corbisier, P., van der Lelie, D., Borremans, B., Provoost, A., de Lorenzo, V., Brown, N.L., et al., 1999. Whole cell- and protein-based biosensors for the detection of bioavailable heavy metals in environmental samples. *Analytica Chimica Acta*. 387, 235-244.
- Croisetière, L., Rouillon, R., Carpentier, R., 2001. A simple mediatorless amperometric method using the cyanobacterium *Synechococcus leopoliensis* for the detection of phytotoxic pollutants. *Applied Microbiology and Biotechnology*. 56, 261-264.
- Charrier, T., Durand, M.J., Jouanneau, S., Dion, M., Perneti, M., Poncelet, D., et al., 2011. A multi-channel bioluminescent bacterial biosensor for the on-line detection of metals and toxicity. Part I: design and optimization of bioluminescent bacterial strains. *Anal Bioanal Chem*. 400, 1051-1060.
- Choi, S.H., Gu, M.B., 2002. A portable toxicity biosensor using freeze-dried recombinant bioluminescent bacteria. *Biosensors and Bioelectronics*. 17, 433-440.
- Chojnacka, K., Chojnacki, A., Górecka, H., Górecki, H., 2005. Bioavailability of heavy metals from polluted soils to plants. *Science of The Total Environment*. 337, 175-182.
- Chou, T.-C., 1976. Derivation and properties of Michaelis-Menten type and Hill type equations for reference ligands. *Journal of Theoretical Biology*. 59, 253-276.
- Chou, T.-C., Talalay, P., 1983. Analysis of combined drug effects: a new look at a very old problem. *Trends in Pharmacological Sciences*. 4, 450-454.
- Chou, T.C., 2006. Theoretical basis, experimental design, and computerized simulation of synergism and antagonism in drug combination studies. *Pharmacol Rev*. 58, 621-681.
- Chou, T.C., Martin, N., 2005. *Compusyn for Drug Combinations: PC Software and User's Guide: A Computer Program for Quantification of Synergism and Antagonism in Drug Combinations and the Determination of ic50 and ed50 and ld50 Values*. ComboSyn, Inc.: Paramus, NJ, USA.
- Chou, T.C., Talalay, P., 1984. Quantitative analysis of dose-effect relationships: the combined effects of multiple drugs or enzyme inhibitors. *Adv Enzyme Regul*. 22, 27-55.
- Darling, C.T.R., Thomas, V.G., 2005. Lead bioaccumulation in earthworms, *Lumbricus terrestris*, from exposure to lead compounds of differing solubility. *Science of The Total Environment*. 346, 70-80.
- Daunert, S., Barrett, G., Feliciano, J.S., Shetty, R.S., Shrestha, S., Smith-Spencer, W., 2000. Genetically engineered whole-cell sensing systems: coupling biological recognition with reporter genes. *Chem Rev*. 100, 2705-2738.
- Dayton, E.A., Basta, N.T., Payton, M.E., Bradham, K.D., Schroder, J.L., Lanno, R.P., 2006. Evaluating the contribution of soil properties to modifying lead phytoavailability and phytotoxicity. *Environ Toxicol Chem*. 25, 719-725.
- de las Heras, A., de Lorenzo, V., 2011. In situ detection of aromatic compounds with biosensor *Pseudomonas putida* cells preserved and delivered to soil in water-soluble gelatin capsules. *Anal Bioanal Chem*. 400, 1093-1104.
- Deheyn, D.D., Bencheikh-Latmani, R., Latz, M.I., 2004. Chemical speciation and toxicity of metals assessed by three bioluminescence-based assays using marine organisms. *Environ Toxicol*. 19, 161-178.
- Delany, I., Rappuoli, R., Scarlato, V., 2004. Fur functions as an activator and as a repressor of putative virulence genes in *Neisseria meningitidis*. *Mol Microbiol*. 52, 1081-1090.
- Demple, B., 1996. Redox signaling and gene control in the *Escherichia coli* soxRS oxidative stress regulon - a review. *Gene*. 179, 53-57.

- DeRuyter, Y.S., Fromme, P. Molecular Structure of the Photosynthetic Apparatus. In *The Cyanobacteria: Molecular Biology, Genomics And Evolution*. Norfolk, U.K.: Caister Academic Press, 2008.
- Di Toro, D.M., Allen, H.E., Bergman, H.L., Meyer, J.S., Paquin, P.R., Santore, R.C., 2001. Biotic ligand model of the acute toxicity of metals. 1. Technical basis. *Environ Toxicol Chem.* 20, 2383-2396.
- Dodds, W.K., 2006. Eutrophication and trophic state in rivers and streams. *Limnology and Oceanography.* 51, 671-680.
- Duran, N., Duran, M., de Jesus, M.B., Seabra, A.B., Favaro, W.J., Nakazato, G., 2016. Silver nanoparticles: A new view on mechanistic aspects on antimicrobial activity. *Nanomedicine.* 12, 789-799.
- Durham, K.A., Porta, D., Twiss, M.R., McKay, R.M., Bullerjahn, G.S., 2002. Construction and initial characterization of a luminescent *Synechococcus* sp. PCC 7942 Fe-dependent bioreporter. *FEMS Microbiol Lett.* 209, 215-221.
- EC/2000/60. Directive 2000/60/EC of the European Parliament and of the Council of 23 October 2000 establishing a framework for Community action in the field of water policy.
- EC/2006/1907. Regulation (EC) No 1907/2006 of the European Parliament and of the Council of 18 December 2006 concerning the Registration, Evaluation, Authorisation and Restriction of Chemicals (REACH).
- EC/2008/105. Directive 2008/105/EC of the European Parliament and of the Council of 16 December 2008 on environmental quality standards in the field of water policy, amending and subsequently repealing Council Directives 82/176/EEC, 83/513/EEC, 84/156/EEC, 84/491/EEC, 86/280/EEC and amending Directive 2000/60/EC of the European Parliament and of the Council.
- EC/2008/1272. Regulation (EC) No 1272/2008 of 16 December 2008 on classification, labelling and packaging of substances and mixtures, amending and repealing Directives 67/548/EEC and 1999/45/EC, and amending Regulation (EC) No 1907/2006.
- EC/2011. Toxicity and assessment of chemical mixtures. Scientific Committee on Health and Environmental Risk, Scientific Committee on Emerging and Newly Identified Health Risks, and Scientific Committee on Consumer Safety. Directorate-General for Health and Consumers.
- Erbe, J.L., Adams, A.C., Taylor, K.B., Hall, L.M., 1996. Cyanobacteria carrying an *smt-lux* transcriptional fusion as biosensors for the detection of heavy metal cations. *J Ind Microbiol.* 17, 80-83.
- Faust, M., Altenburger, R., Backhaus, T., Blanck, H., Boedeker, W., Gramatica, P., et al., 2003. Joint algal toxicity of 16 dissimilarly acting chemicals is predictable by the concept of independent action. *Aquat Toxicol.* 63, 43-63.
- Feliciano, J., Liu, Y., Daunert, S., 2006. Novel reporter gene in a fluorescent-based whole cell sensing system. *Biotechnol Bioeng.* 93, 989-997.
- Ferey, G., 2008. Hybrid porous solids: past, present, future. *Chem Soc Rev.* 37, 191-214.
- Fernandez-Lopez, R., Ruiz, R., de la Cruz, F., Moncalian, G., 2015. Transcription factor-based biosensors enlightened by the analyte. *Front Microbiol.* 6, 648.
- Fernandez-Pinas, F., Leganes, F., Wolk, C.P., 2000. Bacterial lux genes as reporters in cyanobacteria. *Methods Enzymol.* 305, 513-527.
- Fernandez-Pinas, F., Wolk, C.P., 1994. Expression of luxCD-E in *Anabaena* sp. can replace the use of exogenous aldehyde for in vivo localization of transcription by luxAB. *Gene.* 150, 169-174.
- Fernandez-Piñas, F., Mateo, P., Bonilla, I., 1991. Binding of cadmium by cyanobacterial growth media: Free ion concentration as a toxicity index to the cyanobacterium *Nostoc* UAM 208. *Archives of Environmental Contamination and Toxicology.* 21, 425-431.
- Flores, E., Herrero, A., 2010. Compartmentalized function through cell differentiation in filamentous cyanobacteria. *Nat Rev Microbiol.* 8, 39-50.
- Fowler, B.A., Hildebrand, C.E., Kojima, Y., Webb, M., 1987. Nomenclature of metallothionein. *Experientia Suppl.* 52, 19-22.
- Fujimoto, H., Wakabayashi, M., Yamashiro, H., Maeda, I., Isoda, K., Kondoh, M., et al., 2006. Whole-cell arsenite biosensor using photosynthetic bacterium *Rhodovulum sulfidophilum*. *Applied Microbiology and Biotechnology.* 73, 332-338.
- Garcia-Pichel, F., Wojciechowski, M.F., 2009. The evolution of a capacity to build supra-cellular ropes enabled filamentous cyanobacteria to colonize highly erodible substrates. *PLoS One.* 4, e7801.
- Godsey, M.H., Baranova, N.N., Neyfakh, A.A., Brennan, R.G., 2001. Crystal structure of MtaN, a global multidrug transporter gene activator. *J Biol Chem.* 276, 47178-47184.
- Gonzalez-Pleiter, M., Gonzalo, S., Rodea-Palomares, I., Leganes, F., Rosal, R., Boltes, K., et al., 2013. Toxicity of five antibiotics and their mixtures towards photosynthetic aquatic organisms: implications for environmental risk assessment. *Water Res.* 47, 2050-2064.
- Greco, W.R., Bravo, G., Parsons, J.C., 1995. The search for synergy: a critical review from a response surface perspective. *Pharmacol Rev.* 47, 331-385.

- Greer, L.F., 3rd, Szalay, A.A., 2002. Imaging of light emission from the expression of luciferases in living cells and organisms: a review. *Luminescence*. 17, 43-74.
- Griffiths, M.W., 2000. How novel methods can help discover more information about foodborne pathogens. *Can J Infect Dis*. 11, 142-153.
- Gu, M.B., Choi, S.H., Kim, S.W., 2001. Some observations in freeze-drying of recombinant bioluminescent *Escherichia coli* for toxicity monitoring. *J Biotechnol*. 88, 95-105.
- Gu, M.B., Gil, G.C., Kim, J.H., 1999. A two-stage minibioreactor system for continuous toxicity monitoring. *Biosensors and Bioelectronics*. 14, 355-361.
- Guan, G., Pinochet-Barros, A., Gaballa, A., Patel, S.J., Argüello, J.M., Helmann, J.D., 2015. PfeT, a P(1B4)-type ATPase, effluxes ferrous iron and protects *Bacillus subtilis* against iron intoxication. *Molecular microbiology*. 98, 787-803.
- Gutierrez, J.C., Amaro, F., Martin-Gonzalez, A., 2015. Heavy metal whole-cell biosensors using eukaryotic microorganisms: an updated critical review. *Front Microbiol*. 6, 48.
- Hakkila, K., Green, T., Leskinen, P., Ivask, A., Marks, R., Virta, M., 2004. Detection of bioavailable heavy metals in EILATox-Oregon samples using whole-cell luminescent bacterial sensors in suspension or immobilized onto fibre-optic tips. *J Appl Toxicol*. 24, 333-342.
- Hantke, K., 2001. Bacterial zinc transporters and regulators. *Biometals*. 14, 239-249.
- Harms, H., Wells, M.C., van der Meer, J.R., 2006. Whole-cell living biosensors--are they ready for environmental application? *Appl Microbiol Biotechnol*. 70, 273-280.
- Harvie, D.R., Andreini, C., Cavallaro, G., Meng, W., Connolly, B.A., Yoshida, K., et al., 2006. Predicting metals sensed by ArsR-SmtB repressors: allosteric interference by a non-effector metal. *Mol Microbiol*. 59, 1341-1356.
- Hecker, M., Newsted, J.L., Murphy, M.B., Higley, E.B., Jones, P.D., Wu, R., et al., 2006. Human adrenocarcinoma (H295R) cells for rapid in vitro determination of effects on steroidogenesis: hormone production. *Toxicol Appl Pharmacol*. 217, 114-124.
- Helaluddin, A.B.M., Khalid, R.S., Alaama, M., Abbas, S.A., 2016. Main Analytical Techniques Used for Elemental Analysis in Various Matrices. *Tropical Journal of Pharmaceutical Research*. 15, 427.
- Heldwein, E.E., Brennan, R.G., 2001. Crystal structure of the transcription activator BmrR bound to DNA and a drug. *Nature*. 409, 378-382.
- Heys, K.A., Shore, R.F., Pereira, M.G., Jones, K.C., Martin, F.L., 2016. Risk assessment of environmental mixture effects. *RSC Adv*. 6, 47844-47857.
- Higgins, K.A., Giedroc, D., 2014. Insights into Protein Allostery in the CsoR/RcnR Family of Transcriptional Repressors. *Chem Lett*. 43, 20-25.
- Hobman, J.L., Wilkie, J., Brown, N.L., 2005. A design for life: prokaryotic metal-binding MerR family regulators. *Biometals*. 18, 429-436.
- Hoiczky, E., Hansel, A., 2000. Cyanobacterial Cell Walls: News from an Unusual Prokaryotic Envelope. *Journal of Bacteriology*. 182, 1191-1199.
- Huang, X., Shin, J.-H., Pinochet-Barros, A., Su, T.T., Helmann, J.D., 2017. *Bacillus subtilis* MntR coordinates the transcriptional regulation of manganese uptake and efflux systems. *Molecular Microbiology*. 103, 253-268.
- Huckle, J.W., Morby, A.P., Turner, J.S., Robinson, N.J., 1993. Isolation of a prokaryotic metallothionein locus and analysis of transcriptional control by trace metal ions. *Mol Microbiol*. 7, 177-187.
- Intawongse, M., Dean, J.R., 2006. Uptake of heavy metals by vegetable plants grown on contaminated soil and their bioavailability in the human gastrointestinal tract. *Food Addit Contam*. 23, 36-48.
- Ivask, A., George, S., Bondarenko, O., Kahru, A. 2012. Metal-Containing Nano-Antimicrobials: Differentiating the Impact of Solubilized Metals and Particles. In: Cioffi N, Rai M, editors. *Nano-Antimicrobials: Progress and Prospects*. Springer Berlin Heidelberg, Berlin, Heidelberg, 253-290.
- Ivask, A., Virta, M., Kahru, A., 2002. Construction and use of specific luminescent recombinant bacterial sensors for the assessment of bioavailable fraction of cadmium, zinc, mercury and chromium in the soil. *Soil Biology and Biochemistry*. 34, 1439-1447.
- Iwig, J.S., Leitch, S., Herbst, R.W., Maroney, M.J., Chivers, P.T., 2008. Ni(II) and Co(II) sensing by *Escherichia coli* RcnR. *J Am Chem Soc*. 130, 7592-7606.
- Iwig, J.S., Rowe, J.L., Chivers, P.T., 2006. Nickel homeostasis in *Escherichia coli* - the rcnR-rcnA efflux pathway and its linkage to NikR function. *Mol Microbiol*. 62, 252-262.
- Jarque, S., Bittner, M., Blaha, L., Hilscherova, K., 2016. Yeast Biosensors for Detection of Environmental Pollutants: Current State and Limitations. *Trends Biotechnol*. 34, 408-419.
- Johnson, B.T. 2005. Microtox® Acute Toxicity Test. In: Blaise C, Féraud J-F, editors. *Small-scale Freshwater Toxicity Investigations: Toxicity Test Methods*. Springer Netherlands, Dordrecht, 69-105.

- Jouanneau, S., Durand, M.J., Courcoux, P., Blusseau, T., Thouand, G., 2011. Improvement of the identification of four heavy metals in environmental samples by using predictive decision tree models coupled with a set of five bioluminescent bacteria. *Environ Sci Technol.* 45, 2925-2931.
- Jouanneau, S., Durand, M.J., Lahmar, A., Thouand, G., 2015. Main Technological Advancements in Bacterial Bioluminescent Biosensors Over the Last Two Decades. *Adv Biochem Eng Biotechnol.*
- Junghans, M., Backhaus, T., Faust, M., Scholze, M., Grimme, L.H., 2006. Application and validation of approaches for the predictive hazard assessment of realistic pesticide mixtures. *Aquat Toxicol.* 76, 93-110.
- Kabata-Pendias, A., Pendias, H. Trace elements in soils and plants. Boca Raton, Florida: CRC Press, 2001.
- Kahru, A., Dubourguier, H.C., Blinova, I., Ivask, A., Kasemets, K., 2008. Biotests and Biosensors for Ecotoxicology of Metal Oxide Nanoparticles: A Minireview. *Sensors (Basel).* 8, 5153-5170.
- Kim, B.C., Gu, M.B., 2005. A Multi-Channel Continuous Water Toxicity Monitoring System: Its Evaluation and Application to Water Discharged from a Power Plant. *Environmental Monitoring and Assessment.* 109, 123-133.
- Knight, M.R., Campbell, A.K., Smith, S.M., Trewavas, A.J., 1991. Transgenic plant aequorin reports the effects of touch and cold-shock and elicitors on cytoplasmic calcium. *Nature.* 352, 524-526.
- Knoll, A.H. Cyanobacteria and Earth History In *The Cyanobacteria: Molecular Biology, Genomics And Evolution.* Norfolk, U.K.,: Caister Academic Press, 2008.
- Ko, K.S., Kong, I.C., 2017. Application of the freeze-dried bioluminescent bioreporter *Pseudomonas putida* mt-2 KG1206 to the biomonitoring of groundwater samples from monitoring wells near gasoline leakage sites. *Appl Microbiol Biotechnol.* 101, 1709-1716.
- Kohler, S., Belkin, S., Schmid, R.D., 2000. Reporter gene bioassays in environmental analysis. *Fresenius J Anal Chem.* 366, 769-779.
- Kolaj-Robin, O., Russell, D., Hayes, K.A., Pembroke, J.T., Soulimane, T., 2015. Cation Diffusion Facilitator family: Structure and function. *FEBS Lett.* 589, 1283-1295.
- Komárek, J., 2016. A polyphasic approach for the taxonomy of cyanobacteria: principles and applications. *European Journal of Phycology.* 51, 346-353.
- Kong, I.C., 2014. Effects of binary mixtures of inducers (toluene analogs) and of metals on bioluminescence induction of a recombinant bioreporter strain. *Sensors (Basel).* 14, 18993-19006.
- Kortenkamp, A., Backhaus, T., Faust, M., 2009. *State of the Art Report on Mixture Toxicity.* European Commission: Brussels, Belgium.
- Kudla, J., Batistic, O., Hashimoto, K., 2010. Calcium signals: the lead currency of plant information processing. *Plant Cell.* 22, 541-563.
- Lee, S.W., Glickmann, E., Cooksey, D.A., 2001. Chromosomal locus for cadmium resistance in *Pseudomonas putida* consisting of a cadmium-transporting ATPase and a MerR family response regulator. *Appl Environ Microbiol.* 67, 1437-1444.
- Leganes, F., Forchhammer, K., Fernandez-Pinas, F., 2009. Role of calcium in acclimation of the cyanobacterium *Synechococcus elongatus* PCC 7942 to nitrogen starvation. *Microbiology.* 155, 25-34.
- Lemire, J.A., Harrison, J.J., Turner, R.J., 2013. Antimicrobial activity of metals: mechanisms, molecular targets and applications. *Nat Rev Microbiol.* 11, 371-384.
- Li, Q., Mahendra, S., Lyon, D.Y., Brunet, L., Liga, M.V., Li, D., et al., 2008. Antimicrobial nanomaterials for water disinfection and microbial control: Potential applications and implications. *Water Research.* 42, 4591-4602.
- Liu, T., Ramesh, A., Ma, Z., Ward, S.K., Zhang, L., George, G.N., et al., 2007. CsoR is a novel *Mycobacterium tuberculosis* copper-sensing transcriptional regulator. *Nat Chem Biol.* 3, 60-68.
- Loewe, S., 1953. The problem of synergism and antagonism of combined drugs. *Arzneimittelforschung.* 3, 285-290.
- Ma, Z., Jacobsen, F.E., Giedroc, D.P., 2009. Coordination Chemistry of Bacterial Metal Transport and Sensing. *Chemical Reviews.* 109, 4644-4681.
- Marschner, B., Welge, P., Hack, A., Wittsiepe, J., Wilhelm, M., 2006. Comparison of soil Pb in vitro bioaccessibility and in vivo bioavailability with Pb pools from a sequential soil extraction. *Environ Sci Technol.* 40, 2812-2818.
- Martín-de-Lucía, I., Campos-Mañás, M.C., Agüera, A., Rodea-Palomares, I., Pulido-Reyes, G., Leganés, F., et al., 2017. Reverse Trojan-horse effect decreased wastewater toxicity in the presence of inorganic nanoparticles. *Environ. Sci.: Nano.*
- Mateo, P., Leganés, F., Perona, E., Loza, V., Fernández-Piñas, F., 2015. Cyanobacteria as bioindicators and bioreporters of environmental analysis in aquatic ecosystems. *Biodiversity and Conservation.* 24, 909-948.

- Mbeunkui, F., Richaud, C., Etienne, A.L., Schmid, R.D., Bachmann, T.T., 2002. Bioavailable nitrate detection in water by an immobilized luminescent cyanobacterial reporter strain. *Appl Microbiol Biotechnol.* 60, 306-312.
- McGregor, G.B., Rasmussen, J.P., 2008. Cyanobacterial composition of microbial mats from an Australian thermal spring: a polyphasic evaluation. *FEMS Microbiol Ecol.* 63, 23-35.
- McKinlay, A.C., Morris, R.E., Horcajada, P., Ferey, G., Gref, R., Couvreur, P., et al., 2010. BioMOFs: metal-organic frameworks for biological and medical applications. *Angew Chem Int Ed Engl.* 49, 6260-6266.
- Meeks, J.C., Campbell, E.L., Summers, M.L., Wong, F.C., 2002. Cellular differentiation in the cyanobacterium *Nostoc punctiforme*. *Arch Microbiol.* 178, 395-403.
- Meighen, E.A., 1991. Molecular biology of bacterial bioluminescence. *Microbiol Rev.* 55, 123-142.
- Merrington, G., Peters, A., Schlekot, C.E., 2016. Accounting for metal bioavailability in assessing water quality: A step change? *Environ Toxicol Chem.* 35, 257-265.
- Meyer, J.S., Farley, K.J., Garman, E.R., 2015. Metal mixtures modeling evaluation project: 1. Background. *Environ Toxicol Chem.* 34, 726-740.
- Michelini, E., Roda, A., 2012. Staying alive: new perspectives on cell immobilization for biosensing purposes. *Anal Bioanal Chem.* 402, 1785-1797.
- Morby, A.P., Turner, J.S., Huckle, J.W., Robinson, N.J., 1993. SmtB is a metal-dependent repressor of the cyanobacterial metallothionein gene *smtA*: identification of a Zn inhibited DNA-protein complex. *Nucleic Acids Res.* 21, 921-925.
- Munoz-Martin, M.A., Mateo, P., Leganes, F., Fernandez-Pinas, F., 2011. Novel cyanobacterial bioreporters of phosphorus bioavailability based on alkaline phosphatase and phosphate transporter genes of *Anabaena* sp. PCC 7120. *Anal Bioanal Chem.* 400, 3573-3584.
- Munoz-Martin, M.A., Mateo, P., Leganes, F., Fernandez-Pinas, F., 2014. A battery of bioreporters of nitrogen bioavailability in aquatic ecosystems based on cyanobacteria. *Sci Total Environ.* 475, 169-179.
- Nel, A., Xia, T., Madler, L., Li, N., 2006. Toxic potential of materials at the nanolevel. *Science.* 311, 622-627.
- Nevo, Y., Nelson, N., 2006. The NRAMP family of metal-ion transporters. *Biochim Biophys Acta.* 1763, 609-620.
- Newman, M.C., McCloskey, J.T., 1996. Predicting relative toxicity and interactions of divalent metal ions: Microtox® bioluminescence assay. *Environmental Toxicology and Chemistry.* 15, 275-281.
- Nies, D.H., 2003. Efflux-mediated heavy metal resistance in prokaryotes. *FEMS Microbiol Rev.* 27, 313-339.
- Norwood, W.P., Borgmann, U., Dixon, D.G., Wallace, A., 2003. Effects of Metal Mixtures on Aquatic Biota: A Review of Observations and Methods. *Human and Ecological Risk Assessment: An International Journal.* 9, 795-811.
- Ohlsson, A., Cedergreen, N., Oskarsson, A., Ulleras, E., 2010. Mixture effects of imidazole fungicides on cortisol and aldosterone secretion in human adrenocortical H295R cells. *Toxicology.* 275, 21-28.
- Oomen, A.G., Rempelberg, C.J., Van de Kamp, E., Pereboom, D.P., De Zwart, L.L., Sips, A.J., 2004. Effect of bile type on the bioaccessibility of soil contaminants in an in vitro digestion model. *Arch Environ Contam Toxicol.* 46, 183-188.
- Osman, D., Cavet, J.S., 2010. Bacterial metal-sensing proteins exemplified by ArsR-SmtB family repressors. *Nat Prod Rep.* 27, 668-680.
- Outten, F.W., Outten, C.E., Hale, J., O'Halloran, T.V., 2000. Transcriptional activation of an *Escherichia coli* copper efflux regulon by the chromosomal MerR homologue, *cueR*. *J Biol Chem.* 275, 31024-31029.
- Pagenkopf, G.K., 1983. Gill surface interaction model for trace-metal toxicity to fishes: role of complexation, pH, and water hardness. *Environmental Science & Technology.* 17, 342-347.
- Pagenkopf, G.K., Russo, R.C., Thurston, R.V., 1974. Effect of Complexation on Toxicity of Copper to Fishes. *Journal of the Fisheries Research Board of Canada.* 31, 462-465.
- Palmer, A.E., Qin, Y., Park, J.G., McCombs, J.E., 2011. Design and application of genetically encoded biosensors. *Trends in biotechnology.* 29, 144-152.
- Peca, L., Kos, P.B., Mate, Z., Farsang, A., Vass, I., 2008. Construction of bioluminescent cyanobacterial reporter strains for detection of nickel, cobalt and zinc. *FEMS Microbiol Lett.* 289, 258-264.
- Perona, E., Bonilla, I., Mateo, P., 1998. Epilithic cyanobacterial communities and water quality: an alternative tool for monitoring eutrophication in the Alberche River (Spain). *Journal of Applied Phycology.* 10, 183-191.

- Petänen, T., Virta, M., Karp, M., Romantschuk, M., 2001. Construction and Use of Broad Host Range Mercury and Arsenite Sensor Plasmids in the Soil Bacterium *Pseudomonas fluorescens* OS8. *Microb Ecol.* 41, 360-368.
- Prosser, J.I., Killham, K., Glover, L.A., Rattray, E.A., 1996. Luminescence-based systems for detection of bacteria in the environment. *Crit Rev Biotechnol.* 16, 157-183.
- Que, Q., Helmann, J.D., 2000. Manganese homeostasis in *Bacillus subtilis* is regulated by MntR, a bifunctional regulator related to the diphtheria toxin repressor family of proteins. *Mol Microbiol.* 35, 1454-1468.
- Rawson, D.M., Willmer, A.J., Turner, A.P., 1989. Whole-cell biosensors for environmental monitoring. *Biosensors.* 4, 299-311.
- Rengel, Z. 1999. Heavy Metals as Essential Nutrients. *Heavy Metal Stress in Plants: From Molecules to Ecosystems.* Springer Berlin Heidelberg, Berlin, Heidelberg, 231-251.
- Rensing, C., Grass, G., 2003. *Escherichia coli* mechanisms of copper homeostasis in a changing environment. *FEMS Microbiol Rev.* 27, 197-213.
- Reyes-Caballero, H., Campanello, G.C., Giedroc, D.P., 2011. Metalloregulatory proteins: metal selectivity and allosteric switching. *Biophys Chem.* 156, 103-114.
- Rider, T.H., Petrovick, M.S., Nargi, F.E., Harper, J.D., Schwoebel, E.D., Mathews, R.H., et al., 2003. A B cell-based sensor for rapid identification of pathogens. *Science.* 301, 213-215.
- Riether, K., Dollard, M.A., Billard, P., 2001. Assessment of heavy metal bioavailability using *Escherichia coli* zntAp::lux and copAp::lux-based biosensors. *Applied Microbiology and Biotechnology.* 57, 712-716.
- Ripp, S. 2005. *Bioreporter Technology for Monitoring Soil Bioremediation. Monitoring and Assessing Soil Bioremediation.* Springer Berlin Heidelberg, Berlin, Heidelberg, 233-250.
- Roda, A., Roda, B., Cevenini, L., Michelini, E., Mezzanotte, L., Reschiglian, P., et al., 2011. Analytical strategies for improving the robustness and reproducibility of bioluminescent microbial bioreporters. *Anal Bioanal Chem.* 401, 201-211.
- Rodea-Palomares, I., Boltes, K., Fernandez-Pinas, F., Leganes, F., Garcia-Calvo, E., Santiago, J., et al., 2011. Physicochemical characterization and ecotoxicological assessment of CeO₂ nanoparticles using two aquatic microorganisms. *Toxicol Sci.* 119, 135-145.
- Rodea-Palomares, I., Gonzalez-Garcia, C., Leganes, F., Fernandez-Pinas, F., 2009. Effect of pH, EDTA, and anions on heavy metal toxicity toward a bioluminescent cyanobacterial bioreporter. *Arch Environ Contam Toxicol.* 57, 477-487.
- Rodea-Palomares, I., González-Pleiter, M., Martín-Betancor, K., Rosal, R., Fernández-Piñas, F., 2015a. Additivity and Interactions in Ecotoxicity of Pollutant Mixtures: Some Patterns, Conclusions, and Open Questions. *Toxics.* 3, 342-369.
- Rodea-Palomares, I., Makowski, M., Gonzalo, S., Gonzalez-Pleiter, M., Leganes, F., Fernandez-Pinas, F., 2015b. Effect of PFOA/PFOS pre-exposure on the toxicity of the herbicides 2,4-D, Atrazine, Diuron and Paraquat to a model aquatic photosynthetic microorganism. *Chemosphere.* 139, 65-72.
- Rodea-Palomares, I., Petre, A.L., Boltes, K., Leganes, F., Perdigon-Melon, J.A., Rosal, R., et al., 2010. Application of the combination index (CI)-isobologram equation to study the toxicological interactions of lipid regulators in two aquatic bioluminescent organisms. *Water Res.* 44, 427-438.
- Rodriguez, R.R., Basta, N.T., Casteel, S.W., Pace, L.W., 1999. An In Vitro Gastrointestinal Method To Estimate Bioavailable Arsenic in Contaminated Soils and Solid Media. *Environmental Science & Technology.* 33, 642-649.
- Roessner, C.A., Scott, A.I., 1995. Fluorescence-based method for selection of recombinant plasmids. *Biotechniques.* 19, 760-764.
- Roggo, C., van der Meer, J.R., 2017. Miniaturized and integrated whole cell living bacterial sensors in field applicable autonomous devices. *Curr Opin Biotechnol.* 45, 24-33.
- Ron, E.Z., 2007. Biosensing environmental pollution. *Current Opinion in Biotechnology.* 18, 252-256.
- Rosal, R., Rodea-Palomares, I., Boltes, K., Fernandez-Pinas, F., Leganes, F., Gonzalo, S., et al., 2010a. Ecotoxicity assessment of lipid regulators in water and biologically treated wastewater using three aquatic organisms. *Environ Sci Pollut Res Int.* 17, 135-144.
- Rosal, R., Rodea-Palomares, I., Boltes, K., Fernandez-Pinas, F., Leganes, F., Petre, A., 2010b. Ecotoxicological assessment of surfactants in the aquatic environment: combined toxicity of docusate sodium with chlorinated pollutants. *Chemosphere.* 81, 288-293.
- Ruby, M.V., Davis, A., Schoof, R., Eberle, S., Sellstone, C.M., 1996. Estimation of Lead and Arsenic Bioavailability Using a Physiologically Based Extraction Test. *Environmental Science & Technology.* 30, 422-430.

- Ruby, M.V., Schoof, R., Brattin, W., Goldade, M., Post, G., Harnois, M., et al., 1999. Advances in Evaluating the Oral Bioavailability of Inorganics in Soil for Use in Human Health Risk Assessment. *Environmental Science & Technology*. 33, 3697-3705.
- Rutherford, J.C., Bird, A.J., 2004. Metal-Responsive Transcription Factors That Regulate Iron, Zinc, and Copper Homeostasis in Eukaryotic Cells. *Eukaryotic Cell*. 3, 1-13.
- Schmitt, M.P., 2002. Analysis of a DtxR-like metalloregulatory protein, MntR, from *Corynebacterium diphtheriae* that controls expression of an ABC metal transporter by an Mn(2+)-dependent mechanism. *J Bacteriol*. 184, 6882-6892.
- Schneider, D., Fuhrmann, E., Scholz, I., Hess, W.R., Graumann, P.L., 2007. Fluorescence staining of live cyanobacterial cells suggest non-stringent chromosome segregation and absence of a connection between cytoplasmic and thylakoid membranes. *BMC Cell Biol*. 8, 39.
- Scholze, M., Silva, E., Kortenkamp, A., 2014. Extending the applicability of the dose addition model to the assessment of chemical mixtures of partial agonists by using a novel toxic unit extrapolation method. *PLoS One*. 9, e88808.
- Schreiter, E.R., Sintchak, M.D., Guo, Y., Chivers, P.T., Sauer, R.T., Drennan, C.L., 2003. Crystal structure of the nickel-responsive transcription factor NikR. *Nat Struct Biol*. 10, 794-799.
- Schreiter, P.P., Gillor, O., Post, A., Belkin, S., Schmid, R.D., Bachmann, T.T., 2001. Monitoring of phosphorus bioavailability in water by an immobilized luminescent cyanobacterial reporter strain. *Biosens Bioelectron*. 16, 811-818.
- Schroder, J.L., Basta, N.T., Si, J., Casteel, S.W., Evans, T., Payton, M., 2003. In Vitro Gastrointestinal Method To Estimate Relative Bioavailable Cadmium in Contaminated Soil. *Environmental Science & Technology*. 37, 1365-1370.
- Selifonova, O., Burlage, R., Barkay, T., 1993. Bioluminescent sensors for detection of bioavailable Hg(II) in the environment. *Applied and Environmental Microbiology*. 59, 3083-3090.
- Shao, C.Y., Howe, C.J., Porter, A.J.R., Glover, L.A., 2002. Novel Cyanobacterial Biosensor for Detection of Herbicides. *Applied and Environmental Microbiology*. 68, 5026-5033.
- Shih, P.M., Wu, D., Latifi, A., Axen, S.D., Fewer, D.P., Talla, E., et al., 2013. Improving the coverage of the cyanobacterial phylum using diversity-driven genome sequencing. *Proc Natl Acad Sci U S A*. 110, 1053-1058.
- Shing, W.L., Heng, L.Y., Surif, S., 2013. Performance of a cyanobacteria whole cell-based fluorescence biosensor for heavy metal and pesticide detection. *Sensors (Basel)*. 13, 6394-6404.
- Sijm, D., Kraaij, R., Belfroid, A., 2000. Bioavailability in soil or sediment: exposure of different organisms and approaches to study it. *Environmental Pollution*. 108, 113-119.
- Silva, E., Scholze, M., Kortenkamp, A., 2007. Activity of xenoestrogens at nanomolar concentrations in the E-Screen assay. *Environ Health Perspect*. 115 Suppl 1, 91-97.
- Smaldone, G.T., Helmann, J.D., 2007. CsoR regulates the copper efflux operon copZA in *Bacillus subtilis*. *Microbiology*. 153, 4123-4128.
- Smarda, J., Smajs, D., Komrska, J., Krzyzanek, V., 2002. S-layers on cell walls of cyanobacteria. *Micron*. 33, 257-277.
- Sorensen, S.J., Burmole, M., Hansen, L.H., 2006. Making bio-sense of toxicity: new developments in whole-cell biosensors. *Curr Opin Biotechnol*. 17, 11-16.
- Stepanenko, O.V., Verkhusha, V.V., Kuznetsova, I.M., Uversky, V.N., Turoverov, K.K., 2008. Fluorescent proteins as biomarkers and biosensors: throwing color lights on molecular and cellular processes. *Curr Protein Pept Sci*. 9, 338-369.
- Stocker, J., Balluch, D., Gsell, M., Harms, H., Feliciano, J., Daunert, S., et al., 2003. Development of a set of simple bacterial biosensors for quantitative and rapid measurements of arsenite and arsenate in potable water. *Environ Sci Technol*. 37, 4743-4750.
- Tauriainen, S., Karp, M., Chang, W., Virta, M., 1997. Recombinant luminescent bacteria for measuring bioavailable arsenite and antimonite. *Appl Environ Microbiol*. 63, 4456-4461.
- Tauriainen, S., Karp, M., Chang, W., Virta, M., 1998. Luminescent bacterial sensor for cadmium and lead. *Biosensors and Bioelectronics*. 13, 931-938.
- Tauriainen, S., Virta, M., Chang, W., Karp, M., 1999. Measurement of firefly luciferase reporter gene activity from cells and lysates using *Escherichia coli* arsenite and mercury sensors. *Anal Biochem*. 272, 191-198.
- Tay, C.C., Sui, S., Lee, Y.H., 2003. Detection of metals toxicity biosensor using immobilized using immobilized cyanobacteria *Anabaena flos-aquae*. *Asiasense Sensor*, 197-201.
- Tay, C.C., Sui, S., Lee, Y.H., 2009. The Behavior of Immobilized Cyanobacteria *Anabaena torulosa* as an Electrochemical Toxicity Biosensor. *Asian Journal of Biological Science*. 1, 14-20.
- Tchounwou, P.B., Yedjou, C.G., Patlolla, A.K., Sutton, D.J., 2012. Heavy metal toxicity and the environment. *EXS*. 101, 133-164.

- Thelwell, C., Robinson, N.J., Turner-Cavet, J.S., 1998. An SmtB-like repressor from *Synechocystis* PCC 6803 regulates a zinc exporter. *Proc Natl Acad Sci U S A*. 95, 10728-10733.
- Tibazarwa, C., Corbisier, P., Mench, M., Bossus, A., Solda, P., Mergeay, M., et al., 2001. A microbial biosensor to predict bioavailable nickel in soil and its transfer to plants. *Environ Pollut*. 113, 19-26.
- Torrecilla, I., Leganes, F., Bonilla, I., Fernandez-Pinas, F., 2000. Use of recombinant aequorin to study calcium homeostasis and monitor calcium transients in response to heat and cold shock in cyanobacteria. *Plant Physiol*. 123, 161-176.
- Torrecilla, I., Leganés, F., Bonilla, I., Fernández-Piñas, F., 2001. Calcium transients in response to salinity and osmotic stress in the nitrogen-fixing cyanobacterium *Anabaena* sp. PCC7120, expressing cytosolic apoaequorin. *Plant, Cell & Environment*. 24, 641-648.
- Tottey, S., Harvie, D.R., Robinson, N.J., 2005. Understanding how cells allocate metals using metal sensors and metallochaperones. *Acc Chem Res*. 38, 775-783.
- Trang, P.T., Berg, M., Viet, P.H., Van Mui, N., Van Der Meer, J.R., 2005. Bacterial bioassay for rapid and accurate analysis of arsenic in highly variable groundwater samples. *Environ Sci Technol*. 39, 7625-7630.
- Troxell, B., Hassan, H.M., 2013. Transcriptional regulation by Ferric Uptake Regulator (Fur) in pathogenic bacteria. *Front Cell Infect Microbiol*. 3, 59.
- Ulitzur, S., Lahav, T., Ulitzur, N., 2002. A novel and sensitive test for rapid determination of water toxicity. *Environ Toxicol*. 17, 291-296.
- US. Environmental Protection Agency. 2013. National recommended water quality criteria, aquatic life criteria table. Available from: <http://water.epa.gov/scitech/swguidance/standards/criteria/current/index> and <https://www.epa.gov/wqs-tech/copper-biotic-ligand-model>.
- van der Meer, J.R., 2016. Towards improved biomonitoring tools for an intensified sustainable multi-use environment. *Microbial Biotechnology*. 9, 658-665.
- Van der Meer, J.R., Belkin, S., 2010. Where microbiology meets microengineering: design and applications of reporter bacteria. *Nat Rev Microbiol*. 8, 511-522.
- Van der Meer, J.R., Tropel, D., Jaspers, M., 2004. Illuminating the detection chain of bacterial bioreporters. *Environ Microbiol*. 6, 1005-1020.
- Van Straalen, N.M., Donker, M.H., Vijver, M.G., van Gestel, C.A., 2005. Bioavailability of contaminants estimated from uptake rates into soil invertebrates. *Environ Pollut*. 136, 409-417.
- Virta, M., Lampinen, J., Karp, M., 1995. A Luminescence-Based Mercury Biosensor. *Analytical Chemistry*. 67, 667-669.
- Waidmann, M.S., Bleichrodt, F.S., Laslo, T., Riedel, C.U., 2011. Bacterial luciferase reporters: the Swiss army knife of molecular biology. *Bioeng Bugs*. 2, 8-16.
- Waldron, K.J., Rutherford, J.C., Ford, D., Robinson, N.J., 2009. Metalloproteins and metal sensing. *Nature*. 460, 823-830.
- Wang, C., Qian, X., An, X., 2015. In situ green preparation and antibacterial activity of copper-based metal-organic frameworks/cellulose fibers (HKUST-1/CF) composite. *Cellulose*. 22, 3789-3797.
- Waters, L.S., Sandoval, M., Storz, G., 2011. The *Escherichia coli* MntR miniregulon includes genes encoding a small protein and an efflux pump required for manganese homeostasis. *J Bacteriol*. 193, 5887-5897.
- West, A.L., St. John, F., Lopes, P.E.M., MacKerell, A.D., Pozharski, E., Michel, S.L.J., 2010. Holo-Ni(II)HpNikR Is an Asymmetric Tetramer Containing Two Different Nickel-Binding Sites. *Journal of the American Chemical Society*. 132, 14447-14456.
- Whitton, B.A. 1992. Diversity, Ecology, and Taxonomy of the Cyanobacteria. In: Mann NH, Carr NG, editors. *Photosynthetic Prokaryotes*. Springer US, Boston, MA, 1-51.
- Wildt, S., Deuschle, U., 1999. cobA, a red fluorescent transcriptional reporter for *Escherichia coli*, yeast, and mammalian cells. *Nat Biotechnol*. 17, 1175-1178.
- Wilkinson, C.R., Fay, P., 1979. Nitrogen fixation in coral reef sponges with symbiotic cyanobacteria. *Nature*. 279, 527-529.
- Wojciechowska, A., Gagor, A., Wysokinski, R., Trusz-Zdybek, A., 2012. Synthesis, structure and properties of [Zn(L-Tyr)(2)(bpy)](2)3H(2)O.CH(3)OH complex: theoretical, spectroscopic and microbiological studies. *J Inorg Biochem*. 117, 93-102.
- Wong, L.S., Lee, Y.H., Surif, S., 2013. Whole Cell Biosensor Using *Anabaena torulosa* with Optical Transduction for Environmental Toxicity Evaluation. *Journal of Sensors*. 2013, 1-8.
- Yagi, K., 2007. Applications of whole-cell bacterial sensors in biotechnology and environmental science. *Appl Microbiol Biotechnol*. 73, 1251-1258.

- Yannarell, A.C., Steppe, T.F., Paerl, H.W., 2006. Genetic variance in the composition of two functional groups (diazotrophs and cyanobacteria) from a hypersaline microbial mat. *Appl Environ Microbiol.* 72, 1207-1217.
- Zha, S., Xu, X., Hu, H., 2012. A high sensitivity iron-dependent bioreporter used to measure iron bioavailability in freshwaters. *FEMS Microbiol Lett.* 334, 135-142.
- Zhang, H., Zhao, F.J., Sun, B., Davison, W., McGrath, S.P., 2001. A new method to measure effective soil solution concentration predicts copper availability to plants. *Environ Sci Technol.* 35, 2602-2607.
- Zhuang, W., Yuan, D., Li, J.-R., Luo, Z., Zhou, H.-C., Bashir, S., et al., 2012. Highly Potent Bactericidal Activity of Porous Metal-Organic Frameworks. *Advanced Healthcare Materials.* 1, 225-238.

**O
B
J
E
C
T
I
V
E
S**

OBJECTIVES

The present Thesis aims to develop a biological system to detect and evaluate the effects of heavy metals in aquatic environments.

Heavy metals are priority pollutants that persist in the environment, especially, because of anthropogenic activities. Several chemical methods are available to determine the total concentration of these pollutants in the environment; however, this total concentration is not directly related with the toxicity exhibited by these chemicals. In this context, the use of biological systems (whole-cell bioreporters) provides many advantages since the response displayed by these organisms is a result of direct interaction with these pollutants and therefore provides a real data on bioavailability. Thus, a whole-cell bioreporter based on a cyanobacterial (organism of high relevance in aquatic environments) will be developed and used to detect different heavy metals both in culture media and in different environmental matrices including biocidal nanomaterials.

Currently, heavy metals are present as mixtures in the environment. Predicting and evaluating the effect of these mixtures is essential in order to improve risk assessment. Therefore, a predictive mathematical model will be developed and implemented to analyze the response of the bioreporter to heavy metal mixtures.

Furthermore, when using these biological systems an important matter is to maintain the viability and sensitivity along time so that they can be used easily and quickly in environmental assessment. The development and set-up of maintenance systems will be tested and the viability and sensitivity of a turn-off bioreporter along time will be checked in order to generate a system that generalizes the use of these bioreporters in environmental monitoring.

The specific objectives are:

1. Construction of a cyanobacterial lights-on bioreporter strain (based on *Synechococcus elongatus* PCC7942) for detecting bioavailable heavy-metal carrying a transcriptional fusion of the promoter region of the *smt* cyanobacterial locus encoding a cyanobacterial metallothionein (SmtA) and a repressor of its expression (SmtB) to the *luxCDABE* operon. Characterization of the bioreporter response to heavy metals applied singly and in mixtures and development of a mathematical model for predicting and analysing heavy metals mixtures effects.
2. Characterization of free ion bioavailability in different natural matrices including biocidal nanomaterials using the bioreporter strain of bioavailable heavy metals generated in objective 1.
3. Development of freeze-drying protocols for cyanobacterial bioreporters, determining the optimal conditions before and after freeze-drying and characterization of the viability, sensitivity and response to contaminants of freeze-dried bioreporters over time.

Construction of a self-luminescent cyanobacterial bioreporter that detects a broad range of bioavailable heavy metals in aquatic environments

C

H

A

P

T

E

R

II

Construction of a self-luminescent cyanobacterial bioreporter that detects a broad range of bioavailable heavy metals in aquatic environments

Keila Martín-Betancor, Ismael Rodea-Palomares, M. A. Muñoz-Martín, Francisco Leganés and Francisca Fernández-Piñas*

Department of Biology, Universidad Autónoma de Madrid, Madrid, Spain

OPEN ACCESS

Edited by:

Gérald Thouand,
University of Nantes, France

Reviewed by:

Shimshon Belkin,
Hebrew University of Jerusalem, Israel
C French,
University of Edinburgh, UK
Jiangxin Wang,
Arizona State University, USA

*Correspondence:

Francisca Fernández-Piñas,
Department of Biology,
Universidad Autónoma de Madrid,
Darwin Street 2,
Cantoblanco Campus,
28049 Madrid, Spain
francisca.pina@uam.es

Specialty section:

This article was submitted to
Microbiotechnology, Ecotoxicology
and Bioremediation, a section of the
journal *Frontiers in Microbiology*

Received: 15 December 2014

Accepted: 19 February 2015

Published: 09 March 2015

Citation:

Martín-Betancor K, Rodea-Palomares I, Muñoz-Martín MA, Leganés F and Fernández-Piñas F (2015) Construction of a self-luminescent cyanobacterial bioreporter that detects a broad range of bioavailable heavy metals in aquatic environments. *Front. Microbiol.* 6:186. doi: 10.3389/fmicb.2015.00186

A self-luminescent bioreporter strain of the unicellular cyanobacterium *Synechococcus* sp. PCC 7942 was constructed by fusing the promoter region of the *smt* locus (encoding the transcriptional repressor SmtB and the metallothionein SmtA) to *luxCDABE* from *Photobacterium luminescens*; the sensor *smtB* gene controlling the expression of *smtA* was cloned in the same vector. The bioreporter performance was tested with a range of heavy metals and was shown to respond linearly to divalent Zn, Cd, Cu, Co, Hg, and monovalent Ag. Chemical modeling was used to link bioreporter response with metal speciation and bioavailability. Limits of Detection (LODs), Maximum Permissible Concentrations (MPCs) and dynamic ranges for each metal were calculated in terms of free ion concentrations. The ranges of detection varied from 11 to 72 pM for Hg²⁺ (the ion to which the bioreporter was most sensitive) to 1.54–5.35 μM for Cd²⁺ with an order of decreasing sensitivity as follows: Hg²⁺ >> Cu²⁺ >> Ag⁺ > Co²⁺ ≥ Zn²⁺ > Cd²⁺. However, the maximum induction factor reached 75-fold in the case of Zn²⁺ and 56-fold in the case of Cd²⁺, implying that Zn²⁺ is the preferred metal *in vivo* for the SmtB sensor, followed by Cd²⁺, Ag⁺ and Cu²⁺ (around 45–50-fold induction), Hg²⁺ (30-fold) and finally Co²⁺ (20-fold). The bioreporter performance was tested in real environmental samples with different water matrix complexity artificially contaminated with increasing concentrations of Zn, Cd, Ag, and Cu, confirming its validity as a sensor of free heavy metal cations bioavailability in aquatic environments.

Keywords: cyanobacteria, chemical modeling, environmental validation, free ion, heavy metal detection, self-luminescent bioreporter, *smt* locus

Introduction

Heavy metals such as Cu, Ni, Fe, Zn or Co are essential for life as they are required to maintain cellular metabolism (Waldron et al., 2009; Osman and Cavet, 2010). During evolution, bacteria have developed mechanisms to sense and respond to variable fluxes of metals in the environment and try to keep a beneficial intracellular concentration of the essential metals to meet the requirements of the metalloproteins. To avoid toxicity of metals, essential or not, bacteria present detoxification and resistance systems which mainly employ proteins involved in metal efflux

(CPx-ATPases, chemiosmotic efflux systems), enzymatic detoxification or intracellular sequestration of excess metal (O'Halloran, 1993; Silver and Phung, 1996; Busenlehner et al., 2003; Arguello et al., 2007; Osman and Cavet, 2010).

The ArsR-SmtB family of transcriptional repressors are a group of metal sensing transcriptional regulators which bind to proteins involved in the efflux or sequestration of metals. The family is named after the *Synechococcus* sp. PCC 7942 SmtB repressor which negatively regulates the expression of SmtA, a class II cyanobacterial metallothionein (Huckle et al., 1993; Morby et al., 1993; Turner et al., 1996; Robinson et al., 2001). *smtB* and *smtA* are divergently transcribed and repression is alleviated mainly by Zn, although it has been described that Cd, Co, Cr, Cu, Hg, Ni, and Pb increase the abundance of *smtA* transcripts (Huckle et al., 1993). Other ArsR-SmtB representatives include ZiaR which also senses Zn; CadC, Cd, Pb and Zn; CmtR, Cd and Pb; CzrA, Zn and Co; NmtR, Ni and Co; BmxR, Cu, Ag, Zn, Cd, Ni and Co and ArsR which senses As, Sb and Bi (for a review see Busenlehner et al., 2003; Osman and Cavet, 2010).

The metal sensing bacterial systems have been used for the construction of whole cell bioreporters (Hynninen and Virta, 2010). Whole cell bioreporters complement the traditional methods of detection of heavy metals which are based on highly sensitive and specific physical and chemical techniques, such as atomic absorption spectroscopy or mass spectrometry; however, such methods are not able to distinguish between available (potentially hazardous to biological systems) and non-available fractions of metals existing in the environment. In contrast to chemical methods, whole-cell bioreporters measure bioavailable metals, which is the fraction interacting with the cell and capable of passing through cellular membranes. They are also able to integrate the complexity of environmental factors (pH, redox potential, exchangeable cations, biological activity, etc.) that contribute to bioavailability (Kohler et al., 2000). In general, whole-cell bioreporters are intact living cells genetically engineered to produce a dose-dependent measurable signal in response to chemical or physical agents in their environment (Harms et al., 2006; van der Meer and Belkin, 2010). Cyanobacteria are the only prokaryotic organisms carrying out an oxygen-evolving photosynthesis. They originated during the Precambrian era, and as a group they are known to survive a wide spectrum of environmental stresses. As primary producers with a key role in the N and C cycles, they are a dominant component of marine and freshwater phytoplankton, and are well suited for detecting contaminants in aqueous samples (Bachmann, 2003; Rodea-Palomares et al., 2009). Cyanobacteria are ecologically relevant (particularly in aquatic environments), and for that reason, in recent years there has been an interest in developing recombinant bioluminescent cyanobacterial bioreporters which may be useful to assess toxicity in photosynthetic organisms (Shao et al., 2002; Rodea-Palomares et al., 2009; Rodea-Palomares et al., 2010), nutrient bioavailability due to their pivotal role in biogeochemical cycles (Bullerjahn et al., 2010; Munoz-Martin et al., 2011, 2014b) and a few specific pollutants like heavy metals (Erbe et al., 1996; Peca et al., 2008). Regarding the *smtB-smtA* locus, there is only one previous report of a cyanobacterial bioreporter based on the fusion of the complete *Vibrio fischeri luxCDABE* (now denoted as *Aliivibrio*

fischeri) operon to the *smtA* promoter region of *Synechococcus* sp. PCC 7942 (Erbe et al., 1996). However, this bioreporter showed limited production of endogenous aldehyde (the luciferase substrate for the bioluminescence reaction) and needed the exogenous addition of n-decanal; it was tested with only three metals, Zn, Cu, and Cd and was shown to respond to them with varying sensitivities. In the present work, we have fused the *luxCDABE* operon from *Photobacterium luminescens* (Szittner and Meighen, 1990; Fernandez-Pinas et al., 2000) to the promoter region of *smtA* of *Synechococcus* sp. PCC 7942 to develop a novel self-luminescent heavy-metal bioreporter which does not need the addition of exogenous aldehyde; the regulatory *smtB* gene controlling the expression of *smtA* was cloned in the same vector. We have characterized its response to a range of heavy metals: Zn, Cd, Cu, Co, Ag, Hg, Sr, Mg, Fe, Ba, Ni, and Pb. We have found that this bioreporter is induced in the presence of Zn, Cd, Cu, Co, and Hg, but interestingly also in the presence of Ag, a monovalent metal cation to which *smtA* of *Synechococcus* sp. PCC 7942 has never been reported to respond. Furthermore, due to the importance of testing the bioreporter response in real environmental samples, the bioreporter has been tested in river and wastewater samples spiked with heavy metals as case studies; as metal speciation is a relevant issue which has been seldom addressed when testing bioreporters in real samples, we have used chemical modeling (Visual MINTEQ program) in an attempt to link the bioreporter response with metal speciation and bioavailability.

Material and Methods

Bacterial Strains and Culture Conditions

Synechococcus elongatus PCC 7942 cells were grown at 28°C with continuous illumination, at 60 $\mu\text{mol photons m}^{-2}\text{s}^{-1}$ intensity on a rotary shaker in 500 mL Erlenmeyer flasks containing 300 mL of BG11 medium (Rippka, 1988) buffered with 2 mM MOPS and pH = 7.5 (medium composition in Supplementary material Table S1). Culture medium was supplemented with 3.75 $\mu\text{g/mL}$ chloramphenicol (Cm) for the transformed strain *Synechococcus elongatus* PCC 7942 pBG2120.

Chemical Substances

Enzymes required for molecular cloning were from Takara and Fermentas. Kits for plasmid extraction and purification were from Qiagen and Promega. Metal salts used in this study were: ZnCl₂, CdCl₂, AgSO₄, CuSO₄, HgCl₂, CoCl₂, PbNO₃, MgCl₂, NiCl₂, FeCl₂, BaCl₂, and SrCl₂. All metal salts were from Sigma-Aldrich. Concentrated metal salts solutions (1000 mg/L) were prepared in deionized water (Millipore) and stored at 4°C in opaque bottles. Dilutions were carried out in distilled water from this concentrated solution and kept for 1 month at 4°C.

Construction of the *smtAB-luxCDABE* Cyanobacterial Reporter Strain

The cyanobacterial whole cell bioreporter for heavy metals detection was constructed using *Synechococcus elongatus* PCC 7942 as host cell. A sequence containing the *smtB* gene, the *smt* operator/promoter region and the first 50 pb of *smtA* was amplified from the genomic DNA using the primers displayed in

Figure 1. The product of the PCR amplification was cloned in pDrive cloning vector (Qiagen), digested with *KpnI* and *Sall* and cloned into the *KpnI/Sall* sites of plasmid pBG2106 (Munoz-Martin et al., 2011) that harbors the promoterless *luxCDABE* from *Photobacterium luminescens*, generating the plasmid pBG2120 (Figure 1). The resulting plasmid contains a *smt-luxCDABE* transcriptional fusion where the *luxCDABE* operon is regulated under the control of the metal inducible promoter region of *smtAB* and, also contains the regulatory gene *smtB*. The integrity of the construction in *Escherichia coli* (*E. coli*) was confirmed by restriction analysis and DNA sequencing.

This plasmid, pBG2120, was introduced into the cyanobacterial strain by conjugation as described (Elhai and Wolk, 1988; Elhai et al., 1997). The integrity of the transformation in *Synechococcus* sp. PCC 7942 was confirmed by PCR with the forward primer used for the amplification of the promoter and a primer

designated as luxOUT, which anneals in the *luxCDABE* coding sequence: 5'-AGTCATTCAATATTGGCAGG-3' (not included in Figure 1). A scheme depicting plasmid pBG2120 can be found in Figure 1.

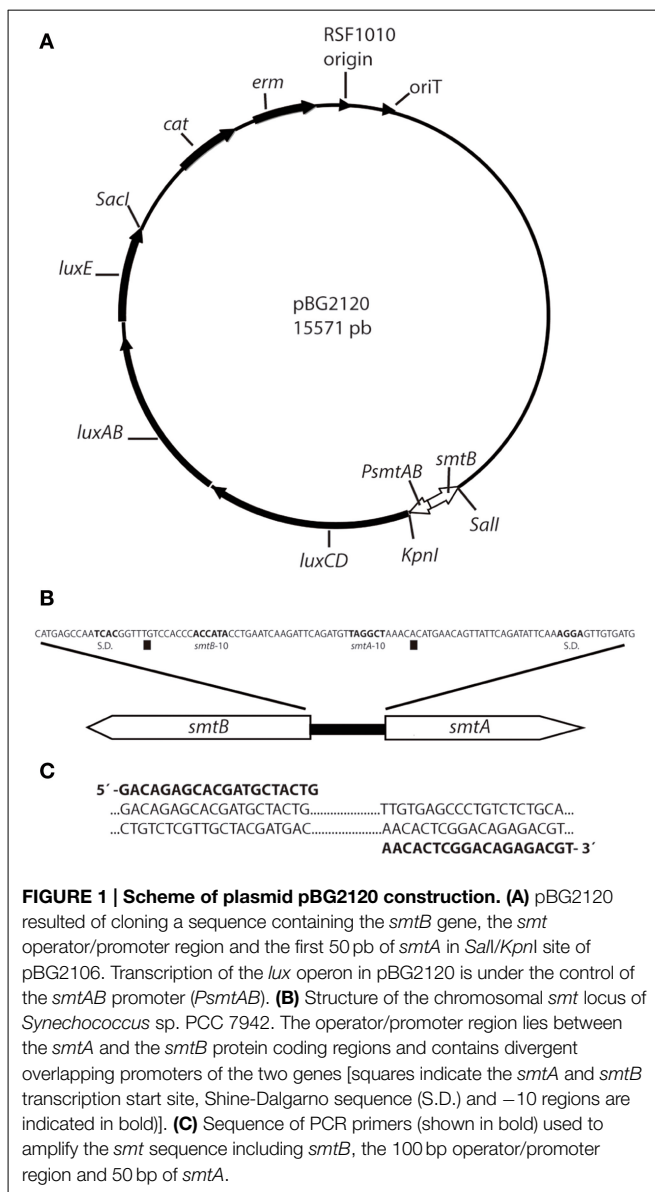
Bioluminescence Assays

The bioreporter strain was grown until reaching the mid-log phase ($OD_{750nm} = 0.6-0.7$) because this growth stage was found to increase luminescence induction (data not shown) and washed twice in a BG11 modified medium lacking Co, Zn, and Cu which might induce the *smt-luxCDABE* reporter system (Huckle et al., 1993) (Supplementary Material Table S1) buffered with 2 mM MOPS and pH = 7.5. For standardization purposes cells were resuspended in the same medium to reach a final $OD_{750nm} = 0.5$ (Rodea-Palomares et al., 2009). Metal salt exposure experiments were performed in transparent 24 well microtiter plates in a 1.5 mL final volume. Metal salts were added to the wells to get the desired final concentrations, which were between 0 and 40 μM for each tested metal.

Plates were incubated at 28°C in light ($60 \mu mol m^{-2} s^{-1}$) on a rotatory shaker up to 6 h. For the luminescence measurements, 100 μl of cell suspensions were transferred to an opaque 96-well microtiter plate and luminescence was recorded every 5 min for 20 min in a Centro LB 960 luminometer (Berthold Technologies GmbH and Co.KG, Bald Wilbad, Germany) and the maximum record (usually at 15–17 min) was taken. All data are expressed as Bioluminescence induction factors (BIFs) calculated by dividing the mean luminescence signal of a treated sample by the mean luminescence signal of the untreated sample. The limits of detection (LODs) were defined as a value two-fold above the background signal plus three times the standard deviation. In addition, the maximum permissive concentrations (MPCs), the highest concentrations that do not cause toxicity to an organism, were determined. The luminescence was measured without supplementation of exogenous aldehyde as the strain harbored the *lux* operon and its endogenously generated aldehyde was not limiting (as tested by the addition of exogenous aldehyde, data not shown).

Toxicity Bioassay

The toxicity of the heavy metals was determined by monitoring growth inhibition of the cyanobacterium *Synechococcus* sp. PCC 7942 pBG2120. Strain manipulation and metal tested concentrations were the same as described for bioluminescence bioassays. The bioreporter strain was grown until reaching the mid-log phase ($OD_{750nm} = 0.6-0.7$), washed twice in a BG11 modified medium lacking Co, Zn, and Cu buffered with 2 mM MOPS and pH = 7.5 and resuspended in the same medium to reach a final $OD_{750nm} = 0.5$. Experiments were performed in 24 well microtiter plates in a 1.5 mL final volume. Metals were added to the wells to get the desired final concentrations. The growth of *Synechococcus* sp. PCC 7942 pBG2120 was monitored for 4 and 20 h and assessed by optical density at 750 nm using a HITACHI U-2000 spectrophotometer. Microplates were maintained at 28°C inside a growing chamber with controlled light intensity ($60 \mu mol photons m^{-2} s^{-1}$) on an orbital shaker.



Three independent experiments with triplicate samples were conducted.

Spiking Experiments: Artificial Contamination of Environmental Water Samples with Heavy Metals

Three environmental water samples with different matrix compositions were selected to validate the response of the metal reporter under real environmental conditions, as explained below:

Two fresh water samples were from the Guadalix River (Glx); this is a tributary of the larger Jarama River and is located in central Spain, near the city of Madrid. It is 38 km long and flows mainly through siliceous substrates (Douterelo et al., 2004). The main flow is about 1 m³/s after the thaw and no more than 0.60 m³/s the rest of the year. The source of the river is at more than 1790 m altitude in the south drainage Guadarrama Mountains and flows into the Jarama River at 600 m altitude. Glx1 sampling point is located near the headwaters at 1500 m and does not have anthropogenic influence, whereas the Glx3 sampling point is near a human settlement, San Agustín de Guadalix. At this point, the river receives industrial and domestic sewage.

Moreover, a wastewater sample was collected from the effluent of the secondary clarifier of the Alcalá de Henares wastewater treatment plant (WWTP) (Rosal et al., 2010; Barran-Berdon et al., 2011). This is the main WWTP in the region and it discharges treated wastewater effluents into the Henares River. The location of the sampling points are shown in Supplementary Material Figure S1. The water sample manipulation, storage and analysis were performed essentially as previously described (Rodea-Palomares et al., 2010; Munoz-Martin et al., 2011). Quantitative analysis of the elemental composition of the waters samples was performed by inductively coupled plasma-mass spectrometry (ICP-MS; Perkin-Elmer Sciex Elan 6000 equipped with an AS 91 autosampler) by the ICP-MS laboratory of the Universidad Autonoma de Madrid. The main environmental water physicochemical characteristics are described in **Table 1**. For the heavy metal spiking experiments, 75 μ l of the concentrated culture was added to the environmental water samples, already pre-incubated with metals for at least 30 min (Fernandez-Pinas et al., 1991), to reach a final OD_{750nm} of 0.5 in a final volume of 1.5 mL. The water samples were supplemented with BG11 (without Cu, Zn and Co, as described above) growth medium, to ensure that any change in luminescence was not due to any nutrient deficiency; 150 μ l ten-fold concentrated medium was added so that, in the final volume of 1.5 mL, the composition of ions in the supplemented samples was the same as that in BG11; dilution of the sample by addition of BG11 did not significantly change Visual MINTEQ predictions. The metals and the range of nominal concentration tested were as follows: ZnCl₂: [3.6–15 μ M], CdCl₂: [2.45–10 μ M], AgSO₄: [0.2–0.5 μ M], and CuSO₄: [0.875–7 μ M]. Plates were incubated at 28°C in light (60 μ mol m²s⁻¹) on a rotatory shaker for 4 h (see Results). For the luminescence measurements, 100 μ l of cell suspensions were transferred to an opaque 96-well microtiter plate and recorded every 5 min for 20 min in a Centro LB 960 luminometer (Berthold Technologies GmbH and Co.KG, Bald Wilbad, Germany) and the maximum record (usually at 15–17 min) was taken. All data are expressed as BIFs calculated by

TABLE 1 | Main physicochemical characteristics of environmental waters used in the study.

Physicochemical parameters	Guadalix river		Alcalá wastewater treatment plant (WWTP)
	Glx1	Glx3	
Water temperature (°C)	8.6	9.9	13
pH	6.9	7.2	7.5
Conductivity (μ S cm ⁻¹)	100	325	702
PO ₃ ³⁻ -P (mg l ⁻¹)	0.05	0.24	1.1
Alkalinity (mg l ⁻¹ CaCO ₃)	14.5	80	472
Hardness (mg l ⁻¹ CaCO ₃)	17.7	109	176
N-NO ₃ ⁻ (mg l ⁻¹)	0.2	0.45	7
N-NH ₄ ⁺ (mg l ⁻¹)	0.05	0.14	1.5
Microelements (μ M)			
Mg	67.64	336.4	786.07
Na	398.78	737.29	3575.92
K	21.20	90.63	447.54
Ca	24.95	986.18	1117.85
Mn	0.027	0.024	0.49
Fe	0.19	0.081	1.05
Co	6.79·10 ⁻⁴	1.02·10 ⁻³	0.012
Ni	5.28·10 ⁻³	8.004·10 ⁻³	0.095
Cu	3.51·10 ⁻³	6.41·10 ⁻³	0.036
Zn	0.74	0.43	0
As	0.065	0.2	0.057
Ag	0	2.78·10 ⁻⁴	8.84·10 ⁻³
Cd	0	0	0
Hg	0	0	2.48·10 ⁻³
Pb	0	0	0.01
Sr	0.47	3.34	10.07
Ba	0.12	0.13	0.05

Glx1, Guadalix river sampling point as a representative of the upstream course, Glx3 as representative of the downstream course; WWTP, effluent of Alcalá de Henares Wastewater Treatment Plant.

dividing the mean luminescence signal of a treated sample by the mean luminescence signal of the untreated sample. Triplicate samples within each experiment were measured in at least three independent experiments.

Modeling of Metal Speciation

The chemical equilibrium model Visual MINTEQ (<http://www.lwr.kth.se/English/OurSoftware/vminteq/index.htm>) was used to predict the metal speciation with the growth medium (BG11) and environmental samples. Assumptions of a fixed pH, fixed potential redox (Eh), closed system and no precipitation of solid phases were made during computations. This chemical model has proved very useful for linking speciation to metal toxicity and biosorption processes in a number of organisms (Newman and McCloskey, 1996; Campbell et al., 2000; Deheyne et al., 2004; Herrero et al., 2005; Rodea-Palomares et al., 2009). In the present work, Visual MINTEQ is used in order to predict metal speciation and link it to the response of the reporter strain in the assay and in the spiking experiments. The LODs, dynamic ranges and MPCs of the bioreporter performance given in the

text were calculated based on the free ion metal concentration as predicted by Visual MINTEQ for the assay and spiking experiments.

Statistical Analysis

The test of statistically significant differences between data sets was performed using One-Way Analyses of Variance (ANOVA); also, to discriminate which data sets were significantly different from the others, the *post-hoc* Tukey's HSD (honestly significant difference) test was performed. All the tests were computed using R software 3.0.2. (copyright©The Foundation for Statistical Computing). All data were obtained from a minimum of three independent experiments with replicates for each assay condition. Toxicity was expressed as effective concentration EC₅₀ which is the metal concentration exerting 50% growth inhibition. To calculate the EC₅₀ values, dose-response curves were fitted by non-linear parametric functions with the R "drc" analysis package (Ritz and Streibig, 2005) (R for windows, 3.0.2 version Development Core Team). Best-fit models were selected by using the "model select" function provided in the *drc* package according to the maximum likelihood and the Akaike's information criterion (Ritz and Streibig, 2005).

Results

Selectivity and Sensitivity of *Synechococcus* sp. PCC 7942 pBG2120 to Heavy Metals

The selectivity and sensitivity profile of *Synechococcus* sp. PCC 7942 pBG2120 was studied as a function of exposure time to twelve different metals: Zn, Cd, Ag, Cu, Hg, Co, Pb, Mg, Ni, Fe, Ba, and Sr. Six metals effectively induced the *smtAB::luxCDABE* reporter system of *Synechococcus* sp. PCC 7942 pBG2120: Zn, Cd, Ag, Cu, Hg, and Co. Their induction profiles for a range of metal concentrations expressed as free ion, and exposure times are shown in **Figure 2**. No significant induction of the *smtAB::luxCDABE* reporter system was observed for any of the other six metals tested: Pb, Mg, Ni, Fe, Ba, and Sr (Supplementary Material Figure S2).

The medium used for the assays was BG11. This is the growth medium for this organism, and it had to be used also as bioassay medium (without trace metals) because in water the bioreporter strain was not induced to the same level as when assay was performed in growth medium. Because the medium used for the assays, BG11 (medium composition in Supplementary Material Table S1), is a rich medium and it has components that can complex heavy metals, such as phosphate, EDTA and ferric ammonium citrate, the chemical program Visual MINTEQ was used to predict metal speciation. The predicted percentages of metal present as free ion in BG11 medium and the other main chemical species in BG11 medium are detailed in Supplementary Material Table S2. The BIFs shown in **Figure 2** were calculated based on free ion metal concentration as predicted by Visual MINTEQ.

As shown in **Figure 2**, for each metal, BIF values increased in a dose-dependent fashion as a function of exposure time up to 4 h. Longer exposure times did not result in a significant higher induction. The maximum BIF for Zn²⁺ (**Figure 2A**) was the highest, near 75-fold induction followed by Cd²⁺ (**Figure 2B**)

with a maximum BIF of 56-fold induction, Ag⁺ (**Figure 2C**) with a maximum BIF of 50-fold induction, Cu²⁺ (**Figure 2D**) with a maximum BIF of 45-fold induction, Hg²⁺ (**Figure 2E**) with a maximum BIF of 30-fold induction and Co²⁺ (**Figure 2F**) with a maximum BIF of 20-fold induction.

The LODs, MPCs and dynamic ranges of performance of *Synechococcus* sp. PCC 7942 pBG2120 for each metal in terms of free ion are summarized in **Table 2**.

Regarding sensitivity, the lowest LOD was found for Hg²⁺, followed in decreasing order of sensitivity by Cu²⁺, Ag⁺, Co²⁺, Zn²⁺, and Cd²⁺. This order of sensitivity was further confirmed by a toxicity bioassay using growth inhibition as the endpoint after 20 h exposure to increasing concentrations of metals (see Supplementary Material Table S3 with EC₅₀ values; exposure times shorter than 20 h did not allow calculations of EC₅₀ values). The observed luminescence decrease, abrupt in many of the cases, at concentrations higher than the MPCs indicated metal toxicity as shown by the quite low EC₅₀ values obtained in the toxicity bioassays.

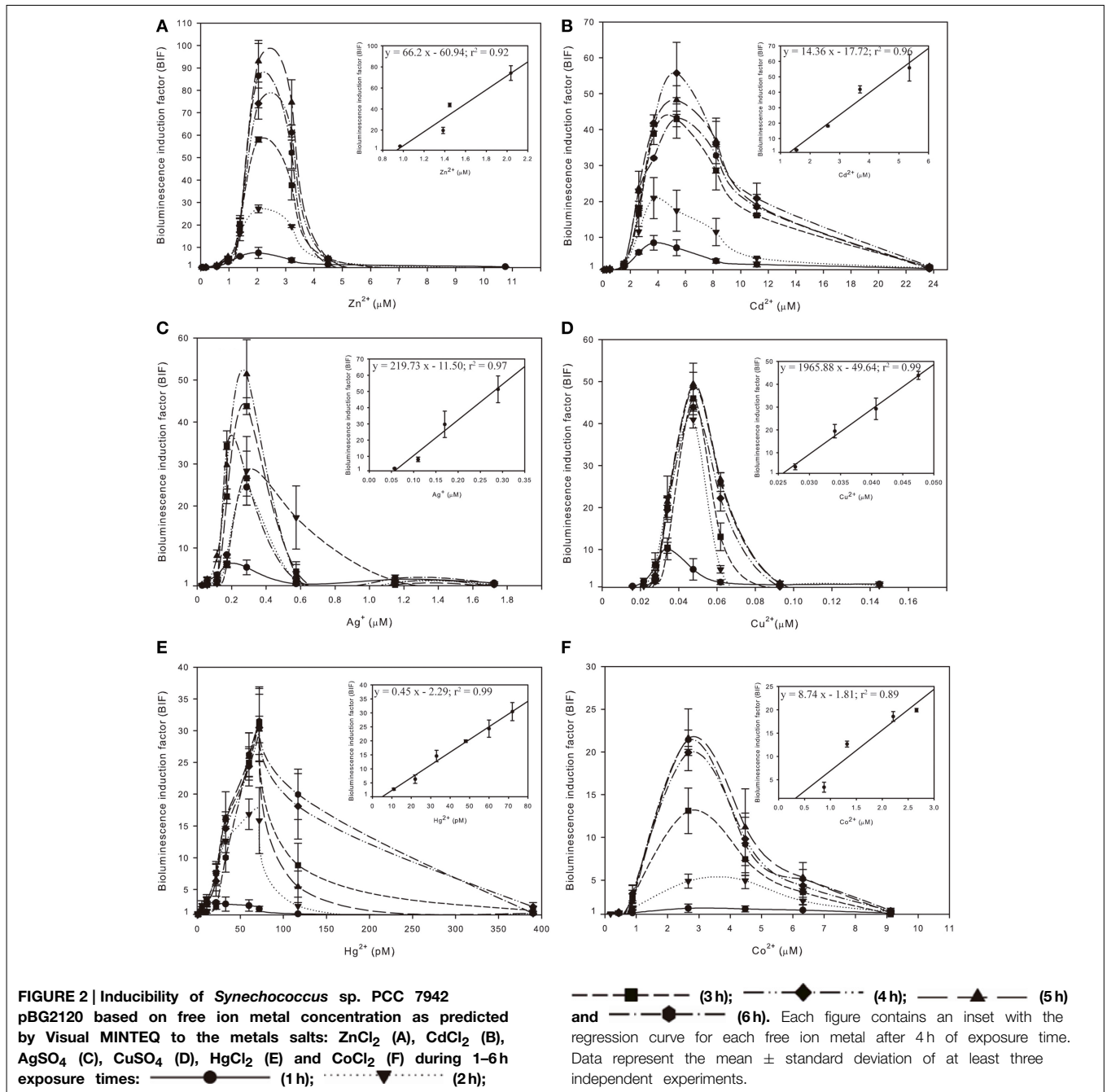
Table 2 also shows the main parameters of the regression curves in the linear ranges of the bioreporter response; further experiments including intermediate concentrations were carried out to confirm the linearity range for each metal; the regression curves were plotted as a fraction of free ion in the exposure medium using chemical modeling (Visual MINTEQ).

Application of *Synechococcus* sp. PCC 7942 pBG2120 as a Bioreporter of Heavy Metal Bioavailability in Environmental Samples: Spiking Experiments

The above experiments indicate that *Synechococcus* sp. PCC 7942 pBG2120 responds in a linear manner to 6 different metals in different detection ranges: Zn²⁺ (0.97–2.04 μM), Cd²⁺ (1.54–5.35 μM), Ag⁺ (0.05–0.29 μM), Cu²⁺ (0.027–0.05 μM), Hg²⁺ (11–72 pM), and Co²⁺ (0.88–2.66 μM). As described before, 4 h was found to be an optimal exposure time for all metals; therefore, environmental assays were performed after 4 h of exposure.

To test the suitability of *Synechococcus* sp. PCC 7942 pBG2120 as a bioreporter of heavy metals in environmental samples, we exposed it to three different water samples. Two samples points were from upstream and downstream of Guadalix River, Glx1 and Glx3, respectively, and the third was from an effluent of the Alcalá WWTP. These samples were artificially contaminated (spiked or doped) with increasing concentrations of Zn, Cd, Ag, and Cu as described in Material and Methods section. All sampling points are located in central Spain (Supplementary Material Figure S1) and the main environmental water physicochemical characteristics are described in the Material and Methods section and **Table 1**.

As can be seen in **Table 1**, there is a wide range of variation in the concentrations of the different parameters between the three water samples. Mainly, Glx1 represents a near pristine water with low electrical conductivity, PO₄³⁻-P, alkalinity, N-NO₃⁻ and N-NH₄⁺, while Glx3 and WWTP present increasing anthropic influence represented by increasing values for those parameters. Also, **Table 1** details the chemically detected concentrations of different metals present in the water samples. The



concentration of the heavy metals present in the water samples were very low and below the limit of detection of the strain; in fact, the water samples did not induce the bioreporter response (data not shown).

Table 3 shows the heavy metal nominal concentrations used to spike the water samples, the predicted free ion metal concentration as predicted by Visual MINTEQ and the bioreporter output as calculated from the calibration curve given in the text, for each metal concentration in each water sample. It is very interesting to note that the predicted free ion metal concentrations were slightly lower in river sample Glx3 and considerably lower in

wastewater sample for all metals added, indicating the complexity of the water matrix in the WWTP.

As can be seen in Table 3, in the case of Zn²⁺, the metal concentration estimated based on the bioreporter output was 53.3% of that predicted by Visual MINTEQ in Glx1 and 60% in Glx3. In the case of Cd²⁺, the metal concentration estimated based on the bioreporter output was an average of 57% of that predicted by Visual MINTEQ in Glx1 and 70% in Glx3. In the WWTP sample, the metal concentration estimated based on the bioreporter output was 86% and 96% of that predicted by Visual MINTEQ for Zn²⁺ and Cd²⁺, respectively. In the case of Ag⁺, the metal

TABLE 2 | Limits of detection (LODs), free ion dynamic ranges, free ion maximum permissible concentrations (MPCs), regression equations and corresponding R^2 values for *Synechococcus* sp. PCC 7942 pBG2120 for each metal tested in terms of free ion.

Metal	Free ion LODs (μM)	Free ion dynamic range (μM)	Free ion MPCs (μM)	Regression equation	R^2
Zn ²⁺	0.97	0.97–2.04	2.04	$y = 66.2x - 60.94$	0.92
Cd ²⁺	1.54	1.54–5.35	5.35	$y = 14.36x - 17.72$	0.96
Ag ⁺	0.05	0.05–0.29	0.29	$y = 219.73x - 11.50$	0.97
Cu ²⁺	0.027	0.027–0.05	0.05	$y = 1965.88x - 49.64$	0.99
Hg ²⁺	11*	11–72*	72*	$y = 0.45x - 2.29$	0.99
Co ²⁺	0.88	0.88–2.66	2.66	$y = 8.74x - 1.81$	0.89

*, Hg²⁺ concentrations are in picomolar (pM); y = bioluminescence induction factor (BIF); x = free ion metal concentration (μM).

TABLE 3 | Heavy metal concentrations tested in water samples in the spiking experiments, predicted free ion heavy metal concentrations by Visual MINTEQ and the bioreporter output (calculated from the calibration curve given in the text) in water samples for two sampling points in Guadalix river (Glx1 as representative of the upstream course and Glx3 as representative of the downstream course) and one sample from the effluent of Alcalá de Henares wastewater treatment plant (WWTP).

METAL	Nominal Conc. (μM)	Sample					
		Glx1		Glx3		WWTP	
		Predicted free ion (μM)	Bioreporter output (μM)	Predicted free ion (μM)	Bioreporter output (μM)	Predicted free ion (μM)	Bioreporter output (μM)
Zn	3.6	0.86	0.96 ± 0.003	0.77	–	0.48	–
	7.3	1.82	0.97 ± 0.01	1.62	0.96 ± 0.01	0.99	0.97 ± 0.01
	10	2.57	–	2.30	–	1.37	1.14 ± 0.12
	15	4.09	–	3.63	–	2.08	1.58 ± 0.33
Cd	2.5	1.51	1.31 ± 0.009	1.38	1.31 ± 0.01	0.89	1.31 ± 0.009
	5	3.04	1.67 ± 0.13	2.77	1.88 ± 0.51	1.88	1.65 ± 0.26
	7	4.28	2.54 ± 0.46	3.89	2.79 ± 0.23	2.71	2.58 ± 0.88
	10	6.14	–	5.60	–	4	4.17 ± 0.45
Ag	0.2	0.10	0.073 ± 0.002	0.10	0.068 ± 0.003	0.03	–
	0.3	0.15	0.09 ± 0.006	0.15	0.083 ± 0.002	0.04	–
	0.5	0.25	0.157 ± 0.002	0.26	0.164 ± 0.002	0.07	0.165 ± 0.012
	1	0.51	–	0.51	–	0.14	0.17 ± 0.01
Cu	1.75	0.03	0.027 ± 0.001	0.03	0.027 ± 0.001	0.022	–
	3.5	0.07	0.036 ± 0.005	0.06	0.042 ± 0.007	0.022	–
	7	0.16	–	0.13	–	0.05	0.03 ± 0.0006
	14	0.37	–	0.28	–	0.13	0.039 ± 0.005

The bioreporter output data represent the average ± standards errors of the mean (n = 3).
–, out of calibration range.

concentration estimated based on the bioreporter output was 65% of that predicted by Visual MINTEQ in Glx1 and 62% in Glx3.

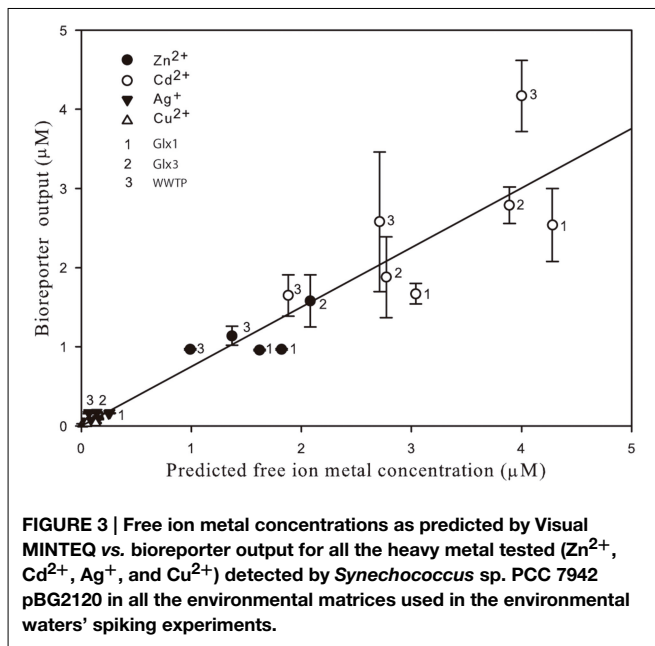
Interestingly, in the WWTP, the amount of Ag⁺ detected by *Synechococcus* sp. PCC 7942 pBG2120 in the water sample with metal concentration within its dynamic range, was higher than that predicted by Visual MINTEQ (around 2-fold).

In the case of Cu²⁺, the metal concentration estimated based on the bioreporter output was 70% and 80% of the concentration predicted by Visual MINTEQ in both river samples, Glx1 and Glx3, respectively; in the WWTP, only the highest concentrations

tested was within the calibration range for this metal and the concentration estimated based on the bioreporter output was 60% of that predicted by Visual MINTEQ.

For some of the spiked samples, the obtained output was out of the calibration range of the bioreporter; in those with metal concentration above the calculated MPCs, the unreliability of the bioreporter was probably due to toxicity (Supplementary Material Table S3).

Figure 3 shows free ion concentrations as predicted by Visual MINTEQ vs. bioreporter output for all the heavy metal tested and all the environmental matrices used as a summary of the



global performance of the *Synechococcus* sp. PCC 7942 pBG2120 estimating bioavailable heavy metals in environmental water matrices. As can be seen in the figure, within its dynamic ranges, the global performance of this bioreporter strain is excellent and, in general, it was very accurate for all metals tested in all water samples. A global high linear correlation ($r^2 = 0.9$) free ion predicted by Visual MINTEQ vs. bioreporter output was obtained.

Discussion

In this study, we report the construction, characterization and testing in actual environmental samples of a self-luminescent cyanobacterial bioreporter sensitive to several heavy metals both essential and non-essential for life. The constructed *Synechococcus* bioreporter is based on the *smt* locus present in the same cyanobacterium. The *smt* locus consists of a regulatory gene, *smtB*, which depending on the bioavailability of certain metals, controls the expression of *smtA*. This gene encodes a metallothionein whose main role is to sequester an excess of the heavy metal ions in the bacterial cell. This is a well-known system of bacterial metal sensing proteins (see Osman and Cavet, 2010 for a thorough review) and may be useful to construct bacterial bioreporters to detect heavy metals. In fact, Erbe et al. (1996) already constructed what can be considered the first cyanobacterial bioreporter able to detect heavy metals; it was also based on the *smt* locus and the host was also *Synechococcus* PCC 7942. However, the genetic construct was different as they fused the *smt* operator/promoter region to *A. fischeri luxCDABE* operon. The resulting recombinant strain was not able to produce enough endogenous aldehyde (the substrate for luciferase), therefore exogenous aldehyde had to be added for the bioluminescent reaction to occur. In contrast, the bioreporter that we have constructed is a fusion of the *smt* operator/promoter region with

Photorhabdus luminescens luxCDABE, which rendered the strain self-luminescent with no need of exogenous aldehyde. The addition of aldehyde increased bioluminescence but did not modify the dynamic ranges of detection by the bioreporter. Furthermore, this bacterial luciferase has the greatest thermal stability among bacterial luciferases (Szittner and Meighen, 1990; Fernandez-Pinas et al., 2000) and allows monitoring at higher temperatures than that of *A. fischeri*. This fact helps to decrease the toxicity caused by the addition of exogenous aldehyde (Fernandez-Pinas et al., 2000; Porta et al., 2003).

Erbe et al. (1996) tested the sensitivity and specificity of the bioreporter toward three metal salts: $ZnCl_2$, $CuSO_4$, and $CdCl_2$. Although calibration curves, LODs or dynamic ranges for detection were not provided, the authors found a linear increase of luminescence with increasing $ZnCl_2$ from 0.5 to 2 μM after 1 h of exposure with 5 μM decreasing luminescence. Regarding $CuSO_4$ and $CdCl_2$, they found that greater concentrations than 15 μM $CuSO_4$ and 1.5 μM $CdCl_2$ reduced luminescence due to toxicity. To our knowledge this bioreporter has not been tested with environmental samples. Regarding our bioreporter, growth of cells and assays were performed in BG11 growth medium (as Erbe et al., 1996) without metal salts added but retaining all the other components that were necessary for growth and induction of the bioreporter. BG11 medium has components such as phosphate, citrate or EDTA which may precipitate/chelate the metal ions and for this reason, chemical modeling (Visual MINTEQ) (Rodea-Palomares et al., 2009) was used to link metal speciation with the bioreporter response. We have calculated the calibration curves and subsequent LODs and dynamic ranges as a function of the free ion which is usually the most bioavailable and toxic metal species (Sunda and Lewis, 1978). This approach is not currently taken when calculating the dynamic ranges of heavy metal bioreporters (Magrisso et al., 2008) except for cyanobacterial iron bioreporters (Durham et al., 2002; Boyanapalli et al., 2007). The dynamic ranges calculated using this method show that the constructed cyanobacterial bioreporter varies in sensitivity with the different metals tested. While Sr, Mg, Fe, Ba, Ni, and Pb did not induce the bioreporter luminescence, the rest of the metals ranges of detection varied from 11 to 72 pM for Hg^{2+} (the ion to which the bioreporter was most sensitive) to 1.54–5.35 μM for Cd^{2+} with an order of decreasing sensitivity as follows: $Hg^{2+} \gg Cu^{2+} \gg Ag^+ > Co^{2+} \geq Zn^{2+} > Cd^{2+}$. This order of decreasing sensitivity was further confirmed by the toxicity bioassay. In general, non-essential ions are detected at much lower concentrations than the essential ones because they are not needed and are usually more toxic (Hynninen and Virta, 2010). However, the sensitivity of bacterial bioreporters also rely on a combination of metal affinities by the sensors and homeostasis/resistance mechanisms that determines the intracellular concentration available for detection. In this regard, if a metal is actively excluded by the cell, its cytoplasmic pool may not reach a threshold level needed for detection by a particular sensor (Cavet et al., 2003). Zn, Cu, and Co are essential for cyanobacteria (Cavet et al., 2003) while Hg, Ag and Cd are not. The fact that Cu, although essential, is the second in order of decreasing sensitivity could be due to the elevated toxicity of this element to the bioreporter as found in the toxicity bioassay. Cu has been reported to adversely

affect phytoplankton, inhibiting photosynthesis and causing serious cell damage through the formation of reactive oxygen species (Wei et al., 2014). From the tested metals, Cd was the least toxic and the bioreporter showed the smallest sensitivity to this ion. Cd is a Zn analog which enters bacterial cells via transport systems for essential divalent cations and, it is known, in many bacteria, that cellular extrusion mechanisms do not usually differentiate between both ions (Hynninen and Virta, 2010). That might be a plausible explanation for the observed similar sensitivity for both Cd and Zn by the SmtB sensor.

The constructed bioreporter shows a broad specificity as it responds, although with varying sensitivities, to Zn^{2+} , Cd^{2+} , Co^{2+} , Cu^{2+} , Hg^{2+} , and Ag^+ . Huckle et al. (1993) already demonstrated *in vitro* that Cd, Co, Cr, Cu, Hg, Ni, and Pb increased the expression of *smtA*. By fusing the upstream region of *smtA* to the reporter gene *lacZ*, they found that, *in vivo*, Zn was the most effective elicitor of *smtA* expression followed by Cu, Cd, Co, and Ni. *In vivo*, we did not get any induction by Pb or Ni; regarding Co, Cavet et al. (2002) using the same cyanobacterial host found that *in vitro* SmtB binds to Co^{2+} but *in vivo*, also using a *lacZ* reporter fusion, Co^{2+} did not induce *smtA* in *Synechococcus*. It is interesting that our bioreporter responded *in vivo* to a monovalent cation, Ag^+ , which had not been found to induce this system before. Nevertheless in the filamentous cyanobacterium *Oscillatoria brevis*, Liu et al. (2004) found a *smtB* ortholog, denoted as *bxmR* encoding a regulatory protein BmxR which has been found to respond both to mono (Ag^+ ; Cu^+) and divalent (Cd^{2+} , Zn^{2+}) metal cations. However, although regarding sensitivity the bioreporter senses Zn^{2+} and Cd^{2+} at concentrations higher than those of other metal ions, it should be pointed out that the maximum induction factor reaches 75-fold in the case of Zn^{2+} and 56-fold in the case of Cd^{2+} , implying that as found by Huckle et al. (1993) Zn^{2+} is the preferred metal *in vivo* for SmtB, followed by Cd^{2+} , Ag^+ and Cu^{2+} (around 45–50-fold induction), Hg^{2+} (30-fold), and finally Co^{2+} (20-fold).

SmtB is an intracellular metal sensor. We do not know which intracellular metal species are sensed by SmtB, however, the free ion could be a good candidate. It has been found that in the case of Zn, free Zn^{2+} is the major form of this nutrient taken up by the phytoplankton (Barnett et al., 2012). Once inside the cells, the intracellular metal pools might vary depending on metalloproteins that may bind essential metal ions as cofactors, metallothioneins which may sequester ions (essential or not) in excess or unknown intracellular ligands which might also chelate the free ions. The metal sensors regulate the abundance of their cognate metal handling protein but, also, there are efflux pumps to provide ion homeostasis both for essential and non-essential ions (Rae et al., 1999; Blindauer, 2008; Choi and Bird, 2014). From studies based on intracellular Cu^{2+} and Zn^{2+} homeostasis, it is known that the high chelation capacity of cells and that both ions' concentrations are tightly controlled. In yeast, it has been found that there is a great cellular capacity for Cu binding, meaning a low availability of Cu^{2+} inside the cells (less than 10^{-18} M in unstressed cells), so, it is extraordinarily restricted (Rae et al., 1999). Regarding Zn^{2+} , it has been found to be tightly controlled as it has been suggested to act as a signaling element (Choi and Bird, 2014). Although the total cellular Zn quota of *E. coli* is in the

micromolar range, *E. coli* was found to sense Zn^{2+} *in vivo* in the nanomolar range and *in vitro* in the femtomolar range (Outten and O'Halloran, 2001; Blindauer, 2008). This difference between *in vitro* and *in vivo* sensing has been attributed to ligands in the cytosol that may play an important role in Zn^{2+} buffering. As suggested by Cavet et al. (2002), there is a need in cyanobacteria and other cell types to identify the chemical form(s) of the labile pool(s) of metals accessible by each metal sensor to understand the observed sensitivities and requirements of metalloproteins, which is essential information to understand the response *in vivo* of the constructed metal bioreporters.

Our bioreporter response has been also tested with actual environmental samples spiked with increasing concentrations of heavy metals. The real samples used reflect water matrices of different complexity (affected or not by anthropogenic influence). This approach is seldom used in the field of bacterial bioreporters (Magrisso et al., 2008; Hynninen and Virta, 2010) although, in the case of cyanobacteria, it has been done for iron bioreporters (Durham et al., 2002; Boyanapalli et al., 2007); P and N bioreporters (Munoz-Martin et al., 2011, 2014a,b) and for Co, Zn, and Ni bioreporters constructed by Peca et al. (2008), using the *coa* and *nrs* detection systems. The concentrations of free ions detected by the bioreporter in the two river spiked samples represented an average of 68% of that predicted by chemical modeling and nearly 100% of that predicted in the spiked WWTP, which may be interpreted as the bioavailable fractions. As discussed earlier, the SmtB sensor only detects the metal ions which accumulate into the cell (the cytoplasmic pool) and this depends on the ion homeostasis of each cell system (i.e., metal exclusion systems or buffer systems such as metallothioneins) (Osman and Cavet, 2010). Besides, a fraction of the ions might not enter the cell and be adsorbed to negatively charged groups of the cell wall. In the case of Ag^+ , the bioavailable Ag^+ as detected by the bioreporter was higher (almost double) than that predicted by chemical modeling, which probably means that all free Ag^+ is bioavailable, but also might indicate, that Visual MINTEQ prediction is underestimating the concentration of this particular free ion, probably due to the complexity of the water matrix of the WWTP. Although the main physicochemical parameters and metal concentrations of this sample were characterized, probably has other uncharacterized components such as dissolved organic matter, unknown to us, which were not included as inputs in the chemical model. In some of the spiked environmental samples, the bioreporter did not give a reliable response as the amount of metal was higher than its MPCs. This means that in highly polluted samples, toxicity might be an issue and false negative results could be found. This drawback could be solved by serial dilution of the sample to decrease toxicity and restore induced responses (Amaro et al., 2011). To detect sample toxicity, it could also be convenient to use, in parallel with the metal bioreporter, a general toxicity bioreporter such as the cyanobacterial bioreporter *Anabaena* CPB4337 (Rodea-Palomares et al., 2009).

In Supplementary Material Table S4, we compare the sensitivity and dynamic ranges of our bioreporter strain with those of several microbial bioreporters which respond to the same metals (see Supplementary Material Table S4 for references). It is not an easy comparison since the sensing elements are quite different;

we have used the promoter of a metallothionein locus while most prokaryotic bioreporters are based on promoters of metal transport systems with sensors displaying different affinities. In the table, we have included eukaryotic bioreporters (based on the ciliate *Tetrahymena thermophila*) which are also based on metallothionein promoters (Amaro et al., 2011). There are also differences in the luciferase systems used in the bioreporters since, although many are based on bacterial luciferases, others are based on the eukaryotic firefly luciferase and the two reporter systems differ in sensitivity. Also, as indicated in Supplementary Material Table S4, different assay media have been used and usually no prediction/calculation of particular metal species has been made. Taking into account these limitations, the cyanobacterial bioreporter constructed in this study is, in general, more sensitive (based in the published LODs) to Hg, Cu, and Ag than other microbial bioreporters. It is less sensitive to Co than the *coaT*-based *Synechocystis* bioreporter. Regarding Zn, it shows a similar sensitivity to that of the ciliate bioreporter and the previous *smtAB*-based cyanobacterial bioreporter, and, it is much more sensitive than the *zntA*-based *E. coli* bioreporter. The constructed bioreporter is generally less sensitive to Cd than the other bioreporters. Cyanobacterial bioreporters should not be envisaged as an alternative to other microbial bioreporters, but as a useful complement as they inform on pollutant bioavailability/toxicity to organisms at the base of the food webs, namely primary producers. Most authors in the field agree that a battery of bioreporters based on organisms of different trophic levels is a useful tool in environmental monitoring.

References

- Amaro, F., Turkewitz, A. P., Martin-Gonzalez, A., and Gutierrez, J. C. (2011). Whole-cell biosensors for detection of heavy metal ions in environmental samples based on metallothionein promoters from *Tetrahymena thermophila*. *Microb. Biotechnol.* 4, 513–522. doi: 10.1111/j.1751-7915.2011.00252.x
- Arguello, J. M., Eren, E., and Gonzalez-Guerrero, M. (2007). The structure and function of heavy metal transport P1B-ATPases. *Biometals* 20, 233–248. doi: 10.1007/s10534-006-9055-6
- Bachmann, T. (2003). Transforming cyanobacteria into bioreporters of biological relevance. *Trends Biotechnol.* 21, 247–249. doi: 10.1016/S0167-7799(03)00114-8
- Barnett, J. P., Millard, A., Ksibe, A. Z., Scanlan, D. J., Schmid, R., and Blindauer, C. A. (2012). Mining genomes of marine cyanobacteria for elements of zinc homeostasis. *Front. Microbiol.* 3:142. doi: 10.3389/fmicb.2012.00142
- Barran-Berdon, A. L., Rodea-Palomares, I., Leganes, F., and Fernandez-Pinas, F. (2011). Free Ca²⁺ as an early intracellular biomarker of exposure of cyanobacteria to environmental pollution. *Anal. Bioanal. Chem.* 400, 1015–1029. doi: 10.1007/s00216-010-4209-3
- Blindauer, C. A. (2008). Zinc-handling in cyanobacteria: an update. *Chem. Biodivers.* 5, 1990–2013. doi: 10.1002/cbdv.200890183
- Boyanapalli, R., Bullerjahn, G. S., Pohl, C., Croot, P. L., Boyd, P. W., and McKay, R. M. (2007). Luminescent whole-cell cyanobacterial bioreporter for measuring Fe availability in diverse marine environments. *Appl. Environ. Microbiol.* 73, 1019–1024. doi: 10.1128/AEM.01670-06
- Bullerjahn, G. S., Boyanapalli, R., Rozmarynowycz, M. J., and McKay, R. M. (2010). Cyanobacterial bioreporters as sensors of nutrient availability. *Adv. Biochem. Eng. Biotechnol.* 118, 165–188. doi: 10.1007/10_2009_23
- Busenlehner, L. S., Pennella, M. A., and Giedroc, D. P. (2003). The SmtB/ArsR family of metalloregulatory transcriptional repressors: structural insights into prokaryotic metal resistance. *FEMS Microbiol. Rev.* 27, 131–143. doi: 10.1016/S0168-6445(03)00054-8
- Like most of the published microbial bioreporters (Ivask et al., 2002; Magrisso et al., 2008; Hynninen and Virta, 2010), the *Synechococcus* bioreporter responds to several metals. In an environmental sample, it will not discriminate between different ones, but metals as well as other potential toxic pollutants are present in the environment as complex mixtures and antagonistic/synergistic interactions might occur between them (Rodea-Palomares et al., 2010; Rodea-Palomares et al., 2012; Jouanneau et al., 2012). For that reason, this bioreporter might be useful as a first screening tool, which will easily determine whether the sample is polluted with metals, but more specific sophisticated chemical analytical methods are still necessary to determine the chemical species and exact quantities of the metals present. At present, we are evaluating the bioreporter response to heavy metal mixtures of increasing complexity in order to study and define experimental/modeling approaches to understand the potential interactions of these pollutants in the environment.

Acknowledgments

This study was funded by MINECO grants CGL2010-15675 and CTM2013-45775-C2-2-R.

Supplementary Material

The Supplementary Material for this article can be found online at: <http://www.frontiersin.org/journal/10.3389/fmicb.2015.00186/abstract>

- Campbell, C. D., Hird, M., Lumsdon, D. G., and Meeussen, J. C. (2000). The effect of EDTA and fulvic acid on Cd, Zn, and Cu toxicity to a bioluminescent construct (pUCD607) of *Escherichia coli*. *Chemosphere* 40, 319–325. doi: 10.1016/S0045-6535(99)00302-1
- Cavet, J. S., Borrelly, G. P., and Robinson, N. J. (2003). Zn, Cu and Co in cyanobacteria: selective control of metal availability. *FEMS Microbiol. Rev.* 27, 165–181. doi: 10.1016/S0168-6445(03)00050-0
- Cavet, J. S., Meng, W., Pennella, M. A., Appelhoff, R. J., Giedroc, D. P., and Robinson, N. J. (2002). A nickel-cobalt-sensing ArsR-SmtB family repressor. Contributions of cytosol and effector binding sites to metal selectivity. *J. Biol. Chem.* 277, 38441–38448. doi: 10.1074/jbc.M207677200
- Choi, S., and Bird, A. J. (2014). Zinc sensing: controlling zinc homeostasis at the transcriptional level. *Metallomics* 6, 1198–1215. doi: 10.1039/c4mt00064a
- Deheyn, D. D., Bencheikh-Latmani, R., and Latz, M. I. (2004). Chemical speciation and toxicity of metals assessed by three bioluminescence-based assays using marine organisms. *Environ. Toxicol.* 19, 161–178. doi: 10.1002/tox.20009
- Douterelo, I., Perona, E., and Mateo, P. (2004). Use of cyanobacteria to assess water quality in running waters. *Environ. Pollut.* 127, 377–384. doi: 10.1016/j.envpol.2003.08.016
- Durham, K. A., Porta, D., Twiss, M. R., McKay, R. M., and Bullerjahn, G. S. (2002). Construction and initial characterization of a luminescent *Synechococcus* sp. PCC 7942 Fe-dependent bioreporter. *FEMS Microbiol. Lett.* 209, 215–221. doi: 10.1111/j.1574-6968.2002.tb11134.x
- Elhai, J., Veprikitskiy, A., Muro-Pastor, A. M., Flores, E., and Wolk, C. P. (1997). Reduction of conjugal transfer efficiency by three restriction activities of *Anabaena* sp. strain PCC 7120. *J. Bacteriol.* 179, 1998–2005.
- Elhai, J., and Wolk, C. P. (1988). Conjugal transfer of DNA to cyanobacteria. *Methods Enzymol.* 167, 747–754. doi: 10.1016/0076-6879(88)67086-8
- Erbe, J. L., Adams, A. C., Taylor, K. B., and Hall, L. M. (1996). Cyanobacteria carrying an *smt-lux* transcriptional fusion as biosensors for the detection of heavy metal cations. *J. Ind. Microbiol.* 17, 80–83. doi: 10.1007/BF01570047

- Fernandez-Pinas, F., Leganes, F., and Wolk, C. P. (2000). Bacterial lux genes as reporters in cyanobacteria. *Methods Enzymol.* 305, 513–527. doi: 10.1016/S0076-6879(00)05510-5
- Fernandez-Pinas, F., Mateo, P., and Bonilla, I. (1991). Binding of cadmium by cyanobacterial growth media: free ion concentration as a toxicity index to the cyanobacterium *Nostoc UAM 208*. *Arch. Environ. Contam. Toxicol.* 21, 425–431. doi: 10.1007/BF01060366
- Harms, H., Wells, M. C., and van der Meer, J. R. (2006). Whole-cell living biosensors—are they ready for environmental application? *Appl. Microbiol. Biotechnol.* 70, 273–280. doi: 10.1007/s00253-006-0319-4
- Herrero, R., Lodeiro, P., Rey-Castro, C., Vilarino, T., and Sastre de Vicente, M. E. (2005). Removal of inorganic mercury from aqueous solutions by biomass of the marine macroalga *Cystoseira baccata*. *Water Res.* 39, 3199–3210. doi: 10.1016/j.watres.2005.05.041
- Huckle, J. W., Morby, A. P., Turner, J. S., and Robinson, N. J. (1993). Isolation of a prokaryotic metallothionein locus and analysis of transcriptional control by trace metal ions. *Mol. Microbiol.* 7, 177–187. doi: 10.1111/j.1365-2958.1993.tb01109.x
- Hynninen, A., and Virta, M. (2010). Whole-cell bioreporters for the detection of bioavailable metals. *Adv. Biochem. Eng. Biotechnol.* 118, 31–63. doi: 10.1007/10_2009_9
- Ivask, A., Virta, M., and Kahru, A. (2002). Construction and use of specific luminescent recombinant bacterial sensors for the assessment of bioavailable fraction of cadmium, zinc, mercury and chromium in the soil. *Soil Biol. Biochem.* 34, 1439–1447. doi: 10.1016/S0038-0717(02)00088-3
- Jouanneau, S., Durand, M. J., and Thouand, G. (2012). Online detection of metals in environmental samples: comparing two concepts of bioluminescent bacterial biosensors. *Environ. Sci. Technol.* 46, 11979–11987. doi: 10.1021/es3024918
- Kohler, S., Belkin, S., and Schmid, R. D. (2000). Reporter gene bioassays in environmental analysis. *Fresenius J. Anal. Chem.* 366, 769–779. doi: 10.1007/s002160051571
- Liu, T., Nakashima, S., Hirose, K., Shibasaki, M., Katsuhara, M., Ezaki, B., et al. (2004). A novel cyanobacterial SmtB/ArsR family repressor regulates the expression of a CPx-ATPase and a metallothionein in response to both Cu(I)/Ag(I) and Zn(II)/Cd(II). *J. Biol. Chem.* 279, 17810–17818. doi: 10.1074/jbc.M310560200
- Magrisso, S., Erel, Y., and Belkin, S. (2008). Microbial reporters of metal bioavailability. *Microb. Biotechnol.* 1, 320–330. doi: 10.1111/j.1751-7915.2008.00022.x
- Morby, A. P., Turner, J. S., Huckle, J. W., and Robinson, N. J. (1993). SmtB is a metal-dependent repressor of the cyanobacterial metallothionein gene *smtA*: identification of a Zn inhibited DNA-protein complex. *Nucleic Acids Res.* 21, 921–925. doi: 10.1093/nar/21.4.921
- Munoz-Martin, M. A., Martinez-Rosell, A., Perona, E., Fernandez-Pinas, F., and Mateo, P. (2014a). Monitoring bioavailable phosphorus in lotic systems: a polyphasic approach based on cyanobacteria. *Sci. Total Environ.* 475, 158–168. doi: 10.1016/j.scitotenv.2013.06.076
- Munoz-Martin, M. A., Mateo, P., Leganes, F., and Fernandez-Pinas, F. (2011). Novel cyanobacterial bioreporters of phosphorus bioavailability based on alkaline phosphatase and phosphate transporter genes of *Anabaena* sp. PCC 7120. *Anal. Bioanal. Chem.* 400, 3573–3584. doi: 10.1007/s00216-011-5017-0
- Munoz-Martin, M. A., Mateo, P., Leganes, F., and Fernandez-Pinas, F. (2014b). A battery of bioreporters of nitrogen bioavailability in aquatic ecosystems based on cyanobacteria. *Sci. Total Environ.* 475, 169–179. doi: 10.1016/j.scitotenv.2013.07.015
- Newman, M. C., and McCloskey, J. T. (1996). Time-to-event analyses of ecotoxicity data. *Ecotoxicology* 5, 187–196. doi: 10.1007/BF00116339
- O'Halloran, T. V. (1993). Transition metals in control of gene expression. *Science* 261, 715–725. doi: 10.1126/science.8342038
- Osman, D., and Cavet, J. S. (2010). Bacterial metal-sensing proteins exemplified by ArsR-SmtB family repressors. *Nat. Prod. Rep.* 27, 668–680. doi: 10.1039/b906682a
- Outen, C. E., and O'Halloran, T. V. (2001). Femtomolar sensitivity of metal-loreulatory proteins controlling zinc homeostasis. *Science* 292, 2488–2492. doi: 10.1126/science.1060331
- Peca, L., Kos, P. B., Mate, Z., Farsang, A., and Vass, I. (2008). Construction of bioluminescent cyanobacterial reporter strains for detection of nickel, cobalt and zinc. *FEMS Microbiol. Lett.* 289, 258–264. doi: 10.1111/j.1574-6968.2008.01393.x
- Porta, D., Bullerjahn, G. S., Durham, K. A., Wilhelm, S. W., Twiss, M. R., and McKay, R. M. L. (2003). Physiological characterization of a *synechococcus* sp. (cyanophyceae) strain pcc 7942 iron-dependent bioreporter for freshwater environments. *J. Phycol.* 39, 64–73. doi: 10.1046/j.1529-8817.2003.02068.x
- Rae, T. D., Schmidt, P. J., Pufahl, R. A., Culotta, V. C., and O'Halloran, T. V. (1999). Undetectable intracellular free copper: the requirement of a copper chaperone for superoxide dismutase. *Science* 284, 805–808. doi: 10.1126/science.284.5415.805
- Rippka, R. (1988). Isolation and purification of cyanobacteria. *Methods Enzymol.* 167, 3–27. doi: 10.1016/0076-6879(88)67004-2
- Ritz, C., and Streibig, J. C. (2005). Bioassay analysis using R. *J. Stat. Softw.* 12, 1–22.
- Robinson, N. J., Whitehall, S. K., and Cavet, J. S. (2001). Microbial metallothioneins. *Adv. Microb. Physiol.* 44, 183–213. doi: 10.1016/S0065-2911(01)44014-8
- Rodea-Palomares, I., Gonzalez-Garcia, C., Leganes, F., and Fernandez-Pinas, F. (2009). Effect of pH, EDTA, and anions on heavy metal toxicity toward a bioluminescent cyanobacterial bioreporter. *Arch. Environ. Contam. Toxicol.* 57, 477–487. doi: 10.1007/s00244-008-9280-9
- Rodea-Palomares, I., Leganes, F., Rosal, R., and Fernandez-Pinas, F. (2012). Toxicological interactions of perfluorooctane sulfonic acid (PFOS) and perfluorooctanoic acid (PFOA) with selected pollutants. *J. Hazard. Mater.* 201–202, 209–218. doi: 10.1016/j.jhazmat.2011.11.061
- Rodea-Palomares, I., Petre, A. L., Boltes, K., Leganes, F., Perdigon-Melon, J. A., Rosal, R., et al. (2010). Application of the combination index (CI)-isobologram equation to study the toxicological interactions of lipid regulators in two aquatic bioluminescent organisms. *Water Res.* 44, 427–438. doi: 10.1016/j.watres.2009.07.026
- Rosal, R., Rodea-Palomares, I., Boltes, K., Fernandez-Pinas, F., Leganes, F., Gonzalez, S., et al. (2010). Ecotoxicity assessment of lipid regulators in water and biologically treated wastewater using three aquatic organisms. *Environ. Sci. Pollut. Res. Int.* 17, 135–144. doi: 10.1007/s11356-009-0137-1
- Shao, C. Y., Howe, C. J., Porter, A. J., and Glover, L. A. (2002). Novel cyanobacterial biosensor for detection of herbicides. *Appl. Environ. Microbiol.* 68, 5026–5033. doi: 10.1128/AEM.68.10.5026-5033.2002
- Silver, S., and Phung, L. T. (1996). Bacterial heavy metal resistance: new surprises. *Annu. Rev. Microbiol.* 50, 753–789. doi: 10.1146/annurev.micro.50.1.753
- Sunda, W. G., and Lewis, J. M. (1978). Effect of complexation by natural organic ligands on the toxicity of copper to a unicellular alga, *Monochrysis lutheri*. *Limnol. Oceanogr.* 23, 870–876. doi: 10.4319/lo.1978.23.5.0870
- Szittner, R., and Meighen, E. (1990). Nucleotide sequence, expression, and properties of luciferase coded by lux genes from a terrestrial bacterium. *J. Biol. Chem.* 265, 16581–16587.
- Turner, J. S., Glands, P. D., Samson, A. C., and Robinson, N. J. (1996). Zn²⁺-sensing by the cyanobacterial metallothionein repressor SmtB: different motifs mediate metal-induced protein-DNA dissociation. *Nucleic Acids Res.* 24, 3714–3721. doi: 10.1093/nar/24.19.3714
- van der Meer, J. R., and Belkin, S. (2010). Where microbiology meets microengineering: design and applications of reporter bacteria. *Nat. Rev. Microbiol.* 8, 511–522. doi: 10.1038/nrmicro2392
- Waldron, K. J., Rutherford, J. C., Ford, D., and Robinson, N. J. (2009). Metalloproteins and metal sensing. *Nature* 460, 823–830. doi: 10.1038/nature08300
- Wei, Y., Zhu, N., Lavoie, M., Wang, J., Qian, H., and Fu, Z. (2014). Copper toxicity to *Phaeodactylum tricorutum*: a survey of the sensitivity of various toxicity endpoints at the physiological, biochemical, molecular and structural levels. *Biometals* 27, 527–537. doi: 10.1007/s10534-014-9727-6

Conflict of Interest Statement: The authors declare that the research was conducted in the absence of any commercial or financial relationships that could be construed as a potential conflict of interest.

Copyright © 2015 Martín-Betancor, Rodea-Palomares, Muñoz-Martín, Leganes and Fernández-Piñas. This is an open-access article distributed under the terms of the Creative Commons Attribution License (CC BY). The use, distribution or reproduction in other forums is permitted, provided the original author(s) or licensor are credited and that the original publication in this journal is cited, in accordance with accepted academic practice. No use, distribution or reproduction is permitted which does not comply with these terms.

**S M
U A
P T
P E
L R
E I
M A
E L
N
T
A
R
Y**

Supplementary Material:

Construction of a self-luminescent cyanobacterial bioreporter that detects a broad range of bioavailable heavy metals in aquatic environments

Keila Martín-Betancor, Ismael Rodea-Palomares, M.A. Muñoz-Martin, Francisco Leganés, Francisca Fernández-Piñas*

Department of Biology, Facultad de Ciencias, Universidad Autónoma de Madrid, 28049 Madrid, Spain

*Corresponding author: Francisca Fernández-Piñas

Mailing address: Departamento de Biología, Facultad de Ciencias, Universidad Autónoma de Madrid. C/ Darwin, 2. 28049, Madrid. Spain.

E-mail: francisca.pina@uam.es

Table of contents:

Supplementary Material Table S1: BG11 medium composition

Supplementary Material Table S2: Heavy metals speciation predicted by Visual MINTEQ

Supplementary Material Table S3: EC₅₀ values of heavy metals towards *Synechococcus* sp. PCC 7942 pBG2120

Supplementary Material Table S4: Comparison of the performance of *Synechococcus* sp. PCC 7942 pBG2120 with other microbial bioreporter assays

Supplementary Material Figure S1: Location of Guadalix River and Alcalá WWTP samples sites

Supplementary Material Figure S2: Performance of *Synechococcus* sp. PCC 7942 pBG2120 with non-inducible heavy metals

Table S1. BG11 medium composition

Composition	Final Concentration (μM)
$\text{MgSO}_4 \cdot 7 \text{H}_2\text{O}$	200
$\text{CaCl}_2 \cdot 2 \text{H}_2\text{O}$	240
NaNO_3	18000
$\text{K}_2\text{HPO}_4 \cdot 3 \text{H}_2\text{O}$	230
EDTA (Tritiplex III)	2.8
Citric acid $\cdot \text{H}_2\text{O}$	31
Ammonium-iron (III) citrate	20
Na_2CO_3	190
H_3BO_3	46
$\text{MnCl}_2 \cdot 4 \text{H}_2\text{O}$	9.1
$\text{ZnSO}_4 \cdot 7 \text{H}_2\text{O}^*$	0.77
$\text{Na}_2\text{MoO}_4 \cdot 2 \text{H}_2\text{O}$	1.6
$\text{CuSO}_4 \cdot 5 \text{H}_2\text{O}^*$	0.32
$\text{Co}(\text{NO}_3)_2 \cdot 6 \text{H}_2\text{O}^*$	0.17
MOPS	2 mM
pH = 7.5	

*Modified medium lacking Co, Ni and Cu was used for bioluminescence assays.

Table S2. Predicted percentages of metal present as free ion and other main chemical species as predicted by Visual MINTEQ for inducing and not inducing metals used. The chosen concentration for all metals is 1 μ M.

Inducing metals	Zn	Cd	Ag	Cu	Hg	Co
	18.594 Zn ²⁺	50.347 Cd ²⁺	57.422 Ag ⁺	1.052 Cu ²⁺	99.989 HgEDTA ²⁻	87.694 Co ²⁺
	7.889 ZnOH ⁺	1.370 CdCl ⁺	40.055 AgCL AQ	0.714 CuCO ₃ AQ		12.306CoEDTA ²⁻
	0.167 Zn(OH) ₂ AQ	1.299 CdNO ₃ ⁺	2.003 AgCL ₂ ⁻	0.436 CuOH ⁺		
	0.240 ZnSO ₄ AQ	0.856 CdSO ₄ AQ	0.119 AgSO ₄ ⁻	9.923 Cu(OH) ₂ AQ		
	1.921 ZnHPO ₄ AQ	4.132 CdHPO ₄ AQ	0.399 AgNO ₃ AQ	34.017 CuEDTA ²⁻		
	0.480 ZnCO ₃ AQ	0.626 CdHCO ₃ ⁺		53.683 Cu-		
	65.861 ZnCITRATE	28.584 CdCITRATE		CITRATE		
	4.090 ZnEDTA ²⁻	12.596 CdEDTA ²⁻				
Not inducing metals	Pb	Mg	Ni	Fe	Ba	Sr
	9.786 Pb ²⁺	93.694 Mg ²⁺	2.681 Ni ²⁺	15.403 Fe ²⁺	96.828 Ba ²⁺	100.000 Sr ²⁺
	4.057 PbOH ⁺	0.109 MgHCO ₃ ⁺	2.571 NiCO ₃ AQ	58.239 FeOH ⁺	3.172 BaCITRATE	
	1.490 PbNO ₃ ⁺	0.977 MgSO ₄ AQ	31.7 NiCITRATE	0.231 FeH ₂ PO ₄ ⁺		
	21.977 PbCO ₃ AQ	0.321 MgPO ₄ ⁻	62.872 NiEDTA ²⁻	3.175 FeHPO ₄ AQ		
	0.732 PbHCO ₃ ⁺	4.129 MgHPO ₄ AQ		21.982 FeCITRATE		
	0.611 Pb-CITRATE	0.648 Mg-CITRATE				
	60.275 PbEDTA ²⁻					

Table S3. Toxicity of heavy metals towards *Synechococcus* sp. PCC 7942 pBG2120 expressed as EC₅₀ values (μM) ± standard deviation after 20 h of exposure time

Metal	<i>Synechococcus</i> sp. PCC 7942 pBG2120 EC ₅₀ (μM)
Zn ²⁺	1.6±0.15
Cd ²⁺	2.37±0.56
Ag ⁺	0.41±0.18
Hg ²⁺	59.5±5.44 (pM)
Cu ²⁺	0.026±0.003
Co ²⁺	0.67±0.21

Table S4. Comparison of the performance of *Synechococcus* sp. PCC 7942 pBG2120 with other microbial bioreporter assays

Promoter	Element	Reporter gene	Host	Linear response (μM)	Time of induction	Medium	Reference
<i>smt</i>	Hg ²⁺	LuxCDABE (<i>P.luminescens</i>)	<i>Synechococcus</i>	11-72 (pM)	240 min	BG-11	This study
	Cu ²⁺			0.027-0.05			
	Ag ⁺			0.05-0.29			
	Co ²⁺			0.88-2.66			
	Zn ²⁺			0.97-2.04			
	Cd ²⁺			1.54-5.35			
<i>smt</i>	Zn ²⁺	<i>LuxCDABE (A.fischeri)</i>	<i>Synechococcus</i>	0.5-2	240 min	BG-11	(Erbe et al., 1996)
	Cd ²⁺			0.5-1.5	60 min		
	Cu ²⁺			2-4	120 min		
<i>MTT5</i>	As ⁵⁺	<i>lucFF</i> (Firefly)	<i>T.termophila</i>	25·10 ⁻³ (LOD)	120 min	Tris-HCl	(Amaro et al., 2011)
	Zn ²⁺			1.5-4.6·10 ⁶			
	Cd ²⁺			5·10 ⁻³ -27			
	Hg ²⁺			2.5·10 ⁻² -7.5			
	Pb ²⁺			5·10 ⁻² -1.5·10 ³			
	Cu ²⁺			1.5-2.2·10 ³			
<i>MTT1</i>	As ⁵⁺	<i>lucFF</i> (Firefly)	<i>T.termophila</i>	50·10 ⁻³ (LOD)	120 min	Tris-HCl	(Amaro et al., 2011)
	Zn ²⁺			0.5-2.29·10 ³			
	Cd ²⁺			2.5·10 ⁻² -8.9			
	Hg ²⁺			2.5·10 ⁻² -5			
	Pb ²⁺			0.5-2.4·10 ²			
	Cu ²⁺			2.5-7.9·10 ²			
<i>coaT</i>	Zn ²⁺	<i>luxAB (A.harveyi)</i>	<i>Synechocystis</i>	1-3		BG-11	(Peca et al., 2008)
	Co ²⁺			0.3-6	180 min		
<i>copA</i>	Ag ⁺	<i>luxCDABE (A.fischeri)</i>	<i>E.coli</i>	0.3-3	80 min	GGM minimal	(Riether et al., 2001)
	Cu ²⁺			3-30			
<i>zntA</i>	Zn ²⁺	<i>lucFF</i> (Firefly)	<i>E.coli</i>	40-15000	120 min	M9	(Ivask et al., 2002)
	Cd ²⁺			0.05-30			

	Hg ²⁺			0.01-1			
<i>merR</i>	Cd ²⁺	<i>lucFF</i> (Firefly)	<i>P.fluorescens</i>	1-10	120 min	PBS	(Petanen et al., 2001)
	Hg ²⁺			10 ⁻⁵ -0.1			
<i>copA</i>	Cd ²⁺	<i>luxCDABE</i> (<i>A.fischeri</i>)	<i>E.coli</i>	0.05 (LOD)		Acetate	(Charrier et al., 2011)
	Hg ²⁺			5 (LOD)			
	Ag ⁺			0.5 (LOD)			

LOD : limit of detection

Amaro, F., Turkewitz, A.P., Martin-Gonzalez, A., and Gutierrez, J.C. (2011). Whole-cell biosensors for detection of heavy metal ions in environmental samples based on metallothionein promoters from *Tetrahymena thermophila*. *Microb Biotechnol* 4, 513-522.

Charrier, T., Durand, M.J., Jouanneau, S., Dion, M., Perneti, M., Poncelet, D., and Thouand, G. (2011). A multi-channel bioluminescent bacterial biosensor for the on-line detection of metals and toxicity. Part I: design and optimization of bioluminescent bacterial strains. *Anal Bioanal Chem* 400, 1051-1060.

Erbe, J.L., Adams, A.C., Taylor, K.B., and Hall, L.M. (1996). Cyanobacteria carrying an *smt-lux* transcriptional fusion as biosensors for the detection of heavy metal cations. *J Ind Microbiol* 17, 80-83.

Ivask, A., Virta, M., and Kahru, A. (2002). Construction and use of specific luminescent recombinant bacterial sensors for the assessment of bioavailable fraction of cadmium, zinc, mercury and chromium in the soil. *Soil Biology and Biochemistry* 34, 1439-1447.

Peca, L., Kos, P.B., Mate, Z., Farsang, A., and Vass, I. (2008). Construction of bioluminescent cyanobacterial reporter strains for detection of nickel, cobalt and zinc. *FEMS Microbiol Lett* 289, 258-264.

Petanen, T., Virta, M., Karp, M., and Romantschuk, M. (2001). Construction and Use of Broad Host Range Mercury and Arsenite Sensor Plasmids in the Soil Bacterium *Pseudomonas fluorescens* OS8. *Microb Ecol* 41, 360-368.

Riether, K.B., Dollard, M.A., and Billard, P. (2001). Assessment of heavy metal bioavailability using *Escherichia coli* *zntAp::lux* and *copAp::lux*-based biosensors. *Appl Microbiol Biotechnol* 57, 712-716.

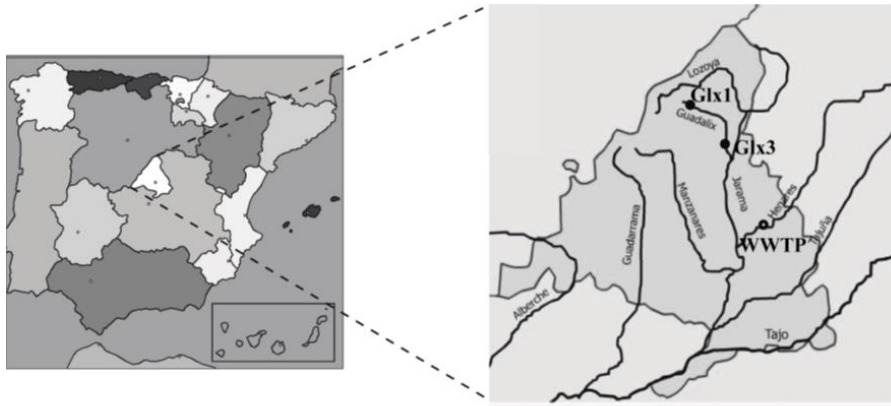


Figure S1. Location of the Guadalix river and Alcalá de Henares wastewater treatment plant and sampling sites Guadalix 1 and 2 (Glx1 and Glx2) and Alcalá de Henares wastewater treatment plant (WWTP)

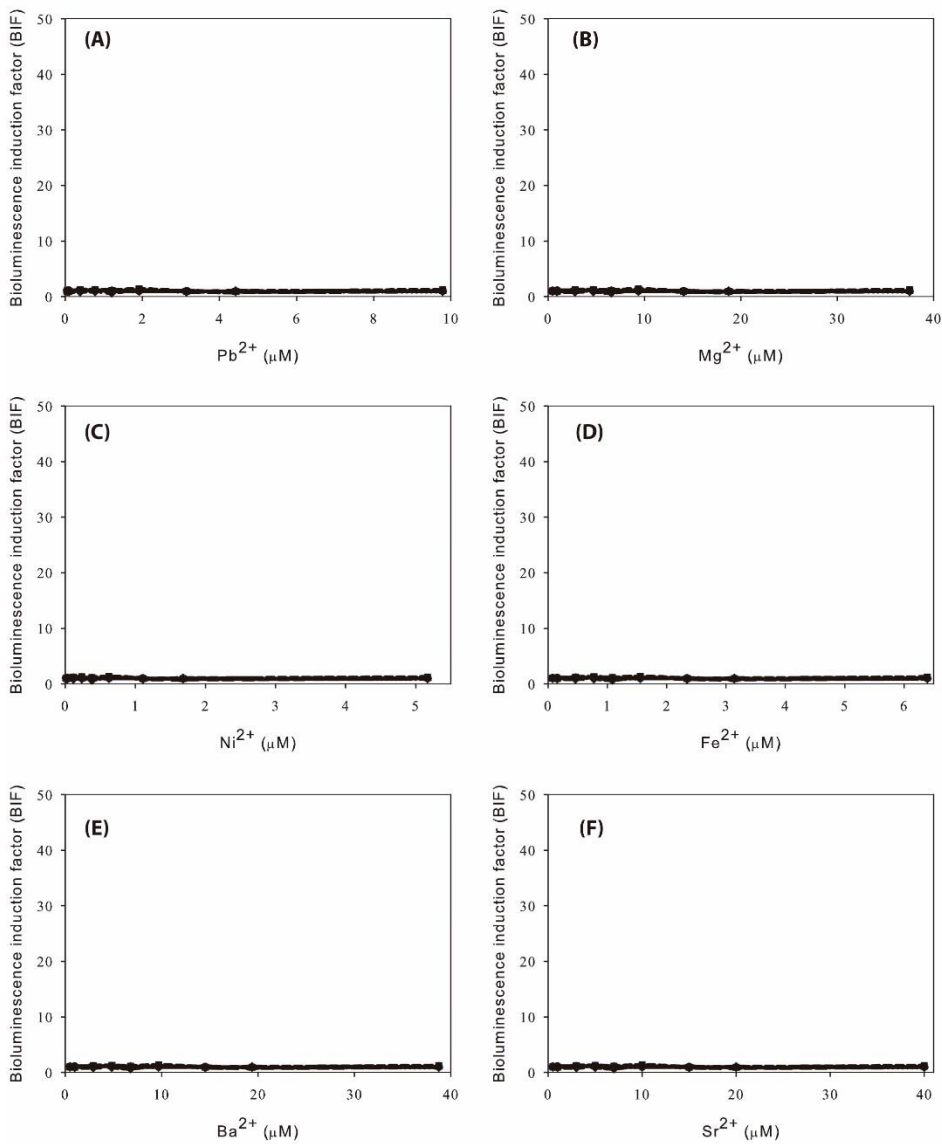


Figure S2. Lack of inducibility of the cyanobacterial bioreporter by Pb, Mg, Ni, Fe, Ba and Sr. Time of exposure from 1-6 h.

**Defining an additivity
framework for mixture
research in inducible whole-
cell biosensors**

C

H

A

P


T

E

R

III

SCIENTIFIC REPORTS



OPEN

Defining an additivity framework for mixture research in inducible whole-cell biosensors

K. Martin-Betancor¹, C. Ritz², F. Fernández-Piñas¹, F. Leganés¹ & I. Rodea-Palomares¹

Received: 14 July 2015

Accepted: 27 October 2015

Published: 26 November 2015

A novel additivity framework for mixture effect modelling in the context of whole cell inducible biosensors has been mathematically developed and implemented in R. The proposed method is a multivariate extension of the *effective dose* (ED_p) concept. Specifically, the extension accounts for differential maximal effects among analytes and response inhibition beyond the maximum permissive concentrations. This allows a multivariate extension of *Loewe additivity*, enabling direct application in a biphasic dose-response framework. The proposed additivity definition was validated, and its applicability illustrated by studying the response of the cyanobacterial biosensor *Synechococcus elongatus* PCC 7942 pBG2120 to binary mixtures of Zn, Cu, Cd, Ag, Co and Hg. The novel method allowed by the first time to model complete dose-response profiles of an inducible whole cell biosensor to mixtures. In addition, the approach also allowed identification and quantification of departures from additivity (interactions) among analytes. The biosensor was found to respond in a near additive way to heavy metal mixtures except when Hg, Co and Ag were present, in which case strong interactions occurred. The method is a useful contribution for the whole cell biosensors discipline and related areas allowing to perform appropriate assessment of mixture effects in non-monotonic dose-response frameworks

The prediction of the expected effect of chemical mixtures when only the effect of individual components is known is a hot topic in pharmacology, toxicology, and ecotoxicology^{1–3}. A central element in mixture research is the definition and mathematical formulation of additivity^{2,4,5}. At present, there are two sound pharmacological definitions of additivity: *Loewe additivity*⁶ and *Bliss independence*⁷, which are the foundations of the so-called *Concentration addition* (CA) and *Independent Action* (IA) additivity models, respectively⁸. Departures from *Loewe additivity* can be quantitatively studied based on the *Combination Index* (CI)^{4,9}. The crucial prerequisite for the applicability of any additivity model is to fulfill certain mathematical assumptions⁵. The basic mathematical feature of *Loewe additivity* is that the effects of the mixture components could be formulated in terms of a common *effective dose* (ED_p). For instance, this requisite is trivially met when all individual mixture components present identical maximal effects, (see Fig. 1a). An important complication occurs with mixtures of chemicals that show differential maximal effects: When this happens, additivity hypothesis can only be formulated up to the effect levels achieved by the less potent compound present in the mixture due to inherent mathematical features of the additivity definition⁵ (Fig. 1b). An additional challenge for formulating the additivity hypothesis occurs when the studied response is susceptible to result in non-monotonic biphasic dose-response patterns (see Fig. 1c). Besides, in biphasic dose-response curves, two different concentrations can result in the same *fractional effect* (Fig. 1c), resulting in misleading conclusions⁵. These problems have hampered the applicability of additivity models in important areas where differential maximal effects and biphasic dose-response patterns are commonly observed, such as in hormetic effects¹⁰, hormone agonists/antagonists research¹¹,

¹Departament of Biology, Facultad de Ciencias, Universidad Autónoma de Madrid, 28049 Madrid, Spain.

²Department of Nutrition, Exercise and Sports, Faculty of Science, University of Copenhagen, Rolighedsvej 30, DK-1958 Frederiksberg C, Denmark. Correspondence and requests for materials should be addressed to I.R.-P. (email: ismael.rodea@uam.es)

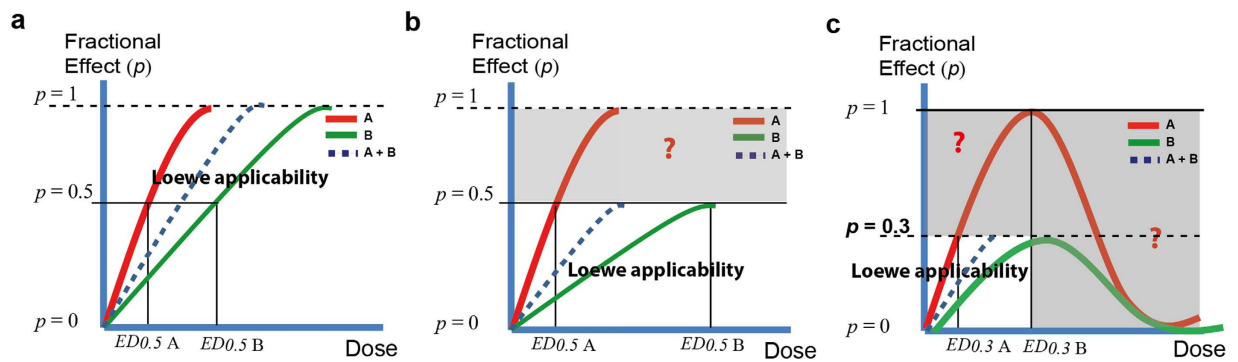


Figure 1. Applicability of Loewe additivity. Typical dose-response profiles for (a) classical monotonic dose-response curves for chemicals A and B showing identical maximal effects, (b) classical monotonic dose-response curves for chemicals A and B presenting differential maximal effects, and (c) biosensor type biphasic dose-response curves for chemicals A and B presenting differential maximal effects and toxicity threshold. The meanings of the terms presented in the figure can be found in theory section.

AhR agonists/antagonists activity research⁵, endocrine disruptors activity research^{12,13}, and in general in the field of inducible (turn-on) whole cell biosensors.

To overcome these bottlenecks, some authors recently suggested the need for a formal mathematical expansion of the additivity formulations that may allow working with differential maximal effects^{14,15}. Other authors have proposed a pragmatic numerical approximation based on a toxic unit extrapolation method to solve the problem⁵.

Inducible whole cell biosensors are a paradigmatic case of a biological system displaying differential maximal effects and usually biphasic dose-response profiles (e.g.,¹⁶) (Fig. 1c). Whole cell biosensors are intact, living cells genetically engineered to produce a dose-dependent measurable signal in response to a specific chemical or physical stimulus in their environment¹⁷. Inducible whole cell biosensors response is usually characterized by a dose-dependent biphasic profile presenting an induction region up to a concentration threshold (*maximum permissive concentration*), and a subsequent inhibition region where the biosensor response decays, possibly due to the inherent toxicity of the analyte above certain concentrations which affects cell viability¹⁸. Whole cell biosensors have been extensively used in the last 3 decades for the detection and quantification of different analytes and stresses of interest (for a review see^{17,19}). Despite they have a clear vocation to be applicable in realistic conditions, mixture effect research using inducible whole-cell biosensors is presently a poorly developed research area. From our point of view, the main reason is the lack of a founded theoretical basis and experimental additivity framework.

In the present work, a novel additivity framework for mixture research in the context of whole cell inducible biosensors has been mathematically developed. The method proposes a multivariate extension of the *effective dose* (ED_p) to take into account the occurrence of differential maximal effects and inhibition beyond the MPCs. In effect, this allows an extension of *Loewe additivity* that enables its direct application in a biphasic dose-response framework. A family of user friendly utilities has been incorporated in the (*drc*) package²⁰ for R. The method has been illustrated studying the response of the cyanobacterial biosensor *Synechococcus elongatus* PCC 7942 pBG2120 to binary mixtures of 6 heavy metals (Zn, Cu, Cd, Ag, Co and Hg). *Synechococcus* sp. PCC 7942 pBG2120 bears a fusion of the promoter region of the *smt* locus of *Synechococcus* sp. PCC 7942 to the *luxCDABE* operon of *Photobacterium luminescens*. It is an inducible self-luminescent *whole cell* biosensor able to respond to a broad range of heavy metal cations which present differential maximal effects and biphasic dose-response curves¹⁶. The method is a useful contribution for the entire whole-cell biosensors discipline and related areas which allows to perform sound mixture-effect research in the framework of biphasic dose-response curves.

Theory

A novel framework for mixture-effect research for whole cell biosensors. We propose a novel framework for modelling mixture effects in *whole cell biosensors* showing biphasic dose-response curves. It is characterized by the following 5 steps: (1) Fitting biphasic dose-response profiles. (2) A dimensional extension of the *effective dose* notation. (3) *Two-dimensional formulation of Loewe additivity*. (4) Prediction of mixture effects based on individual component biphasic dose-response data. (5) Analysis of departures from additivity.

Fitting biphasic dose-response profiles. Inducible whole cell biosensors usually present inverted *v-shaped* biphasic dose-response profiles (Fig. 1c). This specific type of dose-response pattern may be fitted using nonlinear regression model equations Gaussian and LogGaussian. We considered 2 specific inverted *v-shaped* functions f : the *Gaussian* (Eq. 1 below) and the *log Gaussian* (Eq. 2 below) equations, which are defined as follows:

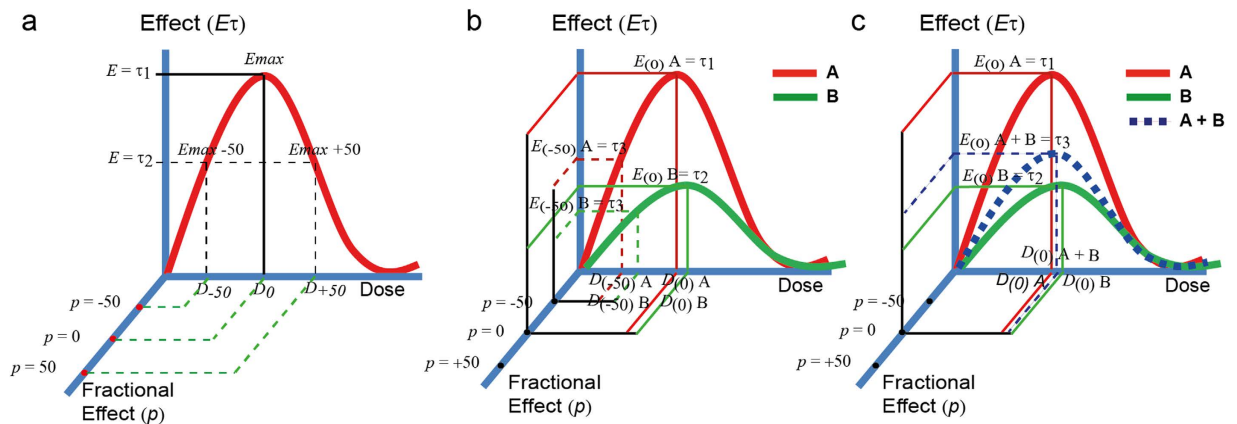


Figure 2. The bi-dimensional fractional effect notation. (a) Fractional effective doses ED_p in biphasic dose-response systems is proposed to be scaled as fractions (p) of the E_{max} defining the fractional effect scale (Ep). The empirical effect scale ($E_{(\tau)}$), in the y axis is decoupled from the fractional effect scale (Ep) which is projected in the z plane. This allows to define fractional effects covering the entire biphasic dose-response curve. (b) The proposed fractional effective notation allows to scale in a common fractional effect scale stimuli A and B showing differential maximal effects. (c) An additive biphasic dose response pattern “A + B” can be formulated for a theoretical mixture of A and B based on the univocal relationship of the fractional effect scale (Ep) with the other two dimensions: $D_{(p)}$ and $E_{(p)}$. For notation meanings in the Figures see section 2.

$$f(x) = c + (d - c) \cdot \exp(-0.5 \cdot \{(x - e)/b\}^f) \tag{1}$$

$$f(x) = c + (d - c) \cdot \exp(-0.5 \cdot |\{\log(x) - \log(e)\}/b|^f) \tag{2}$$

where the parameters c and d correspond to the limits for $x=0$ and x tending to infinity and the parameters b and e control the steepness of the curve and location of the peak, respectively. The parameter f describes asymmetry in the curve (i.e., asymmetry between the left and right sides of the peak).

A multivariate extension of the effective dose notation. In the present work, a notation for fractional effective doses ED_p scaled from the MPCs (hereafter, E_{max}) has been chosen (Fig. 2a). The novelty of the approach is that we maintain the empirical effect scale ($E_{(\tau)}$) in the y axis, and we project the fractional effect scale ($Ep_{(p)}$) in the z plane (see Fig. 2a). Fractional effects (p) in the Ep scale are defined as follows: $-100 \leq p \leq 100$. For $p < 0$, fractional effects on the left side of the E_{max} are obtained (Fig. 2a) (the induction part of the curve), for $p > 0$, fractional effects on the right side of the E_{max} are obtained (the inhibition part of the dose-response curve). $p = 0 = E_{max} = MPC$. Decoupling the fractional effect scale ($Ep_{(p)}$) from the empirical effect ($E_{(\tau)}$) allows to scale inverted v -shaped dose-response curves with differential maximum effects in a unique fractional scale independently of the maximum level of effect (E_{max}) attained (Fig. 2b). However, ED_p needs to be dimensionally extended to account for differences in both the dose (D) and effect (E) scales (Fig. 2b). Therefore we define ED_p as a two-dimensional vector $(D_{(p)}, E_{(p)})$ where $D_{(p)}$ is the dose required to get the desired fractional effect (p) (i.e. 50%), and $E_{(p)}$ is the effect in the empirical effect scale ($E(\tau)$) achieved at this fractional effect (p).

Two-dimensional formulation of Loewe additivity. For classical monotonic dose-response curves, a uni-dimensional effective dose-notation and additivity formulation are enough to perform accurate additive predictions. In the same way that the fractional notation (ED_p) needs to be extended to set a proper common fractional effect scale in biphasic dose-response curves, the existing additivity formulation needs to be extended as well. For this we propose a two-dimensional formulation of *Loewe additivity* computed for the two components of $ED_p = (D_{(p)}, E_{(p)})_p$ (Fig. 2c). The additivity formulation on the dose (D) scale is identical to the original *Loewe additivity* formulation. For notational convenience, we will formulate hereafter *Loewe additivity* as follows:

$$\frac{D_A}{(D_{(p)})_A} + \frac{D_B}{(D_{(p)})_B} = CI_{Dp} \tag{3}$$

where D_A and D_B are the doses of the components A and B which in combination produces a fractional effect p on the measured biological response. $(D_{(p)})_A$ and $(D_{(p)})_B$ are the doses that individually result in a fractional effect p for the components A and B, respectively. In case (Eq. 3) equals 1 *Loewe additivity* holds. Otherwise, Combination Index Theorem holds⁴. If CI_{Dp} denotes the Combination Index in the D dimension (see Fig. 2c) for the considered fractional effect p , $CI_{Dp} < 1$ indicates synergism, $CI_{Dp} > 1$ indicates antagonism. To project *Loewe additivity* to the empirical effect dimension ($E(\tau)$), we simply assume that the effect (E) dimension is equivalent to the Dose (D) dimension in its relationship with the fractional effect (Ep) dimension (Fig. 2c). Therefore, it holds that *Loewe additivity* is computed in the E dimension as follows:

$$\frac{E_A}{(E_{(p)})_A} + \frac{E_B}{(E_{(p)})_B} = CI_{Ep} \quad (4)$$

where E_A and E_B are the effects (in the empirical scale (τ)) of the components A and B which in combination results in a fractional effect p on the measured biological response. $(E_{(p)})_A$ and $(E_{(p)})_B$ are the effects in the empirical effect scale of the components A and B resulting individually in the desired fractional effect p . CI_{Dp} is the Combination Index in the E dimension for the considered fractional effect p .

The proposed two-dimensional formulations are susceptible of extension to n components as follows:

$$\sum_{i=1}^n \frac{D_i}{(D_{(p)})_i} = CI_{Dp} \quad (5)$$

$$\sum_{i=1}^n \frac{E_i}{(E_{(p)})_i} = CI_{Ep} \quad (6)$$

where D_i is the dose of the i^{th} component which in combination produces a fractional effect p . $(D_{(p)})_i$ is the dose of the i^{th} components that individually produces the same fractional effect p . E_i is the effect (τ) of the i^{th} component which in combination produces a fractional effect p . $(E_{(p)})_i$ is the effect (τ) of the i^{th} components that individually produce the same fractional effect p . Thus, CI_{Dp} and CI_{Ep} are the combination index scores for the D and E dimensions at any fractional effect p .

Predictions of the joint effect of a mixture under two-dimensional Loewe additivity.

Equation (5) for $CI_{Dp} = 1$ can be rewritten in a predictive formulation (allowing for *in-silico* predictions of the joint effect of n mixture components based on individual chemical information only) according to Faust, *et al.*²¹, if D_i are expressed as relative proportions j_i of the total dose (D_{mix}), where $j_i = D_i/D_{mix}$. Under the condition that the mixture elicits a p total fractional effect, the total dose of the mixture D_{mix} is defined as the effective dose of the mixture (D_{pmix}) required to produce a fractional effects p . If $CI = 1$, $\Rightarrow D_i$ can be substituted in Eq. (5) by $j_i D_{pmix}$, and by rearrangement, it holds:

$$D_{pmix} = \left(\sum_{i=1}^n \frac{j_i}{D_{pi}} \right)^{-1} \quad (7)$$

According to Gonzalez-Pleiter, *et al.*²², equation (5) can be similarly rewritten as follows when $CI \neq 1$:

$$D_{pmix} = \left(\sum_{i=1}^n \frac{j_i}{D_{pi} \cdot CI_{Dp}} \right)^{-1} \quad (8)$$

Considering the proposed two-dimensional notation $ED_p = (D_{(p)}, D_{(p)})$, the formulation of Equation (7) in the E dimension gives:

$$E_{(p)mix} = \left(\sum_{i=1}^n \frac{j_i}{E_{(p)i}} \right)^{-1} \quad (9)$$

In case $CI \neq 1$:

$$E_{(p)mix} = \left(\sum_{i=1}^n \frac{j_i}{E_{(p)i} \cdot CI_{Ep}} \right)^{-1} \quad (10)$$

Analysis of departures from additivity. The definition in equations (5) and (6) also allows investigating departures from additivity in biphasic dose-response systems. The result from evaluating

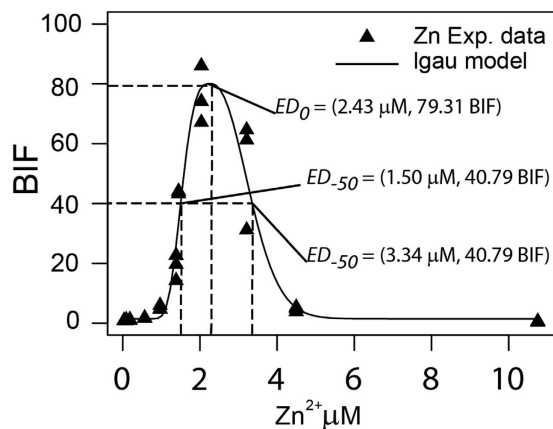


Figure 3. Fitting biphasic profiles with non-linear regression models. Experimental response of *Synechococcus elongatus* PCC 7942 pBG2120 to increasing concentrations of Zn^{2+} . Best fit model for Zn^{2+} logGaussian “lgau2” (see Supplementary Material SM 1) is presented in the figure. Position of selected ED_p vectors ($-50, 0, +50$) are marked in the figure.

equations (5) and (6) are two numerical values of the Combination Index (CI) for the D and E dimensions, which can be expressed as a two-dimensional vector $CI_{p(D,E)} = (CI_{Dp}, CI_{Ep})$. This approach yields 9 theoretical combinations of $CI_{p(D,E)}$ as follows: $CI_{p(D,E)} = (1, 1)$; $(1, <1)$; $(1, >1)$; $(<1, 1)$; $(<1, <1)$; $(<1, >1)$; $(>1, >1)$; $(>1, 1)$; $(>1, <1)$.

For global assessment of departures from additivity, a simplification of the two-dimensional information can be obtained by calculating a weighted index CI_{wp} for any fractional effect p as follows:

$$CI_{wp} = CI_{Dp} \cdot CI_{Ep} \quad (11)$$

where $CI_{wp} > 1$ indicates overall antagonism, $CI_{wp} = 1$ an overall additive effect, and $CI_{wp} < 1$, an overall synergistic effect.

Results

Dose-response profiles of *Synechococcus elongatus* PCC 7942 pBG2120 exposed to Zn, Cu, Cd, Ag, Co and Hg and their binary combinations were fitted using the proposed set of v -shaped non-linear functions described in Theory section. Best fit models for each metal and metal mixture were selected accordingly to the minimum of the residual sum of squares²⁰. Supplementary Material SM1 shows a summary of the selected model function and parameters for each individual metal and metal mixture. Overall, the majority of single metal experimental data were better fitted by log Gaussian function, and only Ag was fitted better by a Gaussian model. On the contrary, the responses of the biosensor to half of the binary metal mixtures were fitted better by Gaussian, and the other half by logGaussian model (see Supplementary Material SM1). Figure 3 shows as an example, the goodness of fit of the v -shaped non-linear function logGaussian “lgau2” to Zn response experimental data (see Supplementary Material SM1 for model parameters). As can be observed, the function fits adequately Zn experimental data at both the induction and the inhibition part of the dose-effect curve. Using the *drc* package we can get ED_p vectors ($D_{(p)}, E_{(p)}$) at any desired fractional effect p . For example, we can calculate the Zn $ED_{-50} = (1.50 \mu\text{M}, 40.79 \text{ BIF})$, Zn $ED_0 = (2.43 \mu\text{M}, 79.31 \text{ BIF})$ and the Zn ED_{+50} to be $(3.34 \mu\text{M}, 40.79 \text{ BIF})$ (Fig. 3) (definitions in Methods section). Since ED_p is two-dimensional, it includes not only the concentration required to produce a specific fractional effect p , but also the actual BIF that the biosensor signal achieves at this specific fractional effect for a specific analyte. A summary of ED_p vectors ($-50, 0, +50$) for the 6 metals can be found in Supplementary Material SM2. As can be seen, the bi-dimensional notation allows to explicitly predict concentrations of the analyte resulting in fractional effects in both the induction and the inhibition regions of the dose-response curves. An illustrative example on how to get ED_p vectors can be found in Supplementary Material SM3.

Once individual metal biphasic response profiles are adequately fitted, and ED_p vectors can be obtained to any fractional effect p , it is possible to predict the biosensor response to any combination of the individual metals evaluating Equations (7) and (9). However, prior to any further analysis, it is required to validate the proposed two-dimensional definition of *Loewe additivity*. Figure 4 shows predicted vs experimental dose-response patterns of sham binary mixtures for Zn:Zn, Cd:Cd and Cu:Cu. A near perfect overlap occurred between the experimental and predicted dose-response curves of sham mixtures for the 3 metals. This validates the proposed multivariate formulation of *Loewe additivity* model for biphasic dose-response curves, even at mixture concentrations where inhibition of the signal occurs (See Fig. 1b).

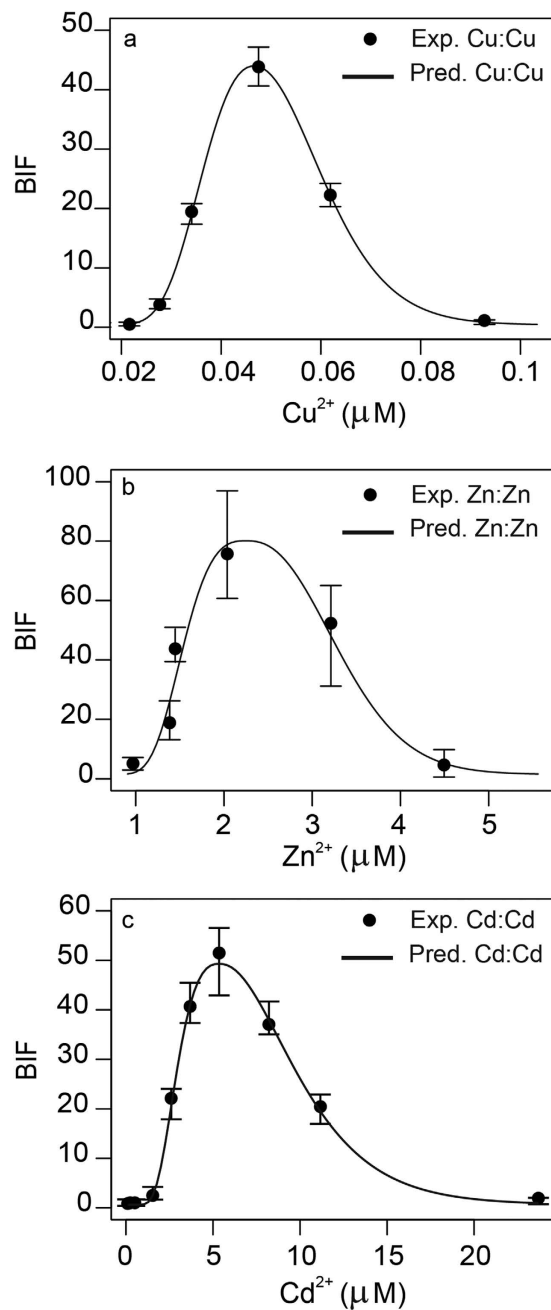


Figure 4. Validation of the additivity definition using sham mixtures. Predicted dose-response patterns of sham binary mixtures for (a) Cu:Cu, (b) Zn:Zn, (c) Cd:Cd. Predicted dose-response patterns were calculated solving the multivariate extension of *Loewe additivity* equation in predictive formulation (eqs (7) and (9)). Error bars are standard errors ($n = 3-4$).

Once the multivariate extension of *Loewe additivity* was validated with the sham mixtures, we applied the method to perform additivity predictions and to study the nature of the interaction (if any) of the response of *Synechococcus elongatus* PCC 7942 pBG2120 to the 15 possible binary mixtures of Zn, Cd, Cu, Ag, Hg and Co. Complete results of the analysis can be found in Supplementary Material SM5. A representative selection of the results is presented in Fig. 5. In the case of the binary mixture Cu:Zn (Fig. 5a), the additivity prediction fitted reasonably well the experimental *dose-response* profile. However, the additivity predictions of the binary mixtures Zn:Cd (Fig. 5b) and Zn:Co (Fig. 5c), deviated from their respective experimental *dose-response* pattern, suggesting a departure from additivity. However, which kind of departure are we observing?

To answer this question, a quantitative analysis of the nature of the interactions is required^{3,4}. Departures from additivity can be quantified solving Equations 5 and 6 for any fractional effect p . As illustrative example, we used *extended p-CI* plots to graphically present the results of the quantification

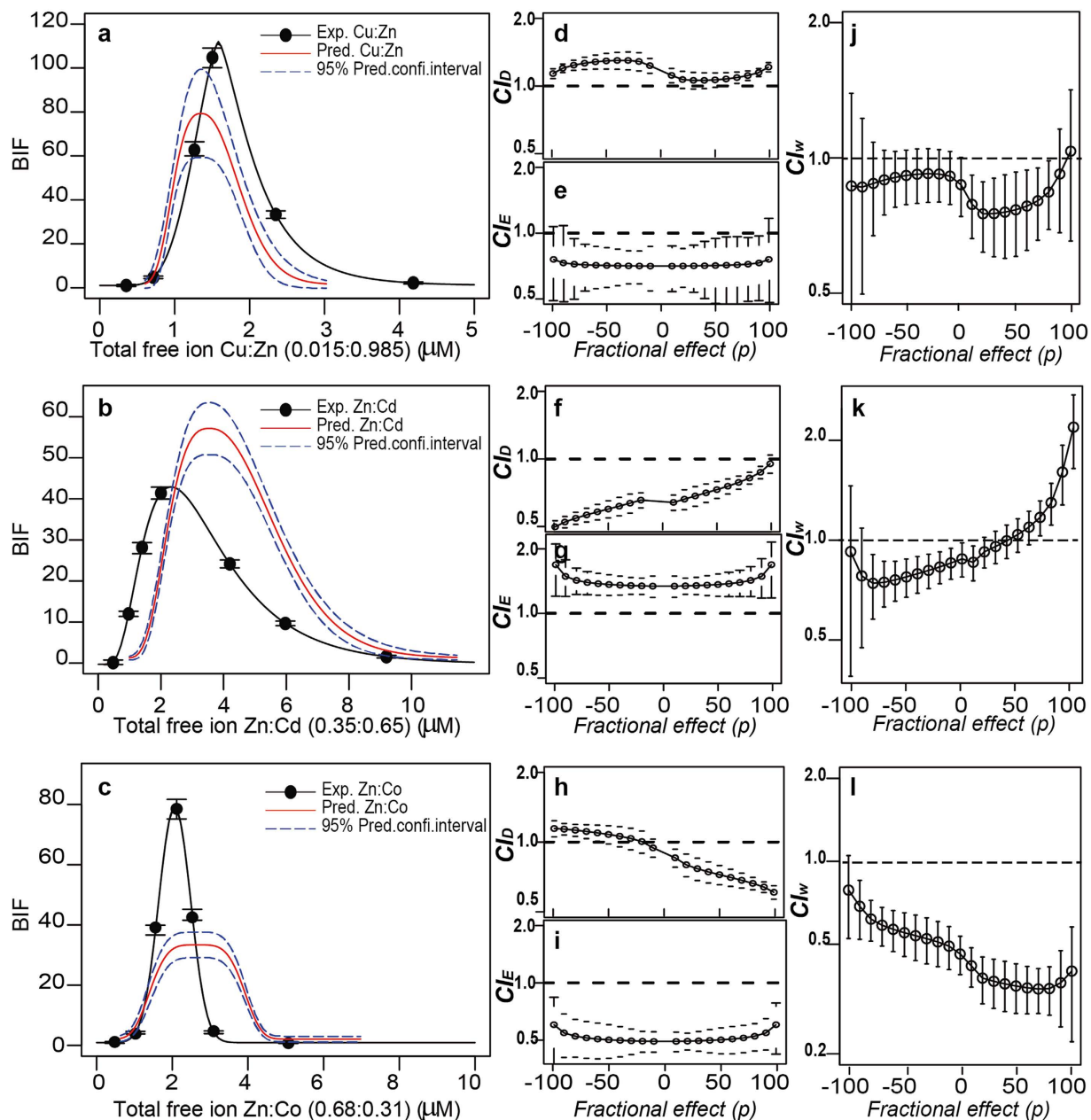


Figure 5. Analysis of departures from additivity. Experimental vs predicted (under additivity) dose-response patterns for Cu:Zn (a), Zn:Cd (b) and Zn:Co (c) binary mixture's, respectively. Extended p -CI plots presenting departures from additivity (as CI values) as a function of the effect level (p) for the D dimension of Cu:Zn (d), Zn:Cd (f) and Zn:Co (h). Extended p -CI plots presenting departures from additivity (as CI values) as a function of the effect level (p) for the E dimension of Cu:Zn (e), Zn:Cd (g) and Zn:Co (i). Extended p - CI_w plots presenting weighted departures from additivity (as CI_w values) as a function of the effect level (p) for Cu:Zn (j), Zn:Cd (k) and Zn:Co (l). Error bars are standard errors ($n=3-4$). Total free ion concentrations presented in the Figures are those of Supplementary Material SM2 presented as ED_0 in Supplementary Material SM2 corrected by MINTEQA2 calculations due to the presence of the two metals used in each mixture.

of the interactions of the three selected mixtures (Cu:Zn, Zn:Cd and Zn:Co). Extended p -CI plots allow to observe the nature of the interactions along the D and E dimensions covering the complete biphasic dose-response curves, representing the deviation from the additivity line ($CI=1$) for any fractional effect p . Figures 5d,f,h and Figure 5e,g,i show extended p -CI plots for the D and E dimensions (respectively), for the three selected metal binary mixtures (Cu:Zn, Zn:Cd and Zn:Co). Extended p -CI plots for D and E axis (Fig. 5d,e, respectively) for the Cu:Zn combination showed CI values near 1 (the additivity line)

along the entire range of fractional effects (p) in both dimensions, confirming the near additive behaviour of this metal combination. The Zn: Cd binary combination presented statistically significant synergism ($CI < 1, p < 0.05$) along the entire range of fractional effects (p) in the D dimension (Fig. 5f), but statistically significant antagonism ($CI > 1, p < 0.05$) in the E dimension (Fig. 5g). On the other hand, the Zn:Co combination showed a p -dependent interaction patterns in the dose (D) axis (going from antagonistic to synergistic), and consistent synergism ($CI < 1, p < 0.05$) in the effect (E) axis along the entire range of effect levels (p) (Fig. 5h,i). See Supplementary Material SM4 for specific p -values for three selected fractional effect levels ($-50, 0, +50$). Figure 5j–l showed *Extended p - CI_w plots* for the mixtures Cu:Zn, Zn: Cd and Zn:Co, respectively. *Extended p - CI_w plots* (see equation 11) can be used as a measure of the overall fitness to additivity of the response of a biosensor to mixtures of analytes. As can be seen in the Fig. 5j, the overall effect of the combination of Cu:Zn combination was additive, that of Zn: Cd combination was p -dependent (Fig. 5k), going from synergistic (below the MPC) to antagonistic (above the MPC). That of Zn:Co was consistently synergistic $CI < 0.5$ along the entire range of effect levels (p) (Fig. 5l).

The effect of the metal ratio on the predictive power of the multivariate extension of Loewe additivity was addressed for selected binary mixtures. Figure 6a–c shows the experimental dose-response patterns and the respective additivity predictions for the three different metal ratios (75:25, 50:50, 25:75, respectively) of the binary metal mixture Cu:Zn. *Extended p - CI plots* for the D and E dimensions for the different metal ratios are presented in Fig. 6d–i. In addition, *extended p - CI_w plots* are presented in Fig. 6j–l. The selection of metal ratios allows to specifically address the possibility of predicting the dose response patterns including metal combinations in which eventually one of the metal may be present below the MPC and the other above the MPC and vice versa. As can be seen in Fig. 6, the main features of the dose-response pattern of the 50:50 mixture of Cu:Zn (Fig. 6b), that is additivity in D , synergism in E , and overall additive effect ($CI_w > 0.5$) is essentially conserved in the 25:75 and the 75:25 ratio. The only differences were the occurrence of a slight tendency to synergism in D in the 25:75 ratio (Fig. 6h), and a slight tendency to synergism in both the 75:25 and 25:75 ratios based on CI_w (but still additive based on the management criterion: $0.5 < CI_w < 2$). Similar results were obtained for ratio variations for the mixture Zn: Cd (Supplementary Material SM4).

The analysis of the departures from additivity for the 15 possible binary combinations of the studied metals revealed a complex scenario where the 9 possible theoretical combinations of the $CI_{D,E}$ vectors anticipated in Theory section were actually found (Supplementary Material SM5). In order to get a global idea on the fitness to additivity of the response of the biosensor to the binary mixtures of metals, we computed CI_w values according to Equation (11) which were summarized as well as *polygonograms*⁴ (for p levels $-50, 0, +50$) in Fig. 7. Interestingly, additive or near additive effects (according to the management criterion: $0.5 < CI_w < 2$) hold for binary mixtures of Zn, Cd, Ag and Cu at the three representative p levels (Fig. 7). However, some mixtures containing Hg, Co and Ag resulted in significant departures from additivity: The mixtures Hg:Co and Hg:Ag resulted in synergism and antagonism, respectively at the three representative p levels ($-50, 0, +50$). In addition, some mixtures resulted in effect-level dependent departures from additivity: the mixture Co:Zn resulted in synergism at $p = 0$ and $p = +50$, and the mixture Ag: Cd resulted in synergism at $p = +50$.

Discussion

Here we present a theoretical framework which allows to perform sound mixture-effect research in inducible whole cell biosensors and related fields. To have a mathematical formulation of additivity is crucial in order to obtain accurate and comprehensive results in mixture research as demonstrated in the last 20 years in pharmacology and eco/toxicology^{2–4}. In these disciplines, *Loewe additivity* is the gold standard for additivity formulations^{2–4}. However, the practical applicability of *Loewe additivity* is historically hampered in biological systems presenting differential maximal effects and non-monotonic responses such as biphasic dose-response curves^{5,14}. In the present work we propose a multivariate extension of *Loewe additivity* which allows its application in the context of differential maximal effects and biphasic dose-response curves. The proposed methodology was validated and tested using the inducible whole-cell self-luminescent metal biosensor *Synechococcus elongatus* PCC 7942 pBG2120 as case study. Our solution is in agreement with the conceptual formulations which Belz, *et al.*¹⁴ proposed in order to extend the applicability of *Loewe additivity* in the context of hormesis (an stimulatory effect found at low doses of toxicants). They postulated that differential maximal hormetic effects among individual mixture components force the need to perform additivity formulations in both dose (D) and effect (E) dimensions independently. As solution, they proposed to use the original *Loewe* equation (Equ. 3) for predictions in the (D) dimension, but a simple summation of fractional effects for predictions in the E dimension. Their predictions were reasonable for the dose (D) dimension, but were, in their own words “more dubious” for the (E) dimension¹⁴. This is because their proposal of *Loewe additivity* formulation for the E dimension was not accurate. We have demonstrated with the sham mixtures that our definition (Eqs 4 and 6) is a true projection of *Loewe additivity* in the (E) dimension. Scholze, *et al.*⁵ recently proposed an elegant approach to the differential maximal effect problem. Since, without multivariate extension, it is impossible to solve *Loewe additivity* equation for systems presenting differential maximal effects, they proposed a numerical approximation as a solution. Basically, they constructed an extrapolated interval of mixture predicted effects based on reasonable maximal and minimal hypothetical contributions of the less potent mixture components. The method worked well with a biosensor based

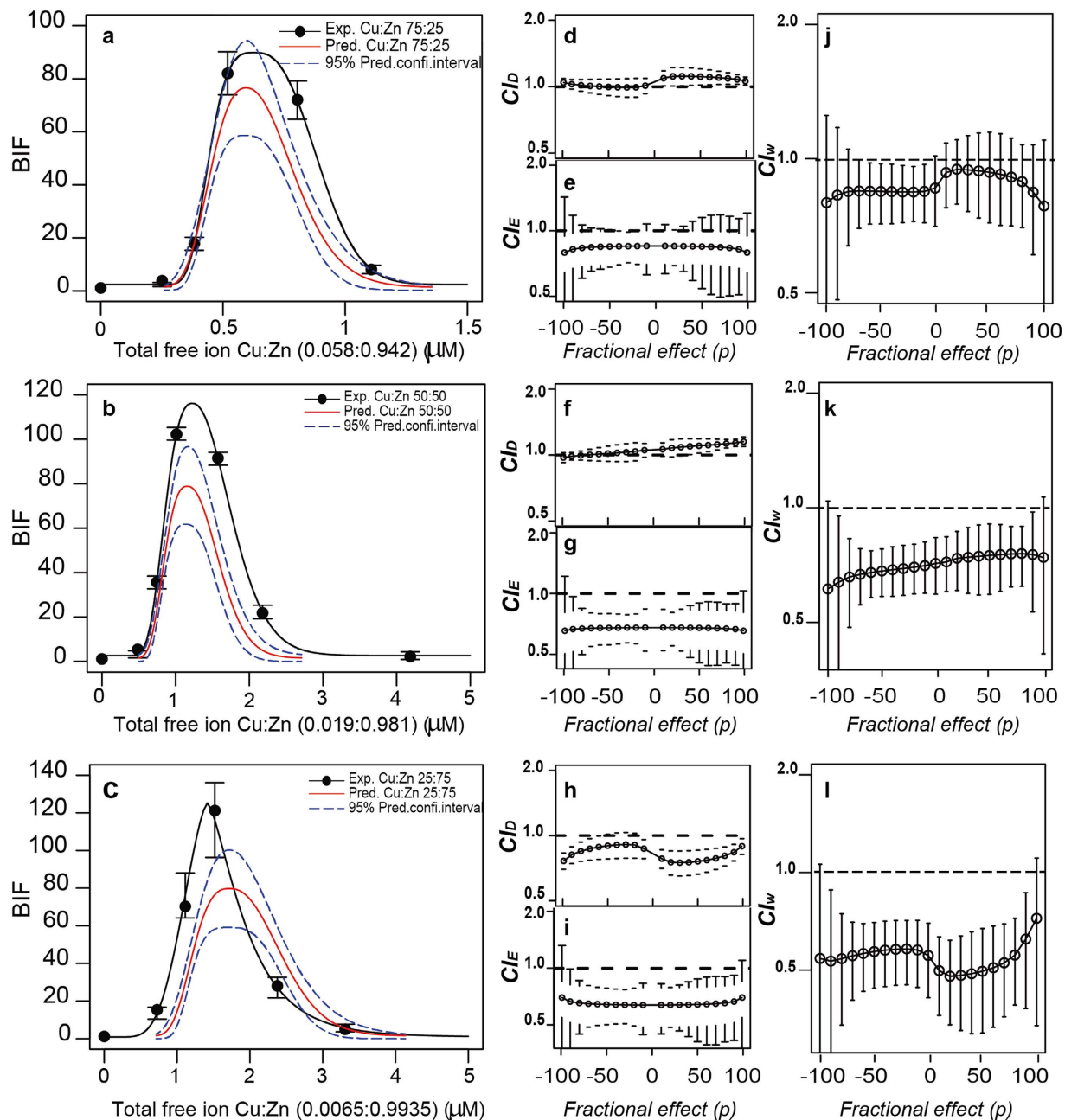


Figure 6. Effect of mixture ratio. Experimental vs predicted (under additivity) dose-response patterns for the mixture Cu:Zn at 75:25 (a), 50:50 (b) and 25:75 (c) ratios based on the D_0 concentration of the metals. Extended p -CI plots presenting departures from additivity (as CI values) as a function of the effect level (p) for the D dimension (d,f,h), and the E dimension (e,g,i). Extended p - CI_w plots presenting weighted departures from additivity (as CI_w values) as a function of the effect level (p) for the binary mixture Cu:Zn at 75:25 (j), 50:50 (k), 25:75 (l) mixture ratios. Error bars are standard errors ($n=3-4$). Total free ion concentrations presented in the Figures are those presented as ED_0 in Supplementary Material SM2 corrected by MINTEQ calculations due to the presence of the two metals used in each mixture.

on partial agonists of aryl hydrocarbon receptor (AhR) used for mixtures including components with varying maximal effects. However, they recognized that it cannot work in systems presenting inhibitory thresholds beyond the MPCs⁵.

The availability of a *Loewe additivity* formulation conceived for inducible whole-cell biosensors is an important milestone in this field of research which may allow for a wider generalization of mixture-effect research. This is especially true if a user friendly utility is available. We have made available all the presented mathematical equations, statistical and graphical utilities in the “dose-response curve” (*drc*) package for R²⁰. Currently the methodology is presently set up for binary mixtures, and only two biphasic

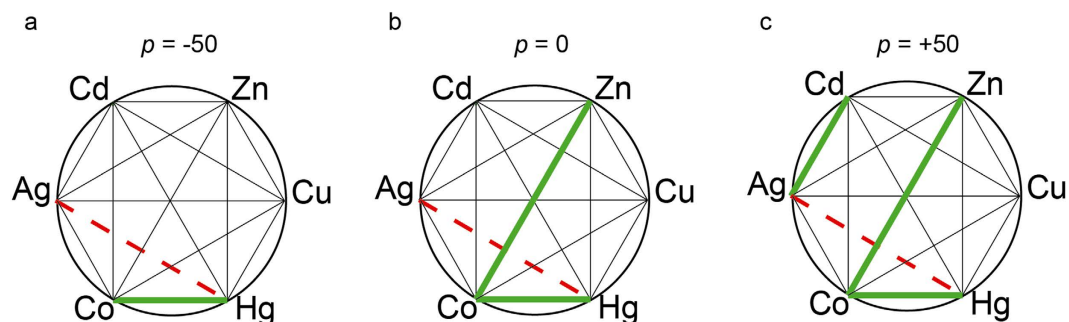


Figure 7. CI_w Polygonograms. Polygonograms summarizing weighted combination index (CI_w) for all the binary combinations of the 6 studied metal cations (Zn, Cu, Cd, Ag, Co and Hg) at three representative fractional effects (p): -50 (a), 0 (b), $+50$ (c). Departures from additivity are based on the risk management criterion (see Methods). Thin solid black lines represent additive effect ($0.5 < CI_w < 2$). Solid green lines indicate synergism ($CI_w < 0.5$). Dashed red lines indicate antagonism ($CI_w > 2$).

models (Gaussian and logGaussian) are available. However, future work will focus on extending the framework to n -component mixtures and more biphasic models.

An important application of the methodology is the possibility, by the first time, of predicting inducible whole cell biosensor responses to mixtures using single chemical experimental information only. As shown by the experiments with varying mixture ratios, this was true even when individual chemicals were present above or below the MPCs. This equals the potential applicability of inducible whole cell biosensors in mixture risk assessment with the same conditions and scope than those of monotonic toxicity tests, or *turn-off* whole cell biosensors such as Microtox^{23,24}. This increases the opportunities of inducible whole cell biosensors to be included in future regulatory frameworks which will explicitly consider mixture risk assessment^{1,25}. A complementary application of the methodology is the possibility of investigating departures from additivity (synergism and antagonism)^{3,4}. In the presented case study with *Synechococcus elongatus* PCC 7942 pBG2120, we found that the response to the binary combinations of the different metals was quite complex when analyzing the two constitutive dimensions (D and E), ranging from additivity to synergism and antagonism. In addition, we found that additivity, synergism or antagonism or any of their permutations, even of opposite effects occurred, for example a combination of synergism in (D), and antagonism in (E). In fact, the occurrence of opposite behaviours in the (D) and (E) dimensions was relatively common. One may wonder what the biological meaning of these patterns is. Most possibly, the answer will depend on the biological receptor used for the biosensor construction. In our case, the observed opposite behaviors in (D) and (E) dimensions for some metal mixtures may reflect the counteracting effects of the metals on the two independent but co-existing biological processes involved in the bioluminescence signal emission: On one hand, a synergistic effect of the metals on the induction of the *smtAB* promoter may result in lower metal concentration required to start to induce the system (synergism in D). However, a synergism in the toxicity of the metals affecting cell metabolism may result in a lower FMNH₂ and ATP pool, inhibiting the bioluminescence signal (antagonism in E). Similar arguments may hold for the different possible combinations of departures from additivity in the two dimensions for other biosensor systems. However, from a practical point of view, one may be more interested in finding out whether or not an overall deviation from additivity in the biosensor response may likely occur with a specific combination of analytes, rather than in a detailed analysis of deviations in the D and E dimensions and their causes. In such case, $CI_w = CI_D \cdot CI_E$, can be used as a measure of the overall fitness to additivity of the response of a biosensor to mixtures of analytes. Intuitively, CI_w will tend to zero when CI_D and CI_E have opposite values, reflecting the counteracting effects of the tendencies in both dimensions. In the other hand, CI_w would be magnified (either in synergism or antagonism) when both CI_D and CI_E show the same kind of interaction. For example, if $CI_D = 0.5$ and $CI_E = 0.5$, $CI_w = 0.25$, this results in increased synergism in the overall response of the biosensor (lower concentration and higher induction than expected to reach the same p level). Therefore, CI_w will allow to easily detect those metal combinations which may result in evident deviations from additivity which may potentially be problematic from a practical view-point. The analysis of CI_w of the biosensor response for the 15 binary metal combinations revealed that the weighted response of *Synechococcus elongatus* PCC 7942 pBG2120 could be considered nearly additive for the mixtures including Cu, Cd, Zn. However, important departures from additivity occurred when Hg, Co and to a lesser extent Ag were present in the mixtures. It is interesting to note that Hg and Co are the weakest inducers of the *smtAB* promoter alone¹⁶, however their impact on the analytical performance of the biosensor would be important. A similar analysis can be applied to any other biosensor strain whose robustness to interaction effects with detectable analytes would be addressed. Despite in the present work we have not performed any correction of the biosensor signal with a cell viability control which may serve to increase the dynamic range or bioanalytical performance of a whole-cell biosensor^{17,18}, the presented analytical method (additivity formulations and

analysis of departures from additivity) is equally applicable when the biosensor signal is corrected by such viability control. Finally, since our solution ultimately relies on a multivariate extension of the effective dose notation, the method may be generalized to other additivity formulations, such as *Bliss independence*⁷. *Bliss independence* may be a functional additivity formulation for stimuli with dissimilar mode of action but whose effects converge in the activation of a common biological effect²⁶. Similarly, the bi-dimensional *Loewe additivity* may be generalized to any number of k extra dimensions which may be required to describe any biological response. For example, one important dimension, which may be approached with the same multivariate extension, is the exposure time. It may be done defining a three-dimensional *Loewe additivity* formulation, and an extension of the effective dose notation in the form $ED_p = (D_{(p)}, E_{(p)}, t_{(p)})$. This method may have important applications in the formulation of additivity hypothesis in studies which may explicitly consider toxicokinetics and toxicodynamics, such as transcriptomics²⁷.

Conclusions

A multivariate extension of the *effective dose* (ED_p) notation in order to take into account the occurrence of differential maximal effects and signal inhibition beyond the MPCs in biphasic dose-response curves has been developed. This allows a multivariate extension of *Loewe additivity* enabling its direct application in a biphasic dose-response framework. The proposed additivity definition has been experimentally validated using sham mixtures, finding excellent agreement between experimental and predicted dose-response patterns. The method was applied to study the response of the cyanobacterial self-luminescent metallothionein-based whole-cell biosensor *Synechococcus elongatus* PCC 7942 pBG2120 to binary mixtures of 6 heavy metals (Zn, Cu, Cd, Ag, Co and Hg). The response of *Synechococcus* to the mixtures can be considered nearly additive except when Hg, Co and to lesser extent Ag were present in the mixtures which resulted in important departures from additivity. The method has different applications and is a useful contribution for the entire whole-cell biosensors field and related areas allowing to perform sound mixture research in non-monotonic dose-response frameworks.

Material and Methods

Chemicals. Chemicals were of analytical grade, culture media and heavy metals stock solutions were prepared in MilliQ water. Heavy metal salts $ZnCl_2$, $CdCl_2$, $AgSO_4$, $CuSO_4$, $HgCl_2$, $CoCl_2$, $PbNO_3$, $MgCl_2$, $NiCl_2$, $FeCl_2$, $BaCl_2$ and $SrCl_2$ were from Sigma-Aldrich (Germany). Concentrated metal salts solutions (1000 mg/L) were prepared in deionized water (Millipore) and stored at 4 °C in opaque bottles. Dilutions and mixtures were freshly prepared in MilliQ water before the experiments.

Heavy metal mixture exposure experiments. Culture conditions and heavy metal exposure of self-luminescent *Synechococcus elongatus* PCC 7942 pBG2120 were as previously described¹⁶. Briefly, exposure was performed in transparent 24 well microtiter plates in 1.5 mL final volume BG11 medium (without Co, Ni, Cu, Zn). Plates were incubated at 28 °C in the light, Ca. 40 $\mu\text{mol photons m}^{-2} \text{s}^{-1}$ during 4 h. Luminescence measurements were performed in a Centro LB 960 luminometer in opaque white 96 well microtiter plates. The biosensor signal was expressed as luminescence induction factor (BIF) as previously reported^{16,28}.

Mixture exposure design was adapted from^{3,29}. Basically, *Synechococcus elongatus* PCC 7942 pBG2120 was exposed to Zn, Cu, Cd, Ag, Co and Hg, and to their 15 possible binary combinations. Binary mixtures were prepared according to a constant ratio design (1:1) based on the individual D_{-50} (the dose required to get half of the MPC of each individual metal). 7 to 9 serial dilutions (factor 2) of each individual metal and binary combination were tested at the same time⁴. At least three independent experiments were performed.

Experimental validation of the additivity definition by sham mixtures. Validation of the additivity definition was performed according to the *sham* mixture procedure³⁰. *sham* mixtures are *false* mixtures in which the two components are exactly the same substance, and therefore, their fractional combination should be perfect additivity³⁰. If an additivity formulation is correct, experimental and predicted dose-response pattern of the *sham* mixtures should perfectly overlap. *sham* mixtures of Cu:Cu, Zn:Zn and Cd:Cd (ratio 1:1) were prepared and tested as described in theory.

Analysis of results. *Fitting biphasic dose-response profiles and obtaining ED_p vectors.* The entire dose-response profiles of the response of *Synechococcus elongatus* PCC 7942 pBG2120 to the different individual heavy metal cations (Zn, Cu, Cd, Ag, Co and Hg) and their binary combinations were fitted using the non-linear functions described in Theory, with and without the use of variance-stabilizing Box-Cox transform-both-sides approach²⁰. Best fit models were selected based on the minimum of the residual sum of squares²⁰. *Effective doses* (ED_p) = ($D_{(p)}, E_{(p)}$) for the different metal cations and combinations were calculated from the fitted *v-shaped* nonlinear functions.

Additivity predictions and departures from additivity. Additive *dose-effect* profiles for the different heavy metal combinations were predicted by solving equation (7) and (9). The molar fractions (j_i) of

the mixture components were fixed according to the experimental mixture metal fractions described in Theory. Two-dimensional Combination Index $CI_{(D, Ep)} = (CI_{Dp}, CI_{Ep})$ and weighted CI_{wp} values were computed accordingly to equations 5, 6 and 11, respectively. An illustrative example of the whole procedure of fitting dose-response curves, additivity formulation and analysis of departures from additivity can be found in Supplementary Material SM3.

Criteria for quantification of departures from additivity. In the present work, two criteria for the definition of departures from additivity are considered. The “pharmacological criterion” considers departures from additivity when $H_0: CI = 1$, is rejected (two-tailed Student’s t-Test), and is equivalent to the criterion used in human pharmacology⁴. The second criterion considered is the “risk management criterion (singular)” which defines departure from additivity as significant based on pragmatic thresholds: $Exp < 0.5 \cdot CA$ (synergism) and $Exp > 2 \cdot CA$ (antagonism)^{31,32}. The equivalent thresholds based on CI are: $0.5 < CI > 2$. Departures from additivity for CI_D and CI_E were analyzed based on the pharmacological criterion, while analysis of departures from additivity in CI_w were based on the risk management (for consistency) criterion.

References

- Altenburger, R. *et al.* Future water quality monitoring—adapting tools to deal with mixtures of pollutants in water resource management. *Sci Total Environ* **512–513**, 540–551, doi: 10.1016/j.scitotenv.2014.12.057 (2015).
- Kortenkamp, A., Backhaus, T. & Faust, M. State of the art report on mixture toxicity. Final Report to the European Commission under Contract Number 070307/2007/485103/ETU/D.1., (European Commission, Brussels, Belgium, 2009).
- Rodea-Palomares, I. *et al.* Application of the combination index (CI)-isobologram equation to study the toxicological interactions of lipid regulators in two aquatic bioluminescent organisms. *Water Res* **44**, 427–438, doi: 10.1016/j.watres.2009.07.026 (2010).
- Chou, T. C. Theoretical basis, experimental design, and computerized simulation of synergism and antagonism in drug combination studies. *Pharmacol Rev* **58**, 621–681, doi: 10.1124/pr.58.3.10 (2006).
- Scholze, M., Silva, E. & Kortenkamp, A. Extending the applicability of the dose addition model to the assessment of chemical mixtures of partial agonists by using a novel toxic unit extrapolation method. *PLoS one* **9**, e88808, doi: 10.1371/journal.pone.0088808 (2014).
- Loewe, S. The problem of synergism and antagonism of combined drugs. *Arzneimittelforschung* **3**, 285–290 (1953).
- Bliss, C. I. The toxicity of poisons applied jointly. *Ann Appl Biol* **26**, 585–615, doi: 10.1111/j.1744-7348.1939.tb06990.x (1939).
- Greco, W. R., Bravo, G. & Parsons, J. C. The search for synergy: a critical review from a response surface perspective. *Pharmacol Rev* **47**, 331–385 (1995).
- Chou, T. C. & Talalay, P. Quantitative analysis of dose-effect relationships: the combined effects of multiple drugs or enzyme inhibitors. *Adv Enzyme Regul* **22**, 27–55 (1984).
- Calabrese, E. J. Hormesis: why it is important to toxicology and toxicologists. *Environ Toxicol Chem* **27**, 1451–1474, doi: 10.1897/07-541 (2008).
- Hecker, M. *et al.* Human adrenocarcinoma (H295R) cells for rapid *in vitro* determination of effects on steroidogenesis: hormone production. *Toxicol Appl Pharmacol* **217**, 114–124, doi: 10.1016/j.taap.2006.07.007 (2006).
- McMahon, T. A. *et al.* The fungicide chlorothalonil is nonlinearly associated with corticosterone levels, immunity, and mortality in amphibians. *Environ Health Perspect* **119**, 1098–1103, doi: 10.1289/ehp.1002956 (2011).
- Silva, E., Scholze, M. & Kortenkamp, A. Activity of xenoestrogens at nanomolar concentrations in the e-screen assay. *Environ Health Perspect* **115**, 91–97, doi: 10.1289/ehp.9363 (2007).
- Belz, R. G., Cedergreen, N. & Sorensen, H. Hormesis in mixtures — Can it be predicted? *Sci Total Environ* **404**, 77–87, doi: http://dx.doi.org/10.1016/j.scitotenv.2008.06.008 (2008).
- Ohlsson, A., Cedergreen, N., Oskarsson, A. & Ulleras, E. Mixture effects of imidazole fungicides on cortisol and aldosterone secretion in human adrenocortical H295R cells. *Toxicology* **275**, 21–28, doi: 10.1016/j.tox.2010.05.013 (2010).
- Martin-Betancor, K., Rodea-Palomares, I., Munoz-Martin, M. A., Leganes, F. & Fernandez-Pinas, F. Construction of a self-luminescent cyanobacterial bioreporter that detects a broad range of bioavailable heavy metals in aquatic environments. *Front Microbiol* **6**, 186, doi: 10.3389/fmicb.2015.00186 (2015).
- van der Meer, J. R. & Belkin, S. Where microbiology meets microengineering: design and applications of reporter bacteria. *Nat Rev Microbiol* **8**, 511–522, doi: 10.1038/nrmicro2392 (2010).
- Roda, A. *et al.* Analytical strategies for improving the robustness and reproducibility of bioluminescent microbial bioreporters. *Anal Bioanal Chem* **401**, 201–211, doi: 10.1007/s00216-011-5091-3 (2011).
- Yagi, K. Applications of whole-cell bacterial sensors in biotechnology and environmental science. *Appl Microbiol Biotechnol* **73**, 1251–1258, doi: 10.1007/s00253-006-0718-6 (2007).
- Ritz, C. & Streibig, J. C. Bioassay Analysis using R. *J Stat Softw* **12**, 17 (2005).
- Faust, M. *et al.* Predicting the joint algal toxicity of multi-component s-triazine mixtures at low-effect concentrations of individual toxicants. *Aquat Toxicol* **56**, 13–32, doi: http://dx.doi.org/10.1016/S0166-445X(01)00187-4 (2001).
- Gonzalez-Pleiter, M. *et al.* Toxicity of five antibiotics and their mixtures towards photosynthetic aquatic organisms: implications for environmental risk assessment. *Water Res* **47**, 2050–2064, doi: 10.1016/j.watres.2013.01.020 (2013).
- Fernandez-Pinas, F., Rodea-Palomares, I., Leganes, F., Gonzalez-Pleiter, M. & Angeles Munoz-Martin, M. Evaluation of the ecotoxicity of pollutants with bioluminescent microorganisms. *Adv Biochem Eng Biotechnol* **145**, 65–135, doi: 10.1007/978-3-662-43619-6_3 (2014).
- Wernersson, A.-S. *et al.* The European technical report on aquatic effect-based monitoring tools under the water framework directive. *Env Sci Eur* **27**, 7 (2015).
- Brack, W. *et al.* The SOLUTIONS project: challenges and responses for present and future emerging pollutants in land and water resources management. *Sci Total Environ* **503–504**, 22–31, doi: 10.1016/j.scitotenv.2014.05.143 (2015).
- Junghans, M., Backhaus, T., Faust, M., Scholze, M. & Grimme, L. H. Application and validation of approaches for the predictive hazard assessment of realistic pesticide mixtures. *Aquat Toxicol* **76**, 93–110, doi: http://dx.doi.org/10.1016/j.aquatox.2005.10.001 (2006).
- Altenburger, R., Scholz, S., Schmitt-Jansen, M., Busch, W. & Escher, B. I. Mixture Toxicity Revisited from a Toxicogenomic Perspective. *Environ Sci Technol* **46**, 2508–2522, doi: 10.1021/es2038036 (2012).

28. Jouanneau, S., Durand, M. J., Courcoux, P., Blusseau, T. & Thouand, G. Improvement of the identification of four heavy metals in environmental samples by using predictive decision tree models coupled with a set of five bioluminescent bacteria. *Environ Sci Technol* **45**, 2925–2931, doi: 10.1021/es1031757 (2011).
29. Rodea-Palomares, I. F.-P., F. González-García, C. & Leganes, F. in *Nova Science Publishers, Inc. New York. USA.* (2009).
30. Dawson, D. A., Allen, J. L., Schultz, T. W. & Pösch, G. Time-dependence in mixture toxicity with soft-electrophiles: 2. Effects of relative reactivity level on time-dependent toxicity and combined effects for selected Michael acceptors. *J Environ Sci Health A* **43**, 43–52, doi: 10.1080/10934520701750371 (2007).
31. Altenburger, R., Backhaus, T., Boedeker, W., Faust, M. & Scholze, M. Simplifying complexity: Mixture toxicity assessment in the last 20 years. *Environ Toxicol Chem* **32**, 1685–1687, doi: 10.1002/etc.2294 (2013).
32. Cedergreen, N. Quantifying Synergy: A Systematic Review of Mixture Toxicity Studies within Environmental Toxicology. *PLoS one* **9**, e96580, doi: 10.1371/journal.pone.0096580 (2014).

Acknowledgements

This research was supported by MINECO grants CGL2010-15675 and CTM2013-45775-C2-2-R.

Author Contributions

All authors have made essential contributions to this study. Experimental design: I.R., K.M., F.L. and F.F.P. Programation of R scripts C.R., I.R. and K.M. Experimental execution: K.M., F.L. and I.R. Data analysis: K.M. and I.R. Manuscript drafting: I.R., F.F.P. and C.R. All authors critically read and approved the final manuscript.

Additional Information

Supplementary information accompanies this paper at <http://www.nature.com/srep>

Accession codes: Data used in the present manuscript is publicly available at: Doi: <http://dx.doi.org/10.6084/m9.figshare.1476176>

Competing financial interests: The authors declare no competing financial interests.

How to cite this article: Martin-Betancor, K. *et al.* Defining an additivity framework for mixture research in inducible whole-cell biosensors. *Sci. Rep.* **5**, 17200; doi: 10.1038/srep17200 (2015).



This work is licensed under a Creative Commons Attribution 4.0 International License. The images or other third party material in this article are included in the article's Creative Commons license, unless indicated otherwise in the credit line; if the material is not included under the Creative Commons license, users will need to obtain permission from the license holder to reproduce the material. To view a copy of this license, visit <http://creativecommons.org/licenses/by/4.0/>

**S M
U A
P T
P E
L R
E I
M A
E L
N
T
A
R
Y**

Supplementary Material:

Defining an additivity framework for mixture research in inducible whole-cell biosensors

Martin-Betancor, K¹; Ritz, C²; Fernández-Piñas, F¹; Leganés, F¹; & Rodea-Palomares I^{1*}

¹ Department of Biology, Facultad de Ciencias, Universidad Autónoma de Madrid. 28049 Madrid, Spain.

² Department of Nutrition, Exercise and Sports, Faculty of Science, University of Copenhagen, Rolighedsvej 30, DK-1958 Frederiksberg C, Denmark.

*Corresponding author: Ismael Rodea-Palomares

Mailing address: Departamento de Biología, Facultad de Ciencias, Universidad Autónoma de Madrid. C/ Darwin, 2. 28049, Madrid. Spain.

Tel.: +34 914978180

Fax: +34 914978344

E-mail: ismael.rodea@uam.es

Table of contents:

Supplementary Material SM1 (Table). Summary of non-linear models and estimated parameters

Supplementary Material SM2 (Table). *ED_p* vectors (-50, 0, +50) for Cu, Cd, Zn, Cu, Hg and Co.

Supplementary Material SM3 (Tutorial). Complete non-monotonic dose-response profiles and analysis of departures from additivity based on Loewe additivity and Combination Index using R.

Supplementary Material SM4 (Figure). Effect of mixture ratio for the Zn:Cu binary mixture

Supplementary Material SM5 (Table). Combination index (CI) values for the dose (*D*) and empirical effect (*E*) dimensions together with relevant statistical information for 3 selected fractional effect levels (*p*) of the 15 binary metal mixtures of Cu, Cd, Zn, Cu, Hg and Co.

Supplementary Material SM1 (Table). Summary of non-linear models and estimated parameters together with relevant statistical information of the model fits for the response of *Synechococcus elongatus* PCC 7942 pBG2120 to 6 heavy metals and their binary mixtures (Zn, Cu, Cd, Ag, Co and Hg)

Metal	Model Function	Parameter estimates				Residual Standard Error	
		Estimate value	Std.Error	t-value	p-		
Zn	lgau2	b	0.351996	0.048207	7.301822	0.0000	0.1698429
		c	1.475965	0.597634	2.469679	0.0199	
		d	80.099960	9.894407	8.095479	0.0000	
		e	2.245102 (2245.102) ^a	0.043678	51.401066	0.0000	
		f	2.662339	0.829132	3.210994	0.0033	
		Cd	lgau2	b	0.562495	0.039451	
c	1.039686	0.314707		3.303666	0.0031		
d	49.728622	3.290085		15.114693	0.0000		
e	5.340496 (5340.496) ^a	0.093375		57.193828	0.0000		
f	2.358463	0.293418		8.037883	0.0000		
Ag	gau2	b		0.1443642	0.0093814	15.3883702	0.0000
c		1.3247561	0.3296468	4.0187134	0.0007		
d		54.6960138	3.3118291	16.5153493	0.0000		
e		0.3292834 (329.2834) ^a	0.0045334	72.6353256	0.0000		
f		3.4229734	0.4677340	7.3182051	0.0000		
Co		lgau2	b	0.532205	0.066033	8.059677	0.0000
c	0.955349		0.336941	2.835362	0.0119		
d	18.297557		1.270958	14.396664	0.0000		
e	2.413876 (2413.876) ^a		0.084272	28.643759	0.0000		
f	2.028618		0.403140	5.032046	0.0001		
Cu	lgau2		b	0.24392	0.0096496	25.277	0.0000
c		0.40810	0.18429	2.2145	0.0354		
d		43.998	1.6215	27.134	0.0000		
e		0.046606 (46.606) ^a	0.00028072	166.02	0.0000		
f		2.1294	0.13881	15.341	0.0000		
Hg		lgau2	b	0.3284459 ^a	0.0724137	4.5356872	0.0002
c	0.9965343 ^a		0.5464225	1.8237431	0.0818		
d	33.5822889 ^a		2.9519420	11.3763375	0.0000		
e	0.0679623 ^a		0.0017048	39.8664205	0.0000		
f	1.0307636 ^a		0.1737224	5.9333959	0.0000		
Cu: Cd	Gau2		b	0.833872	0.087886	9.488139	0.0000
c		1.587702	0.559394	2.838253	0.0098		
d		32.661863	2.571750	12.700250	0.0000		
e		2.526442	0.039160	64.515964	0.0000		
f		2.226572	0.326413	6.821331	0.0000		
Cu: Zn		Lgau2	b	0.210524	0.020723	10.159021	0.0000
c	1.058583		0.215034	4.922875	0.0002		
d	111.998627		5.055904	22.152047	0.0000		
e	1.584642		0.016992	93.255607	0.0000		
f	1.442243		0.112803	12.785522	0.0000		

Zn:Cd	Lgau2	b	0.555188	0.015215	36.489732	0.0000	0.02654068
		c	-0.290451	0.583670	-0.497628	0.626	
		d	42.910857	0.943991	45.456837	0.0000	
		e	2.321820	0.012425	186.867587	0.0000	
		f	2.024344	0.134982	14.997109	0.0000	
Cu:Hg	Lgau2	b	0.6340408	0.0362401	17.4955546	0.0000	0.05278326
		c	2.2452456	0.3135964	7.1596667	0.0000	
		d	74.6073845	3.0968760	24.0911760	0.0000	
		e	0.0260586	0.0004689	55.5735249	0.0000	
		f	3.1835757	0.3918444	8.1245914	0.0000	
Cu:Co	Gau2	b	0.85374	0.010441	81.771	0.0000	0.03405409
		c	1.3777	0.13300	10.359	0.0000	
		d	21.115	0.52473	40.239	0.0000	
		e	1.4961	0.0070987	210.75	0.0000	
		f	6.0718	0.35879	16.923	0.0000	
Co:Cd	Lgau2	b	0.26824	0.0098237	27.305	0.0000	0.05352349
		c	1.8005	0.18445	9.7614	0.0000	
		d	35.467	1.2264	28.920	0.0000	
		e	3.2161	0.013300	241.81	0.0000	
		f	2.8076	0.26146	10.738	0.0000	
Ag:Cd	Gau2	b	0.59045	0.017055	34.620	0.0000	0.0487012
		c	1.4009	0.19988	7.0088	0.0000	
		d	77.971	2.1637	36.037	0.0000	
		e	2.7331	0.0078159	349.69	0.0000	
		f	2.1606	0.079377	27.220	0.0000	
Cu:Ag	Lgau2	b	0.34083	0.013952	24.429	0.0000	0.05808011
		c	1.8282	0.24210	7.5516	0.0000	
		d	78.149	2.8113	27.798	0.0000	
		e	0.20627	0.0010609	194.43	0.0000	
		f	2.2139	0.12447	17.787	0.0000	
Zn:Ag	Gau2	b	0.28513	0.0077488	36.797	0.0000	0.04642924
		c	1.1717	0.18042	6.4942	0.0000	
		d	123.94	3.2011	38.717	0.0000	
		e	1.5822	0.0039700	398.53	0.0000	
		f	2.0776	0.061918	33.553	0.0000	
Co:Ag	Gau2	b	0.40242	0.038248	10.521	0.0000	0.04745158
		c	1.7071	0.30221	5.6487	0.0000	
		d	11.328	0.99761	11.356	0.0000	
		e	1.0509	0.0099931	105.16	0.0000	
		f	3.0655	0.74799	4.0984	0.0007	
Zn:Co	Gau2	b	0.42157	0.0097373	43.295	0.0000	0.03552789
		c	1.7071	0.30221	5.6487	0.0000	
		d	11.328	0.99761	11.356	0.0000	
		e	2.0648	0.0047810	431.88	0.0000	
		f	2.0479	0.054401	37.644	0.0000	
Cu:Hg	Lgau2	b	0.6340408	0.0362401	17.49555	0.0000	0.05278326
		c	2.2452456	0.3135964	7.1596667	0.0000	
		d	74.6073845	3.0968760	24.0911760	0.0000	
		e	0.0260586	0.0004689	55.5735249	0.0000	
		f	3.1835757	0.3918444	8.1245914	0.0000	
Cd:Hg	Lgau2	b	0.335736	0.010892	30.824749	0.0000	0.03659033
		c	1.487436	0.158866	9.362838	0.0000	
		d	71.957893	1.550272	46.416307	0.0000	
		e	2.487738	0.017196	144.672177	0.0000	

		f	2.508632	0.142398	17.617043	0.0000	
Zn:Hg	Gau2	b	0.28384	0.015798	17.967	0.0000	0.07234654
		c	1.3458	0.29692	4.5326	0.0001	
		d	154.63	8.0164	1.9290	0.0000	
		e	1.3592	0.0060743	223.76	0.0000	
		f	2.2107	0.13004	16.999	0.0000	
Hg:Co	Lgau2	b	0.464864	0.054759	8.489311	0.0000	0.05336395
		c	2.154873	0.322521	6.681348	0.0000	
		d	65.070756	2.618477	24.850612	0.0000	
		e	0.754579	0.030447	24.783295	0.0000	
		f	2.812375	0.814988	3.450817	0.0000	
Hg:Ag	Gau2	b	0.071195	0.0014252	49.954	0.0000	0.02301
		c	-0.0050033	0.12298	-0.040684	0.968	
		d	34.655	0.58610	59.128	0.0000	
		e	0.18673	0.00079776	234.07	0.0000	
		f	1.9507	0.062492	31.215	0.0000	

^a (nM)

gau and lgau refers to the Normal and log-normal biphasic dose-response models described in the gaussian {drc} functions in *drc* R package ¹. Parameter estimates and estimated residual standard errors are calculated using the function *drm* {drc} which is based on the function *optim* {stats} ² which relies on the minimisation of the minus log likelihood function. For a quantitative response this reduces to least squares estimation, which is carried out by minimising the following sums of squares

$$\sum_{i=1}^N [w_i (y_i - f_i)]^2$$

where y_i , f_i , and w_i correspond to the observed value, expected value, and the weight respectively, for the i th observation (from 1 to N).

Supplementary Material SM2 (Table). *EDp* vectors (-50, 0, +50) for Cu, Cd, Zn, Cu, Hg and Co.

Metal	Fractional effect	<i>EDp</i> (μM , BIF)	
		<i>D(p)</i> (μM)	<i>E(p)</i> (BIF)
Zn	<i>ED</i> ₋₅₀	1.508±0.082	40.79±3.33
	<i>ED</i> ₀	2.8±0.11	79.31±8.89
	<i>ED</i> ₊₅₀	3.34±0.18	4.79±7.38
Cd	<i>ED</i> ₋₅₀	2.8±0.11	25.38±1.69
	<i>ED</i> ₀	5.94±0.18	49.24±3.03
	<i>ED</i> ₊₅₀	10.19±0.39	25.38±1.49
Ag	<i>ED</i> ₋₅₀	0.17±0.006	28.01±1.79
	<i>ED</i> ₀	0.37±0.013	54.16±3.12
	<i>ED</i> ₊₅₀	0.49±0.012	28.01±4.39
Co	<i>ED</i> ₋₅₀	1.29±0.07	9.63±15
	<i>ED</i> ₀	2.61±0.1	18.12±1.17
	<i>ED</i> ₊₅₀	4.51±0.24	9.63±0.76
Cu	<i>ED</i> ₋₅₀	0.035±0.0004	22.2±0.97
	<i>ED</i> ₀	0.048±0.0003	43.56±1.53
	<i>ED</i> ₊₅₀	0.062±0.0007	22.2±0.95
Hg ^a	<i>ED</i> ₋₅₀	0.043±0.003	17.29±1.24
	<i>ED</i> ₀	0.068±0.001	33.25±3.04
	<i>ED</i> ₊₅₀	0.11±0.008	17.29±1.08

±: Standard error. Standard error are estimated from the non-linear fitted model. Fitted non-linear models and estimated parameters can be found in Table SM1.

^a (nM).

Supplementary Material SM3 (Tutorial)

Fitting non-monotonic dose-response with differential maximal effects and analysis of departures from additivity based on multivariate Loewe additivity using R.

From: *Defining an additivity framework for mixture research in inducible whole-cell biosensors.*

Martin-Betancor, K¹; Ritz, C²; Fernández-Piñas, F¹; Leganés, F¹; & Rodea-Palomares I^{1*}

¹ Department of Biology, Facultad de Ciencias, Universidad Autónoma de Madrid. 28049 Madrid, Spain.

² Department of Nutrition, Exercise and Sports, Faculty of Science, University of Copenhagen, Rolighedsvej 30, DK-1958 Frederiksberg C, Denmark.

*Corresponding author: Ismael Rodea-Palomares

Mailing address: Departamento de Biología, Facultad de Ciencias, Universidad Autónoma de Madrid. C/ Darwin, 2. 28049, Madrid. Spain.

Tel.: +34 914978180

Fax: +34 914978344

E-mail: ismael.rodea@uam.es

A novel additivity framework for mixture-effect research in the framework of whole-cell inducible biosensors has been mathematically developed. The method proposes a multivariate extension of the effective dose (ED_p) notation in order to take into account the occurrence of differential maximal effects and inhibition beyond the maximum permissive concentrations (MPCs). This allow a dimensional extension of Loewe additivity which enables its direct application in a biphasic dose-response framework. The utilities that allow to achieve this new approach have been incorporated in the (*drc*) package for R¹.

#Example data:

The dataset “metaldata.csv” and the functional R-script “SM3_Script_R.R” used in the present example are freely available from <http://dx.doi.org/10.6084/m9.figshare.1476176>

In the present tutorial, we will explain how to use the novel method developed in order to model dose-response profiles of an inducible whole cell biosensor to individual *stimuli* and mixtures (in the present case, different heavy metals). We will analyse the “metaldata.csv” dataset. This dataset includes the raw data resulted from the individual exposure of the inducible whole cell biosensor *Synechococcus elongatus* PCC 7942 pBG2120³ to six metals and their 15 possible binary combinations.

The dataset is importable as data.frame in R as follows: (from the root directory:

```
metaldata<-read.csv(file="metaldata.csv")
```

The data frame have 3 variables: “metal” (factor), “conc” (numeric), “IR” (induction factor, the same as BIF in the main text) (numeric). In the tutorial, we will explain the *drc* extension using the data for Zn, Cd and its mixture, ZnCd.

#Make a subset with the Zn data

```
Zn <- metaldata[metaldata$metal=="Zn",]
```

```
Zn
```

	metal	conc	IR
1	Zn	0.0369	0.9142857
2	Zn	0.0369	0.9756098
3	Zn	0.0369	0.8974359
4	Zn	0.0925	0.9523810
5	Zn	0.0925	0.8780488
6	Zn	0.0925	1.1666667
7	Zn	0.1859	0.9523810
8	Zn	0.1859	1.1707317
9	Zn	0.1859	1.2115385
10	Zn	0.5693	1.7523810
11	Zn	0.5693	1.6585366
12	Zn	0.5693	1.7948718
13	Zn	0.9684	5.9809524
14	Zn	0.9684	4.6341463
15	Zn	0.9684	4.8461538
16	Zn	1.3836	14.2857143
17	Zn	1.3836	19.7073171
18	Zn	1.3836	22.7051282
19	Zn	1.4472	43.9500000
20	Zn	1.4472	44.0869565
21	Zn	1.4472	43.2000000
22	Zn	2.0371	67.1238095
23	Zn	2.0371	74.0975610
24	Zn	2.0371	86.0192308
25	Zn	3.2111	31.1619048
26	Zn	3.2111	61.2195122
27	Zn	3.2111	64.6153846
28	Zn	4.4946	3.8857143
29	Zn	4.4946	4.8292683
30	Zn	4.4946	5.3846154
31	Zn	10.7532	0.3428571
32	Zn	10.7532	0.5853659
33	Zn	10.7532	0.6730769

#Fitting biphasic dose-response profiles:

Inducible whole cell biosensors usually present inverted v-shaped biphasic dose-response profiles. This specific type of dose-response pattern may be fitted using nonlinear regression model equations as Gaussian (gau) or LogGaussian (lgau) with or without the use of variance-stabilizing Box-Cox transform-both-sides approach. (For more detail see section 2.1 *Fitting biphasic dose-response profiles* of the manuscript).

#gaussian function:

```
Zn.gau <- drm(IR~conc, data=Zn, fct=gaussian(), na.action=na.omit)
```

```
summary(Zn.gau)
```

Model fitted: Gaussian (5 parms)

Parameter estimates:

	Estimate	Std. Error	t-value	p-value
b:(Intercept)	8.8613e-01	9.3682e-03	9.4589e+01	0.0000
c:(Intercept)	2.1660e+00	1.2821e+00	1.6895e+00	0.1022
d:(Intercept)	7.5746e+01	3.3920e+00	2.2331e+01	0.0000
e:(Intercept)	2.3418e+00	8.6316e-03	2.7131e+02	0.0000

```
f:(Intercept) 1.3880e+01 2.8981e+00 4.7894e+00 0.0000
```

Residual standard error:

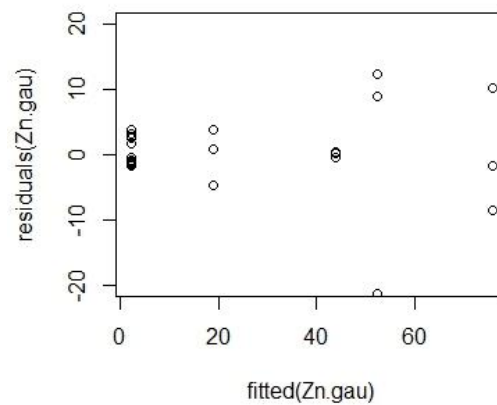
5.87511 (28 degrees of freedom)

For complete information of the `drm {drc}` consult the tutorial of `drc` package <http://cran.r-project.org/web/packages/drc/index.html>

Model checking

Best-fit models can be selected based on the residual standard error that is indicated in the model summary. For visual observation they can be plotted:

```
plot(fitted(Zn.gau), residuals(Zn.gau), ylim = c(-20, 20))
```



Gaussian function with Box-Cox transform

```
Zn.gau2 <- drm(IR~conc, data=Zn, fct=gaussian(), na.action=na.omit, bcVal = 0, bcAdd = 10)
```

```
summary(Zn.gau2)
```

Model fitted: Gaussian (5 parms)

Parameter estimates:

	Estimate	Std. Error	t-value	p-value
b:(Intercept)	0.793259	0.075520	10.503961	0.0000
c:(Intercept)	1.613775	0.500908	3.221697	0.0032
d:(Intercept)	81.080825	10.982114	7.382989	0.0000
e:(Intercept)	2.422227	0.042576	56.892278	0.0000
f:(Intercept)	3.115795	0.624967	4.985533	0.0000

Residual standard error:

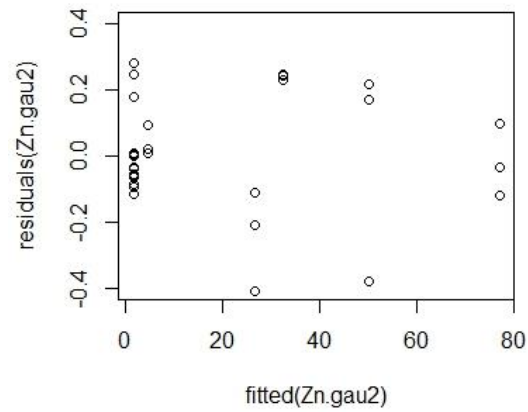
0.17677 (28 degrees of freedom)

Non-normality/heterogeneity adjustment through optimal Box-Cox transformation

Specified lambda: 0

Model checking

```
plot(fitted(Zn.gau2), residuals(Zn.gau2), ylim = c(-0.4, 0.4))
```



#lgaussian function

```
Zn.lgau <- drm(IR~conc, data=Zn, fct=lgaussian(), na.action=na.omit)
summary(Zn.lgau)
```

Model fitted: Log-Gaussian (5 parms)

Parameter estimates:

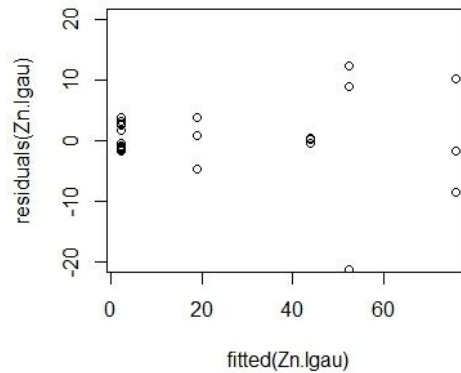
	Estimate	Std. Error	t-value	p-value
b:(Intercept)	4.0134e-01	6.4603e-03	6.2124e+01	0.0000
c:(Intercept)	2.1661e+00	1.2821e+00	1.6895e+00	0.1022
d:(Intercept)	7.5747e+01	3.3920e+00	2.2331e+01	0.0000
e:(Intercept)	2.1746e+00	1.2839e-02	1.6938e+02	0.0000
f:(Intercept)	9.1066e+00	1.8773e+00	4.8510e+00	0.0000

Residual standard error:

5.87511 (28 degrees of freedom)

#Model checking

```
plot(fitted(Zn.lgau), residuals(Zn.lgau), ylim = c(-20, 20))
```

lgaussian function with Box-Cox transform

```
Zn.lgau2 <- drm(IR~conc, data=Zn, fct=lgaussian(), na.action=na.omit, bcVal = 0, bcAdd = 10)
```

```
summary(Zn.lgau2)
```

Model fitted: Log-Gaussian (5 parms)

Parameter estimates:

	Estimate	Std. Error	t-value	p-value
b:(Intercept)	0.351996	0.048207	7.301822	0.0000
c:(Intercept)	1.475965	0.597634	2.469679	0.0199
d:(Intercept)	80.099960	9.894407	8.095479	0.0000
e:(Intercept)	2.245102	0.043678	51.401066	0.0000
f:(Intercept)	2.662339	0.829132	3.210994	0.0033

Residual standard error:

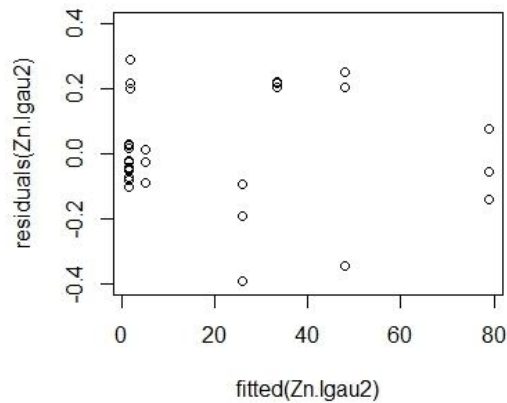
0.1698429 (28 degrees of freedom)

Non-normality/heterogeneity adjustment through optimal Box-Cox transformation

Specified lambda: 0

#Model checking

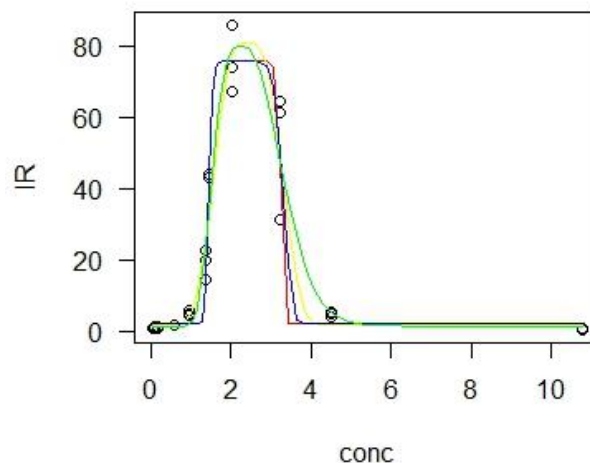
```
plot(fitted(Zn.lgau2), residuals(Zn.lgau2), ylim = c(-0.4, 0.4))
```



#plot:

We can visually observe all the functions used in order to have a visual overview of the models fitted.

```
plot(Zn.gau, type = "obs", col= "black", log = "")
plot(Zn.gau, type = "none", add = TRUE, col = "red")
plot(Zn.gau2, type = "none", add = TRUE, col = "yellow")
plot(Zn.lgau, type = "none", add = TRUE, col = "blue")
plot(Zn.lgau2, type = "none", add = TRUE, col = "green")
```



Based on the residuals standard errors and the visual examination, we can conclude that the LogGaussian with Box-Cox modification (green line) is the model that fit better the experimental data, therefore it will be used for fitting Zn response in the rest of calculations.

#Effective doses (ED_p) calculation:

Using the `ED {drc}` function, we can get the $D(p)$ vectors at any desired fractional effect p . We selected the three representative p levels: -50 (half of the E_{max} , in the induction region), 99.9 (E_{max}) and +50 (half of the E_{max} , in the inhibition region) (*Equivalent to the -50, 0, +50 p levels in the manuscript*). For more details, see section 2.2 *a multivariate extension of the effective dose notation of the manuscript*. Note: to get the $E(p)$ values, for the moment it is required to use the `indicesFct {drc}` function which will be described in next sections.

```
ED(Zn.lgau2, -50, interval = "delta", bound = FALSE)
```

```
Estimate Std. Error Lower Upper
1:-50 1.508038 0.082849 1.338329 1.6777
```

```
ED(Zn.lgau2, 99.9,interval = "delta")
```

```
Estimate Std. Error Lower Upper
1:99.9 2.32300 0.10458 2.10877 2.5372
```

```
ED(Zn.lgau2, 50, interval = "delta")
```

```
Estimate Std. Error Lower Upper
1:50 3.34241 0.18363 2.96627 3.7186
```

#Cd fit:

Now, we are going to fit the second data component, in that case, Cd. For that, we use the same steps as for Zn.

#Make a subset with the Cd data

```
Cd <- metaldata[metaldata$metal=="Cd",]
```

```
Cd
```

#Fitting biphasic dose-response profiles:

#gaussian function

```
Cd.gau <- drm(IR~conc, data=Cd, fct=gaussian(), na.action=na.omit)
```

```
summary(Cd.gau)
```

```
Model fitted: Gaussian (5 parms)
```

```
Parameter estimates:
```

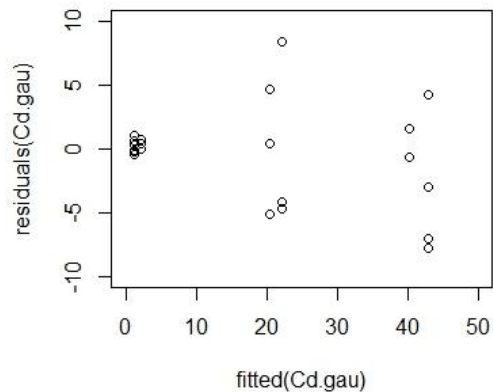
```
Estimate Std. Error t-value p-value
b:(Intercept) 4.079689 0.115139 35.432648 0.0000
c:(Intercept) 1.283627 1.275138 1.006657 0.3246
d:(Intercept) 42.981885 1.907644 22.531393 0.0000
e:(Intercept) 6.850150 0.070015 97.838717 0.0000
f:(Intercept) 7.805005 3.237173 2.411056 0.0243
```

```
Residual standard error:
```

```
4.4849 (23 degrees of freedom)
```

#Model checking

```
plot(fitted(Cd.gau), residuals(Cd.gau), ylim = c(-10, 10))
```



#Gaussian function with Box-Cox transform

```
Cd.gau2 <- drm(IR~conc, data=Cd, fct=gaussian(), na.action=na.omit, bcVal = 0, bcAdd = 10)
```

```
summary(Cd.gau2)
```

Model fitted: Gaussian (5 parms)

Parameter estimates:

	Estimate	Std. Error	t-value	p-value
b:(Intercept)	4.056422	0.090069	45.036766	0.0000
c:(Intercept)	1.202271	0.352358	3.412072	0.0024
d:(Intercept)	42.700145	2.340528	18.243805	0.0000
e:(Intercept)	6.851570	0.053432	128.230478	0.0000
f:(Intercept)	7.234677	1.057973	6.838241	0.0000

Residual standard error:

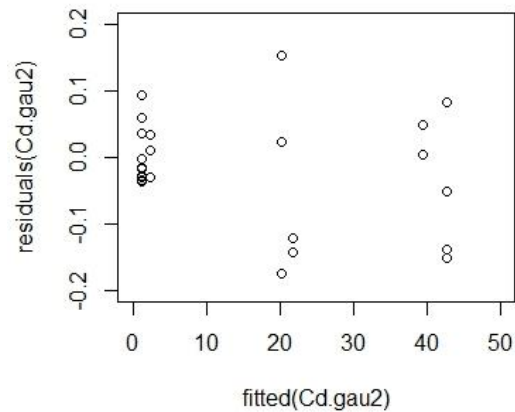
0.1088791 (23 degrees of freedom)

Non-normality/heterogeneity adjustment through optimal Box-Cox transformation

Specified lambda: 0

#Model checking

```
plot(fitted(Cd.gau2), residuals(Cd.gau2), ylim = c(-0.2, 0.2))
```



#lgaussian function

```
Cd.lgau <- drm(IR~conc, data=Cd, fct=lgaussian(), na.action=na.omit)
```

```
summary(Cd.lgau)
```

Model fitted: Log-Gaussian (5 parms)

Parameter estimates:

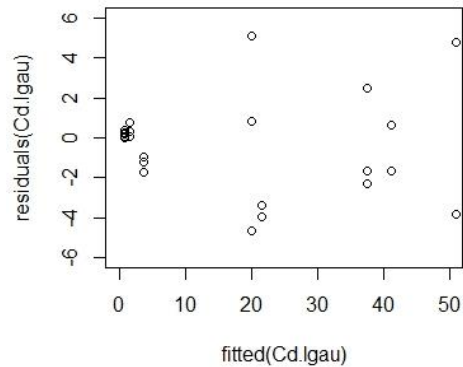
	Estimate	Std. Error	t-value	p-value
b:(Intercept)	0.544683	0.032578	16.719520	0.0000
c:(Intercept)	0.806563	0.920847	0.875893	0.3901
d:(Intercept)	51.009281	2.143174	23.800808	0.0000
e:(Intercept)	5.315768	0.093498	56.854176	0.0000
f:(Intercept)	2.105116	0.261655	8.045382	0.0000

Residual standard error:

3.086809 (23 degrees of freedom)

#Model checking

```
plot(fitted(Cd.lgau), residuals(Cd.lgau), ylim = c(-6, 6), xlim = c(0, 50))
```



#lgaussian function with Box-Cox transform

```
Cd.lgau2 <- drm(IR~conc, data=Cd, fct=lgaussian(), na.action=na.omit, bcVal = 0, bcAdd = 10)
```

```
summary(Cd.lgau2)
```

Model fitted: Log-Gaussian (5 parms)

Parameter estimates:

	Estimate	Std. Error	t-value	p-value
b:(Intercept)	0.562495	0.039451	14.258093	0.0000
c:(Intercept)	1.039686	0.314707	3.303666	0.0031
d:(Intercept)	49.728622	3.290085	15.114693	0.0000
e:(Intercept)	5.340496	0.093375	57.193828	0.0000
f:(Intercept)	2.358463	0.293418	8.037883	0.0000

Residual standard error:

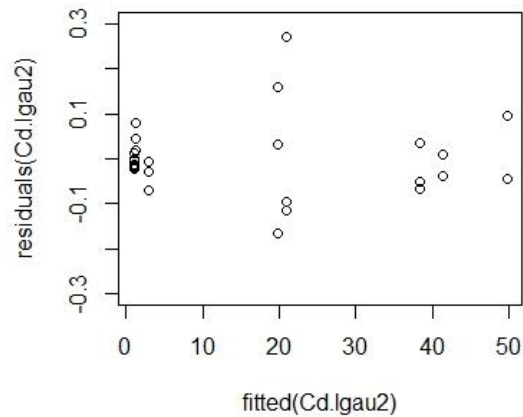
0.09005292 (23 degrees of freedom)

Non-normality/heterogeneity adjustment through optimal Box-Cox transformation

Specified lambda: 0

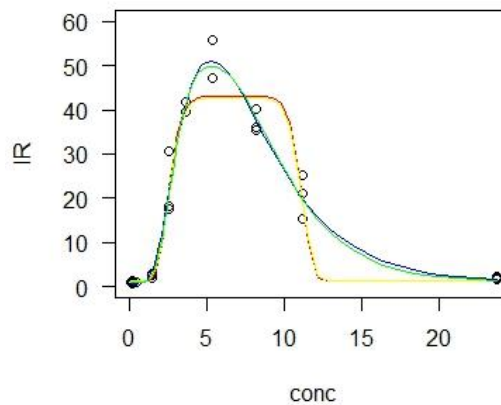
#Model checking

```
plot(fitted(Cd.lgau2), residuals(Cd.lgau2), ylim = c(-0.3, 0.3))
```



#plot:

```
plot(Cd.gau, type = "obs", col= "black", log = "", ylim = c(0, 60))
plot(Cd.gau, type = "none", add = TRUE, col = "red")
plot(Cd.gau2, type = "none", add = TRUE, col = "yellow")
plot(Cd.lgau, type = "none", add = TRUE, col = "blue")
plot(Cd.lgau2, type = "none", add = TRUE, col = "green")
```



Based on the residuals standard errors and the visual examination, we can observed that the LogGaussian with Box-Cox modification (green line) is the model that fits better Cd experimental data, therefore it will be used for fitting Cd response in the rest of calculations.

#Effective doses ($D(p)$) calculation:

```
ED(Cd.lgau2, -50, interval = "delta", bound = FALSE)
```

	Estimate	Std. Error	Lower	Upper
1:-50	2.79902	0.10714	2.57737	3.0207

```
ED(Cd.lgau2, 99.9,interval = "delta")
```

```
Estimate Std. Error Lower Upper  
1:99.9 5.56039 0.11333 5.32594 5.7948
```

```
ED(Cd.lgau2, 50,interval = "delta")
```

```
Estimate Std. Error Lower Upper  
1:50 10.18961 0.39005 9.38273 10.996
```

#Fitting mixture data:

In order to predict the biosensor response to any combination of the individual metals and also, to be able to analyse departures from additivity, it is required to fit the mixture data to a nonlinear regression model equation. Zn and Cd mixture data are used as example.

Make a subset with the ZnCd data

```
ZnCd <- metaldata[metaldata$metal=="ZnCd",]
```

#gaussian function

```
ZnCd.gau <- drm(IR~conc, data=ZnCd, fct=gaussian(), na.action=na.omit)
```

```
summary(ZnCd.gau)
```

```
Model fitted: Gaussian (5 parms)
```

```
Parameter estimates:
```

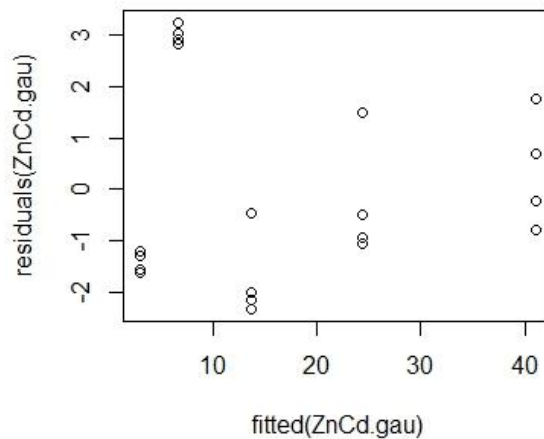
```
Estimate Std. Error t-value p-value  
b:(Intercept) 9.1892e-03 NA NA NA  
c:(Intercept) 2.3311e+00 1.1228e+00 2.0760e+00 0.0555  
d:(Intercept) 1.0401e+03 NA NA NA  
e:(Intercept) 2.8890e+00 2.3606e-02 1.2239e+02 0.0000  
f:(Intercept) 4.1168e-01 1.6657e-02 2.4716e+01 0.0000
```

```
Residual standard error:
```

```
2.123171 (15 degrees of freedom)
```

#Model checking

```
plot(fitted(ZnCd.gau), residuals(ZnCd.gau))
```

#Gaussian function with Box-Cox transform

```
ZnCd.gau2 <- drm(IR~conc, data=ZnCd, fct=gaussian(), na.action=na.omit, bcVal = 0, bcAdd = 10)
```

```
summary(ZnCd.gau2)
```

Model fitted: Gaussian (5 parms)

Parameter estimates:

	Estimate	Std. Error	t-value	p-value
b:(Intercept)	0.040441	0.032399	1.248238	0.2311
c:(Intercept)	0.561210	1.249161	0.449269	0.6597
d:(Intercept)	330.288516	136.118307	2.426481	0.0283
e:(Intercept)	2.899675	0.049022	59.151001	0.0000
f:(Intercept)	0.473996	0.074228	6.385670	0.0000

Residual standard error:

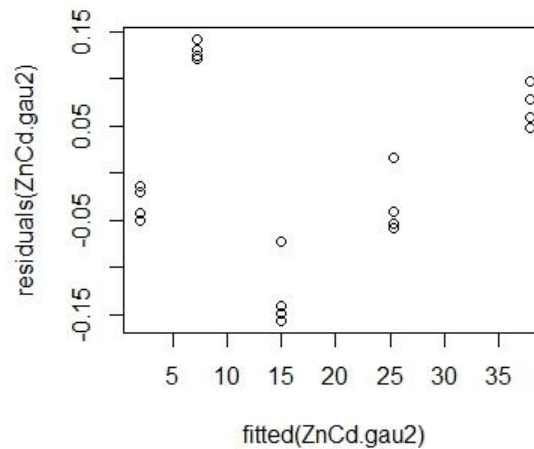
0.1078746 (15 degrees of freedom)

Non-normality/heterogeneity adjustment through optimal Box-Cox transformation

Specified lambda: 0

#Model checking

```
plot(fitted(ZnCd.gau2), residuals(ZnCd.gau2), ylim = c(-0.15, 0.15))
```



#lgaussian function

```
ZnCd.lgau <- drm(IR~conc, data=ZnCd, fct=lgaussian(), na.action=na.omit)
```

```
summary(ZnCd.lgau)
```

Model fitted: Log-Gaussian (5 parms)

Parameter estimates:

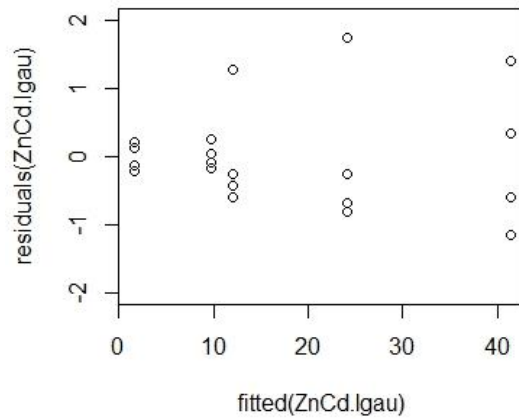
	Estimate	Std. Error	t-value	p-value
b:(Intercept)	0.555663	0.015419	36.038564	0.0000
c:(Intercept)	-0.274800	1.032831	-0.266065	0.7938
d:(Intercept)	42.904780	0.747360	57.408441	0.0000
e:(Intercept)	2.321479	0.018413	126.077969	0.0000
f:(Intercept)	2.028462	0.164444	12.335300	0.0000

Residual standard error:

0.834502 (15 degrees of freedom)

#Model checking

```
plot(fitted(ZnCd.lgau), residuals(ZnCd.lgau), ylim = c(-2, 2))
```



#lgaussian function with Box-Cox transform

```
ZnCd.lgau2 <- drm(IR~conc, data=ZnCd, fct=lgaussian(), na.action=na.omit, bcVal = 0, bcAdd = 10)
```

```
summary(ZnCd.lgau2)
```

Model fitted: Log-Gaussian (5 parms)

Parameter estimates:

	Estimate	Std. Error	t-value	p-value
b:(Intercept)	0.555188	0.015215	36.489732	0.000
c:(Intercept)	-0.290451	0.583670	-0.497628	0.626
d:(Intercept)	42.910857	0.943991	45.456837	0.000
e:(Intercept)	2.321820	0.012425	186.867587	0.000
f:(Intercept)	2.024344	0.134982	14.997109	0.000

Residual standard error:

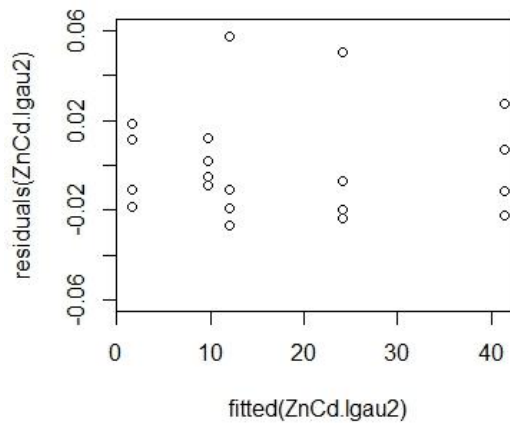
0.02654068 (15 degrees of freedom)

Non-normality/heterogeneity adjustment through optimal Box-Cox transformation

Specified lambda: 0

#Model checking

```
plot(fitted(ZnCd.lgau2), residuals(ZnCd.lgau2), ylim = c(-0.06, 0.06))
```



#Plot:

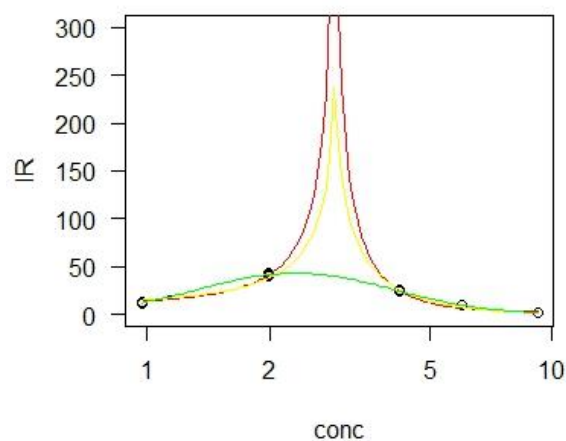
```
plot(ZnCd.gau, type = "obs", col= "black", ylim = c(0, 300))
```

```
plot(ZnCd.gau, type = "none", add = TRUE, col = "red")
```

```
plot(ZnCd.gau2, type = "none", add = TRUE, col = "yellow")
```

```
plot(ZnCd.lgau, type = "none", add = TRUE, col = "blue")
```

```
plot(ZnCd.lgau2, type = "none", add = TRUE, col = "green")
```



Based on the residuals standard errors and visual observation, we can infer that the LogGaussian with Box-Cox modification (green line) is the model that fits better the experimental data, therefore it will be used for fitting ZnCd response in the rest of calculations.

#Effective doses ($D(p)$) calculation:

```
ED(ZnCd.lgau2, -50, interval = "delta", bound = FALSE)
```

	Estimate	Std. Error	Lower	Upper
1:-50	1.209189	0.014632	1.178001	1.2404

```
ED(ZnCd.lgau2, 99.9, interval = "delta")
```

	Estimate	Std. Error	Lower	Upper
1:99.9	2.382456	0.015367	2.349703	2.4152

```
ED(ZnCd.lgau2, 50, interval = "delta")
```

	Estimate	Std. Error	Lower	Upper
1:50	4.458236	0.053948	4.343248	4.5732

#Additivity predictions and departures from additivity:

$E(p)$ calculation

We apply the method to perform additivity predictions and to study the nature of the interaction through the *indicesFct* {drc} command. The first datum that has to be indicated is the ratio in which metals are present in the mixture. After that, we have to introduce the list with the model equations fitted for the mixture and the individual metals, respectively. The ratio only has to be indicated for the individual metal indicated first. (For example, in the case below, the ratio Zn: Cd is 0.355:0.645, therefore, as Zn is the first individual metal introduced, we indicated is 0.355 as ratio data). In c() vector we indicated the fractional effect (p) which we want to be considered.

```
indicesFct(0.355, list(ZnCd.lgau2, Zn.lgau2, Cd.lgau2), c(-0.2, -0.5, -1, -2, -5, -10, -20, -30, -40, -50, -60, -70, -80, -90, -99, 99, 80, 70, 60, 50, 40, 30, 20, 10, 5, 2, 1, 0.5, 0.2))
```

#ECmat: Matrix with the fitted nonlinear regression model equations concentration data for the mixture (ECmix, Zn: Cd), the first individual metal indicated (EC1, Zn) and the second individual metal indicated (EC2, Cd) and the standard error, respectively. These data correspond to the $D(p)$ data for all the fractional effect indicated in indicesFct.

#Emat: Matrix with the fitted nonlinear regression model equations effect data for the mixture (ECmix, Zn: Cd), the first individual metal indicated (EC1, Zn) and the second individual metal indicated (EC2, Cd) and the standard error, respectively. These data correspond to the $E(p)$ data for all the fractional effect indicated.

```
#ECmat
```

```
$ECmat
  ECmix  EC1  EC2  SEMix  SE1  SE2
-0.2 0.3377212 0.9063974 1.038593 0.04011755 0.13046075 0.14144360
-0.5 0.3908416 0.9554918 1.155985 0.03941034 0.11453523 0.13457294
-1 0.4403353 0.9982981 1.262736 0.03821894 0.10068741 0.12756483
-2 0.5008234 1.0475599 1.390481 0.03621944 0.08504322 0.11864606
-5 0.6052838 1.1265598 1.605791 0.03175981 0.06167670 0.10360652
-10 0.7130718 1.2020991 1.823015 0.02636580 0.04433297 0.09065132
-20 0.8635123 1.3004321 2.121074 0.01865975 0.03990628 0.08155946
-30 0.9854817 1.3758876 2.360446 0.01376951 0.05191294 0.08431427
```

-40	1.0980212	1.4431499	2.580827	0.01236843	0.06724096	0.09380770
-50	1.2091890	1.5080376	2.799017	0.01463218	0.08284889	0.10714382
-60	1.3247947	1.5744593	3.027361	0.01900860	0.09824789	0.12269719
-70	1.4513381	1.6465755	3.280125	0.02418490	0.11340309	0.13948356
-80	1.5994438	1.7311354	3.581510	0.02937550	0.12816148	0.15641649
-90	1.7951676	1.8452853	3.993509	0.03323070	0.14111191	0.17001128
-99	2.1420593	2.0701401	4.797048	0.02491718	0.13005296	0.14361250
99	2.5166671	2.4348518	5.945510	0.02927474	0.15296534	0.17799479
80	3.3704531	2.9116638	7.963371	0.06190199	0.21555976	0.34778696
70	3.7144001	3.0611923	8.695064	0.06189626	0.21083069	0.36974764
60	4.0691968	3.2014066	9.421043	0.05838621	0.19977109	0.38182950
50	4.4582362	3.3424130	10.189613	0.05394832	0.18362621	0.39004910
40	4.9096050	3.4926962	11.051070	0.05530320	0.16273586	0.40168347
30	5.4702694	3.6634419	12.082839	0.07643259	0.13822354	0.43159454
20	6.2429337	3.8760073	13.446443	0.13490439	0.11894280	0.51704222
10	7.5600385	4.1930688	15.644902	0.27953208	0.15463881	0.77795888
5	8.9063184	4.4742271	17.761275	0.46732288	0.24495419	1.14596724
2	10.7639755	4.8116429	20.511540	0.77844851	0.39061976	1.75019587
1	12.2426021	5.0490772	22.586587	1.06259775	0.50924519	2.28175498
0.5	13.7929269	5.2752772	24.672378	1.39080342	0.63234981	2.87221259
0.2	15.9624260	5.5610094	27.461096	1.89615994	0.80041434	3.73986448

\$Emat

	Emix	E1	E2	SEmix	SE1	SE2
-0.2	-0.2040480	1.633213	1.137063	0.5205959	0.4644456	0.2752171
-0.5	-0.0744441	1.869085	1.283130	0.4604050	0.7311427	0.2751321
-1	0.1415624	2.262205	1.526575	0.3871991	1.2358878	0.3226767
-2	0.5735755	3.048445	2.013464	0.2880300	2.0127812	0.4429080
-5	1.8696147	5.407164	3.474132	0.1717987	3.3361324	0.6960765
-10	4.0296801	9.338364	5.908579	0.2052600	4.1595662	0.8915007
-20	8.3498109	17.200764	10.777473	0.2567516	4.0115727	1.0526113
-30	12.6699416	25.063163	15.646367	0.3034367	3.2581518	1.2316369
-40	16.9900724	32.925563	20.515260	0.4120100	2.9174574	1.4676017
-50	21.3102031	40.787962	25.384154	0.5412729	3.3301463	1.6940712
-60	25.6303338	48.650362	30.253047	0.6439274	4.0714852	1.8533158
-70	29.9504646	56.512761	35.121941	0.6877660	4.7374010	1.9219699
-80	34.2705953	64.375161	39.990835	0.6544011	5.2893357	1.9432093
-90	38.5907261	72.237560	44.859728	0.5856322	6.2821053	2.1387117
-99	42.4788438	79.313720	49.241733	0.8282188	9.1805150	3.0337516
99	42.4788438	79.313720	49.241733	0.8505941	8.8935420	3.0498938
80	34.2705953	64.375161	39.990835	0.5437934	7.9318629	1.6544342
70	29.9504646	56.512761	35.121941	0.5390104	8.5289396	1.5638688
60	25.6303338	48.650362	30.253047	0.4828725	8.3180725	1.5340835
50	21.3102031	40.787962	25.384154	0.3876131	7.3784991	1.4919847
40	16.9900724	32.925563	20.515260	0.2912417	5.9051575	1.4375273
30	12.6699416	25.063163	15.646367	0.2511280	4.2123056	1.3878589
20	8.3498109	17.200764	10.777473	0.2655813	2.9172177	1.3277733
10	4.0296801	9.338364	5.908579	0.2112043	2.6130773	1.1303774
5	1.8696147	5.407164	3.474132	0.1460100	2.2864276	0.8458768
2	0.5735755	3.048445	2.013464	0.2697191	1.4925741	0.5097317
1	0.1415624	2.262205	1.526575	0.3772735	0.9548770	0.3522130
0.5	-0.0744441	1.869085	1.283130	0.4551203	0.6017063	0.2840370
0.2	-0.2040480	1.633213	1.137063	0.5183190	0.4483813	0.2753855

#CAx: data frame including a series of relevant parameters from the mixture models:

CAX\$ComInd is the Combination Index calculated for the dose dimension for each p level, CAX\$seCI is the standard errors of the combination index, CAX\$Diff is the difference from 1 of the Combination index, CAX\$CAdiffp: p-value of the two tailed Student T-test of the Null hypothesis $CI=1$. CAX\$PredAdd is the prediction of the dose (D) required to produce each p level under the hypothesis of additivity, and CAX\$sePredAdd is the standard error of the dose (D) required to produce each p level under the hypothesis of additivity.

#CAy: The same that **#CAx** but for the empirical effect (E) axis.

CAx

	combInd	seCI	CAdiff	ciloCAdiff	cihiCAdiff	CAdiffp	PredAdd	sePredAdd
-0.2	0.3420080	0.05318707	-0.65799204	0.2377613	0.4462546	0.000000e+00	0.987466	0.09911044
-0.5	0.3632882	0.04784768	-0.63671184	0.2695067	0.4570696	0.000000e+00	1.075845	0.09115646
-1	0.3815069	0.04315301	-0.61849311	0.2969270	0.4660868	0.000000e+00	1.154200	0.08371682
-2	0.4020365	0.03779096	-0.59796346	0.3279663	0.4761068	0.000000e+00	1.245716	0.07480133
-5	0.4338613	0.02955270	-0.56613872	0.3759380	0.4917846	0.000000e+00	1.395109	0.06059542
-10	0.4628736	0.02259682	-0.53712644	0.4185838	0.5071633	0.000000e+00	1.540533	0.04910660
-20	0.4983135	0.01643862	-0.50168648	0.4660938	0.5305332	0.000000e+00	1.732870	0.04319287
-30	0.5235555	0.01542966	-0.47644447	0.4933134	0.5537977	0.000000e+00	1.882287	0.04884191
-40	0.5445192	0.01718988	-0.45548075	0.5108271	0.5782114	0.000000e+00	2.016497	0.05946825
-50	0.5632927	0.02011918	-0.43670733	0.5238591	0.6027263	0.000000e+00	2.146644	0.07213750
-60	0.5809637	0.02340490	-0.41903632	0.5350901	0.6268373	0.000000e+00	2.280340	0.08584242
-70	0.5982965	0.02666656	-0.40170354	0.5460300	0.6505629	0.000000e+00	2.425784	0.10027830
-80	0.6160407	0.02959570	-0.38395927	0.5580332	0.6740483	0.000000e+00	2.596328	0.11525769
-90	0.6352995	0.03143490	-0.36470046	0.5736871	0.6969119	0.000000e+00	2.825703	0.12966401
-99	0.6553495	0.02578785	-0.34465050	0.6048053	0.7058937	0.000000e+00	3.268576	0.12286943
99	0.6399498	0.02556564	-0.36005016	0.5898412	0.6900585	0.000000e+00	3.932601	0.15029770
80	0.6839299	0.03500694	-0.31607013	0.6153163	0.7525435	0.000000e+00	4.928068	0.23544563
70	0.7062854	0.03399879	-0.29371461	0.6396478	0.7729230	0.000000e+00	5.259064	0.23750546
60	0.7298207	0.03209315	-0.27017933	0.6669181	0.7927232	0.000000e+00	5.575612	0.23176311
50	0.7557176	0.02961498	-0.24428238	0.6976723	0.8137630	2.220446e-16	5.899341	0.21988492
40	0.7855666	0.02697002	-0.21443342	0.7327053	0.8384278	1.776357e-15	6.249763	0.20268872
30	0.8220989	0.02531321	-0.17790112	0.7724850	0.8717128	2.095213e-12	6.654029	0.18257472
20	0.8712462	0.02819427	-0.12875384	0.8159854	0.9265069	4.955426e-06	7.165522	0.17260888
10	0.9517409	0.04511972	-0.04825907	0.8633063	1.0401756	2.848093e-01	7.943378	0.23568287
5	1.0300894	0.06966783	0.03008942	0.8935405	1.1666384	6.658154e-01	8.646160	0.36895879
2	1.1326403	0.10816823	0.13264027	0.9206305	1.3446500	2.201082e-01	9.503437	0.59274946
1	1.2103851	0.14078794	0.21038505	0.9344407	1.4863294	1.350868e-01	10.114634	0.78322652
0.5	1.2887785	0.17615178	0.28877851	0.9435210	1.6340360	1.011356e-01	10.702325	0.98752619
0.2	1.3939205	0.22701557	0.39392053	0.9489700	1.8388711	8.270296e-02	11.451461	1.27584661

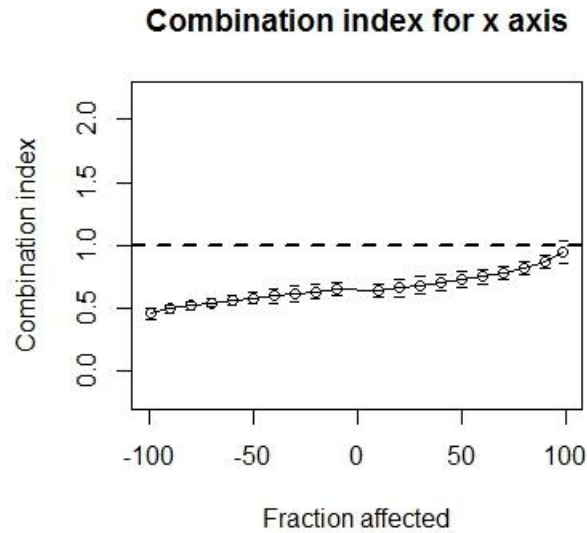
\$CAy

	combInd	seCI	CAdiff	ciloCAdiff	cihiCAdiff	CAdiffp	PredAdd	sePredAdd	
-0.2	-6.246141	15.98104655	-7.2461407	-37.56899190	25.076711	6.502457e-01	1.274513	0.2445852	
-0.5	-19.394622	120.00348198	-20.3946216	-254.60144624	215.812203	8.650493e-01	1.443815	0.2728977	
-1	12.191095	33.44643940	11.1910951	-53.36392614	77.746116	7.379287e-01	1.725801	0.3687187	
-2	3.991448	2.21941650	2.9914484	-0.35860794	8.341505	1.777055e-01	2.289397	0.5466498	
-5	2.128313	0.50514537	1.1283131	1.13822818	3.118398	2.550674e-02	3.979126	0.8707750	
-10	1.686106	0.28392387	0.6861065	1.12961568	2.242597	1.566985e-02	6.794470	1.0905217	
-20	1.488006	0.14727617	0.4880064	1.19934505	1.776668	9.212100e-04	12.424572	1.1688759	
-30	1.424987	0.10187579	0.4249871	1.22531058	1.624664	3.024410e-05	18.054504	1.2161818	
-40	1.394013	0.08747537	0.3940133	1.22256162	1.565465	6.659910e-06	23.684387	1.3707492	
-50	1.375597	0.08196254	0.3755970	1.21495038	1.536244	4.593528e-06	29.314251	1.5799862	
-60	1.363389	0.07675733	0.3633885	1.21294418	1.513833	2.198644e-06	34.944103	1.7605632	
-70	1.354702	0.06969076	0.3547019	1.21810797	1.491296	3.587174e-07	40.573950	1.8677796	
-80	1.348205	0.06198961	0.3482051	1.22670549	1.469705	1.941297e-08	46.203793	1.9325552	
-90	1.343163	0.05981961	0.3431629	1.22591650	1.460409	9.657907e-09	51.833633	2.1703342	
-99	1.339502	0.07761812	0.3395018	1.18737028	1.491633	1.219894e-05	56.900487	3.1048805	
99	1.339502	0.07750054	0.3395018	1.18760072	1.491403	1.183326e-05	56.900487	3.0886847	
80	1.348205	0.06306100	0.3482051	1.22460557	1.471805	3.356992e-08	46.203793	2.0329821	
70	1.354702	0.07300699	0.3547019	1.21160816	1.497796	1.182997e-06	40.573950	2.0610678	
60	1.363389	0.08273892	0.3633885	1.20122026	1.525557	1.123176e-05	34.944103	2.0158471	
50	1.375597	0.09101584	0.3755970	1.19720591	1.553988	3.679729e-05	29.314251	1.8648365	
40	1.394013	0.09968792	0.3940133	1.19862501	1.589402	7.734919e-05	23.684387	1.6443250	
30	1.424987	0.11575340	0.4249871	1.19811046	1.651864	2.411433e-04	18.054504	1.4222600	
20	1.488006	0.15814184	0.4880064	1.17804835	1.797964	2.029524e-03	12.424572	1.2599316	
10	1.686106	0.28267095	0.6861065	1.13207141	2.240142	1.521475e-02	6.794470	1.0819760	
5	2.128313	0.47901587	1.1283131	1.18944201	3.067184	1.849871e-02	3.979126	0.8399322	
2	3.991448	2.08412857	2.9914484	-0.09344358	8.076340	1.511881e-01	2.289397	0.5196061	
1	12.191095	32.58457772	11.1910951	-51.67467725	76.056867	7.312618e-01	1.725801	0.3510270	
0.5	-19.394622	118.62396439	-20.3946216	-251.89759175	213.108349	8.634952e-01	1.443815	0.2646745	
0.2	-6.246141	15.91107245	-7.2461407	-37.43184268	24.939561	6.488107e-01	1.274513	0.2433053	

#Plot the CI for the x axis:

```
plotFACI(0.355,list(ZnCd.lgau2, Zn.lgau2, Cd.lgau2), "x", ylim = c(-0.2, 2.2), faValues = c(-10, -20, -30, -40, -50, -60, -70, -80, -90, -99, 99, 90, 80, 70, 60, 50, 40, 30, 20, 10), showPoints = TRUE)
```

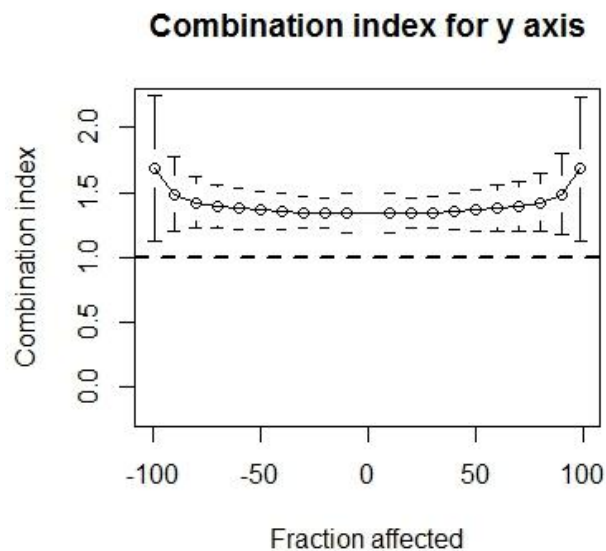
```
title("Combination index for x axis")
```



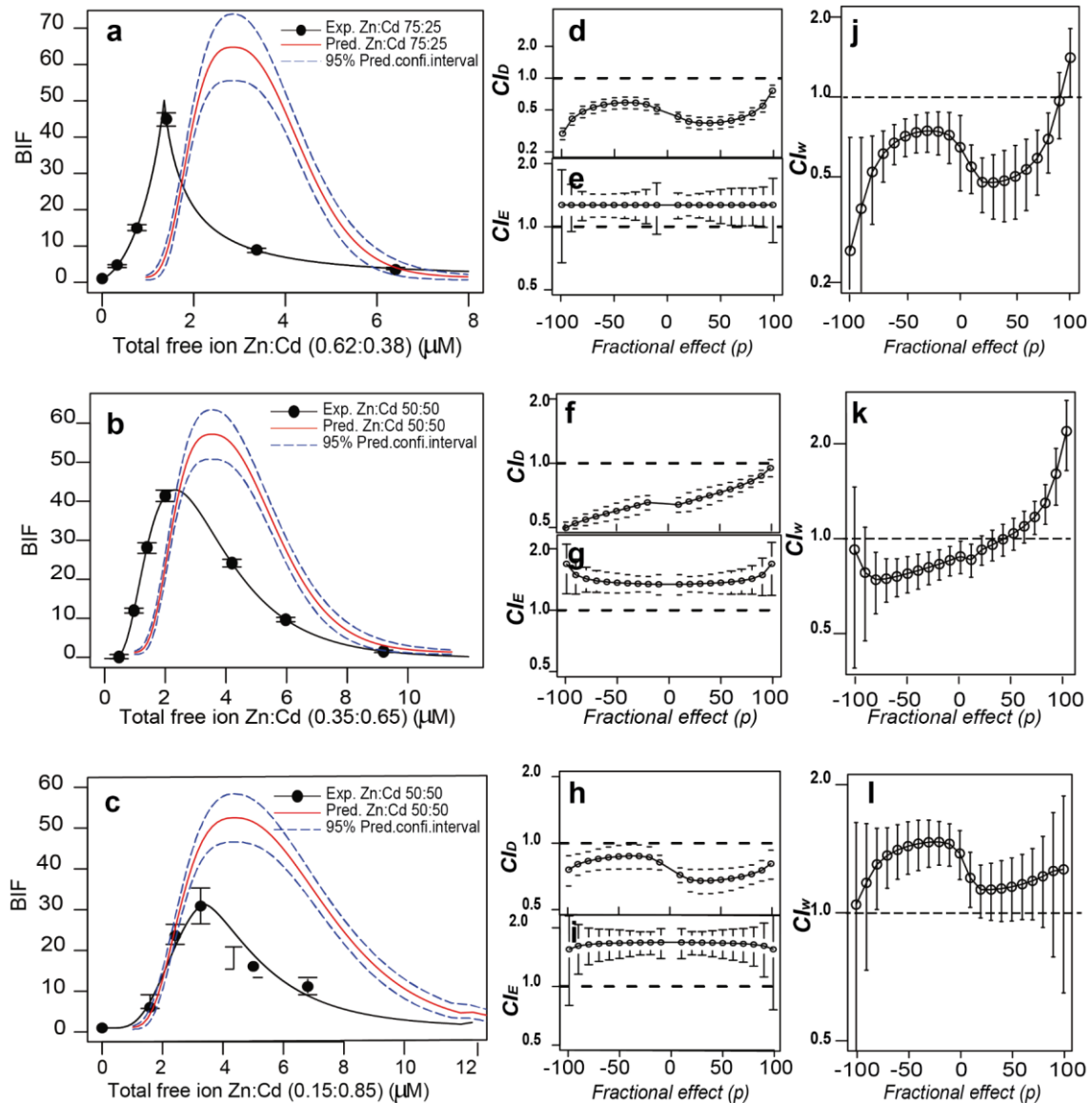
#Plot CI for the y axis

```
plotFACI(0.355,list(ZnCd.lgau2, Zn.lgau2, Cd.lgau2), "y", ylim = c(-0.2, 2.2), faValues = c(-10, -20, -30, -40, -50, -60, -70, -80, -90, -99, 99, 90, 80, 70, 60, 50, 40, 30, 20, 10), showPoints = TRUE)
```

```
title("Combination index for y axis")
```



Supplementary Material SM4 (Figure).



Effect of mixture ratio for the Zn:Cd binary mixture. Experimental vs predicted (under additivity) dose-response patterns for the mixture Zn:Cd at 75:25 (a), 50:50 (b) and 25:75 (c) mixture ratios based on the D_0 concentration of the metals. Extended p -CI plots presenting departures from additivity (as CI values) as a function of the effect level (p) for the D dimension (d, f, h), and the E dimension (e, g, i). Extended p - CI_w plots presenting weighted departures from additivity (as CI_w values) as a function of the effect level (p) for the binary mixture Zn:Cd at 75:25 (j), 50:50 (k), 25:75 (l) mixture ratios. Error bars are standard errors ($n = 3-4$). Total free ion concentrations presented in the Figures are those presented as ED_0 in Supplementary Material SM2 corrected by MINTEQ calculations due to the presence of the two metals used in each mixture.

Supplementary Material SM5 (Table). Combination index (CI) values for the dose (*D*) and empirical effect (*E*) dimensions together with relevant statistical information for 3 selected fractional effect levels (*p*) of the 15 binary metal mixtures of Cu, Cd, Zn, Cu, Hg and Co.

Metal mixture	Fractional affect (<i>p</i>)	CI _D	<i>p</i> -values	CI _E	<i>p</i> -values	CI _w
Cu:Cd	-50	0.89± 0.05	0.03	1.48± 0.15	< 0.01	1.32± 0.2
	0	0.86± 0.03	< 0.01	1.52± 0.14	< 0.01	1.31±0.17
	50	0.77± 0.03	< 0.01	1.48± 0.18	< 0.01	1.14±0.21
Cu:Zn	-50	1.28± 0.05	< 0.01	0.71± 0.08	< 0.01	0.91±0.13
	0	1.11± 0.04	< 0.01	0.7± 0.08	< 0.01	0.77± 0.12
	50	1.07± 0.04	0.04	0.71±0.13	0.02	0.76±0.17
Zn:Cd	-50	0.56± 0.02	< 0.01	1.37± 0.08	< 0.01	0.77±0.1
	0	0.64± 0.02	< 0.01	1.34± 0.08	< 0.01	0.86±0.1
	50	0.75± 0.03	< 0.01	1.37± 0.09	< 0.01	1.03±0.12
Cu:Hg	-50	1.18±0.07	< 0.01	0.58±0.06	< 0.01	0.68±0.13
	0	1.89±0.07	< 0.01	0.59±0.03	< 0.01	1.11±0.10
	50	2.19±0.13	< 0.01	0.58±0.05	< 0.01	1.27±0.18
Co:Cd	-50	1.05 ± 0.03	0.01	1.03±0.09	0.76	1.08±0.12
	0	0.73± 0.02	< 0.01	1.04±0.06	0.45	0.76±0.08
	50	0.53± 0.02	< 0.01	1.03±0.06	0.68	0.54±0.08
Hg:Cd	-50	1.39±0.06	< 0.01	0.69±0.06	< 0.01	0.95±0.12
	0	1.22±0.02	< 0.01	0.69±0.04	< 0.01	0.84±0.06
	50	1.04±0.05	< 0.01	0.69±0.05	< 0.01	0.72±0.10
Ag:Cd	-50	1.41±0.04	< 0.01	0.64±0.04	< 0.01	0.9±0.08
	0	1.07±0.02	< 0.01	0.64±0.04	< 0.01	0.68±0.06
	50	0.73±0.02	< 0.01	0.64±0.04	< 0.01	0.47±0.06 [§]
Zn:Hg	-50	3.61±0.23	< 0.01	0.52±0.05	< 0.01	1.87±0.28
	0	3.10±0.07	< 0.01	0.52±0.06	< 0.01	1.61±0.13
	50	2.45±0.16	< 0.01	0.52±0.09	< 0.01	1.27±0.25
Hg:Co	-50	1.11±0.06	< 0.01	0.29±0.09	< 0.01	0.32±0.15 [§]
	0	1.24±0.04	< 0.01	0.28±0.02	< 0.01	0.35±0.06 [§]
	50	1.17±0.07	< 0.01	0.29±0.02	< 0.01	0.34±0.09 [§]
Cu:Ag	-50	1.13±0.03	< 0.01	0.68±0.04	< 0.01	0.77±0.07
	0	0.97±0.02	0.02	0.68±0.04	< 0.01	0.66±0.06
	50	1.06±0.02	< 0.01	0.68±0.09	< 0.01	0.72±0.11
Zn:Ag	-50	1.54±0.05	< 0.01	0.62±0.05	< 0.01	0.95±0.1
	0	1.07±0.04	< 0.01	0.61±0.06	< 0.01	0.65±0.1
	50	0.94±0.03	0.05	0.62±0.09	< 0.01	0.57±0.12
Hg:Ag	-50	1.26±0.06	< 0.01	1.62±0.10	< 0.01	2.04±0.16 [§]
	0	1.32±0.03	< 0.01	1.58±0.09	< 0.01	2.08±0.12 [§]
	50	1.26±0.05	< 0.01	1.62±0.25	0.01	2.04±0.3 [§]
Co:Ag	-50	1.11±0.07	0.01	1.71±0.27	< 0.01	1.9±0.34
	0	1±0.05	0.94	1.87±0.18	< 0.01	1.87±0.23
	50	0.91±0.03	< 0.01	1.71±0.16	< 0.01	1.56±0.19
Zn:Co	-50	1.1±0.04	0.02	0.50±0.05	< 0.01	0.55±0.09
	0	0.85±0.04	< 0.01	0.49±0.03	< 0.01	0.42±0.07 [§]
	50	0.7±0.03	< 0.01	0.5±0.04	< 0.01	0.35±0.07 [§]
Cu:Co	-50	0.92±0.03	< 0.01	0.87±0.14	0.33	0.8±0.17
	0	1.85±0.04	< 0.01	0.88±0.06	0.04	1.63±0.1
	50	1.60±0.03	< 0.01	0.87±0.08	0.10	1.39±0.11

±: standard errors. For CI_D and CI_E, *P*-values were obtained using the function *Indices.fct* {drc}¹ which essentially performs a two-tailed Student's t-Test against the null hypothesis Ho: CI = 1. Statistical

significance is assumed to exist for p -values lesser than 0.05. For CI_w , it is not possible to directly perform a Student's t -Test since they are not directly computed with a dedicated *drc* function. In this case, statistical significance can be inferred from the absence of overlapping with 1 of the 95% confidence interval ($IC_{95\%} = 1.95 \cdot \text{Estandard deviation}$) for each CI_w value. However, in the paper and in the present Table, the criteria for the analysis of departures from additivity for CI_w is based on the pragmatic thresholds: $Exp < 0.5 \cdot CA$ (synergism) and $Exp > 2 \cdot CA$ (antagonism)^{4,5}, and it is marked by an [§].

References

- 1 Ritz, C. & Streibig, J. C. Bioassay Analysis using R. *Journal of statistical software* **12**, 17 (2005).
- 2 The R Stats Package v. 3.3.0 (2015).
- 3 Martin-Betancor, K., Rodea-Palomares, I., Munoz-Martin, M. A., Leganes, F. & Fernandez-Pinas, F. Construction of a self-luminescent cyanobacterial bioreporter that detects a broad range of bioavailable heavy metals in aquatic environments. *Frontiers in microbiology* **6**, 186, doi:10.3389/fmicb.2015.00186 (2015).
- 4 Altenburger, R., Backhaus, T., Boedeker, W., Faust, M. & Scholze, M. Simplifying complexity: Mixture toxicity assessment in the last 20 years. *Environmental toxicology and chemistry / SETAC* **32**, 1685-1687, doi:10.1002/etc.2294 (2013).
- 5 Cedergreen, N. Quantifying Synergy: A Systematic Review of Mixture Toxicity Studies within Environmental Toxicology. *PloS one* **9**, e96580, doi:10.1371/journal.pone.0096580 (2014).

**Co, Zn and Ag-MOFS
evaluation as biocidal
materials towards
photosynthetic organisms**

C

H

A

P

T

E

R

IV



Co, Zn and Ag-MOFs evaluation as biocidal materials towards photosynthetic organisms



Keila Martín-Betancor^a, Sonia Aguado^b, Ismael Rodea-Palomares^a, Miguel Tamayo-Belda^a, Francisco Leganés^a, Roberto Rosal^b, Francisca Fernández-Piñas^{a,*}

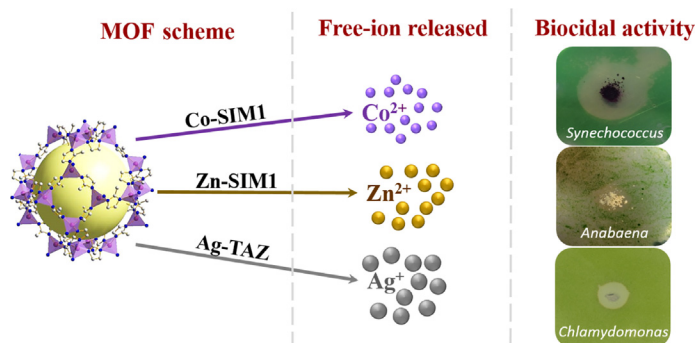
^a Department of Biology, Facultad de Ciencias, Universidad Autónoma de Madrid, 28049 Madrid, Spain

^b Department of Chemical Engineering, Universidad de Alcalá, Alcalá de Henares, 28871 Madrid, Spain

HIGHLIGHTS

- Three metal organic frameworks (MOFs) were evaluated as biocidal materials.
- The three MOFs showed strong biocidal activity towards cyanobacteria.
- The Ag-based MOF was the most effective against the green alga.
- MOFs biocidal activity was due to bioavailable released metal.
- MOFs can be used as reservoirs of metal ions for sustained biocidal activity.

GRAPHICAL ABSTRACT



ARTICLE INFO

Article history:

Received 13 January 2017

Received in revised form 24 March 2017

Accepted 27 March 2017

Available online xxxx

Keywords:

Biocidal material
Heavy metal bioreporter
Metal bioavailability
MOFs
Photosynthetic organisms

ABSTRACT

In the present study, the biocidal activity of three different metal organic frameworks (MOFs) based on Co (Co-SIM1), Zn (Zn-SIM1) and Ag (Ag-TAZ) has been evaluated towards one green alga and two cyanobacteria. These organisms are present in fresh- and seawater and take part in the early stages of the biofouling process. The biocidal activity of these materials was evaluated by measuring chlorophyll *a* concentration and by inhibition zone testing. After 24 h of exposure the three different MOFs caused >50% of chlorophyll *a* concentration inhibition towards both cyanobacteria, however, although the green alga presented a great sensitivity for Ag-TAZ (reaching 90% of chlorophyll *a* concentration inhibition), it was much more resistant to the rest of MOFs. Bioavailability of these metals was studied using ICP-MS, the chemical speciation program Visual MINTEQ, and a heavy metal bioreporter bioanalytical tool. We have elucidated that the biocidal activity presented by these MOFs was due to the dissolved metals released from them and more exactly, it depended on the bioavailability presented by these metal ions, which was closely related with the free ion concentration. This article highlights the potential use of different MOFs as biocidal material towards photosynthetic organisms and reveals important differences in the sensitivity between these organisms that should be taken into account in order to increase the biocidal spectrum of these materials.

© 2017 Elsevier B.V. All rights reserved.

1. Introduction

Metal-organic frameworks (MOFs) are one of the latest developments in nanotechnology (Ferey, 2008; McKinlay et al., 2010; Spokoyney et al.,

* Corresponding author.

E-mail address: francisca.pina@uam.es (F. Fernández-Piñas).

2009). These new porous inorganic-organic hybrid materials are constructed by controlled crystallization, joining metal-containing units with multifunctional organic ligands. Due to the inherent porous structure of MOFs, changeable surface functional groups and different choice of metal and ligands, different types of MOFs can be developed. Their structure give them great potential for a wide range of applications, such as gas storage, catalysis, chemical sensing, drug delivery (Beg et al., 2016; Furukawa et al., 2013; Getman et al., 2012; Horcajada et al., 2010; Kreno et al., 2012; Kuppler et al., 2009; Yaghi et al., 2003) and the most recent application as biocidal materials (Wyszogrodzka et al., 2016). The use of some MOFs as biocide material in water treatment and biomedical applications has been evaluated (Prince et al., 2014; Quirós et al., 2015). Some advantages of using MOFs based materials instead of traditional chemical disinfectants are their high durability, wide antimicrobial spectrum, high effectiveness and thermal-optical stabilities.

Other porous structures used as biocide material are zeolites or silica based materials. Zeolites are porous crystalline alumina silicate minerals with uniform molecular-sized pores. They contain metal ions, which can readily be exchanged by other metals such as silver, copper, and zinc ions via ion-exchange post-synthesis treatment for their use as antimicrobial agents due to the easily metal ion extraction from the zeolites (Dong et al., 2014; Sánchez et al., 2017; Zhou et al., 2014). Many different kinds of silica-supported materials have been proposed for antimicrobial applications. Basic copper chloride structures supported on silica nanoparticles showed similar antibacterial activity against *Escherichia coli* and *Staphylococcus aureus* than copper-exchanged mordenite zeolite microparticles (Palza et al., 2015). Reduced copper on the surface of spherical silica nanoparticles displayed significant antibacterial ability (Kim et al., 2006). Mesoporous silica has also been used as support for metals because thanks to its high surface area and uniform pore distribution offers the possibility of dispersing metal nanoparticles inside a non-nano support. Copper oxide and reduced silver have been dispersed in the form of nanoparticles inside a highly ordered mesoporous SBA with antifungal and antibacterial activities (Díez et al., 2017; Quiros et al., 2016). The mechanism of zeolite and silica-supported metals is different from that of MOF-based antimicrobials. Whereas zeolites are cation-exchangers and supported metals or oxides must change its oxidation state or dissolve before becoming bioavailable, MOFs are constructed directly with the desired metal linked by covalent bonds. The structures of MOFs can be designed at the atomic scale by an appropriate choice of metal and organic ligand, which define their antimicrobial activity and allowing a more controlled release of the metal ions. Furthermore, these metals coordination polymers could provide some advantages over the use of nanoparticles (NPs) as biocidal material (Lu et al., 2014).

In the last years, several MOFs have been successfully tested as biocides materials, especially those based on silver (Berchel et al., 2011; Liu et al., 2010; Lu et al., 2014; Rueff et al., 2015). Silver-based biocidal materials are well known for their antimicrobial properties (Egger et al., 2009; Laluzza et al., 2011; Lemire et al., 2013; Matsumura et al., 2003; Rai et al., 2009; Sondi and Salopek-Sondi, 2004). However, silver is an expensive metal and the indiscriminate use of it in many antimicrobial materials is suspected to promote not only a general toxic risk but also bacterial resistance (Blaser et al., 2008; Merlino and Kennedy, 2010).

New MOFs based on different metals such as Co, Zn or Cu have also emerged. In most cases, these MOFs have been successfully tested towards heterotrophic organisms like *Pseudomonas putida*, *E. coli*, *Saccharomyces cerevisiae* or *S. aureus* (Aguado et al., 2014; Wang et al., 2015; Wojciechowska et al., 2012; Zhuang et al., 2012) and to marine bacteria as *Cobetia marina* (Sancet et al., 2013). However, studies to examine the biocidal effect of MOFs to photosynthetic organisms as cyanobacteria or algae are lacking (Wyszogrodzka et al., 2016).

Cyanobacteria and algae are photosynthetic, aquatic organisms present in both freshwater and seawater. As primary producers, they are relevant organisms in these environments; however, along with bacteria, they have other implications also as organisms that take part in the

early stages of the biofouling process (Briand, 2009; Mieszkin et al., 2013; Rosenhahn et al., 2010; Salta et al., 2013). Biofouling is the accumulation of microorganisms, algae, plants or/and animals on surfaces, mainly in the aquatic environments with a great economic impact on shipping or water filtration (Nguyen et al., 2012; Schultz et al., 2011). The colonization of these structures by unicellular microorganisms such as bacteria, cyanobacteria, unicellular algae and protozoa is denominated “microfouling” or “slime” and normally constitute the early stage of biofilm formation. For a deeper understanding of the colonization process, see the review by Dang and Lovell (2016) and Rosenhahn et al. (2010).

In the present article, we have evaluated the biocidal activity of two zeolite imidazolate frameworks (ZIF), a sub-family of MOFs, consisting of transition metal ions, Co^{2+} and Zn^{2+} , and imidazolate ligands, denominated Co-SIM1 and Zn-SIM1, respectively (Aguado et al., 2010; Aguado et al., 2011; Farrusseng et al., 2009). Different to their MOF analogues with carboxylates ligands, a number of ZIF exhibit exceptional thermal, hydrothermal and chemical stability (Banerjee et al., 2009; Phan et al., 2010). Furthermore, we analysed one silver-triazole coordination polymer (Ag-TAZ) prepared with a polyazaheteroaromatic compound, 1,2,4-triazole, a well-known intermediate compound of industrial relevance (Haasnoot, 2000), which is also widely used as ligand (Zhang et al., 2005).

The biocidal activity of these three different MOFs towards potential biofouling photosynthetic organisms: one filamentous (*Anabaena* sp. PCC 7120, hereinafter *Anabaena*), and one unicellular (*Synechococcus* sp. PCC 7942, hereinafter *Synechococcus*) cyanobacteria, and one unicellular green alga (*Chlamydomonas reinhardtii*, hereinafter *Chlamydomonas*) is reported.

The study of the antimicrobial mechanism of nanomaterials has been of great interest by the scientific community (Durán et al., 2016; Franklin et al., 2007; Rai et al., 2009; Wyszogrodzka et al., 2016). Most of the literature has established that the biocidal activities of metallic nanomaterials are due to the dissolved metal ions. In order to better understand the mechanism of action of these MOFs, three different approaches were used. Metal released from these MOFs and bioavailability of these metals were studied using ICP-MS, the chemical speciation program, Visual MINTEQ, and a heavy metal bioreporter bioanalytical tool, the cyanobacterium *Synechococcus elongatus* PPC7942 pBG2120 (hereinafter *Synechococcus* pBG2120) (Martin et al., 2015). This bioreporter bears a fusion of the promoter region of the *smt* locus (encoding the transcriptional repressor SmtB and the metallothionein SmtA) to the *luxCDABE* operon of *Photobacterium luminescens* and is able to detect six different heavy metals (Zn, Ag, Cu, Co, Hg and Cd) in medium but also in environmental water samples.

To our knowledge, this work is the first study that reports the effects of these materials on photosynthetic organisms.

2. Materials and methods

2.1. Synthesis and characterization of materials

Zn-SIM1, Co-SIM1 and Ag-TAZ were synthesized by solvothermal procedure as reported elsewhere (Banerjee et al., 2008; Farrusseng et al., 2009; Huang et al., 2006). All of them were characterized by X-ray diffraction (XRD) in order to assess their crystallinity. A brief description of each synthesis, the diffractogram and the scanning electron microscope (SEM) micrographs of crystals can be seen in Supplementary text S1 and Supplementary Figs. S1 and S2.

2.2. Microorganism culture

In this study three different photosynthetic microorganisms were used, two different cyanobacterial strains, one filamentous, *Anabaena* sp. PCC 7120 and one unicellular, *Synechococcus* sp. PCC 7942 and one unicellular green alga strain, *Chlamydomonas reinhardtii* Dangeard

(strain CCAP 11/32A mt +). Each strain was grown in its specific medium. *Anabaena* cells were grown in AA/8 supplemented with nitrate (5 mM) (Allen and Arnon, 1955), *Synechococcus* in BG11 (Rippka, 1988) and *Chlamydomonas* in Tris-minimal phosphate medium (TAP-) (Hooper, 1989). All the media were adjusted to pH 7.5. The composition of these media are detailed in supplementary Table S1. All of them were grown on a rotatory shaker set under controlled conditions: 28 °C at 60 $\mu\text{mol photons m}^{-2} \text{s}^{-1}$ light intensity. For the free metal detection assays, a modified cyanobacterium based on *Synechococcus* sp. PCC 7942 was used, *Synechococcus elongatus* PBG2120, this strain was grown in BG11 medium supplemented with 3.2 $\mu\text{g mL}^{-1}$ of chloramphenicol (Cm) (Martin et al., 2015).

2.3. Antimicrobial activity tests

2.3.1. Zone inhibition technique

The biocidal materials were subjected to an antimicrobial experiment using the diffusion method described by Fiebelkorn et al. (2003). Agar plate diffusion assay is the standardized method recommended by the National Committee for Clinical Laboratory standards, based on the method described by Bauer et al. (1966). Petri dishes were prepared with 20 mL of appropriate culture media plus 1% Agar. The cellular concentration in inocula was adjusted to $\text{OD}_{750\text{nm}} = 1$ for cyanobacteria and $\text{OD}_{750\text{nm}} = 0.5$ for the alga, using the corresponding culture medium. 500 μL of each microbial suspension were transferred to plates for inoculation, spread and allowed to dry at room temperature. The cells were allowed to grow during five days under 20 $\mu\text{mol photons m}^{-2} \text{s}^{-1}$ before the addition of the antimicrobials. All materials were used in powder form by placing 1 and 10 mg directly onto the inoculated agar plate. As a control of the toxicity exhibited by the ligands individually, 1 and 10 mg of each ligand were placed directly onto the inoculated agar plate at the same time. In all cases, the amount of ligand in these experiments was higher than that released by 1 or 10 mg of each MOF. Zone radius was measured from the outermost part of the MOF to the highest growth inhibition spot in the plates after 4, 24 and 48 h. Control plates were incubated at the same time without antimicrobial agents to check correct microbial growth.

2.3.2. MOFs suspensions bioassays

Microorganisms were exposed to 1 mg of each MOF in a final volume of 20 mL of each specific medium (50 mg L^{-1} final concentration). The procedure used was as follows: the three organisms were allowed to grow for five days, until they reached $\text{OD}_{750\text{nm}} = 1$ for cyanobacteria and $\text{OD}_{750\text{nm}} = 0.5$ for the alga. After the organisms reached the indicated OD, they were washed three times with each appropriate culture medium and 4 mL of each culture were added to 16 mL of culture media reaching $\text{OD}_{750\text{nm}} = 0.2$ for *Anabaena* and *Synechococcus* and $\text{OD}_{750\text{nm}} = 0.1$ for *Chlamydomonas*. MOFs were added fresh in each test. Before adding the microorganisms, 1 mg of each MOFs was weighed, added to the medium and in order to homogenize the MOFs in all the experiments, sonicated using a Ultrasonic bath (Ultrasons) during 1 min. Then, the organisms were grown on a rotatory shaker during the experiments time with the same conditions as described before. The initial cellular densities were selected in order to maintain all microorganisms in the exponential growth phase during the entire time of exposure (48 h). The pH was measured during the whole incubation period (up to 48 h). In the case of AA/8 + N (*Anabaena* medium), the mean pH during the whole experiment was 7.37 ± 0.02 , 7.35 ± 0.04 and 7.35 ± 0.05 for Ag-TAZ, Co-SIM1 and Zn-SIM1 exposure, respectively. In the case of BG11 (*Synechococcus* medium), the mean pH during the whole experiment was 7.37 ± 0.05 , 7.49 ± 0.05 and 7.43 ± 0.01 , for Ag-TAZ, Co-SIM1 and Zn-SIM1 exposure, respectively. For TAP- (*Chlamydomonas* medium), the pH evolution during the experiment time was 7.27 ± 0.03 , 7.29 ± 0.08 and 7.26 ± 0.03 for Ag-TAZ, Co-SIM1 and Zn-SIM1 exposure, respectively. Microbial growth as measured by increase in $\text{OD}_{750\text{nm}}$ could not be used due to potential

attachment of MOFs to the microorganisms, for that, chlorophyll *a* concentration was used as endpoint as described for diatoms (Bazes et al., 2009; Briand, 2009; Tsoukatou et al., 2002). As a control of the toxicity exhibited by the ligands individually, the microorganisms were exposed at the same time to 50 mg L^{-1} of each ligand. The amount of the total ligand available from 50 mg L^{-1} of each MOF was 38.75 mg L^{-1} and 39.75 mg L^{-1} of SIM1 ligand for Zn-SIM1 and Co-SIM1, respectively, and 19.6 mg L^{-1} of TAZ ligand for Ag-TAZ. Thus, in all cases, the amount of ligand in these experiments was higher than that released by 50 mg L^{-1} of each MOF. Specifically, 50 mg L^{-1} of SIM-1 ligand (Co-SIM1 and Zn-SIM1 ligand) correspond to 1.25 and 1.3 fold more ligand than that released by 50 mg L^{-1} of Co-SIM1 and Zn-SIM1, respectively. In the case of TAZ ligand (Ag-TAZ ligand), the amount of TAZ is 2.5 times higher than that available in the release of 50 mg L^{-1} of Ag-TAZ.

In addition, the biocidal activity of the pure metal salts were also studied. The three microorganisms were exposed to the equivalent metal ion concentration presented in 50 mg L^{-1} of each MOF, specifically, 11.5 mg L^{-1} of Zn^{2+} [52.32 mg L^{-1} of $\text{Zn}(\text{NO}_3)_2 \cdot 6\text{H}_2\text{O}$], 10.65 mg L^{-1} of Co^{2+} [52.5 mg L^{-1} of $\text{Co}(\text{NO}_3)_2 \cdot 6\text{H}_2\text{O}$] and 30.68 mg L^{-1} of Ag^+ (48 mg L^{-1} of AgNO_3).

After 4, 24 and 48 h, chlorophyll was extracted from 1 mL of each experiment in methanol at 4 °C for 24 h in darkness and the chlorophyll *a* concentration of the cyanobacteria estimated according to Marker (1972) and in a 90% acetone aqueous solution for the alga according to Jeffrey and Humphrey (1975). The absorbance was determined by measuring the extract using a HITACHI U-2000 spectrophotometer at appropriate wavelengths. Two replicates of 1 mL were used and the experiments were performed in triplicate. The data are expressed as the percentage of the chlorophyll *a* concentration of the treated samples in function of the chlorophyll *a* concentration of the untreated samples.

2.3.3. MOFs filtrate bioassays

In order to analyse which part of the MOFs toxicity was due to the dissolved metals released from the MOFs, MOFs filtrate experiments were performed as follows: 1 mg of each MOF was weighed, added to 20 mL of each medium and sonicated during 1 min. MOF sonicated suspensions were kept for 24 h and centrifuged (4500 g 15 min) in 50-kDa molar mass cut-off VIVASPIN ultrafiltration membranes (Sartorius) for separating the ion released from the MOFs. 16 mL of the filtrate were used as the experimental medium. The organisms were prepared as in the Section 2.3.2. (see above) and the chlorophyll *a* concentration was measured after 24 h in the same way as described before. Each media without MOFs were also centrifuged and used as controls.

2.4. Detection of dissolved metals from MOFs by ICP-MS

The concentration of the dissolved metals present in MOFs filtrates in each medium (see above), and also, the concentration of the dissolved metals released from MOFs (50 mg L^{-1}) in distilled water was measured by inductively coupled plasma-mass spectrometry (ICP-MS; Perkin-Elmer Sciex Elan 6000 equipped with an AS91 auto-samples), by the ICP-MS laboratory of the Universidad Autonoma de Madrid, after removing the solids by 50-kDa VIVASPIN ultrafiltration membranes (Sartorius) after 4, 24 and 48 h of exposure.

2.5. Detection of the dissolved metals from MOFs by a heavy metal bioreporter

The bioluminescence strain, *Synechococcus* pBG2120, was prepared as described previously (Martin et al., 2015). Briefly, 50 mg L^{-1} of each MOF in distilled water were centrifuged in 50-kDa VIVASPIN ultrafiltration membranes after 24 h and the concentration of the dissolved metal present in these filtrates measured by ICP-MS (see above). The filtrates collected were diluted several times and 300 μL of these dilutions were added to 1200 μL of the bioreporter culture in 24 well plates. The plates were incubated at 28 °C in light (60 $\mu\text{mol m}^{-2} \text{s}^{-1}$) on a rotatory

shaker up to 4 h. For the luminescence measurements, 100 μL of cell suspensions were transferred to an opaque 96-well microtiter plate and luminescence was recorded every 5 min for 20 min in a CentroLB960 luminometer (Berthold Technologies GmbH and Co. KG, Bald Wilbad, Germany).

2.6. Modeling of metal speciation

The chemical equilibrium model Visual MINTEQ was used to predict the metal speciation in the three growth media, BG11, AA/8 + N and TAP-. Assumptions of a fixed pH, fixed potential redox (Eh), closed system and no precipitation of solid phases were made during computations. This chemical model was used previously to predict metal speciation and link it to the response of the reporter strain *Synechococcus* pBG2120 (Martin et al., 2015).

2.7. Statistical analysis

The test of statistically significant differences between datasets was performed using One-Way Analyses of Variance (ANOVA); also, to discriminate which datasets were significantly different from the others, the *post-hoc* Tukey's HSD (honestly significant difference) test was performed. All the tests were computed using R software 3.0.2. (copyright© The Foundation for Statistical Computing).

3. Results and discussion

3.1. Antimicrobial activity tests

3.1.1. Inhibition zone testing bioassay

The three organisms were exposed to 1 and 10 mg of each MOF up to 48 h. When exposed to 1 mg, both cyanobacteria were more sensitive to Co-SIM, presenting an inhibition radius of around 3 mm for *Synechococcus* and 5 mm for *Anabaena*. In the case of *Synechococcus*, Zn-SIM1 and Ag-TAZ produced an inhibition radius of 2 and 1 mm, respectively. *Anabaena* exhibited an inhibition radius of 1 mm and 3 mm for Zn-SIM1 and Ag-TAZ, respectively, after 24 h. In the case of *Chlamydomonas*, none of the MOFs caused any inhibition after 24 h of

exposure (Fig. 1), and, after 48 h, only the MOF based on Ag, Ag-TAZ, caused an inhibition radius of 4 mm to this alga (not shown).

When organisms were exposed to 10 mg of each MOF, also Co-SIM1 was the most toxic MOF for both cyanobacteria, *Synechococcus* and *Anabaena*, causing 8 and 6 mm of inhibition radius after 24 h of exposure, respectively. Again, Ag-TAZ was the only MOF that caused growth inhibition to *Chlamydomonas*, around 5 mm of inhibition radius after 24 h of exposure (Fig. S3). Exposure to 1 or 10 mg of ligands did not exceed 1 mm or 2 mm of inhibition radius respectively.

As previously reported by Aguado et al. (2014) Co-SIM1 showed a significant antimicrobial activity. They found that Co-SIM exhibited higher biocidal activity towards *S. cerevisiae*, *P. putida* and *E. coli* than Ag-TAZ, however, although a high biocidal effect towards both cyanobacteria was found, the results showed that it was not effective towards the green alga *Chlamydomonas* at the concentration tested. Other authors (Refat et al., 2008; Wojciechowska et al., 2012) have investigated the biological activities of Zn based complexes, specifically, in the case of L-tyrosinato Zinc(II) complex, Refat et al. (2008) found moderate activity of this complex against *E. coli* but strong activity against *Bacillus subtilis*, *Serratia* and *Pseudomonas aeruginosa*. Wojciechowska et al. (2012) incorporated ligand modifications to these L-tyrosinato complexes, as a molecule of secondary ligand such as 2,2'-bipyridine or imidazole. They found that only the complexes based on imidazole ligands presented large antibacterial activity, suggesting that the biocidal activity was strongly correlated with the presence of the imidazole molecule in its structure. However, the results reported in this study did not show toxicity of the imidazole, suggesting that the biocidal activity of Zn-SIM1 and Co-SIM1 against the cyanobacteria might be due to the dissolved metal. The biocidal effects of Ag based MOFs are well-documented, Lu et al. (2014) showed that two silver carboxylate MOFs, $[\text{Ag}_2(\text{O-IPA})(\text{H}_2\text{O}) \cdot (\text{H}_3\text{O})]$ and $[\text{Ag}_5(\text{PYDC})_2(\text{OH})]$ exhibited excellent antibacterial activities towards *E. coli* and *S. aureus*. Berchel et al. (2011) presented a silver MOF material based on a 3-phosphonobenzoate ligand which placing 1 mg onto an agar plate resulted in a strong growth inhibition upon six different strains of *S. aureus*, *E. coli* and *P. aeruginosa*. All these previous studies studied the antimicrobial properties of these materials on heterotrophic organisms. Our experiments showed that all MOFs used were able to diffuse in the cyanobacterial media and inhibit

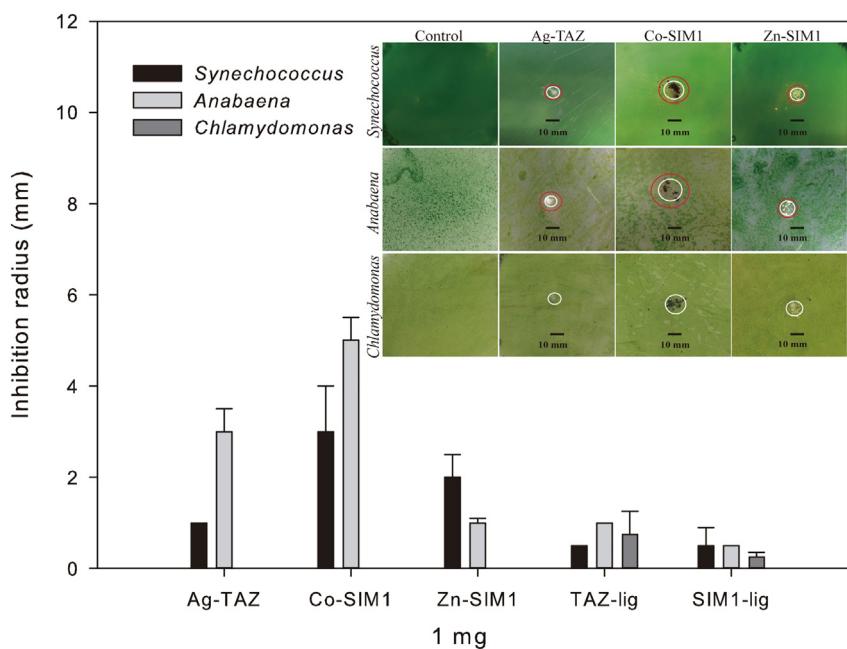


Fig. 1. Zone inhibition technique experiment to estimate antimicrobial activity towards *Synechococcus*, *Anabaena* and *Chlamydomonas* after exposure to 1 mg of Ag-TAZ, Co-SIM1 and Zn-SIM1 MOFs and TAZ-lig and SIM1-lig (ligands) for 24 h. Inhibition radii (mm) and photos of the agar plates showing the inhibition zones are included. The white circles indicate deposited material and the red circles indicate inhibition zones. (For interpretation of the references to color in this figure legend, the reader is referred to the web version of this article.)

their growth. However, only the Ag-TAZ was able to inhibit the growth of the alga at the tested concentration. The inhibition zone in each plate remained at least three months so that the biocidal activity was kept over time (not shown).

3.1.2. MOFs suspension bioassays

To further study the mechanism of action of these MOFs, we also performed tests to determine the biocidal effect of the tested materials in suspension. The three microorganisms were exposed to 50 mg L⁻¹ of each MOF. As controls, the microorganisms were also exposed to 50 mg L⁻¹ of each organic ligand and to the equivalent metal ion concentration presented in 50 mg L⁻¹ of each MOF as metal salts (see Materials and Methods). Chlorophyll *a* concentration was measured after 4, 24 and 48 h of exposure. All the experiments were performed in the culture medium specific for each organism (Table S1) and with the organisms in their exponential growth phase. Fig. 2 shows the results of these experiments.

As observed in Fig. 2A, for *Synechococcus* all MOFs caused around 50% of chlorophyll *a* concentration inhibition after 24 h of exposure. After 48 h of exposure, both Co-SIM1 and Zn-SIM1, reached 80% of chlorophyll *a* concentration inhibition and Ag-TAZ was slightly more toxic, exceeding 85% of inhibition. *Anabaena* was more sensitive to Ag-TAZ and Zn-SIM1, exposure to these MOFs resulted in around 80% of chlorophyll *a* concentration inhibition after 24 h of exposure. In the case of Co-SIM1, it provoked 50% of chlorophyll *a* concentration inhibition after 24 h and near 80% of inhibition after 48 h of exposure (Fig. 2B). Unlike the results observed according to the inhibition zone testing, in liquid media all MOFs caused practically the same degree of inhibition towards both cyanobacteria. In fact, in the case of *Anabaena*, toxicity caused by Ag-TAZ and Zn-SIM1 was higher than that caused by Co-SIM1. These results showed an increased biocidal activity in liquid media vs. agar plate suggesting an increase in the release of dissolved metals or an increase in the cell contact with these materials. This fact has a very important implication when these materials are designed to be in contact with aqueous media. *Chlamydomonas* presented high sensitivity to Ag-TAZ, causing 90% of chlorophyll *a* concentration inhibition after 24 h of exposure, as observed by the inhibition zone method (Fig. 1 and Fig. S1). However, Co-SIM1 and Zn-SIM1 were much less toxic, causing 40 and 30% of inhibition after 48 h, respectively, (Fig. 2C). As observed, in general, both ligands did not show a significant toxicity, only TAZ ligand towards *Anabaena*, (Fig. 2B), showed a significant inhibition of 35%. However, this concentration of ligand was 2.5 fold higher than that released by 50 mg L⁻¹ of Ag-TAZ (see Materials and Methods); implying that the ligand actually released from the MOFs was not relevant for toxicity.

Regarding the activity of pure metal salts, in all cases, we obtained a highest antimicrobial action of the metal salts compared to the biocidal action exhibited by the MOFs, which can be attributed to the immediate bioavailability of these metal ions (Fig. S4).

3.1.3. MOFs filtrate bioassays

Most of the literature has established that the biocidal activities of metallic nanomaterials are due to the dissolved metal ions (Aruoja et al., 2009; Li et al., 2015; Navarro et al., 2008; Wyszogrodzka et al., 2016), however, in some cases, direct contact between the organism and the material could be also responsible of the observed toxicity (Rodea-Palomares et al., 2011; Zhuang et al., 2012). To determine the contribution of dissolved metals to MOFs toxicity, MOF filtrates experiments were performed. The dissolved metal present in each MOF filtrate was designed as Co_d, Zn_d or Ag_d.

First of all, the dissolved metal concentration released from these three different MOFs in distilled water and in each culture medium along time was measured by ICP-MS (Fig. 3). In all cases, a rapid increase of the metal concentration was observed during the first hours, probably due to the release of surface metals, which occurs first. Then, the metal concentration linearly increased within 48 h. In general, all

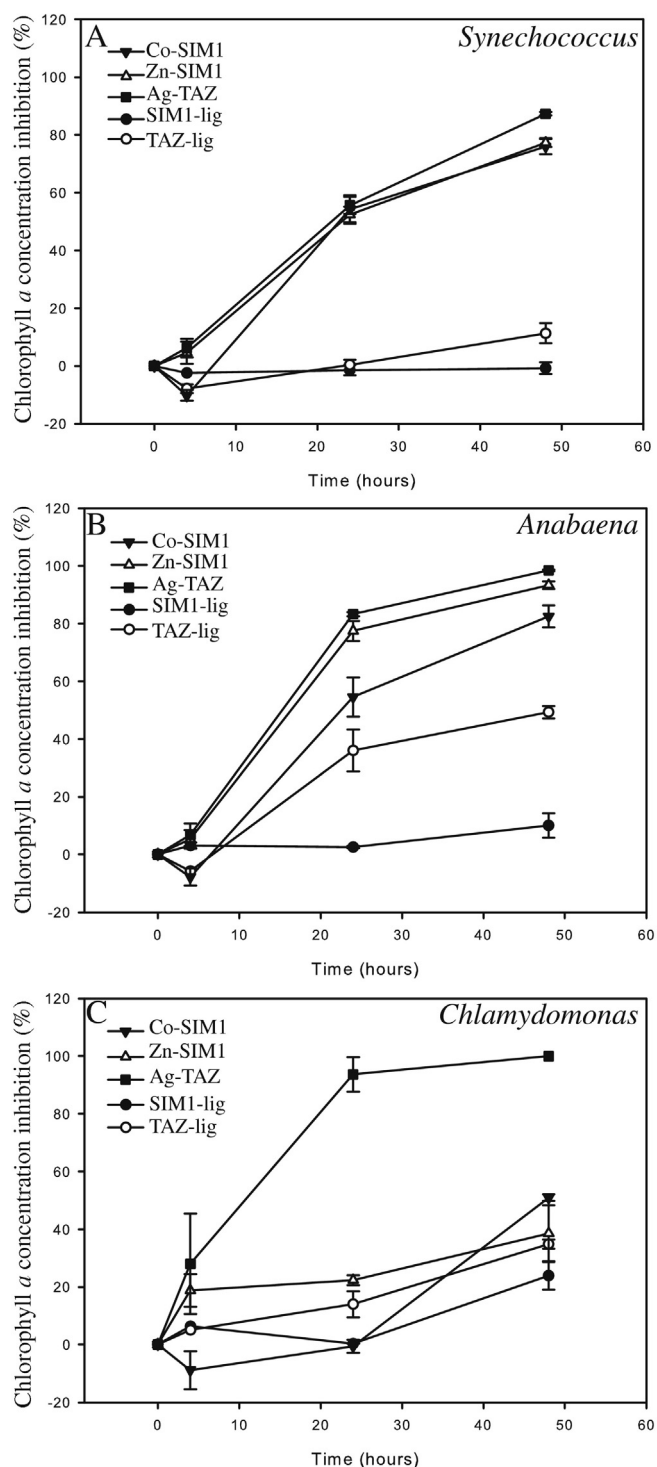


Fig. 2. Chlorophyll *a* concentration inhibition caused by exposure to Ag-TAZ, Co-SIM1 and Zn-SIM1 MOFs and TAZ-lig and SIM1-lig (ligands) of (A) *Synechococcus*, (B) *Anabaena* and (C) *Chlamydomonas* to 50 mg L⁻¹. Data represent the mean \pm standard deviation of at least three independent experiments.

MOFs showed similar quantity of metal released in the different media (Fig. 3), being Co-SIM1 which released more quantity of metal, achieving concentrations of 10, 8 and 12 mg L⁻¹ of Co_d in AA/8 + N, BG11 and TAP- after 24 h, respectively. However, it is remarkable that Co-SIM1 released lesser quantity of cobalt in distilled water than in the other media (Fig. 3). Zn-SIM1 released around 2 mg L⁻¹ of Zn_d in all media after 24 h; Ag-TAZ was by far the MOF which released less

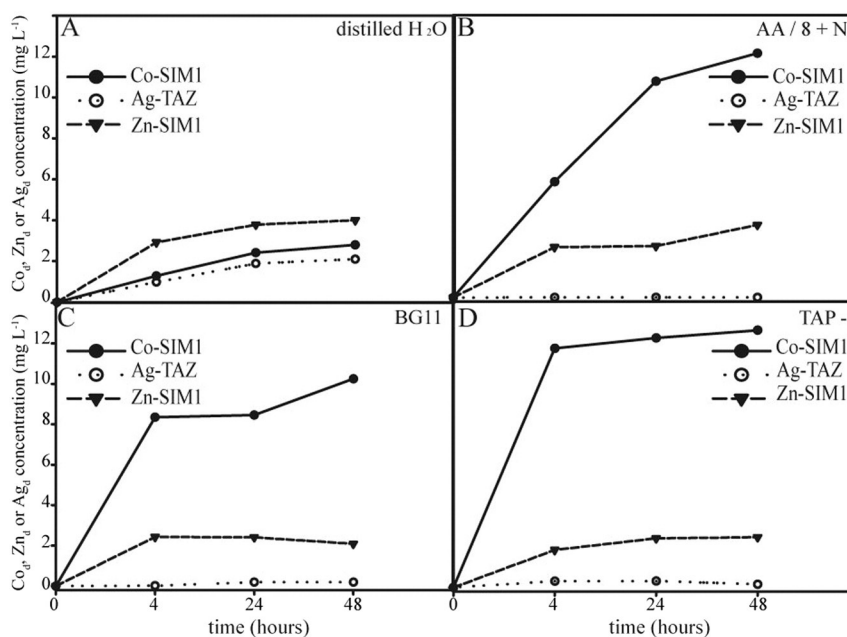


Fig. 3. Time evolution of dissolved metal (Co_d , Ag_d , Zn_d) released from Co-SIM1, Ag-TAZ and Zn-SIM1 MOFs, respectively in (A) distilled water, (B) AA/8 + N, (C) BG11 and (D) TAP- (MOF initial concentration 50 mg L^{-1}).

metal amount, reaching 0.0128 , 0.1896 and 0.3158 mg L^{-1} of Ag_d in AA/8 + N, BG11 and TAP- after 24 h, respectively.

As shown in Fig. 4, dissolved metals can explain the biocidal activity of the tested MOFs. There were no significant differences for the three organisms when performing MOF suspensions (MOF_s) bioassays or when using MOF filtrates (MOF_f), except for Ag-TAZ. Regarding *Synechococcus*, Ag-TAZ filtrate (Ag-TAZ_f) caused significantly ($p < 0.05$) more toxicity than the toxicity exhibited by Ag-TAZ suspensions (Ag-TAZ_s). However, in the case of *Anabaena* and *Chlamydomonas*, Ag-TAZ_s was significantly ($p < 0.001$ and $p < 0.01$, respectively) more toxic than Ag-TAZ_f. These differences may be due to slight differences in dissolved metals released from MOFs in the presence of the organisms as has been reported before (Aguado et al., 2014; Navarro et al., 2008).

All together the results present evidences that the toxicity of these MOFs is strongly mediated by the dissolved metals leaked from them. These results are consistent with other studies (Aguado et al., 2014; Berchel et al., 2011; Lu et al., 2014). These authors found that these MOFs could act as a reservoir of ions and the slow release of these metal ions leads to an excellent and long-term microbial activity. In order to elucidate how long the different MOFs might be releasing these metals, we calculated the release rate in distilled water. The initial time point of the experiment was not included in the calculations to disregard the initial surface metal released from the MOFs. In the case of Co-SIM1, the rate of Co_d release was equal to $0.68 \pm 0.20 \text{ mg Co}_d \cdot \text{g MOF}^{-1} \cdot \text{h}^{-1}$. Zn-SIM1

and Ag-TAZ, presented a metal release rate of $0.48 \pm 0.17 \text{ mg Zn}_d \cdot \text{g MOF}^{-1} \cdot \text{h}^{-1}$ and $0.50 \pm 0.18 \text{ mg Ag}_d \cdot \text{g MOF}^{-1} \cdot \text{h}^{-1}$, respectively. Taking into account the total metal concentration present in the different MOFs, the Co_d release would remain 314 h, 1235 h in the case of Ag_d release from Ag-TAZ and 482 h for Zn_d released from Zn-SIM1. This can ensure the biocidal capacity of the MOFs over time as observed in the inhibition zone testing bioassays.

As reported by other authors (Lu et al., 2014; Ruyra et al., 2015), there is a correlation between the structure and the biocidal activity of the MOFs. The different frameworks may have discriminating capacities to release metal ions, which lead to differences between their biocidal activities. In addition, those that released sufficiently high amounts of soluble metal ions known to be moderately or highly toxic in their free form will exhibit a greater biocidal capacity. While, those MOFs that release significant amounts of soluble metal ions, but whose constituent metal ion is not toxic in the free form will show little or no biocidal capacity. However, the biocidal capacity may also be influenced by the speciation of these metals in the different media and the sensitivity of the microorganism tested. Although these previous studies have related the toxicity with the dissolved ions, speciation of these dissolved metals in the different media used for the toxicity assays were not performed.

As metal speciation is a relevant issue determining the availability and therefore the toxicity of metals (Campbell, 1995; Campbell et al.,

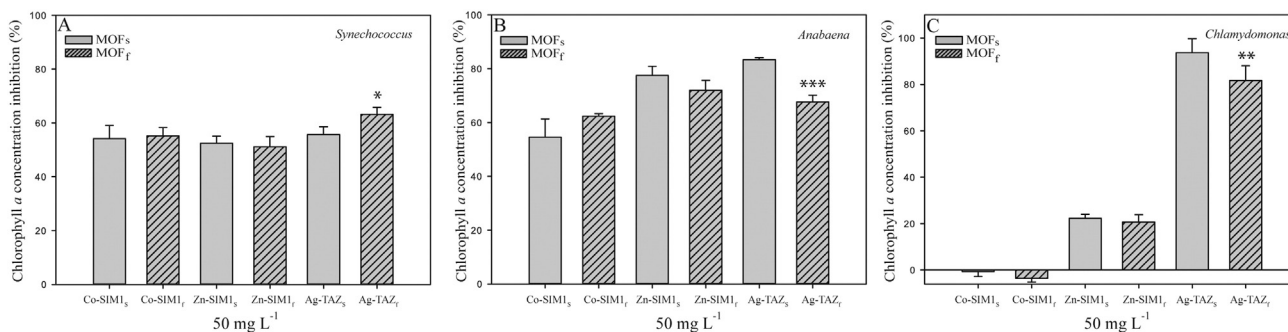


Fig. 4. Chlorophyll *a* concentration inhibition of (A) *Synechococcus*, (B) *Anabaena* and (C) *Chlamydomonas* exposed to 50 mg L^{-1} of Co-SIM1, Zn-SIM1 and Ag-TAZ MOFs. Comparison between MOFs suspensions (MOF_s) and MOFs filtrates (MOF_f) bioassays are shown. Statistically differences are indicated by * * = $p < 0.05$, * ** = $p < 0.01$ and * *** = $p < 0.001$. Data represent the mean \pm standard deviation of at least three independent experiments.

2002; Paquin et al., 2002), the chemical speciation program, Visual MINTEQ, was used in order to elucidate if these differences between organisms sensitivity to the different MOFs are due to differences in bioavailability of the dissolved metals released from these MOFs in the different media. In Table S2, the percentages of the main species predicted by Visual MINTEQ for the dissolved metals released from 50 mg L⁻¹ of MOFs in each medium after 24 h are shown.

As can be seen, each medium presented different percentages of free ion, which has been described as the main bioavailable specie according to the Free Ion Model (FIM) (Campbell et al., 2002). In accordance with the speciation modeling, the Co²⁺ available is significantly higher than the other ions due to the high release capacity of this MOF in the media and to the high predicted Co²⁺ percentage in all media. The percentage of Zn and Co free ion in the green alga medium (TAP-) was slightly higher than in the other media. However, only 2% of the total Ag dissolved in this medium was presented as Ag⁺ in comparison with 57% and 49% presented in BG11 and AA/8 + N, respectively.

As detailed before, at the same concentration tested, both cyanobacteria presented over 50% of chlorophyll *a* concentration inhibition for the three MOFs after 24 h of exposure, however, the green alga only showed a clear sensitivity to Ag-TAZ, reaching 90% of chlorophyll *a* concentration inhibition after 24 h. In order to explain the different sensitivity shown by the three microorganisms, it has to be considered, as previously described for *Chlamydomonas*, that for this alga silver internalization is very rapid (Fortin and Campbell, 2000; Lee et al., 2005). On the other hand, Macfie et al. (1994) and Macfie and Welbourn (2000) studied the effect of the cell wall of *Chlamydomonas* as a barrier towards heavy metals uptake such as Cd, Co, Cu and Ni. They concluded that the algal cell wall offered some protection from potentially toxic concentrations of certain metals, in the case of Co²⁺, this tolerance appeared to be related to the binding of this metal to the cell wall (Macfie and Welbourn, 2000), although the protection varied with each metal and was limited to a specific range of concentration. Therefore, if Zn and Co-MOFs concentrations exposed towards the alga were increased (Fig. 5), cell wall might no longer have a protective effect leading to the occurrence of toxicity. As can be seen in Fig. 5, at 200 mg L⁻¹, Zn-MOF cause 20% of inhibition and Co-SIM 40% after 24 h of exposure while after 48 h, both MOFs caused nearly 80% of chlorophyll *a* concentration inhibition. As highlighted by other authors (Li et al., 2015), it is very important to take into account the diversity in cell wall composition or surface architecture in studies of algal interaction with nanomaterials.

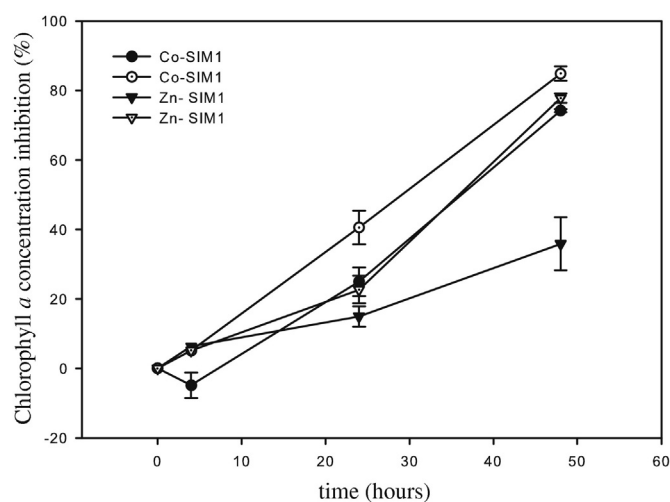


Fig. 5. Chlorophyll *a* concentration inhibition of *Chlamydomonas* exposed to 100 mg L⁻¹ (black symbols) and 200 mg L⁻¹ (white symbols) of Co-SIM and Zn-SIM1 MOFs. Data represent the mean ± standard deviation of at least three independent experiments.

Summarizing, Ag-TAZ was the most toxic MOF for the three microorganisms with a metal ion released rate slower than Co-SIM1, which showed the highest ion released rate.

3.2. Heavy metal bioreporter detection assays

In order to complete the information about the bioavailability of the dissolved metals released from these MOFs, a new approach using a heavy metal whole-cell bioreporter was implemented. In contrast to chemical methods, heavy metals whole-cell bioreporters measure the bioavailable metal, which is the fraction that interacts with the cell and consequently is detected by the organisms. Usually, this fraction correspond to the free ion species, capable of passing through cellular membranes. For that, bioavailability of the dissolved metals (Ag_d, Zn_d and Co_d) released from MOFs was compared between the free ion concentration predicted by Visual MINTEQ and a heavy metal bioreporter based on a cyanobacterium, *Synechococcus elongatus* pBG2120. As shown in Table 1, in the case of Ag_d and Co_d the concentration detected by the bioreporter was very close to the free ion concentration predicted by Visual MINTEQ program. However, regarding Zn_d, the concentration detected by the bioreporter was much higher than the free ion concentration predicted by the program. One plausible explanation of that, as reported by other authors, is the uptake of a metal-ligand complex across the biological membrane (Krom et al., 2000; Zhao et al., 2016). Besides, Errecalde et al. (1998) have elucidated that the toxicity of Cd²⁺ and Zn²⁺ is enhanced in the presence of citrate against the green alga, *Pseudokirchneriella subcapitata*. They have concluded that the bioavailability of divalent metals in the presence of citrate may well diverge from the predictions of the Free ion model (FIM). As can be seen in Table S2, in the bioreporter medium assay (BG11) the 54% of the total Zn_d appeared as Zn-citrate complex, which could be increasing the concentration of Zn detecting by the bioreporter.

We can conclude that the free ion metal is most likely the species available and detected by photosynthetic microorganisms and it is probably the chemical species responsible of the toxicity shown by these MOFs although some metal-complexes could interact with these organisms as well.

4. Conclusions

In summary, these Co, Zn and Ag-MOFs presented high antimicrobial activity towards photosynthetic organisms such as cyanobacteria or algae after a very short time of exposure. These characteristics make these materials suitable for use as antimicrobial materials against bio-fouling process, specifically, “slime” constitution.

Table 1
Comparison between free ion predicted concentration by Visual MINTEQ and the bioreporter output.

Metal dissolved	Free-ion predicted by Visual MINTEQ (mg L ⁻¹)	Bioreporter output (mg L ⁻¹)
Zn _d	0.007	N.D.
	0.015	N.D.
	0.029	0.132 ± 0.012
	0.058	0.209 ± 0.120
	0.117	0.446 ± 0.033
Ag _d	0.007	N.D.
	0.014	0.020 ± 0.001
	0.028	0.027 ± 0.013
	0.056	0.042 ± 0.010
	0.112	N.D.
Co _d	0.014	N.D.
	0.028	N.D.
	0.056	0.068 ± 0.005
	0.112	0.112 ± 0.005
	0.224	0.188 ± 0.001

N.D. Not detected.

Also, a combined analytical chemistry, chemical modeling and bioanalytical strategy was used to better understand the antibiofouling properties of these materials. Based on these different approaches we have elucidated that the biocidal activity presented by these MOFs was due to the dissolved metals released from them and more exactly, it depended on the bioavailability presented by these metal ions, which was closely related with the free ion concentration.

Bioavailability and toxicity of the free ions as well as the release rate of these ions from the MOFs determine the biocidal capacity of each MOF. Thus, due to the slower release rate of Ag^+ from Ag-TAZ and the toxic capacity of this metal ion, Ag-TAZ presents the best characteristics for practical applications. However, taking into account the metal release capacity of the different MOFs and the sensitivity of the target microorganisms, MOFs based on other metals such as Co and Zn can be also designed and used as biocides. The different sensitivities between species have to be taken into account, especially, if these materials are designed to prevent colonization of surfaces by different organisms. Furthermore, the gradual release of the metal ions would provide a sustained long-term biocidal activity towards photosynthetic organisms.

Supplementary data to this article can be found online at <http://dx.doi.org/10.1016/j.scitotenv.2017.03.250>.

Acknowledgements

This research was supported by the Spanish Ministry of Economy, CTM2013-45775-C2-1-R and CTM2013-45775-C2-2-R.

References

- Aguado, S., Canivet, J., Farrusseng, D., 2010. Facile shaping of an imidazolate-based MOF on ceramic beads for adsorption and catalytic applications. *Chem. Commun.* 46, 7999–8001.
- Aguado, S., Canivet, J., Farrusseng, D., 2011. Engineering structured MOF at nano and macroscales for catalysis and separation. *J. Mater. Chem.* 21, 7582–7588.
- Aguado, S., Quiros, J., Canivet, J., Farrusseng, D., Boltes, K., Rosal, R., 2014. Antimicrobial activity of cobalt imidazolate metal-organic frameworks. *Chemosphere* 113, 188–192.
- Allen, M.B., Arnon, D.I., 1955. Studies on nitrogen-fixing blue-green algae. I. Growth and nitrogen fixation by *Anabaena cylindrica* Lemm. *Plant Physiol.* 30, 366–372.
- Aruoja, V., Dubourguier, H.C., Kasemets, K., Kahru, A., 2009. Toxicity of nanoparticles of CuO, ZnO and TiO₂ to microalgae *Pseudokirchneriella subcapitata*. *Sci. Total Environ.* 407, 1461–1468.
- Banerjee, R., Phan, A., Wang, B., Knobler, C., Furukawa, H., O’Keeffe, M., et al., 2008. High-throughput synthesis of zeolitic imidazolate frameworks and application to CO₂ capture. *Science* 319, 939–943.
- Banerjee, R., Furukawa, H., Britt, D., Knobler, C., O’Keeffe, M., Yaghi, O.M., 2009. Control of pore size and functionality in isorecticular zeolitic imidazolate frameworks and their carbon dioxide selective capture properties. *J. Am. Chem. Soc.* 131, 3875–3877.
- Bauer, A.W., Kirby, W.M., Sherris, J.C., Turck, M., 1966. Antibiotic susceptibility testing by a standardized single disk method. *Am. J. Clin. Pathol.* 45 (4), 493–496.
- Bazes, A., Silkina, A., Douzenel, P., Fay, F., Kervarec, N., Morin, D., et al., 2009. Investigation of the antifouling constituents from the brown alga *Sargassum muticum* (Yendo) Fensholt. *J. Appl. Phycol.* 21, 395–403.
- Beg, S., Rahman, M., Jain, A., Saini, S., Midoux, P., Pichon, C., et al., 2016. Nanoporous metal organic frameworks as hybrid polymer-metal composites for drug delivery and biomedical applications. *Drug Discov. Today*.
- Berchel, M., Gall, T.L., Denis, C., Hir, S.L., Quentel, F., Elléouet, C., et al., 2011. A silver-based metal-organic framework material as a ‘reservoir’ of bactericidal metal ions. *New J. Chem.* 35, 1000–1003.
- Blaser, S.A., Scheringer, M., Macleod, M., Hungerbühler, K., 2008. Estimation of cumulative aquatic exposure and risk due to silver: contribution of nano-functionalized plastics and textiles. *Sci. Total Environ.* 390, 396–409.
- Briand, J.F., 2009. Marine antifouling laboratory bioassays: an overview of their diversity. *Biofouling* 25, 297–311.
- Campbell, P.C., 1995. Interactions between trace metals and aquatic organisms: a critique of the free-ion activity model. In: Tessier, A., Turner, D.R. (Eds.), *Metal Speciation and Bioavailability in Aquatic Systems*. 3, pp. 45–102.
- Campbell, P.C., Errecalde, O., Fortin, C., Hiriart-Baer, V.P., Vigneault, B., 2002. Metal bioavailability to phytoplankton—applicability of the biotic ligand model. *Comp. Biochem. Physiol. C Toxicol. Pharmacol.* 133, 189–206.
- Dang, H., Lovell, C.R., 2016. Microbial surface colonization and biofilm development in marine environments. *Microbiol. Mol. Biol. Rev.* 80, 91–138.
- Díez, B., Roldán, N., Martín, A., Sotto, A., Perdigón-Melón, J.A., Arsuaga, J., et al., 2017. Fouling and biofouling resistance of metal-doped mesostructured silica/polyethersulfone ultrafiltration membranes. *J. Membr. Sci.* 526, 252–263.
- Dong, B., Belkhair, S., Zaarour, M., Fisher, L., Verran, J., Tosheva, L., et al., 2014. Silver confined within zeolite EMT nanoparticles: preparation and antibacterial properties. *Nano* 6, 10859–10864.
- Durán, N., Durán, M., de Jesus, M.B., Seabra, A.B., Fávoro, W.J., Nakazato, G., 2016. Silver nanoparticles: a new view on mechanistic aspects on antimicrobial activity. *Nanomed. Nanotechnol. Biol. Med.* 12, 789–799.
- Egger, S., Lehmann, R.P., Height, M.J., Loessner, M.J., Schuppler, M., 2009. Antimicrobial properties of a novel silver-silica nanocomposite material. *Appl. Environ. Microbiol.* 75, 2973–2976.
- Errecalde, O., Seidl, M., Campbell, P.G.C., 1998. Influence of a low molecular weight metabolite (citrate) on the toxicity of cadmium and zinc to the unicellular green alga *Selenastrum capricornutum*: an exception to the free-ion model. *Water Res.* 32, 419–429.
- Farrusseng, D., Aguado, S., Canivet, J., 2009. Zeolitic organic-inorganic functionalised imidazolate material, method for preparing same and uses thereof. *Eur. Pat. WO.* 2011033233.
- Ferey, G., 2008. Hybrid porous solids: past, present, future. *Chem. Soc. Rev.* 37, 191–214.
- Fiebelkorn, K.R., Crawford, S.A., McElmeel, M.L., Jorgensen, J.H., 2003. Practical disk diffusion method for detection of inducible clindamycin resistance in *Staphylococcus aureus* and coagulase-negative staphylococci. *J. Clin. Microbiol.* 41, 4740–4744.
- Fortin, C., Campbell, P.G.C., 2000. Silver uptake by the green alga *Chlamydomonas reinhardtii* in relation to chemical speciation: influence of chloride. *Environ. Toxicol. Chem.* 19, 2769–2778.
- Franklin, N.M., Rogers, N.J., Apte, S.C., Batley, G.E., Gadd, G.E., Casey, P.S., 2007. Comparative toxicity of nanoparticulate ZnO, bulk ZnO, and ZnCl₂ to a freshwater microalga (*Pseudokirchneriella subcapitata*): the importance of particle solubility. *Environ. Sci. Technol.* 41, 8484–8490.
- Furukawa, H., Cordova, K.E., O’Keeffe, M., Yaghi, O.M., 2013. The chemistry and applications of metal-organic frameworks. *Science* 341, 1230444.
- Getman, R.B., Bae, Y.S., Wilmer, C.E., Snurr, R.Q., 2012. Review and analysis of molecular simulations of methane, hydrogen, and acetylene storage in metal-organic frameworks. *Chem. Rev.* 112, 703–723.
- Haasnoot, J.G., 2000. Mononuclear, oligonuclear and polynuclear metal coordination compounds with 1,2,4-triazole derivatives as ligands. *Coord. Chem. Rev.* 200–202, 131–185.
- Hooper, J.K., 1989. The *Chlamydomonas* sourcebook. In: Harris, Elizabeth H. (Ed.), *A Comprehensive Guide to Biology and Laboratory Use*. 246. Academic Press, San Diego, pp. 1503–1504 (Science).
- Horcajada, P., Chalati, T., Serre, C., Gillet, B., Sebrie, C., Baati, T., et al., 2010. Porous metal-organic-framework nanoscale carriers as a potential platform for drug delivery and imaging. *Nat. Mater.* 9, 172–178.
- Huang, X.C., Lin, Y.Y., Zhang, J.P., Chen, X.M., 2006. Ligand-directed strategy for zeolite-type metal-organic frameworks: zinc(II) imidazolates with unusual zeolitic topologies. *Angew. Chem. Int. Ed. Engl.* 45, 1557–1559.
- Jeffrey, S.W., Humphrey, G.F., 1975. New spectrophotometric equations for determining chlorophylls a, b, c1 and c2 in higher plants, algae and natural phytoplankton. *Biochem. Physiol. Pflanz.* 167, 191–194.
- Kim, Y.H., Lee, D.K., Cha, H.G., Kim, C.W., Kang, Y.C., Kang, Y.S., 2006. Preparation and characterization of the antibacterial Cu nanoparticle formed on the surface of SiO₂ nanoparticles. *J. Phys. Chem.* 110, 24923–24928.
- Kreno, L.E., Leong, K., Farha, O.K., Allendorf, M., Van Duyn, R.P., Hupp, J.T., 2012. Metal-organic framework materials as chemical sensors. *Chem. Rev.* 112, 1105–1125.
- Krom, B.P., Warner, J.B., Konings, W.N., Lolkema, J.S., 2000. Complementary metal ion specificity of the metal-citrate transporters CitM and CitH of *Bacillus subtilis*. *J. Bacteriol.* 182, 6374–6381.
- Kuppler, R.J., Timmons, D.J., Fang, Q.-R., Li, J.-R., Makal, T.A., Young, M.D., et al., 2009. Potential applications of metal-organic frameworks. *Coord. Chem. Rev.* 253, 3042–3066.
- Laluzza, P., Monzón, M., Arruebo, M., Santamaría, J., 2011. Bactericidal effects of different silver-containing materials. *Mater. Res. Bull.* 46, 2070–2076.
- Lee, D.Y., Fortin, C., Campbell, P.G., 2005. Contrasting effects of chloride on the toxicity of silver to two green algae, *Pseudokirchneriella subcapitata* and *Chlamydomonas reinhardtii*. *Aquat. Toxicol.* 75, 127–135.
- Lemire, J.A., Harrison, J.J., Turner, R.J., 2013. Antimicrobial activity of metals: mechanisms, molecular targets and applications. *Nat. Rev. Microbiol.* 11, 371–384.
- Li, X., Schirmer, K., Bernard, L., Sigg, L., Pillai, S., Behra, R., 2015. Silver nanoparticle toxicity and association with the alga *Euglena gracilis*. *Environ. Sci. Nano* 2, 594–602.
- Liu, Y., Xu, X., Xia, Q., Yuan, G., He, Q., Cui, Y., 2010. Multiple topological isomerism of three-connected networks in silver-based metal-organoboron frameworks. *Chem. Commun.* 46, 2608–2610.
- Lu, X., Ye, J., Zhang, D., Xie, R., Bogale, R.F., Sun, Y., et al., 2014. Silver carboxylate metal-organic frameworks with highly antibacterial activity and biocompatibility. *J. Inorg. Biochem.* 138, 114–121.
- Macfie, S.M., Welbourn, P.M., 2000. The cell wall as a barrier to uptake of metal ions in the unicellular green alga *Chlamydomonas reinhardtii* (Chlorophyceae). *Arch. Environ. Contam. Toxicol.* 39, 413–419.
- Macfie, S.M., Tarmohamed, Y., Welbourn, P.M., 1994. Effects of cadmium, cobalt, copper, and nickel on growth of the green alga *Chlamydomonas reinhardtii*: the influences of the cell wall and pH. *Arch. Environ. Contam. Toxicol.* 27, 454–458.
- Marker, A.F.H., 1972. The use of acetone and methanol in the estimation of chlorophyll in the presence of phaeophytin. *Freshw. Biol.* 2, 361–385.
- Martin, K., Rodea, I., Munoz, M.A., Leganes, F., Fernandez-Pinas, F., 2015. Construction of a self-luminescent cyanobacterial bioreporter that detects a broad range of bioavailable heavy metals in aquatic environments. *Front. Microbiol.* 6, 186.
- Matsumura, Y., Yoshikata, K., Kunisaki, S., Tsuchido, T., 2003. Mode of bactericidal action of silver zeolite and its comparison with that of silver nitrate. *Appl. Environ. Microbiol.* 69, 4278–4281.

- McKinlay, A.C., Morris, R.E., Horcjada, P., Ferey, G., Gref, R., Couvreur, P., et al., 2010. BioMOFs: metal-organic frameworks for biological and medical applications. *Angew. Chem. Int. Ed. Engl.* 49, 6260–6266.
- Merlino, J., Kennedy, P., 2010. Resistance to the biocidal activity of silver in burn wound dressings – is it a problem? *Microbiol. Aust.* 31, 168–170.
- Mieszkin, S., Callow, M.E., Callow, J.A., 2013. Interactions between microbial biofilms and marine fouling algae: a mini review. *Biofouling* 29, 1097–1113.
- Navarro, E., Piccapietra, F., Wagner, B., Marconi, F., Kaegi, R., Odzak, N., et al., 2008. Toxicity of silver nanoparticles to *Chlamydomonas reinhardtii*. *Environ. Sci. Technol.* 42, 8959–8964.
- Nguyen, T., Roddick, F.A., Fan, L., 2012. Biofouling of water treatment membranes: a review of the underlying causes, monitoring techniques and control measures. *Membranes* 2, 804–840.
- Palza, H., Delgado, K., Curotto, N., 2015. Synthesis of copper nanostructures on silica-based particles for antimicrobial organic coatings. *Appl. Surf. Sci.* 357, 86–90.
- Paquin, P.R., Gorsuch, J.W., Apte, S., Batley, G.E., Bowles, K.C., Campbell, P.G., et al., 2002. The biotic ligand model: a historical overview. *Comp. Biochem. Physiol. C Toxicol. Pharmacol.* 133, 3–35.
- Phan, A., Doonan, C.J., Uribe-Romo, F.J., Knobler, C.B., O’Keeffe, M., Yaghi, O.M., 2010. Synthesis, structure, and carbon dioxide capture properties of zeolitic imidazolate frameworks. *Acc. Chem. Res.* 43, 58–67.
- Prince, J.A., Bhuvana, S., Anbharasi, V., Ayyanar, N., Boodhoo, K.V., Singh, G., 2014. Self-cleaning Metal Organic Framework (MOF) based ultra filtration membranes—a solution to bio-fouling in membrane separation processes. *Sci. Rep.* 4, 6555.
- Quiros, J., Boltes, K., Aguado, S., de Villoria, R.G., Vilatela, J.J., Rosal, R., 2015. Antimicrobial metal-organic frameworks incorporated into electrospun fibers. *Chem. Eng. J.* 262, 189–197.
- Quiros, J., Gonzalo, S., Jalvo, B., Boltes, K., Perdigon-Melon, J.A., Rosal, R., 2016. Electrospun cellulose acetate composites containing supported metal nanoparticles for antifungal membranes. *Sci. Total Environ.* 563–564, 912–920.
- Rai, M., Yadav, A., Gade, A., 2009. Silver nanoparticles as a new generation of antimicrobials. *Biotechnol. Adv.* 27, 76–83.
- Refat, M.S., El-Korashy, S.A., Ahmed, A.S., 2008. Preparation, structural characterization and biological evaluation of l-tyrosinate metal ion complexes. *J. Mol. Struct.* 881, 28–45.
- Rippka, R., 1988. Isolation and purification of cyanobacteria. *Methods Enzymol.* 167, 3–27.
- Rodea-Palomares, I., Boltes, K., Fernandez-Pinas, F., Leganes, F., Garcia-Calvo, E., Santiago, J., et al., 2011. Physicochemical characterization and ecotoxicological assessment of CeO₂ nanoparticles using two aquatic microorganisms. *Toxicol. Sci.* 119, 135–145.
- Rosenhahn, A., Schilp, S., Kreuzer, H.J., Grunze, M., 2010. The role of “inert” surface chemistry in marine biofouling prevention. *Phys. Chem. Chem. Phys.* 12, 4275–4286.
- Rueff, J.M., Perez, O., Caignaert, V., Hix, G., Berchel, M., Quentel, F., et al., 2015. Silver-based hybrid materials from meta- or para-phosphonobenzoic acid: influence of the topology on silver release in water. *Inorg. Chem.* 54, 2152–2159.
- Ruyra, A., Yazdi, A., Espin, J., Carne-Sanchez, A., Roher, N., Lorenzo, J., et al., 2015. Synthesis, culture medium stability, and in vitro and in vivo zebrafish embryo toxicity of metal-organic framework nanoparticles. *Chemistry* 21, 2508–2518.
- Salta, M., Wharton, J.A., Blache, Y., Stokes, K.R., Briand, J.F., 2013. Marine biofilms on artificial surfaces: structure and dynamics. *Environ. Microbiol.* 15, 2879–2893.
- Sancet, M.P., Hanke, M., Wang, Z., Bauer, S., Azucena, C., Arslan, H.K., et al., 2013. Surface anchored metal-organic frameworks as stimulus responsive antifouling coatings. *Biointerphases* 8, 29.
- Sánchez, M.J., Mauricio, J.E., Paredes, A.R., Gamero, P., Cortés, D., 2017. Antimicrobial properties of ZSM-5 type zeolite functionalized with silver. *Mater. Lett.* 191, 65–68.
- Schultz, M.P., Bendick, J.A., Holm, E.R., Hertel, W.M., 2011. Economic impact of biofouling on a naval surface ship. *Biofouling* 27, 87–98.
- Sondi, I., Salopek-Sondi, B., 2004. Silver nanoparticles as antimicrobial agent: a case study on *E. coli* as a model for Gram-negative bacteria. *J. Colloid Interface Sci.* 275, 177–182.
- Spokoyny, A.M., Kim, D., Sumrein, A., Mirkin, C.A., 2009. Infinite coordination polymer nano- and microparticle structures. *Chem. Soc. Rev.* 38, 1218–1227.
- Tsoukatou, M., Hellio, C., Vagias, C., Harvala, C., Roussis, V., 2002. Chemical defense and antifouling activity of three Mediterranean sponges of the genus *Ircinia*. *Z. Naturforsch. C* 57, 161–171.
- Wang, C., Qian, X., An, X., 2015. In situ green preparation and antibacterial activity of copper-based metal-organic frameworks/cellulose fibers (HKUST-1/CF) composite. *Cellulose* 22, 3789–3797.
- Wojciechowska, A., Gagor, A., Wysokinski, R., Trusz-Zdybek, A., 2012. Synthesis, structure and properties of [Zn(L-Tyr)(2)(bpy)](2)3H(2)O.CH(3)OH complex: theoretical, spectroscopic and microbiological studies. *J. Inorg. Biochem.* 117, 93–102.
- Wyszogrodzka, G., Marszalek, B., Gil, B., Dorozynski, P., 2016. Metal-organic frameworks: mechanisms of antibacterial action and potential applications. *Drug Discov. Today* 21, 1009–1018.
- Yaghi, O.M., O’Keeffe, M., Ockwig, N.W., Chae, H.K., Eddaoudi, M., Kim, J., 2003. Reticular synthesis and the design of new materials. *Nature* 423, 705–714.
- Zhang, J.-P., Lin, Y.-Y., Huang, X.-C., Chen, X.-M., 2005. Copper(I) 1,2,4-triazolates and related complexes: studies of the solvothermal ligand reactions, network topologies, and photoluminescence properties. *J. Am. Chem. Soc.* 127, 5495–5506.
- Zhao, C.-M., Campbell, P.G.C., Wilkinson, K.J., 2016. When are metal complexes bioavailable? *Environ. Chem.*
- Zhou, Y., Deng, Y., He, P., Dong, F., Xia, Y., He, Y., 2014. Antibacterial zeolite with a high silver-loading content and excellent antibacterial performance. *RSC Adv.* 4, 5283–5288.
- Zhuang, W., Yuan, D., Li, J.R., Luo, Z., Zhou, H.C., Bashir, S., et al., 2012. Highly potent bactericidal activity of porous metal-organic frameworks. *Adv. Healthc. Mater.* 1, 225–238.

**S M
U A
P T
P E
L R
E I
M A
E L
N
T
A
R
Y**

Supplementary Material:

Co, Zn and Ag-MOFs evaluation as biocidal materials towards photosynthetic organisms

Keila Martín-Betancor^a, Sonia Aguado^b, Ismael Rodea-Palomares^a, Miguel Tamayo-Belda^a, Francisco Leganés^a, Roberto Rosal^b and Francisca Fernández-Piñas^{a*}

^a Department of Biology, Facultad de Ciencias, Universidad Autónoma de Madrid, 28049 Madrid, Spain

^b Department of Chemical Engineering de Alcalá, Alcalá de Henares, 28871, Spain

*Corresponding author: Francisca Fernández-Piñas

E-mail: francisca.pina@uam.es

Table of contents:

Supplementary Material text S1. Preparation of materials

Supplementary Material Table S1: Composition of culture media

Supplementary Material Table S2: Metal dissolved concentration from MOFs calculated by ICP-MS and percentage of main species predicted by Visual MINTEQ

Supplementary Material Figure S1: XRD patterns of Ag-TAZ, Zn-SIM1 and Co-SIM1

Supplementary Material Figure S2: SEM pictures of Ag-TAZ, Zn-SIM1 and Co-SIM1

Supplementary Material Figure S3: Zone inhibition technique experiment to estimate MOFs antimicrobial activity

Supplementary text S1. Preparation of materials

- Zn-SIM-1 synthesis

In a typical synthesis a solid mixture of 0.179 g (0.68 mmol) of $\text{Zn}(\text{NO}_3)_2 \cdot 4\text{H}_2\text{O}$ and 0.301 g (2.7 mmol) of 4-methyl-5-imidazolecarboxaldehyde is dissolved in 5 ml of DMF. Afterwards the solution is poured into a vial and heated in an oven at 373 K for 72 h. After the synthesis, the resulting powder is washed 3 times with DMF then with EtOH. The samples are dried at 373K overnight.

Empirical formula $\text{C}_{10}\text{H}_{10}\text{ZnN}_4\text{O}_2$

- Co-SIM-1 synthesis

In a typical synthesis a solid mixture of 0.199 g (0.68 mmol) of $\text{Co}(\text{NO}_3)_2 \cdot 6\text{H}_2\text{O}$ and 0.301 g (2.7 mmol) of 4-methyl-5-imidazolecarboxaldehyde is dissolved in 5 ml of DMF. Afterwards the solution is poured into a vial and heated in an oven at 358 K for 72 h. After the synthesis, the resulting powder is washed 3 times with DMF then with EtOH. The samples are dried at 373K overnight.

Empirical formula $\text{C}_{10}\text{H}_{10}\text{CoN}_4\text{O}_2$

- AgTAZ synthesis

A mixture of AgNO_3 (1.70 g, 10 mmol), aqueous ammonia (25%, 20 mL), and 1,2,4-triazole (0.69 g, 10 mmol) was sealed in a 45 mL Teflon-lined reactor and heated in an oven at 373 K for 60 h. After the synthesis, the resulting powder is washed 3 times with EtOH. The samples are dried at 373K overnight.

Empirical formula $\text{C}_2\text{H}_2\text{AgN}_3$

Table S1. Composition of media for culture of *Synechococcus* (BG11), *Anabaena* (AA/8 + N) and *Chlamydomonas* (TAP-).

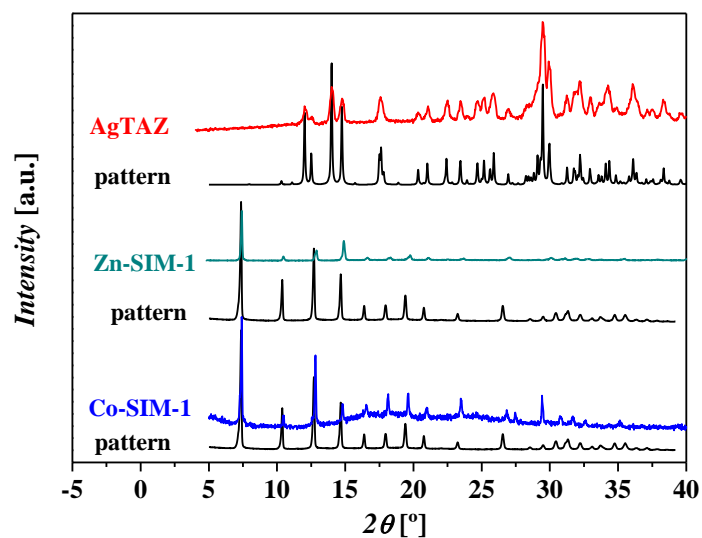
BG11*		AA/8 + N*		TAP-*	
Element	Concen. (μ M)	Element	Concen. (μ M)	Element	Concen. (μ M)
NaNO ₃	18000	MgSO ₄	125	NH ₄ CL	7015
MgSO ₄	200	CaCl ₂	62.5	MgSO ₄	831
CaCl ₂	240	NaCl	500	CaCl ₂	454
K ₂ HPO ₄	230	K ₂ HPO ₄	250	K ₂ HPO ₄	0.62
EDTA	2.80	NaNO ₃	2500	KH ₂ PO ₄	0.39
Citric acid	31	KNO ₃	2500	NO ₃	211
Ammonium ferric citrate	20	Na ₂ EDTA	9.59375	PO ₄ ³⁻	17.72
Na ₂ CO ₃	190	FeSO ₄	8.645	Fe	10.66
H ₃ BO ₃	46	MnCl ₂	1.13625	Zn	0.47
MnCl ₂	9.1	MoO ₃	0.15625	Mn	0.47
ZnSO ₄	0.77	ZnSO ₄	0.095625	Mo	0.34
Na ₂ MoO ₄	1.6	CuSO ₄	0.0395	Co	0.05
CuSO ₄	0.32	H ₃ BO ₃	5.78125	Cu	0.047
Co(NO ₃) ₂	0.17	NH ₄ VO ₃	0.0245	Thiamine HCL	0.026
MOPS	2 (mM)	CoCl ₂	0.021	Biotin	0.002
				Cyanocobalamim	0.00036

*Adjusted to pH 7.5

Table S.2 Metal dissolved concentration released from 50 mg L⁻¹ of each MOF calculated by ICP-MS after 24 h of exposure in each medium and percentage of main species predicted by VISUAL MINTEQ

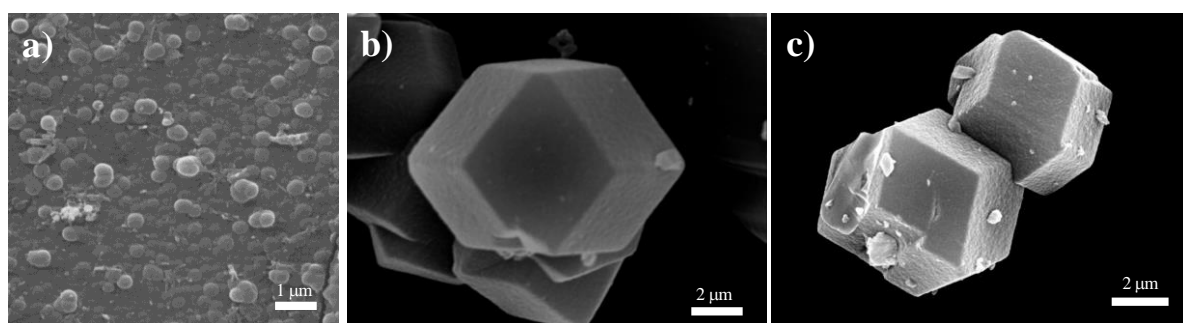
Medium	BG11		AA/8+N		TAP-	
MOFs	Metal dissolved calculated by ICP-MS (mg L ⁻¹)	Main species predicted by VISUAL MINTEQ (%)	Metal dissolved calculated by ICP-MS (mg L ⁻¹)	Main species predicted by VISUAL MINTEQ (%)	Metal dissolved calculated by ICP-MS (mg L ⁻¹)	Main species predicted by VISUAL MINTEQ (%)
Ag-TAZ	0.1896	57.439 Ag ⁺ 40.040 AgCl 2.001 AgCl ₂ ⁻ 0.119 AgSO ₄ ⁻ 0.399 AgNO ₃	0.0128	49.016 Ag ⁺ 47.489 AgCl 2.984 AgCl ₂ ⁻ 0.403 AgSO ₄ ⁻ 0.104 AgNO ₃	0.3158	2.187 Ag ⁺ 41.251 AgCl 55.498 AgCl ₂ ⁻ 1.025 AgCl ₃ ²⁻ 0.039 AgCl ₄ ³⁻
Zn-SIM1	2.4073	26.287 Zn ²⁺ 0.020 ZnCl ⁺ 11.150 ZnOH ⁺ 0.237 Zn(OH) ₂ 0.338 ZnSO ₄ 0.031 ZnH ₂ PO ₄ ⁺ 2.699 ZnHPO ₄ 0.679 ZnNO ₃ ⁺ 0.311 ZnHCO ₃ ⁺ 0.677 ZnCO ₃ 54.503 Zn-CITRATE 3.046 Zn-EDTA ²⁻	2.556	43.571 Zn ²⁺ 0.051 ZnCl ⁺ 21.291 ZnOH ⁺ 0.475 Zn(OH) ₂ 0.018 ZnOHCl 2.696 ZnSO ₄ 0.077 ZnH ₂ PO ₄ ⁺ 7.024 ZnHPO ₄ 0.378 ZnNO ₃ ⁺ 0.015 Zn(SO ₄) ₂ ²⁻ 24.402 Zn-EDTA ²⁻	2.4033	68.542 Zn ²⁺ 1.425 ZnCl ⁺ 28.479 ZnOH ⁺ 0.590 Zn(OH) ₂ 0.468 ZnOHCl 0.464 ZnHPO ₄ 0.021 ZnNO ₃ ⁺
Co-SIM1	8.4586	98.324 Co ²⁺ 1.676 Co-EDTA ²⁻	10.7365	95.380 Co ²⁺ 4.620 Co-EDTA ²⁻	12.2019	100.000 Co ²⁺

Figure S1. XRD patterns of Ag-TAZ, Zn-SIM1 and Co-SIM1.



The XRD measurements on the materials were recorded in the 10–90° 2θ range (scan speed = 20 s, step = 0.04°) by powder X-Ray diffraction (PXRD) using a Shimadzu 600 Series Diffractometer employing $\text{CuK}\alpha$ radiation ($\lambda=1.5418 \text{ \AA}$).

Figure S2. SEM pictures of Ag-TAZ, Zn-SIM1 and Co-SIM1.



The morphology of the as-synthesized materials was examined by scanning electron microscopy (SEM) using a DSM-950 (Zeiss) microscope.

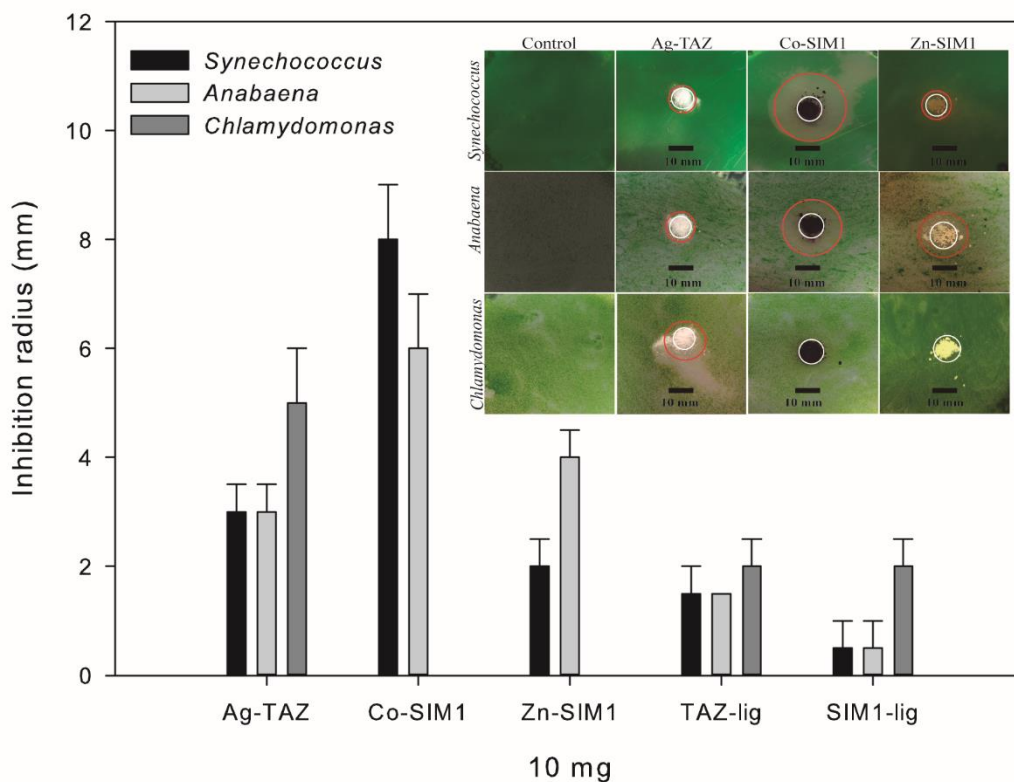


Fig. S3. Zone inhibition technique experiment to estimate MOF antimicrobial activity towards *Synechococcus*, *Anabaena* and *Chlamydomonas* after exposure to 10 mg of Ag-TAZ, Co-SIM1 and Zn-SIM1 MOFs and TAZ-lig and SIM1-lig (ligands) for 24 h. Inhibition radii (mm) and photos of the agar plates showing the inhibition zones are included. The white circles indicate deposited material and the red circles indicate inhibition zones.

High-throughput freeze-dried cyanobacterial bioassay for fresh-waters environmental monitoring

C

H

A

P

T

E

R

V

High-throughput freeze-dried cyanobacterial bioassay for fresh-waters environmental monitoring

Keila Martín-Betancor^a, Marie-José Durand^b, Gérald Thouand^b, Francisco-Leganés^a, Francisca Fernández-Piñas^a, Ismael Rodea-Palomares^a

^aDepartment of Biology, Facultad de Ciencias, Universidad Autónoma de Madrid, 28049 Madrid, Spain.

^bUniversity of Nantes, UMR CNRS 6144 GEPEA, France

Abstract

Microorganisms have been very useful in environmental monitoring due to their constant sensing of the surrounding environment, their easy maintenance and low cost. Some freeze-dried toxicity kits based on naturally bioluminescent bacteria are commercially available and commonly used to assess the toxicity of environmental samples such as Microtox (*Aliivibrio fischeri*) or ToxScreen (*Photobacterium leiognathi*), however, due to the marine origin of these bacteria, they could not be the most appropriate for fresh-waters monitoring. Cyanobacteria are one of the most representative microorganisms of aquatic environments, and are well suited for detecting contaminants in aqueous samples. This study presents the development and application of the first freeze-dried cyanobacterial bioassay for fresh-water contaminants detection. The effects of different cell growth phases, cryoprotectants, freezing protocols, rehydration solutions and incubation conditions methods were evaluated and the optimal freeze-drying protocol selected. The study include detailed characterization of sensitivity towards reference pollutants, as well as, comparison with the standard assays. Moreover, long-term viability and sensitivity were evaluated after 3 years of storage. Freeze-dried cyanobacteria showed, in general, higher sensitivity than the standard assays and viability of the cells remained after 3 years of storage. Finally, the validation of the bioassay using a wastewater sample was also evaluated. Freeze-drying of cyanobacterium in 96-well plates presents a simple, fast and high-throughput method for environmental monitoring.

1. Introduction

A rapid and simple method for toxicity detection is a key aspect of environmental monitoring. Whole-cell bioreporters constitute one of the best approaches in environmental assessment due to their ability to integrate several reactions that can exist only in an intact, functioning cell (Eltzov and Marks, 2011; Nurul Aisyah et al., 2014; Pasco et al., 2011). Microorganisms are advantageous for that purpose, due to their constant sensing of the surrounding environment and their easy maintenance. In addition, the susceptibility of many to be genetically modified makes them ideal for developing genetically engineered microorganisms-based bioreporters for determining the bioavailability and /or toxicity of pollutants practically on demand (He

et al., 2016; Park et al., 2013; Su et al., 2011; Van der Meer and Belkin, 2010; Xu et al., 2013). In general, two different whole-cell microbial bioreporters can be distinguished regarding their sensing ability (Belkin, 2003; Gu et al., 2004; Sorensen et al., 2006). Turn-on bioreporters, which are activated in response to a target compound or stress response, and turn-off bioreporters, which respond with a decrease of the metabolic endpoint to toxicity of a sample. In both, bioluminescence has been largely used as effective reporter signal due to the simple operation, rapid response and low cost (Ma et al., 2014; Nivens et al., 2004; Yagur-Kroll and Belkin, 2011) originating the so-called lights-on (luminescence is induced) and lights-off bioreporters (luminescence is inhibited). In natural environments, pollutants occur in

complex mixtures of different nature (antibiotics, phenols, heavy metals...). There is a huge demand for simple, fast and cost-effective methods that can be used for the screening and monitoring of a wide range of toxic contaminants in aquatic environments (Eltzov and Marks, 2011). Thus, lights-off type bioreporters able to measure general toxicity in chemical mixtures are required (Hassan et al., 2016).

There are several freeze-dried toxicity kits based on naturally bioluminescent bacteria commercially available commonly used to assess the toxicity of water samples, for instance, Microtox based on *Aliivibrio fischeri* (previously known as *Vibrio fischeri*) (Johnson, 2005) or ToxScreen test with *Photobacterium leiognathi* (Ulitzur et al., 2002). However, these marine bacteria operate at salt concentrations around 2-3 %, which has been found to influence the speciation and subsequent toxicity of metals and may alter the solubility of some organic substances producing turbid solutions (Ankley et al., 1989; Deheyn et al., 2004; Farré and Barceló, 2003; Hinwood and McCormick, 1987; Newman and McCloskey, 1996) Thus, the inherent properties of freshwater samples may be altered when these marine bacteria tests are used.

There is an increasing interest in finding freshwater luminous bacteria for this type of samples. Ma et al. (1999) isolated the freshwater luminescent bacterium *Vibrio qinhaiensis* sp.-Q67. Several studies based on this bacterium have found that it is as effective and reliable as conventional *A. fischeri* assays (Liu et al., 2009; Ma et al., 2012; Ma et al., 2011; Zhang et al., 2011). However, no stabilizing process of this bacterium have been performed.

Finally, apart from natural, engineered bioluminescent freeze-dried bacteria for environmental monitoring have also been developed. Most of them are based on *Escherichia coli* (Choi and Gu, 2002; Gu et al., 2001; Jouanneau et al., 2011), but also in widespread microorganisms like *Pseudomonas*, from which bioluminescent strains have been used, mostly for soil ecotoxicity assessment (de

las Heras and de Lorenzo, 2011; Ko and Kong, 2017). Moreover, Cho et al. (2004) used the bacterium *Janthinobacterium lividum*, isolated from groundwater, as lyophilized bioassay that was more sensitive for freshwaters environments monitoring than Microtox®. However, freeze-dried bioluminescent bioassays based on freshwater ecologically relevant organisms are still lacking.

Cyanobacteria are one of the most representative microorganisms of aquatic environments. They are the only prokaryotic organisms carrying out an oxygen-evolving photosynthesis. As primary producers with a key role in the N and C cycles, they are a dominant component of marine and freshwater phytoplankton, and are well suited for detecting contaminants in aqueous samples. Cyanobacteria are ecologically relevant, and for that reason, in recent years, there has been an interest in developing recombinant bioluminescent cyanobacterial bioreporters (Bachmann, 2003). Although these bioreporters have been useful to assess toxicity in photosynthetic organisms (González-Pleiter et al., 2013; Rodea-Palomares et al., 2009a; Rodea-Palomares et al., 2009b; Rodea-Palomares et al., 2016; Rodea-Palomares et al., 2015; Rodea-Palomares et al., 2010; Shao et al., 2002) or nutrient bioavailability due to their pivotal role in biogeochemical cycles (Boyanapalli et al., 2007; Bullerjahn et al., 2010; Durham et al., 2002; Gillor et al., 2010; Munoz-Martin et al., 2011; Munoz-Martin et al., 2014; Porta et al., 2003), development of preservation methods for cyanobacterial bioreporters remains scarce. Solely, Schreiter et al. (2001) and Mbeunkui et al. (2002) have developed two immobilized bioluminescent cyanobacterial reporter strains for nutrients monitoring in aquatic ecosystems denominated CyanoSensors. Both CyanoSensors were successfully immobilized in 24-well plates using agar as a matrix, remaining stable up to one month of storage. These immobilized cyanobacteria-based bioassays are lights-on type, able to detect phosphate or nitrate deprivation.

Long-term viability and activity of whole-cell bioreporters are essential for the development of cell-based devices and for their widespread

practical use in routine environmental monitoring. Several methods for storage and preservation of microbial bioreporters have been described (Bjerketorp et al., 2006; Michelini et al., 2013; Roda et al., 2011). The most used are immobilization (Polyak et al., 2001; Rajan Premkumar et al., 2002) and freeze-drying or lyophilisation (Camanzi et al., 2011; Wenfeng et al., 2013). However, as reported by some authors, lyophilisation is more suitable for long-term maintenance of the organisms' stability due to the lack of cellular growth (Bjerketorp et al., 2006; Jouanneau et al., 2015) and because they can be stored for a long period without changes. In addition, freeze-drying does not require any entrapped matrix which may hamper the optical signal detection. However, the main drawback of freeze-drying is that not all the species are susceptible to be freeze-dried and to keep the viability and sensitivity after rehydration.

There are only few studies on cyanobacterial freeze-drying (Corbett and Parker, 1976; Esteves-Ferreira et al., 2012; Holm-Hansen, 1967; Watanabe, 1959) in most cases, cyanobacteria presented very low levels of viability after freeze-drying. However, the successful lyophilisation of the cyanobacterium *Nostoc muscorum* (Holm-Hansen, 1967) with no observed reduction of viability after 5 years have been reported. Moreover, Estevez et al. (2013) have reported that lyophilisation was adequate for both heterocystous cyanobacteria (orden Nostocales) and other strains that were able to differentiate hormogonia or to synthesize thick layers of exopolysaccharides.

Here, we report the development of the first freeze-dried cyanobacterial bioassay. It is based on a constitutively bioluminescent bioreporter based on a freshwater filamentous cyanobacterium, *Anabaena* PCC 7120. Prior to this work, this cyanobacterium was successfully tested as general toxicity bioreporter against heavy metals (Rodea-Palomares et al., 2009a; Rodea-Palomares et al., 2009b), single and mixtures of priority and emerging pollutants (González-Pleiter et al., 2013; Rodea-Palomares et al., 2016; Rodea-Palomares et al., 2015; Rodea-Palomares et al., 2010; Rosal et al., 2010a; Rosal et al., 2010b) and nanomaterials

(Martín-de-Lucía et al., 2017; Rodea-Palomares et al., 2012). All these approaches make this cyanobacterium a perfect candidate to generate an easy and long-term stable bioreporter. In addition, in order to develop a rapid, simple and high-throughput bioassay, the cyanobacterial bioreporter was freeze-dried in 96-well plates ready-to-use.

In order to develop a rapid *Anabaena*-based bioassay, the main factors affecting freeze-drying have to be elucidated. A full factorial design covering all the possible combinations of several parameters (see 2.1 *Full factorial design*) was performed, and the most optimal protocol of freeze-drying indicated. Moreover, viability and sensitivity of the cells towards reference pollutants upon 3 years of storage were performed. Finally, the use of the bioassay in a natural environmental sample was tested.

2. Materials and methods

2.1 Full factorial design

In order to perform the best freeze-drying protocol for *Anabaena* CPB4337, different scenarios were studied, for all these conditions luminescence was recorded after freeze-drying and compared with that measured in the sample before freeze-drying (see 2.7 *Measurements of bioluminescence after 96-well plates cell reconstitution*). The different conditions tested were (i) the optimal growth phase (early, exponential or stationary); (ii) the cryoprotectant addition (sucrose 12 % in ddH₂O or in BG11 medium); (iii) the freezing condition (slower or rapid freezing); (iv) the rehydration solution (ddH₂O or BG11 medium) and (v) the incubation condition (under light or darkness). To elucidate the main factors affecting freeze-drying, a full factorial design covering all the possible combinations of these parameters was performed (Figure 1).

2.2 *Anabaena* culture conditions

Self-bioluminescent *Anabaena* sp. PCC 7120 strain CPB4337 (hereinafter *Anabaena* CPB4337), which bears in the chromosome a Tn5 derivative with *luxCDABE* from the luminescent terrestrial bacterium *Photorehabdus*

luminescens (formerly *Xenorhabdus luminescens*), was used to optimize the freeze-drying conditions. *Anabaena* CPB4337 was routinely grown at 28 °C in the light, ca. 60 $\mu\text{mol photons m}^{-2}\text{s}^{-1}$ on a rotatory shaker in 100 mL BG11 pH 7.5 cyanobacterial growth medium (Rippka, 1988) supplemented with 10 mg/mL of neomycin sulphate (Nm). Cultures were grown until they reached the growth phase used in the assays: early growth phase: O.D._{750nm} = 0.2-0.3, exponential growth phase: O.D._{750nm} = 0.5-0.8 and in the early stationary growth phase: O.D._{750nm} = 0.8-1.2.

suspended in fresh BG11 growth medium to obtain an O.D._{750nm} = 1. These cultures were mixed with the cryoprotectant stocks solutions (detailed above) in 1:1 v/v reaching *Anabaena* CPB4337 cells an O.D._{750nm} = 0.5 and the cryoprotectant the desire final concentration (12 %). 100 μl of culture were transferred to each well in white 96-well plates. To avoid prolonged exposure to toxic solute concentrations (cryoprotectant solution), 96-well plates were fitted with a plastic cover and rapidly frozen using the two different freezing protocols detailed below (figure 1).

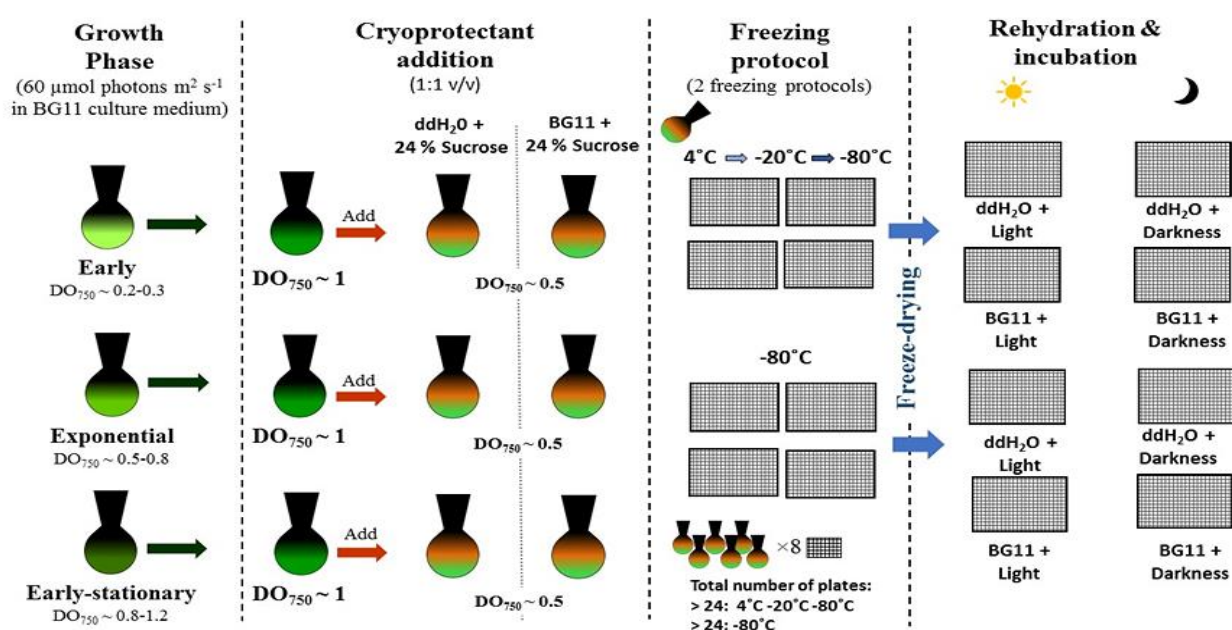


Fig. 1 Full factorial design of freeze-drying protocol optimization.

2.3 Cryoprotectant solutions

Sucrose was tested as cryoprotectant at a final concentration of 12 %. Stock solutions were prepared at 2X concentration (24 % of sucrose) in doubled distilled water (ddH₂O) or cyanobacterial growth medium BG11 and sterilization by filtration (0.22 μm). Stocks solutions were kept in ice during sample preparation.

2.4 Freeze-drying material in 96-well plates

Anabaena CPB4337 was grown until the specific growth phase (early, exponential and early stationary) was reached as described before and then harvested, washed twice (centrifuged at 4500 rpm for 10 min) and re-

2.5 Freeze-drying protocols

The prepared samples were frozen using two freezing conditions. One of the freezing protocol consisted of a slower and more carefully controlled cooling rate, keeping the 96-well plates 20 min at 4 °C following a step at -20 °C during 4.30 h. and at least 20 h. at -80 °C. The other freezing protocol consisted of placing the plates directly at -80 °C during 24 h and 50 min (see figure 1). After that time, the plates were freeze-dried at -50 °C and under 0.025 mbar pressure for one day (this time was enough to completely dry the sample) using a Christ Alpha 1-2 lyophilizer (Bioblock Scientific). After this process was completed, plates were stored at -20 °C until used.

2.6 Rehydration and incubation protocol

Rehydration of the samples with ddH₂O or BG11 medium was compared. In all cases, 100 µl of ddH₂O or BG11 were added to each freeze-dried well and the incubation was at room temperature. As photoautotrophic organisms are very sensitive to light, and this could be a factor that modifies the sensitivity of the bioreporter, incubation under darkness or light (40 µmol photons m⁻²s⁻¹) was applied. Schematically, four different conditions of rehydration and incubation were tested: ddH₂O under light/ ddH₂O under darkness/ BG11 under light and BG11 under darkness (see figure 1).

2.7 Measurements of bioluminescence after 96-well plates cell reconstitution

The optimal cryoprotectant, temperature for freezing, rehydration and incubation protocol was determined by comparing the bioluminescence of the samples for the different conditions, before and after the freeze-drying process and was expressed as % bioluminescence of cells after freeze-drying with respect to bioluminescence of cells before freeze-drying:

$$\text{LUMI (\%)} = (\text{RLU aft.} / \text{RLU bef.}) \times 100 \quad (1)$$

where RLU aft. are the relative luminescence units of freeze-dried cells, and RLU bef. are the relative luminescence units of cells before freeze-dried. For protocol optimization, the freeze-dried plates were taken from the -20 °C storage freezer 24 hours after freeze-dried. At least two plates and three wells per plate were used to study each different condition. To determine the effect of long-term storage in viability of samples, plates were reconstituted after 1 week, 1 month, 1 year and 3 years after freeze-drying, using the optimal freeze-drying protocol (see Results: 3.1 Main factors affecting freeze-drying and figure 2). Long-term viability was determined as % of bioluminescence measured as indicated before.

2.8 Toxicity bioassays

96-well plates were prepared following the optimal freeze-drying protocol and toxicity bioassay was carried out with selected pollutants

to estimate the sensitivity of the freeze-dried cells.

The chemicals chosen for toxicity monitoring were three heavy metals, copper (Cu), zinc (Zn) and cadmium (Cd), one herbicide, atrazine (Atz) and one solvent, phenol. For the heavy metals, in order to compare the sensitivity of the freeze-dried cells, toxicity assays were performed before and after 24 hours, 1 week, 1 month, 1 year and 3 years after freeze-drying. 25 µl of the stock solutions were added to each well reaching a final concentration range between 0-14 mg L⁻¹ and 0-8 mg L⁻¹ for the heavy metals assays before and after freeze-drying, respectively. In the cases of atrazine and phenol, toxicity assays were performed 1 month after freeze-drying. 25 µl of the stock solutions were added to each well reaching a final concentration range of 0-5 mg L⁻¹ and 0-40 mg L⁻¹ of atrazine and phenol, respectively. Bioluminescence measurements were performed after one hour of chemical exposure. At least two plates and three wells per plate were used for each chemical concentration.

2.9 Analysis of results

Bioluminescence was measured as described before in 2.7 *Measurements of bioluminescence after 96-well plates cell reconstitution*. For toxicity bioassays, dose-response curves were fitted by non-linear parametric functions with the R “drc” analysis package (Ritz and Streibig, 2005) (R for Windows, 3.0.1 version Development Core Team). A four parameter log-logistic model (LL.4) (2) was selected for fitting all dose-response curves in the study (Ritz et al., 2015; Ritz and Streibig, 2005).

$$f(x) = c + \frac{d-c}{1+\exp(b(\log(x)-\log(e)))} \quad (2)$$

where d is the upper limit, c is the lower limit, b is the slope and e is the EC₅₀ of the dose-response curve. Toxicity was expressed as effective concentrations (EC_x), which are the concentrations of the chemicals exerting $x\%$ percent bioluminescence inhibition. EC₅₀ was selected as representative of medium toxicity concentration. Mean values and standard error of EC_x values were computed using the function ED.drc on fitted LL.4 models (Ritz and Streibig, 2005).

For the analysis of the sensitivity of freeze-dried cells to pollutants along time, we compared fitted dose-response models for the freeze-dried cells exposed to heavy metals after 24 hours, 1 week, 1 month, 1 year and 3 years using compParm (drc) function (Ritz and Streibig, 2005). CompParm function compares estimated parameters for the same non-linear model fitted for different assays. The comparison can be performed either for ratios of means or differences of means. CompParm allows for automatic statistical testing of differences. The option of comparisons of ratios of the model parameter e (EC_{50}) of the LL.4 model was selected for the comparisons (see Eq. (2)). The EC_{50a}/EC_{50b} ratio allowed to identify increased/decreased toxicity over time, where a denotes 24 h after freeze-drying and b denotes any of the possible time-points after freeze-drying: 1 week (1 w), 1 month (1 m), 1 year (1 yr) and 3 years (3 yrs) (table S1).

2.10 Wastewater spiking experiments

In order to validate the use of the bioassay in environmental monitoring, a water sample from a wastewater effluent was used for spiking experiments with heavy metals (Cu, Zn and Cd), atrazine and phenol. This wastewater sample was collected from the secondary clarifier of a wastewater treatment plant (WWTP) located in Madrid. This plant treats a mixture of domestic and industrial wastewater with a nominal capacity of 13000 m³/h of raw wastewater. Table S2 lists the main characterization parameters for wastewater and table S3 shows the concentration of the main pollutants present in this water sample. The manipulation of the water sample and the detection and quantification of the microcontaminants was performed previously by Martin-de-Lucia et al. (2017).

For the wastewater spiking experiments, the EC_{50} s previously determined for the heavy metals, atrazine and phenol were used (*see Results 3.2 Impact of freeze-drying on the bioassay performance and 3.4 Comparison of the freeze-dried cyanobacterium bioassay performance with that of other freeze-dried bioassays*). The stocks solutions of the

chemicals were made directly in the wastewater. 25 μ l of each pollutant stock solution were added to each well reaching the EC_{50} previously determined as the final concentration. At the same time, 25 μ l of the wastewater sample without chemicals were also used. At least two plates and three wells per plate were used for each chemical concentration.

3. Results and Discussion

3.1 Main factors affecting freeze-drying

a) Growth phase

In order to elucidate how the growth phase of the cells affect the viability measured as bioluminescence after freeze-drying, three representative growth phases were studied. As can be seen in figure 2, when cells were in the early growth phase ($O.D._{750nm} = 0.2-0.3$), the viability after freeze-drying was minimal regardless of the different protocols used. Stepping up the growth phase of the cells increases the survival capacity after freeze-drying. Cells in early stationary growth phase ($O.D._{750nm} = 0.8-1.2$.) showed higher viability than cells in exponential growth phase ($O.D._{750nm} = 0.5-0.8$) in all cases tested. As pointed out by (Morgan et al., 2006), the stationary phase induces various physiological states within the cells, normally due to nutrient sources limitation that triggers stress responses to allow survival of the cell population. This survival response may also protects the cell in other adverse conditions, such as freeze-drying. Esteves-Ferreira et al. (2013) also found that stationary growth phase was better for viability of cyanobacteria after freeze-drying.

b) Freezing protocol and cryoprotectant

As can be seen in figure 2, in all cases, the freezing protocol that consisted in placing the cells directly at $-80\text{ }^{\circ}\text{C}$ was better than the slower and more carefully controlled cooling rate protocol. As reported by other authors (Gu et al., 2001), these differences between both temperature protocols could be due to the slow freezing, above $-30\text{ }^{\circ}\text{C}$. This slow and steady removal of water by freezing increases the

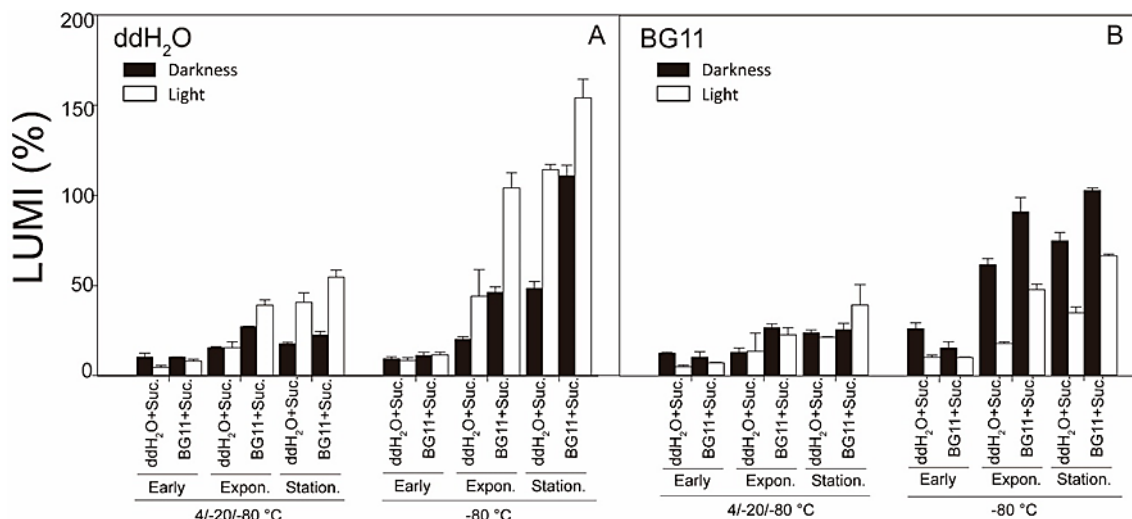


Fig.2 Luminescence percentage of freeze-dried *Anabaena* CPB4337 with respect to the control (before freeze-drying) for two freezing protocols (4/-20/-80 °C or -80 °C) using three different growth stages (early, exponential and early stationary). The final cryoprotectant concentration was 12 % of sucrose added as a ddH₂O solution (ddH₂O+Suc.) or as a BG11 (cyanobacterial medium) solution (BG11+Suc.). The rehydration solution was ddH₂O (A) or BG11 (B) and two different incubation protocols [under darkness or light conditions (40 μmol photons m⁻²s⁻¹)]. Cells were rehydrated after 24 h of freeze-drying and luminescence measured after 30 min of incubation.

concentration of solutes in the remaining aqueous phase, thus lowering the freezing point. As the temperature is further reduced, more ice forms and the residual solution becomes increasingly concentrated which resulted in exposure of the cells to high salt concentration (Morris et al., 1988; Perry, 1995) and consequently to an increase of the osmotic stress. In addition, large ice crystal formation can cause damage to fragile cell membranes and increasing the rate of freezing can reduce these large crystals formation (Morgan et al., 2006).

Using BG11 + 24 % sucrose solution (12% sucrose final concentration) as cryoprotectant substantially increased the percentage of cells luminescence after freeze-drying compared to using ddH₂O + 24 % sucrose solution as cryoprotectant. This may be because mixing the cryoprotectant with the medium forms a more homogeneous mixture and also maintains the optimal concentrations of the nutrients for maintaining cells viability.

c) rehydration solution

As can be observed, incubation under light or darkness condition seems to correlate with the chosen rehydrating solution. When cells were rehydrated in ddH₂O, the percentage of

luminescence was higher if they were incubated under light conditions, however, when BG11 was used as rehydration medium, incubation under darkness condition increased the percentage of luminescence after freeze-drying. Although, the higher level of luminescence was observed in cells rehydrated with ddH₂O incubated under light condition. It is known that numerous biological processes in cyanobacteria such as nutrient uptake or metabolism activation are regulated by light (Golden, 1995; Litchman et al., 2004; Muramatsu and Hihara, 2012). Both, light and nutrient input (with BG11 addition as rehydration solution) may result in an increased osmotic pressure detected by the organisms, affecting them and resulting in a decrease of luminescence.

In summary, given the results detailed above, the following protocol was chosen as optimal and implemented for the rest of the assays: Prior to freeze-drying, cells were grown to the early stationary phase and frozen directly at -80 °C using BG11 + 24 % sucrose solution as cryoprotectant. After freeze-drying, cells were stored at -20 °C and rehydrated with ddH₂O and incubated under light conditions.

3.2 Impact of freeze-drying on the bioassay performance

In order to evaluate how the freeze-drying process affect the performance of the bioassay, the freeze-dried cells were exposed to three different heavy metals before and 24 hours after freeze-drying and the concentration that caused the 50 % of bioluminescence inhibition was calculated (EC_{50}). In the three cases, the EC_{50} decreased one order of magnitude after freeze-

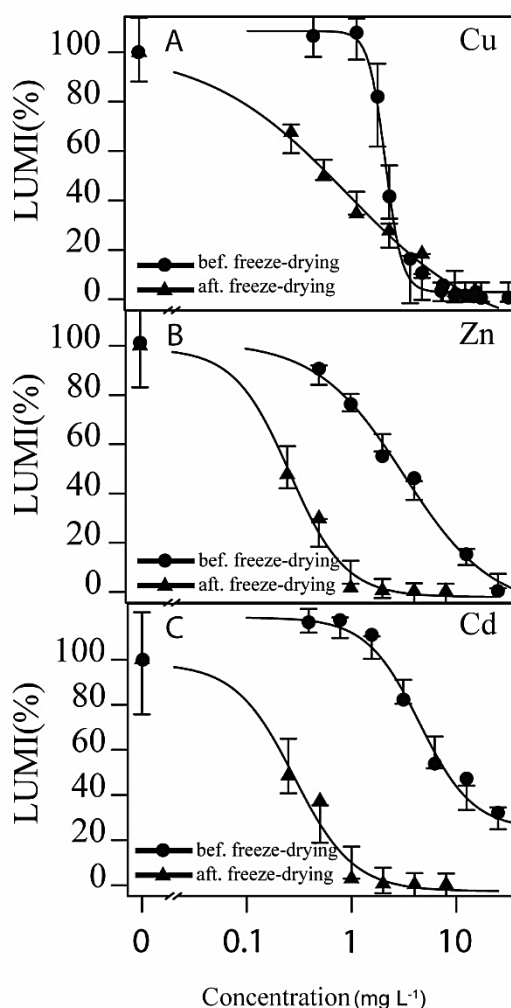


Fig. 3 Dose-response curves of *Anabaena* CPB4337 (as % of luminescence with respect to the control) before and after 24 h of freeze-dried exposed to (A) Copper (Cu); (B) Zinc (Zn); and (C) Cadmium (Cd). Lines represent fitted log logistic models (LL.4) and the standard error of the fitted model for each cation before and after freeze-dried.

drying (Figure 3). For example, in the case of Cu, the EC_{50} decreased from 1.787 ± 0.207 to 0.619 ± 0.155 . Regarding Zn and Cd the EC_{50} after freeze-drying were 0.262 ± 0.061 and 0.281

± 0.044 , respectively. As reported by other authors, the cell membrane can be damaged by the freeze-drying process (Mazur, 1970) and this may result in increased membrane permeability (Sinskey and Silverman, 1970) that may cause an increase in sensitivity to pollutants.

3.3 Effect of long-term preservation on performance of the cyanobacterial bioassay

The maintenance of viability and sensitivity over time are the most critical aspects when evaluating potential long-term functionality of a whole-cell bioreporter. The basal bioluminescence of the freeze-dried cyanobacteria was measured after 24 hours (24 h), 1 week (1 w), 1 month (1 m), 1 year (1 yr) and 3 years (3 yrs) after freeze-drying (figure 4). The bioluminescence remained stable over time however, after 1 year or 3 years of storage, the basal bioluminescence of the cells decreased one order of magnitude, probably due to loss of

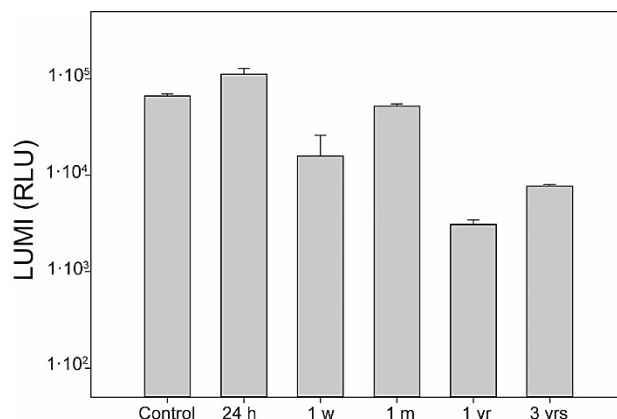


Fig. 4 Long-term stability of luminescence of *Anabaena* CPB4337 (expressed as RLU, Relative Luminescence Units). Basal luminescence of the control (before freeze-drying) and after 24 hours (24 h), 1 week (1 w), 1 month (1 m), 1 year (1 yr) and 3 years (3 yrs) of freeze-drying. Cells were reconstituted using the optimal protocol and luminescence measured after 30 min of incubation.

viability of the cells, but they still presented enough basal luminescence for the bioassays.

To investigate the sensitivity of the bioassay over time, toxicity detection was performed also after 1 w, 1 m, 1 yr and 3 yrs after freeze-drying for the heavy metals Cu, Zn and Cd and it was compared with the results obtained after 24 h of freeze-drying as benchmark reference. Table 1 and figure S1 shows the EC_{50} calculated for the three metals at different times after freeze-

drying (the EC₅₀ before and after 24 h of freeze-drying was also included in table 1 for

Table 1. Sensitivity of freeze-dried *Anabaena* CPB4337 cells before and after different times of freeze-dried, 24 hours (24 h), 1 week (1 w), 1 month (1 m), 1 year (1 yr) and 3 years (3 yrs) towards heavy metals. Cells were exposed to the heavy metals during 1 hour except for 3 yrs¹.

Heavy metals	Time	EC ₅₀ (mg L ⁻¹)
Cu	Before freeze-drying	1.787 ± 0.207
	After freeze-drying:	
	24 h	0.619 ± 0.155
	1 w	0.669 ± 0.043
	1 m	0.483 ± 0.140
	1 yr	0.172 ± 0.052
3 yrs ¹	0.122 ± 0.017	
Zn	Before freeze-drying	3.222 ± 0.403
	After freeze-drying:	
	24 h	0.262 ± 0.061
	1 w	0.219 ± 0.023
	1 m	0.272 ± 0.028
	1 yr	0.171 ± 0.032
3 yrs ¹	0.068 ± 0.006	
Cd	Before freeze-drying	4.472 ± 0.504
	After freeze-drying:	
	24 h	0.281 ± 0.044
	1 w	0.214 ± 0.074
	1 m	0.275 ± 0.064
	1 yr	0.251 ± 0.038
3 yrs ¹	0.226 ± 0.185	

¹Cells were exposed to heavy metals during 30 minutes.

comparison). As can be seen in the table, in general, the EC₅₀ remained stable over time. For a more thorough analysis, and in order to determine if there were significant differences in the EC₅₀ obtained for the three metals over time, the compParm function that compares estimated parameters for the same non-linear model fitted for different assays was carried out. The results of this analysis as EC_{50a}/EC_{50b} (see *Material and Methods*) are detailed in Table S1. This analysis revealed that there were no significant differences in the EC₅₀ of each of the metals over time, except for the case of Cu after 1 year (p < 0.1) and 3 years (p < 0.05) and Zn, whose EC₅₀ after 3 years of freeze-dying decreased significantly one order of magnitude (p < 0.05).

3.4 Comparison of the freeze-dried cyanobacterium bioassay performance with that of other freeze-dried bioassays

Freeze-dried *Anabaena* CPB4337 was sensitive to three heavy metals (Cu, Zn and Cd) commonly present in drinking water, wastewater effluent, and surface water. The EC₅₀s for the three tested heavy metals were one or even two orders of magnitude lower than those of Microtox (*A. fischeri*), according to the data available from the literature (table 2). ToxScreen (*P. leiognathi*) presented greater sensitivity for Cu and Cd than *Anabaena* CPB4337 and Microtox but it presented one order of magnitude lower sensitivity for Zn than freeze-dried *Anabaena* CPB4337. With respect to *J. lividum* YH9, a freeze-dried organism proposed for freshwaters samples, *Anabaena* CPB4337 presented one order of magnitude of more sensitivity for all the tested metals (table 2).

Since organic toxic compounds are also commonly found in fresh or wastewater, we compared freeze-dried *Anabaena* CPB4337 sensitivity with that of the other available freeze-dried bioassays. For this, we chose two toxic organic compounds of different nature, the herbicide, atrazine and the solvent, phenol. The freeze-dried *Anabaena* CPB4337 bioassay showed more sensitivity to atrazine reaching the EC₅₀ at 0.644 ± 0.062 mg L⁻¹ of this compound. In the case of phenol, the EC₅₀ was determined at 11.35 ± 2.365 mg L⁻¹ (figure S2). Compared to Microtox, *Anabaena* CPB4337 was more sensitive for both organic compounds being more accused for atrazine. The EC₅₀ for phenol

Table 2. EC₅₀s comparison between the most relevant freeze-dried toxicity bioassays and the freeze-dried *Anabaena* CPB4337.

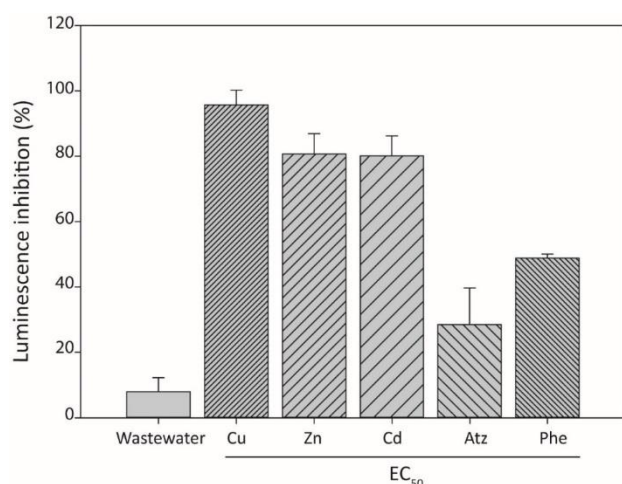
Chemicals	EC ₅₀ (mg L ⁻¹)			
	<i>V. fischeri</i> (Microtox)	<i>P. leiognathi</i> (ToxScreen)	<i>J. lividum</i> YH9	<i>Anabaena</i> CPB4337 ^a
Heavy metals				
Cu	8 ^a , 36 ^b	0.007 ^c	10.5 ^b	0.483 ± 0.140
Zn	2.5 ^a , 13.4 ^b 2–49 ^c	2 ^c	1.3 ^b	0.272 ± 0.028
Cd	21.8 ^b , 41.4 ^c	0.06 ^c	1.1 ^b	0.275 ± 0.064
Organic compounds				
Phenol	25 ^a , 112.9 ^b	NF	12.7 ^b	11.35 ± 2.365
Atrazine	39.87 ^d	NF	NF	0.644 ± 0.062

^a Bulich and Icenberg, 1981 (5 min of exposure); ^b Cho et al., 2004 (30 min of exposure); ^c Ulitzur et al., 2002 (40–50 min of exposure); ^d Tchounwou et. al., 2000 (15 min of exposure); ^e this study (1 hour of exposure). NF: Not found.

was in the same order of magnitude as that of *J. lividum* YH9.

3.5 Application of the bioassay to an environmental sample

Finally, to illustrate the use of the freeze-dried cyanobacterial bioassay in environmental monitoring, a natural water from a wastewater effluent was used as matrix. The characteristics and pollutants present in the wastewater sample are detailed in table S2 and table S3. Figure 5 shows the results of the spiking of the



wastewater sample with the EC_{50} of the heavy metals Cu, Zn, Cd and the organic compounds, atrazine and phenol.

As can be seen in figure 5, when assessing the toxicity of the wastewater effluent without spiking, it provoked 10 % of luminescence inhibition therefore showing low toxicity. When heavy metals were added at their EC_{50} concentration, increased toxicity was observed. Spiking with heavy metals induced a bioluminescence inhibition higher than the 50 % previously determined (EC_{50} s in ddH₂O, see 3.2 *Impact of freeze-drying on the bioassay performance*). Cu addition provoked a bioluminescence inhibition near 100%, while Zn and Cd bioluminescence inhibition was 80 %. In the case of atrazine and phenol addition, luminescence inhibition was practically 50 %.

Fig. 5 Luminescence inhibition (%) of the freeze-dried *Anabaena* CPB4337 exposed to a wastewater sample and a wastewater sample spiked with the EC_{50} of the heavy metals Cu, Zn, Cd and the organic compounds, atrazine and phenol.

Differences in the bioassay performance in a natural matrix may be the consequence of the water chemistry characteristics, which can influence pollutant bioavailability and ultimately, toxicity, especially for heavy metals, or due to interactions between heavy metals and other pollutants in the environmental sample, which induced higher toxicity towards the cyanobacterial bioreporter than when assayed in ddH₂O.

4. Conclusions

The bioluminescent cyanobacterium *Anabaena* CPB4337 was successfully freeze-dried and its potential use as a general toxicity fresh-water bioassay tested. This freeze-dried cyanobacterium was, in general, more sensitive to heavy metals (Cu, Zn and Cd) and to organic chemicals (atrazine and phenol) than standard assays. Freeze-drying in 96-well plate, allows a simple, fast, high throughput and ready-to-use method for testing the toxicity of environmental contaminants.

Moreover, the long-term viability and sensitivity upon 1 year of storage makes freeze-drying an advantageous method for the development of cyanobacterial-based bioassays. However, further analyses using different species of cyanobacteria and also specific inducible bioreporters (lights-on or turn-on) have to be performed to generalize the use of this method.

Acknowledgements

This research was supported by the Spanish Ministry of Economy, CTM2013-45775-C2-1-R and and the Research Programm (MATIERE 2013-2017) from Pays de la Loire, France

References

- Ankley, G., Hoke, R., Giesy, J., Winger, P., 1989. Evaluation of the toxicity of marine sediments and dredge spoils with the Microtox^R bioassay. *Chemosphere*. 18, 2069-2075.
- Bachmann, T., 2003. Transforming cyanobacteria into bioreporters of biological relevance. *Trends in Biotechnology*. 21, 247-249.
- Belkin, S., 2003. Microbial whole-cell sensing systems of environmental pollutants. *Current Opinion in Microbiology*. 6, 206-212.
- Bjerketorp, J., Hakansson, S., Belkin, S., Jansson, J.K., 2006. Advances in preservation methods:

- keeping biosensor microorganisms alive and active. *Curr Opin Biotechnol.* 17, 43-49.
- Boyanapalli, R., Bullerjahn, G.S., Pohl, C., Croot, P.L., Boyd, P.W., McKay, R.M., 2007. Luminescent whole-cell cyanobacterial bioreporter for measuring Fe availability in diverse marine environments. *Appl Environ Microbiol.* 73, 1019-1024.
- Bulich, A.A., Isenberg, D.L., 1981. Use of the luminescent bacterial system for the rapid assessment of aquatic toxicity. *ISA Trans.* 20, 29-33.
- Bullerjahn, G.S., Boyanapalli, R., Rozmarynowycz, M.J., McKay, R.M., 2010. Cyanobacterial bioreporters as sensors of nutrient availability. *Adv Biochem Eng Biotechnol.* 118, 165-188.
- Camanzi, L., Bolelli, L., Maiolini, E., Girotti, S., Matteuzzi, D., 2011. Optimal conditions for stability of photoemission and freeze drying of two luminescent bacteria for use in a biosensor. *Environ Toxicol Chem.* 30, 801-805.
- Corbett, L.L., Parker, D.L., 1976. Viability of lyophilized cyanobacteria (blue-green algae). *Applied and Environmental Microbiology.* 32, 777-780.
- Cho, J.C., Park, K.J., Ihm, H.S., Park, J.E., Kim, S.Y., Kang, I., et al., 2004. A novel continuous toxicity test system using a luminously modified freshwater bacterium. *Biosens Bioelectron.* 20, 338-344.
- Choi, S.H., Gu, M.B., 2002. A portable toxicity biosensor using freeze-dried recombinant bioluminescent bacteria. *Biosens Bioelectron.* 17, 433-440.
- de las Heras, A., de Lorenzo, V., 2011. In situ detection of aromatic compounds with biosensor *Pseudomonas putida* cells preserved and delivered to soil in water-soluble gelatin capsules. *Anal Bioanal Chem.* 400, 1093-1104.
- Deheyn, D.D., Bencheikh-Latmani, R., Latz, M.I., 2004. Chemical speciation and toxicity of metals assessed by three bioluminescence-based assays using marine organisms. *Environ Toxicol.* 19, 161-178.
- Durham, K.A., Porta, D., Twiss, M.R., McKay, R.M., Bullerjahn, G.S., 2002. Construction and initial characterization of a luminescent *Synechococcus* sp. PCC 7942 Fe-dependent bioreporter. *FEMS Microbiol Lett.* 209, 215-221.
- Eltzov, E., Marks, R.S., 2011. Whole-cell aquatic biosensors. *Anal Bioanal Chem.* 400, 895-913.
- Esteves-Ferreira, A.A., Corrêa, D.M., Carneiro, A.P.S., Rosa, R.M., Loterio, R., Araújo, W.L., 2012. Comparative evaluation of different preservation methods for cyanobacterial strains. *Journal of Applied Phycology.* 25, 919-929.
- Farré, M., Barceló, D., 2003. Toxicity testing of wastewater and sewage sludge by biosensors, bioassays and chemical analysis. *Trends in Analytical Chemistry.* 22, 299-310.
- Gillor, O., Hadas, O.R.A., Post, A.F., Belkin, S., 2010. Phosphorus and nitrogen in a monomictic freshwater lake: employing cyanobacterial bioreporters to gain new insights into nutrient bioavailability. *Freshwater Biology.* 55, 1182-1190.
- Golden, S.S., 1995. Light-responsive gene expression in cyanobacteria. *Journal of Bacteriology.* 177, 1651-1654.
- González-Pleiter, M., Gonzalo, S., Rodea-Palomares, I., Leganés, F., Rosal, R., Boltes, K., et al., 2013. Toxicity of five antibiotics and their mixtures towards photosynthetic aquatic organisms: Implications for environmental risk assessment. *Water Research.* 47, 2050-2064.
- Gu, M.B., Choi, S.H., Kim, S.W., 2001. Some observations in freeze-drying of recombinant bioluminescent *Escherichia coli* for toxicity monitoring. *J Biotechnol.* 88, 95-105.
- Gu, M.B., Mitchell, R.J., Kim, B.C., 2004. Whole-Cell-Based Biosensors for Environmental Biomonitoring and Application. *Adv Biochem Engin/Biotechnol* 87, 269-305.
- Hassan, S.H., Van Ginkel, S.W., Hussein, M.A., Abskharon, R., Oh, S.E., 2016. Toxicity assessment using different bioassays and microbial biosensors. *Environ Int.* 92-93, 106-118.
- He, W., Yuan, S., Zhong, W.H., Siddikee, M.A., Dai, C.C., 2016. Application of genetically engineered microbial whole-cell biosensors for combined chemosensing. *Appl Microbiol Biotechnol.* 100, 1109-1119.
- Hinwood, A.L., McCormick, M.J., 1987. The effect of ionic solutes on EC50 values measured using the microtox test. *Toxicity Assessment.* 2, 449-461.
- Holm-Hansen, O., 1967. Factors affecting the viability of lyophilized algae. *Cryobiology.* 4, 17-23.
- Johnson, B.T. 2005. Microtox® Acute Toxicity Test. In: Blaise C, Féraud J-F, editors. *Small-scale Freshwater Toxicity Investigations: Toxicity Test Methods.* Springer Netherlands, Dordrecht, 69-105.
- Jouanneau, S., Durand, M.J., Courcoux, P., Blusseau, T., Thouand, G., 2011. Improvement of the identification of four heavy metals in environmental samples by using predictive decision tree models coupled with a set of five bioluminescent bacteria. *Environ Sci Technol.* 45, 2925-2931.
- Jouanneau, S., Durand, M.J., Lahmar, A., Thouand, G., 2015. Main Technological Advancements in Bacterial Bioluminescent Biosensors Over the Last Two Decades. *Adv Biochem Eng Biotechnol.*
- Ko, K.S., Kong, I.C., 2017. Application of the freeze-dried bioluminescent bioreporter *Pseudomonas putida* mt-2 KG1206 to the biomonitoring of groundwater samples from monitoring wells near gasoline leakage sites. *Appl Microbiol Biotechnol.* 101, 1709-1716.
- Litchman, E., Klausmeier, C.A., Bossard, P., 2004. Phytoplankton nutrient competition under

- dynamic light regimes. *Limnology and Oceanography*. 49, 1457-1462.
- Liu, S.S., Song, X.Q., Liu, H.L., Zhang, Y.H., Zhang, J., 2009. Combined photobacterium toxicity of herbicide mixtures containing one insecticide. *Chemosphere*. 75, 381-388.
- Ma, M., Tong, Z., Wang, Z., Zhu, W., 1999. Acute toxicity bioassay using the freshwater luminescent bacterium *Vibrio-qinghaiensis* sp. Nov.-Q67. *Bull Environ Contam Toxicol*. 62, 247-253.
- Ma, X., Wang, X., Ngo, H., Guo, W., 2012. Application of *vibrio qinghaiensis* sp. Q67 for ecotoxic assessment of environmental waters: A mini review. *Journal of Water Sustainability*. 2, 209 - 220.
- Ma, X.Y., Wang, X.C., Liu, Y.J., 2011. Study of the variation of ecotoxicity at different stages of domestic wastewater treatment using *Vibrio-qinghaiensis* sp.-Q67. *J Hazard Mater*. 190, 100-105.
- Ma, X.Y., Wang, X.C., Ngo, H.H., Guo, W., Wu, M.N., Wang, N., 2014. Bioassay based luminescent bacteria: interferences, improvements, and applications. *Sci Total Environ*. 468-469, 1-11.
- Martín-de-Lucía, I., Campos-Mañas, M.C., Agüera, A., Rodea Palomares, I.M., Pulido-Reyes, G., Leganes, f., et al., 2017. Reverse Trojan-horse effect decreased wastewater toxicity in the presence of inorganic nanoparticles. *Environ. Sci.: Nano*.
- Mazur, P., 1970. Cryobiology: the freezing of biological systems. *Science*. 168, 939-949.
- Mbeunkui, F., Richaud, C., Etienne, A.L., Schmid, R.D., Bachmann, T.T., 2002. Bioavailable nitrate detection in water by an immobilized luminescent cyanobacterial reporter strain. *Appl Microbiol Biotechnol*. 60, 306-312.
- Michelini, E., Cevenini, L., Calabretta, M.M., Spinozzi, S., Camborata, C., Roda, A., 2013. Field-deployable whole-cell bioluminescent biosensors: so near and yet so far. *Anal Bioanal Chem*. 405, 6155-6163.
- Morgan, C.A., Herman, N., White, P.A., Vesey, G., 2006. Preservation of micro-organisms by drying; a review. *J Microbiol Methods*. 66, 183-193.
- Morris, G.J., Coulson, G.E., Clarke, K.J., 1988. Freezing injury in *Saccharomyces cerevisiae*: The effect of growth conditions. *Cryobiology*. 25, 471-482.
- Munoz-Martin, M.A., Mateo, P., Leganes, F., Fernandez-Pinas, F., 2011. Novel cyanobacterial bioreporters of phosphorus bioavailability based on alkaline phosphatase and phosphate transporter genes of *Anabaena* sp. PCC 7120. *Anal Bioanal Chem*. 400, 3573-3584.
- Munoz-Martin, M.A., Mateo, P., Leganes, F., Fernandez-Pinas, F., 2014. A battery of bioreporters of nitrogen bioavailability in aquatic ecosystems based on cyanobacteria. *Sci Total Environ*. 475, 169-179.
- Muramatsu, M., Hihara, Y., 2012. Acclimation to high-light conditions in cyanobacteria: from gene expression to physiological responses. *J Plant Res*. 125, 11-39.
- Newman, M.C., McCloskey, J.T., 1996. Predicting relative toxicity and interactions of divalent metal ions: Microtox® bioluminescence assay. *Environmental Toxicology and Chemistry*. 15, 275-281.
- Nivens, D.E., McKnight, T.E., Moser, S.A., Osbourn, S.J., Simpson, M.L., Saylor, G.S., 2004. Bioluminescent bioreporter integrated circuits: potentially small, rugged and inexpensive whole-cell biosensors for remote environmental monitoring. *Journal of Applied Microbiology*. 96, 33-46.
- Nurul Aisyah, W., Jusoh, W., Shing, L., 2014. Exploring the potential of whole cell biosensor: A review in environmental applications. *International Journal of Chemical, Environmental & Biological Sciences*. 2, 52-56.
- Park, M., Tsai, S.L., Chen, W., 2013. Microbial biosensors: engineered microorganisms as the sensing machinery. *Sensors* 13, 5777-5795.
- Pasco, N.F., Weld, R.J., Hay, J.M., Gooneratne, R., 2011. Development and applications of whole cell biosensors for ecotoxicity testing. *Analytical and Bioanalytical Chemistry*. 400, 931-945.
- Perry, S.F., 1995. Freeze-drying and cryopreservation of bacteria. *Methods Mol Biol*. 38, 21-30.
- Polyak, B., Bassis, E., Novodvoretz, A., Belkin, S., Marks, R.S., 2001. Bioluminescent whole cell optical fiber sensor to genotoxicants: system optimization. *Sensors and Actuators B: Chemical*. 74, 18-26.
- Porta, D., Bullerjahn, G.S., Durham, K.A., Wilhelm, S.W., Twiss, M.R., McKay, R.M.L., 2003. Physiological Characterization of *Asynechococcus* sp. (Cyanophyceae) Strain PCC 7942 Iron-Dependent Bioreporter for Freshwater Environments. *Journal of Phycology*. 39, 64-73.
- Rajan Premkumar, J., Rosen, R., Belkin, S., Lev, O., 2002. Sol-gel luminescence biosensors: Encapsulation of recombinant *E. coli* reporters in thick silicate films. *Analytica Chimica Acta*. 462, 11-23.
- Rippka, R., 1988. Isolation and purification of cyanobacteria. *Methods Enzymol*. 167, 3-27.
- Ritz, C., Baty, F., Streibig, J.C., Gerhard, D., 2015. Dose-Response Analysis Using R. *PLoS One*. 10, e0146021.
- Ritz, C., Streibig, J.C., 2005. Bioassay Analysis Using R. 2005. 12, 22.
- Roda, A., Cevenini, L., Michelini, E., Branchini, B.R., 2011. A portable bioluminescence engineered cell-based biosensor for on-site applications. *Biosens Bioelectron*. 26, 3647-3653.
- Rodea-Palomares, I., Fernández-Piñas, F., González García, C., Leganes, F. Use of lux-marked cyanobacterial bioreporters for assessment of individual and combined toxicities of metals in

- aqueous samples. New York. USA.: Nova Science Publishers, 2009a.
- Rodea-Palomares, I., Gonzalez-Garcia, C., Leganes, F., Fernandez-Pinas, F., 2009b. Effect of pH, EDTA, and anions on heavy metal toxicity toward a bioluminescent cyanobacterial bioreporter. *Arch Environ Contam Toxicol.* 57, 477-487.
- Rodea-Palomares, I., Gonzalez-Pleiter, M., Gonzalo, S., Rosal, R., Leganes, F., Sabater, S., et al., 2016. Hidden drivers of low-dose pharmaceutical pollutant mixtures revealed by the novel GSA-QHTS screening method. *Science Advances.* 2.
- Rodea-Palomares, I., Gonzalo, S., Santiago-Morales, J., Leganes, F., Garcia-Calvo, E., Rosal, R., et al., 2012. An insight into the mechanisms of nanoceria toxicity in aquatic photosynthetic organisms. *Aquat Toxicol.* 122-123, 133-143.
- Rodea-Palomares, I., Makowski, M., Gonzalo, S., Gonzalez-Pleiter, M., Leganes, F., Fernandez-Pinas, F., 2015. Effect of PFOA/PFOS pre-exposure on the toxicity of the herbicides 2,4-D, Atrazine, Diuron and Paraquat to a model aquatic photosynthetic microorganism. *Chemosphere.* 139, 65-72.
- Rodea-Palomares, I., Petre, A.L., Boltes, K., Leganes, F., Perdigon-Melon, J.A., Rosal, R., et al., 2010. Application of the combination index (CI)-isobologram equation to study the toxicological interactions of lipid regulators in two aquatic bioluminescent organisms. *Water Res.* 44, 427-438.
- Rosal, R., Rodea-Palomares, I., Boltes, K., Fernandez-Pinas, F., Leganes, F., Gonzalo, S., et al., 2010a. Ecotoxicity assessment of lipid regulators in water and biologically treated wastewater using three aquatic organisms. *Environ Sci Pollut Res Int.* 17, 135-144.
- Rosal, R., Rodea-Palomares, I., Boltes, K., Fernandez-Pinas, F., Leganes, F., Petre, A., 2010b. Ecotoxicological assessment of surfactants in the aquatic environment: combined toxicity of docusate sodium with chlorinated pollutants. *Chemosphere.* 81, 288-293.
- Schreiter, P.P., Gillor, O., Post, A., Belkin, S., Schmid, R.D., Bachmann, T.T., 2001. Monitoring of phosphorus bioavailability in water by an immobilized luminescent cyanobacterial reporter strain. *Biosens Bioelectron.* 16, 811-818.
- Shao, C.Y., Howe, C.J., Porter, A.J.R., Glover, L.A., 2002. Novel Cyanobacterial Biosensor for Detection of Herbicides. *Applied and Environmental Microbiology.* 68, 5026-5033.
- Sinsky, T.J., Silverman, G.J., 1970. Characterization of injury incurred by *Escherichia coli* upon freeze-drying. *J Bacteriol.* 101, 429-437.
- Sorensen, S.J., Burmolle, M., Hansen, L.H., 2006. Making bio-sense of toxicity: new developments in whole-cell biosensors. *Curr Opin Biotechnol.* 17, 11-16.
- Su, L., Jia, W., Hou, C., Lei, Y., 2011. Microbial biosensors: a review. *Biosens Bioelectron.* 26, 1788-1799.
- Tchounwou, P.B., Wilson, B., Ishaque, A., Ransome, R., Huang, M.-J., Leszczynski, J., 2000. Toxicity Assessment of Atrazine and Related Triazine Compounds in the Microtox Assay, and Computational Modeling for Their Structure-Activity Relationship. *International Journal of Molecular Sciences.* 1, 63-74.
- Ulitzur, S., Lahav, T., Ulitzur, N., 2002. A novel and sensitive test for rapid determination of water toxicity. *Environ Toxicol.* 17, 291-296.
- Van der Meer, J.R., Belkin, S., 2010. Where microbiology meets microengineering: design and applications of reporter bacteria. *Nat Rev Microbiol.* 8, 511-522.
- Watanabe, A., 1959. Some devices for preserving blue-green algae in viable state. *J. Gen. Appl. Microbiol.* 5, 153-157.
- Wenfeng, S., Gooneratne, R., Glithero, N., Weld, R.J., Pasco, N., 2013. Appraising freeze-drying for storage of bacteria and their ready access in a rapid toxicity assessment assay. *Appl Microbiol Biotechnol.* 97, 10189-10198.
- Xu, T., Close, D.M., Sayler, G.S., Ripp, S., 2013. Genetically modified whole-cell bioreporters for environmental assessment. *Ecol Indic.* 28, 125-141.
- Yagur-Kroll, S., Belkin, S., 2011. Upgrading bioluminescent bacterial bioreporter performance by splitting the lux operon. *Anal Bioanal Chem.* 400, 1071-1082.
- Zhang, J., Liu, S.S., Dou, R.N., Liu, H.L., Zhang, J., 2011. Evaluation on the toxicity of ionic liquid mixture with antagonism and synergism to *Vibrio qinghaiensis* sp.-Q67. *Chemosphere.* 82, 1024-1029.

**S M
U A
P T
P E
L R
E I
M A
E L
N
T
A
R
Y**

Supplementary Material:

High-throughput freeze-dried cyanobacterial bioassay for fresh-waters environmental monitoring

Keila Martín-Betancor^a, Marie-José Durand^b, Gérald Thouand^b, Francisco-Leganés^a, Francisca Fernández-Piñas^a, Ismael Rodea-Palomares^a

^aDepartment of Biology, Facultad de Ciencias, Universidad Autónoma de Madrid, 28049 Madrid, Spain.

^bUniversity of Nantes, UMR CNRS 6144 GEPEA, France

*Corresponding author: Francisca Fernández-Piñas

E-mail: francisca.pina@uam.es

Table of contents:

Supplementary Material Table S1: EC_{50a}/ EC_{50b} ratios for *Anabaena* CPB4337 response to the three heavy metals after different times after freeze-drying

Supplementary Material Table S2: Wastewater characterization parameters

Supplementary Material Table S3: Concentrations of pollutants in the wastewater sample

Supplementary Material Figure S1: Comparison of dose-response curves of *Anabaena* CPB4337 after different times of freeze-dried storage

Supplementary Material Figure S2: Dose-response curves of *Anabaena* CPB4337 after one month of freeze-dried exposed to Atrazine and Phenol

Table S1. EC_{50 a}/ EC_{50 b} ratios for *Anabaena* CPB4337 response to the three heavy metals after different times after freeze-drying.

EC _{50 a} / EC _{50 b}	Estimate	Std. Error	<i>t</i> -value	<i>p</i> -value
Comparison of parameter 'EC₅₀': Cu				
EC _{50 24h} / EC _{50 1w}	0.92284	0.29108	-0.26508	0.7923
EC _{50 24h} / EC _{50 1m}	1.27987	0.51201	0.54662	0.5878
EC _{50 24h} / EC _{50 1yr}	3.5836	1.5101	1.7109	0.0957
EC _{50 24h} / EC _{50 3yrs}	5.1097	1.6895	2.4325	0.0198
Comparison of parameter 'EC₅₀': Zn				
EC _{50 24h} / EC _{50 1w}	1.19482	0.30584	0.63701	0.5253
EC _{50 24h} / EC _{50 1m}	0.96506	0.24689	-0.14150	0.8877
EC _{50 24h} / EC _{50 1yr}	1.52913	0.47406	1.11616	0.2664
EC _{50 24h} / EC _{50 3yrs}	3.85907	0.97038	2.94633	0.0038
Comparison of parameter 'EC₅₀': Cd				
EC _{50 24h} / EC _{50 1w}	1.316114	0.816909	0.386964	0.6995
EC _{50 24h} / EC _{50 1m}	1.02195	0.57574	0.03813	0.9696
EC _{50 24h} / EC _{50 1yr}	1.11963	0.59919	0.19965	0.8421
EC _{50 24h} / EC _{50 3yrs}	1.24371	1.19955	0.203172	0.8394

“a” denotes after 24 hours of exposure; “b” denotes any of the possible time-points after freeze-drying: 1 week (1 w), 1 month (1 m), 1 year (1 yr) and 3 years (3 yrs).

Table S2. Wastewater characterization parameters.

Parameters	value	Anions and cations	(mg L ⁻¹)
pH	7.8	Nitrate	0.38
Turbidity (NTU)	1.4	Chloride	125.5
Conductivity (mS/cm)	1.23 ± 0.03	Sulphate	143.7
COD (mg/L)	49.2 ± 1.2	Fluoride	<0.80
NPOC (mg/L)	17.2 ± 0.5	Nitrite	<0.10
Alkalinity (mg CaCO₃/L)	286	Bicarbonate	348.4
Total-P (mg/L)	0.1	Sodium	95.3
Total-N (mg/L)	2.3	Potassium	23.4
		Magnesium	14.3
		Calcium	49
		Ammonium	68.4

Table S3. Concentrations of pollutants in wastewater

No.	Compound	Concentration (ng L ⁻¹)
1	4-Aminoantipyrine (4-AA)	137
2	N-acetyl-4-aminoantipyrine (4-AAA)	1050
3	N-formyl-4-aminoantipyrine (4-FAA)	904
4	Antipyrine	49
5	Atenolol	421
6	Azithromycin	184
7	Bezafibrate	170
8	Caffeine	255
9	Carbamazepine	167
10	Carbamazepine epoxide	41
11	Ciprofloxacin	273
12	Citalopram	162
13	Clarithromycin	169
14	Diatrizoic acid	1185
15	Diazepam	25
16	Erythromicin	140
17	Famotidine	30
18	Fenofibric acid	455
19	Furosemide	528
20	Gemfibrozil	625
21	Hydrochlorothiazide	783
22	Indomethacin	35
23	Iopamidol	703
24	Ketoprofen	241
25	Lincomycin	8
26	Mepivacaine	26
27	Metoclopramide	32
28	Metoprolol	84
29	Metronidazole	391
30	Naproxen	207
31	Nicotine	368
32	Ofloxacin	291
33	Paraxanthine	184
34	Pentoxifylline	371
35	Pravastatin	138
36	Primidone	345
37	Propranolol	57
38	Propyphenazone	20
39	Ranitidine	591
40	Sotalol	61
41	Sucralose	974
42	Sulfamethoxazole	300
43	Sulfapyridine	204
44	Theophylline	87
45	Trimethoprim	303
46	Venlafaxine	338

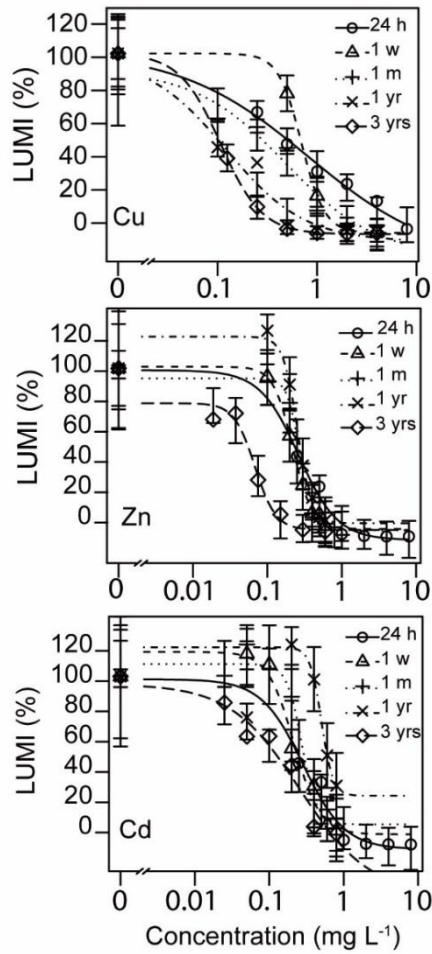


Fig. S1 Comparison of dose-response curves of freeze-dried *Anabaena* CPB4337 (as % of luminescence with respect to the control) after different times of freeze-dried storage (24 hours, 1 week, 1 month, 1 year and 3 years) exposed to Copper (Cu); Zinc (Zn); and Cadmium (Cd). Lines represent fitted log logistic models (LL.4) and the standard error of the fitted model for each cation.

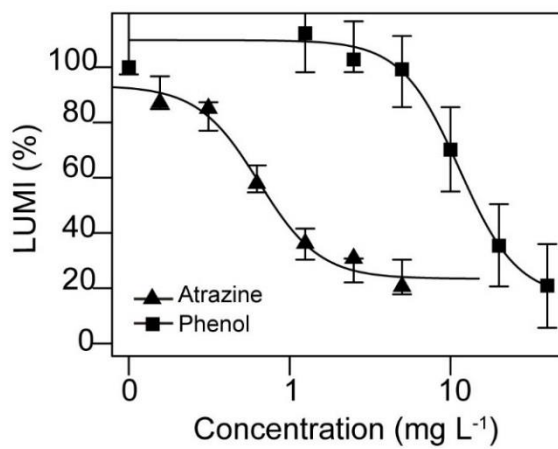


Fig. S2 Dose-response curves of *Anabaena* CPB4337 after one month of freeze-dried exposed to Atrazine and Phenol. Lines represent fitted log logistic models (LL.4) and the standard error of the fitted model for each chemical.

**D
I
S
C
U
S
S
I
O
N**

DISCUSSION

The aim of the present thesis was to construct and characterize a turn-on self-bioluminescent whole-cell bioreporter for bioavailable heavy metals detection. One of the contributions of this thesis was the use of a relevance aquatic organism, specifically the unicellular cyanobacterium, *Synechococcus elongatus* PCC 7942 for the bioreporter development. In order to illustrate and advance the potential use of the bioreporter in real environmental monitoring, the response of this bioreporter was deeply characterized both in culture medium and in different environmental matrices including real waters with different levels of background pollution and source, complex mixtures of heavy metals and biocidal nanomaterials. To further complement this experimental characterization of the bioreporter functioning, a mathematical model for predicting and studying mixtures interactions was developed and validated, which may be a relevant advance in the mixture pharmacology and toxicology sciences. Finally, a preservation system was successfully developed for a turn-off cyanobacterial bioreporter, with the aim of extending it to other cyanobacterial bioreporters in the future.

Through this thesis, and existing literature, (Girotti et al., 2008; Harms et al., 2006; Ma et al., 2014; Ron, 2007; van der Meer and Belkin, 2010; Yagi, 2007) it has become clear that whole-cell bioreporters have many advantages over the use of chemical methods to determine the presence of a pollutant in the environment, however, why are not they used regularly in environmental assessment? There are certain limitations that have to be overcome in order for bioreporters to become something more than just laboratory proof of principles. Some of these disadvantages have been tried to be overcome through this thesis.

A novel whole cell cyanobacterial bioreporter for bioavailable heavy metals detection

In the chapter II of this thesis, a cyanobacterial self-bioluminescent bioreporter strain (denoted as *Synechococcus* sp. PCC 7942 pBG2120) based on the unicellular cyanobacterium *Synechococcus* sp. PCC 7942 was constructed for detecting bioavailable heavy metals in aquatic environments. Currently, several bioreporters are available to

detect heavy metals; however, most of them are based in the bacterium *E. coli* (Magrisso et al., 2008). Although these bioreporters have been widely used to determine heavy metals in aquatic environments, they are not constituted by relevant organisms of these environments. Conversely, cyanobacteria are ecological relevant and abundant group of primary producers (dominant in some aquatic and terrestrial ecosystems) which are prokaryotic in nature and are at the very base of the trophic webs. Due to their key role in the N and C cycles, they are a dominant component of marine and freshwater phytoplankton and they are well suited for detecting contaminants in aqueous samples (Bachmann, 2003; Rodea-Palomares et al., 2009). Therefore, the use of these organisms can contribute to obtain more relevant data about the status of aquatic environments.

The cyanobacterial bioreporter strain was constructed using the *smt* locus present in the same cyanobacterium, which encodes a metallothionein (SmtA), and its repressor (SmtB) fused to *luxCDABE* genes from *P. luminescens*. The SmtB repressor belongs to the ArsR/SmtB family of the transcriptional repressors whose interaction with heavy metals cause de-repression of the *smtA* gene (in the bioreporter strain, of the *luxCDABE* genes) Since it is the sensing element of the bioreporter strain its affinity to heavy metals will determine the bioreporter's specificity and sensitivity. Several studies (Huckle et al., 1993; Morby et al., 1993; Robinson et al., 2001; Turner et al., 1996) have elucidate that the SmtB-repression can be alleviated mainly by Zn but also by Cd, Co, Cr, Cu, Hg, Ni and Pb. In this study, SmtB was, for the first time, described to respond to Ag. Apart from this, the sensitivity among reporter organisms also depends on the metal homeostasis/resistance systems of each organism and the reporter system chosen for the bioreporter construction (Hynninen and Virta, 2010).

The constructed *Synechococcus* bioreporter responded to six different heavy metals, with the following order of sensitivity and range of detections: Hg^{2+} (11-72 pM) > Cu^{2+} (0.027-0.05 μM) > Ag^+ (0.05-0.29 μM) > Co^{2+} (0.88-2.66 μM) \geq Zn^{2+} (0.97-2.04 μM) > Cd^{2+} (1.54-5.35 μM). Prior to this work, Erbe et al. (1996) constructed what can be considered the first cyanobacterial bioreporter able to detect heavy metals based on the *smt* locus fused to the *luxCDABE* of *A. fischeri* and using the same host, *Synechococcus* PCC 7942. This cyanobacterial bioreporter was tested towards Zn, Cd and Cu. For both cyanobacterial bioreporters, Zn^{2+} was the most significant effector and they showed similar sensitivity to this metal. *Synechococcus* sp. PCC 7942 pBG2120 was less sensitive to Cd but two orders of magnitude more sensitive to Cu. However, the main difference

between these bioreporters strains is that the bioreporter developed in this thesis, *Synechococcus* sp. PCC 7942 pBG2120, did not need the addition of exogenous aldehyde.

Regarding the other heavy metals bioreporters available (see *Table 1 of Introduction or Chapter II of this thesis*), *Synechococcus* sp. PCC 7942 pBG2120 was, in general, more sensitive to Hg, Cu and Ag than other microbial heavy metal bioreporters (Amaro et al., 2011; Riether et al., 2001). It was less sensitive to Co than the *coaT*-based *Synechocystis* bioreporter (Peca et al., 2008) and regarding Zn, it showed a similar sensitivity of that of the ciliate bioreporter (Amaro et al., 2011) and it was much more sensitive than the *zntA*-based *E. coli* bioreporter (Riether et al., 2001). In general, it was less sensitive to Cd than other bioreporters (Amaro et al., 2011; Charrier et al., 2011; Erbe et al., 1996; Riether et al., 2001). The cyanobacterial bioreporter developed in this thesis adds to the battery of heavy metal bioreporters of different trophic levels already constructed.

Performance of the whole cell cyanobacterial bioreporter in complex water matrices

Prior to use a whole-cell bioreporter for detecting an environmental pollutant and especially in case of heavy metals, several factors that can influence the performance of the bioassay have to be taken into account. These factors range from the physiological state of the cell or duration of the assay to the chemical composition of the test medium used for the assay (Sharma et al., 2013; Tauriainen et al., 1998). Most studies take into account the first two factors as a part of the characterization of the bioreporter before its use. However, the medium composition for the experimental procedures are very rarely considered (Tauriainen et al., 1998).

The chemical composition of the medium is a major contributor to the bioavailability of the heavy metals, therefore, to the real metal concentration detected by the organism. Unfortunately, it is not possible to use one defined medium for all bioavailability tests since different organisms have different requirements. When performing these bioassays, it is important to consider that components of the test medium may affect metal complexation (Errecalde et al., 1998; Lee et al., 2005; Zhao et al., 2016). The concentrations of organic ligands (and some inorganic ligands) are considered to be the main factors that influence metal speciation in test media and it has been demonstrated that the components of complex media may bind metal ions, and thereby reduce the

toxicity of these metals. Thus, in this study, a chemical speciation model was used to link the response of the bioreporter with the free ion metal concentration, which is the most probably bioavailable specie and the LOD for each heavy metal was giving as free-ion LOD. This is also important when comparing with other bioreporters, whose LODs are normally given as heavy metal nominal concentration.

As highlighted by some authors (Hynninen and Virta, 2010), to facilitate comparisons between studies, a standardized testing protocol for heavy metal bioreporters should be developed. This standardized testing protocol should draw attention to the assay condition, such as bacterial growth phases, growth medium, incubation time and sample preparation. Of these, the most important consideration is the use of media that do not change the bioavailability of metals in the tested sample. If it is impossible, it will be a great improvement to incorporate a chemical speciation model that allows relating the response of the bioreporter with the bioavailable heavy metal species.

On the other hand, testing environmental samples in the characterization of a bioreporter is a great advantage that allows getting closer to reality. Bioreporters designs have been accompanied, in most cases, by simple laboratory experiments; however, assaying more complex real-world samples is obviously more challenging because of the possible presence of inhibitory compounds, the unknown confounding effects of chemical mixtures on bioreporter behaviour and the absorption effects of matrices. Some studies have gone a step beyond this and have validated bioreporter assays using environmental samples (Boyanapalli et al., 2007; Durham et al., 2002; Jouanneau et al., 2012; Magrisso et al., 2008; Munoz-Martin et al., 2011). In the present thesis, the bioreporter performance was tested in three real environmental samples spiked with increasing concentrations of Zn, Cd, Ag and Cu. The real samples used reflect water matrices of different complexities, two river samples (affected or not by anthropogenic influence) and one wastewater effluent sample. In this case, the response of the bioreporter was also linked to the free ion heavy metal concentration through the chemical speciation program, Visual MINTEQ. The concentrations of the free ions detected by the bioreporter in the two river spiked samples represented an average of 68 % of that predicted by chemical modelling and nearly 100 % of that predicted in the spiked wastewater effluent sample. In some of the spiked environmental samples, the bioreporter did not give a reliable response, as the amount of metal was higher than its MPCs. This means that in highly polluted samples, the sample will have to be diluted previously to avoid false negatives; furthermore,

several proposals have been made in order to overcome the effects of testing complex samples. One of the most interesting is to include the same reporter strain with a constitutively reporter signal and tested it in parallel. Some configurations are been proposed to develop this control strain, the used of a modified metal-response system (usually the promoter) that is no longer controlled by the metal and instead drives a constitutively expression of the reporter system (Barkay et al. 1997) or a constitutively production of a reporter protein instead of the metal-inducible promoter (Ivask et al. 2007; Tom-Petersen 2001; Hakkila et al. 2004; Tauriainen 1997; Virta et al. 1995; Ivask et al. 2004, Karhu et al. 2005). For this context, a significant advance would be to incorporate two reporter signals in the same reporter strain (van Rossum et al., 2017). This is a potential way to improve the constructed cyanobacterial bioreporter strain in the future.

Applications of whole cell bioreporters are not limited to testing contaminated water or soil waters, and determining potential risk of pollution. Whole-cell bioreporters have also been used to monitor changes in bioavailable metal concentrations in different processes and are very useful in evaluating efficiency of different remediation/immobilization treatments (Bahar et al., 2008; Heijerick et al., 2002; Sandberg et al., 2007). Moreover, in the last years, given the increased production and application of nanomaterials, the use of heavy metal bioreporters have been also proposed to determine the effect of the metal ion released from the nanomaterials (Ivask et al., 2012; Kahru et al., 2008).

In this thesis, the heavy metal bioreporter constructed was also used to study the antimicrobial effects of three different MOFs based on Zn, Co or Ag towards two cyanobacterial strains and one green alga. The use of three different approaches, the *Synechococcus* PCC 7942 PBG2120 reporter strain, ICP-MS determination and the speciation program Visual MINTEQ, allowed us to elucidate that the biocidal activity presented by these MOFs was mainly due to the concentration of free metal ion released from these MOFs. Moreover, different sensitivities between species were found; the green alga *Chamydomonas* appeared very sensitive to the Ag-MOF but much more resistant to the rest of MOFs, whereas the strains of cyanobacteria were just as sensitive to the three different MOFs. These differences between species are probably due to differences in the cell wall and they are very important to be considered when developing these materials specially if are designed to prevent colonization of surfaces by different organisms.

Despite the variety of applications of bioreporters, nowadays their use is still very limited. The greatest limitation in using whole-cell bioreporters for environmental assessment is the lack of specificity. As reported before, it is the sensing element that determines the sensitivity (detectable concentration) and specificity (detected metals), although these factors also depend greatly on microbial metal homeostasis/resistance systems (uptake proteins, efflux proteins and intracellular sequestering proteins) that determine the intracellular concentration of metals that is ultimately available for detection by the bioreporters. Due to the limited possibilities for coordinate binding between proteins and metal ions, metal-activated transcription factors usually sense several different heavy metal ions with similar properties (Fernandez-Lopez et al., 2015; Reyes-Caballero et al., 2011; Waldron et al., 2009). Thus, it is generally not possible in practice to construct a bioreporter that senses only one metal. This fact makes the examples of specific bioreporters for metals very scarce (Corbisier et al., 1999; Ivask et al., 2002; Selifonova et al., 1993).

As the lack of specificity is a fact to which most of inducible bioreporters studies have to deal, practical solutions for addressing the effects of chemical mixtures have been proposed. The most successfully proposal is the use of an array of bioreporter strains with overlapping detection specificities but using the same reporter protein output. Such a strain panel may be particularly useful in toxicity screening and several groups have presented a proof of principle (Ahn et al., 2004; Belkin, 1998; Elad et al., 2008; Galluzzi and Karp, 2006; Ron, 2007). Furthermore, Jouanneau et al. (2011) developed a statistical model to identify and quantify four metals (As, Cd, Hg and Cu) from a panel of five bioluminescent bacterial strains. This statistical model called “Metalsoft” was able to provide semi quantitative information after 60 minutes without pretreating the samples. In a further study, the use of the data from the software Metalsoft was able to monitor and estimate these four heavy metals levels in environmental samples online with high reliability (Jouanneau et al., 2012).

These methods are a real advance in the use of whole-cell bioreporters for on-line environmental monitoring. However, they do not provide information about mixtures interactions. Until now, no methods are available to study the nature of mixture interactions (synergism and antagonism) along the entire biphasic curve (including toxic concentrations) and there are not predictive models for mixtures effects in turn-on bioreporters frameworks.

A theoretical contribution to mixture effect research in inducible whole-cell bioreporters

In the regulatory field, there is an increasing concern about the pollutants mixtures effects (Carvalho et al., 2014; Farley et al., 2015; Meyer et al., 2015). As described before, environmental regulation on aquatic ecosystems are based predominantly on assessment carried out on individual substances, however, the empirical evidences that mixture effects are uncovered by the individual chemical-chemical investigations have led regulatory authorities to introduce mixture risk assessment (EC/2011). The lack of models to study mixture interactions in inducible systems and to predict the combined effect of any environmental mixture are the main limitations in using inducible systems in environmental assessment.

In chapter III of this thesis, a novel mathematical model for mixture effect modelling in the context of whole-cell inducible bioreporters was developed. This method, based on a multivariate extension of the *Loewe additivity*, was able to predict and study heavy metals interactions, taking into account differential maximal effects and the entire biphasic dose-response curve given by the inducible bioreporter output. An important application of the methodology proposed is the possibility, for the first time, of predicting inducible whole cell bioreporters responses to mixtures using only experimental information from individual chemicals. This equals the potential applicability of inducible whole cell bioreporters in mixture risk assessment than those of monotonic toxicity tests, or turn-off bioreporters such as Microtox (Johnson, 2005) and increases the opportunity of inducible whole cell bioreporter to be included in regulatory frameworks. On the other hand, study of possible departures from additivity was also performed. As results from this study, the *Synechococcus* reporter strain responded to heavy metal binary mixtures in a nearly additive way in all the mixtures studied except when Hg, Co, and to lesser extent Ag, were present in the mixtures which resulted in important departures from additivity. This model could provide information about the occurrence of mixtures interactions when inducible systems are been used and also may help to understand the confounding responses generate by the bioreporters when exposing to pollutant mixtures.

Since a general theoretical contribution was done in this chapter, this model may also be used in the study of other systems that generates biphasic dose-response curves as

hormetic effects studies, hormone agonist/antagonist research or endocrine disruptors activity research for which completely accurate methods are not yet available (Belz et al., 2008; Belz and Piepho, 2017; Scholze et al., 2014).

Towards a functional long-term preservation method for cyanobacterial bioreporter strains

Finally, another clear technical hurdle for routine use of whole cell bioreporters is the difficulty to preserve them in an active form for prolonged time. As reported before, it is of great interest in cyanobacterial-based bioreporters since the maintenance methods tested are very limited. The most widely used method to maintain cyanobacteria-based bioreporters is immobilization in pHEMA (poly (2-hydroxyethyl methacrylate)) (Shing et al., 2013; Tay et al., 2003; Tay et al., 2009) or in agar matrices (Mbeunkui et al., 2002; Schreiter et al., 2001). However, in general, the stability along time is very limited, remaining stable up to only one month of storage in the better cases.

In the chapter V of this thesis, a freeze-dried method was applied for the first time to a cyanobacterial-based bioreporter, especially, to the constitutively bioluminescent bioreporter *Anabaena* CPB4337. As highlighted in this study, the cyanobacterial bioreporter sensitivity remain stable upon 1 year and viability of the cells upon 3 years of storage. This freeze-dried cyanobacterium was, in general, more sensitive to heavy metals (Cu, Zn and Cd) and to organic chemicals (atrazine and phenol) than standard assays such as Microtox (Johnson, 2005) or ToxScreen (Ulitzur et al., 2002). The development of these methods of maintenance will extend the use of cyanobacteria, which are more ecologically relevant organisms in aquatic environments, for aquatic environmental monitoring. In addition, the cyanobacterial freeze-dried protocol was carried out in 96-well plates, generating a simple, fast, high throughput and ready-to-use method for testing the toxicity of environmental contaminants.

Through this thesis, some solutions to the most challenging present drawbacks in using whole cell bioreporters were sought. Although exciting new approaches and methods have been proposed and evaluated, many with great success, further studies can improve these advances in order to secure the future use of this and other bioreporters in real environmental monitoring.

References

- Ahn, J.-M., Mitchell, R.J., Gu, M.B., 2004. Detection and classification of oxidative damaging stresses using recombinant bioluminescent bacteria harboring *sodA::*, *pqi::*, and *katG::luxCDABE* fusions. *Enzyme and Microbial Technology*. 35, 540-544.
- Amaro, F., Turkewitz, A.P., Martin-Gonzalez, A., Gutierrez, J.C., 2011. Whole-cell biosensors for detection of heavy metal ions in environmental samples based on metallothionein promoters from *Tetrahymena thermophila*. *Microb Biotechnol*. 4, 513-522.
- Bachmann, T., 2003. Transforming cyanobacteria into bioreporters of biological relevance. *Trends Biotechnol*. 21, 247-249.
- Bahar, B., Herting, G., Wallinder, I.O., Hakkila, K., Leygraf, C., Virta, M., 2008. The interaction between concrete pavement and corrosion-induced copper runoff from buildings. *Environ Monit Assess*. 140, 175-189.
- Belkin, S., 1998. A panel of stress-responsive luminous bacteria for monitoring wastewater toxicity. *Methods Mol Biol*. 102, 247-258.
- Belz, R.G., Cedergreen, N., Sorensen, H., 2008. Hormesis in mixtures -- can it be predicted? *Sci Total Environ*. 404, 77-87.
- Belz, R.G., Piepho, H.P., 2017. Predicting biphasic responses in binary mixtures: Pelargonic acid versus glyphosate. *Chemosphere*. 178, 88-98.
- Boyanapalli, R., Bullerjahn, G.S., Pohl, C., Croot, P.L., Boyd, P.W., McKay, R.M., 2007. Luminescent whole-cell cyanobacterial bioreporter for measuring Fe availability in diverse marine environments. *Appl Environ Microbiol*. 73, 1019-1024.
- Carvalho, R.N., Arukwe, A., Ait-Aissa, S., Bado-Nilles, A., Balzamo, S., Baun, A., et al., 2014. Mixtures of chemical pollutants at European legislation safety concentrations: how safe are they? *Toxicol Sci*. 141, 218-233.
- Corbisier, P., van der Lelie, D., Borremans, B., Provoost, A., de Lorenzo, V., Brown, N.L., et al., 1999. Whole cell- and protein-based biosensors for the detection of bioavailable heavy metals in environmental samples. *Analytica Chimica Acta*. 387, 235-244.
- Charrier, T., Durand, M.J., Jouanneau, S., Dion, M., Perneti, M., Poncelet, D., et al., 2011. A multi-channel bioluminescent bacterial biosensor for the on-line detection of metals and toxicity. Part I: design and optimization of bioluminescent bacterial strains. *Anal Bioanal Chem*. 400, 1051-1060.
- Durham, K.A., Porta, D., Twiss, M.R., McKay, R.M., Bullerjahn, G.S., 2002. Construction and initial characterization of a luminescent *Synechococcus* sp. PCC 7942 Fe-dependent bioreporter. *FEMS Microbiol Lett*. 209, 215-221.
- EC/2011. Toxicity and assessment of chemical mixtures. Scientific Committee on Health and Environmental Risk, Scientific Committee on Emerging and Newly Identified Health Risks, and Scientific Committee on Consumer Safety. Directorate-General for Health and Consumers.
- Elad, T., Benovich, E., Magrisso, S., Belkin, S., 2008. Toxicant identification by a luminescent bacterial bioreporter panel: application of pattern classification algorithms. *Environ Sci Technol*. 42, 8486-8491.
- Erbe, J.L., Adams, A.C., Taylor, K.B., Hall, L.M., 1996. Cyanobacteria carrying an *smt-lux* transcriptional fusion as biosensors for the detection of heavy metal cations. *J Ind Microbiol*. 17, 80-83.
- Errecalde, O., Seidl, M., Campbell, P.G.C., 1998. Influence of a low molecular weight metabolite (citrate) on the toxicity of cadmium and zinc to the unicellular green alga *Selenastrum Capricornutum*: An exception to the free-ion model. *Water Research*. 32, 419-429.
- Farley, K.J., Meyer, J.S., Balistrieri, L.S., De Schampelaere, K.A., Iwasaki, Y., Janssen, C.R., et al., 2015. Metal mixture modeling evaluation project: 2. Comparison of four modeling approaches. *Environ Toxicol Chem*. 34, 741-753.

- Fernandez-Lopez, R., Ruiz, R., de la Cruz, F., Moncalian, G., 2015. Transcription factor-based biosensors enlightened by the analyte. *Front Microbiol.* 6, 648.
- Galluzzi, L., Karp, M., 2006. Whole cell strategies based on lux genes for high throughput applications toward new antimicrobials. *Comb Chem High Throughput Screen.* 9, 501-514.
- Girotti, S., Ferri, E.N., Fumo, M.G., Maiolini, E., 2008. Monitoring of environmental pollutants by bioluminescent bacteria. *Analytica Chimica Acta.* 608, 2-29.
- Harms, H., Wells, M.C., van der Meer, J.R., 2006. Whole-cell living biosensors--are they ready for environmental application? *Appl Microbiol Biotechnol.* 70, 273-280.
- Heijerick, D.G., Janssen, C.R., Karlen, C., Wallinder, I.O., Leygraf, C., 2002. Bioavailability of zinc in runoff water from roofing materials. *Chemosphere.* 47, 1073-1080.
- Huckle, J.W., Morby, A.P., Turner, J.S., Robinson, N.J., 1993. Isolation of a prokaryotic metallothionein locus and analysis of transcriptional control by trace metal ions. *Mol Microbiol.* 7, 177-187.
- Hynninen, A., Virta, M., 2010. Whole-cell bioreporters for the detection of bioavailable metals. *Adv Biochem Eng Biotechnol.* 118, 31-63.
- Ivask, A., George, S., Bondarenko, O., Kahru, A. 2012. Metal-Containing Nano-Antimicrobials: Differentiating the Impact of Solubilized Metals and Particles. In: Cioffi N, Rai M, editors. *Nano-Antimicrobials: Progress and Prospects.* Springer Berlin Heidelberg, Berlin, Heidelberg, 253-290.
- Ivask, A., Virta, M., Kahru, A., 2002. Construction and use of specific luminescent recombinant bacterial sensors for the assessment of bioavailable fraction of cadmium, zinc, mercury and chromium in the soil. *Soil Biology and Biochemistry.* 34, 1439-1447.
- Johnson, B.T. 2005. Microtox® Acute Toxicity Test. In: Blaise C, Féraud J-F, editors. *Small-scale Freshwater Toxicity Investigations: Toxicity Test Methods.* Springer Netherlands, Dordrecht, 69-105.
- Jouanneau, S., Durand, M.J., Thouand, G., 2012. Online detection of metals in environmental samples: comparing two concepts of bioluminescent bacterial biosensors. *Environ Sci Technol.* 46, 11979-11987.
- Kahru, A., Dubourguier, H.C., Blinova, I., Ivask, A., Kasemets, K., 2008. Biotests and Biosensors for Ecotoxicology of Metal Oxide Nanoparticles: A Minireview. *Sensors (Basel).* 8, 5153-5170.
- Lee, D.Y., Fortin, C., Campbell, P.G., 2005. Contrasting effects of chloride on the toxicity of silver to two green algae, *Pseudokirchneriella subcapitata* and *Chlamydomonas reinhardtii*. *Aquat Toxicol.* 75, 127-135.
- Ma, X.Y., Wang, X.C., Ngo, H.H., Guo, W., Wu, M.N., Wang, N., 2014. Bioassay based luminescent bacteria: Interferences, improvements, and applications. *Science of The Total Environment.* 468, 1-11.
- Magrisso, S., Erel, Y., Belkin, S., 2008. Microbial reporters of metal bioavailability. *Microbial biotechnology.* 1, 320-330.
- Mbeunkui, F., Richaud, C., Etienne, A.L., Schmid, R.D., Bachmann, T.T., 2002. Bioavailable nitrate detection in water by an immobilized luminescent cyanobacterial reporter strain. *Appl Microbiol Biotechnol.* 60, 306-312.
- Meyer, J.S., Farley, K.J., Garman, E.R., 2015. Metal mixtures modeling evaluation project: 1. Background. *Environ Toxicol Chem.* 34, 726-740.
- Morby, A.P., Turner, J.S., Huckle, J.W., Robinson, N.J., 1993. SmtB is a metal-dependent repressor of the cyanobacterial metallothionein gene *smtA*: identification of a Zn inhibited DNA-protein complex. *Nucleic Acids Res.* 21, 921-925.
- Munoz-Martin, M.A., Mateo, P., Leganes, F., Fernandez-Pinas, F., 2011. Novel cyanobacterial bioreporters of phosphorus bioavailability based on alkaline phosphatase and

- phosphate transporter genes of *Anabaena* sp. PCC 7120. *Anal Bioanal Chem.* 400, 3573-3584.
- Peca, L., Kos, P.B., Mate, Z., Farsang, A., Vass, I., 2008. Construction of bioluminescent cyanobacterial reporter strains for detection of nickel, cobalt and zinc. *FEMS Microbiol Lett.* 289, 258-264.
- Reyes-Caballero, H., Campanello, G.C., Giedroc, D.P., 2011. Metalloregulatory proteins: metal selectivity and allosteric switching. *Biophys Chem.* 156, 103-114.
- Riether, K., Dollard, M.A., Billard, P., 2001. Assessment of heavy metal bioavailability using *Escherichia coli* zntAp::lux and copAp::lux-based biosensors. *Applied Microbiology and Biotechnology.* 57, 712-716.
- Robinson, N.J., Whitehall, S.K., Cavet, J.S., 2001. Microbial metallothioneins. *Adv Microb Physiol.* 44, 183-213.
- Rodea-Palomares, I., Gonzalez-Garcia, C., Leganes, F., Fernandez-Pinas, F., 2009. Effect of pH, EDTA, and anions on heavy metal toxicity toward a bioluminescent cyanobacterial bioreporter. *Arch Environ Contam Toxicol.* 57, 477-487.
- Ron, E.Z., 2007. Biosensing environmental pollution. *Current Opinion in Biotechnology.* 18, 252-256.
- Sandberg, J., Odnevall Wallinder, I., Leygraf, C., Virta, M., 2007. Release and chemical speciation of copper from anti-fouling paints with different active copper compounds in artificial seawater. *Materials and Corrosion.* 58, 165-172.
- Scholze, M., Silva, E., Kortenkamp, A., 2014. Extending the Applicability of the Dose Addition Model to the Assessment of Chemical Mixtures of Partial Agonists by Using a Novel Toxic Unit Extrapolation Method. *PLOS ONE.* 9, e88808.
- Schreiter, P.P., Gillor, O., Post, A., Belkin, S., Schmid, R.D., Bachmann, T.T., 2001. Monitoring of phosphorus bioavailability in water by an immobilized luminescent cyanobacterial reporter strain. *Biosens Bioelectron.* 16, 811-818.
- Selifonova, O., Burlage, R., Barkay, T., 1993. Bioluminescent sensors for detection of bioavailable Hg(II) in the environment. *Applied and Environmental Microbiology.* 59, 3083-3090.
- Sharma, P., Asad, S., Ali, A., 2013. Bioluminescent bioreporter for assessment of arsenic contamination in water samples of India. *Journal of Biosciences.* 38, 251-258.
- Shing, W.L., Heng, L.Y., Surif, S., 2013. Performance of a cyanobacteria whole cell-based fluorescence biosensor for heavy metal and pesticide detection. *Sensors (Basel).* 13, 6394-6404.
- Tauriainen, S., Karp, M., Chang, W., Virta, M., 1998. Luminescent bacterial sensor for cadmium and lead. *Biosensors and Bioelectronics.* 13, 931-938.
- Tay, C.C., Sui, S., Lee, Y.H., 2003. Detection of Metals Toxicity Biosensor Using Immobilized Cyanobacteria *Anabaena flos-aquae* AsiaSensor Sensor, 197-201.
- Tay, C.C., Sui, S., Lee, Y.H., 2009. The Behavior of Immobilized Cyanobacteria *Anabaena torulosa* as an Electrochemical Toxicity Biosensor. *Asian Journal of Biological Sciences.* 1, 14-20.
- Turner, J.S., Glands, P.D., Samson, A.C., Robinson, N.J., 1996. Zn²⁺-sensing by the cyanobacterial metallothionein repressor SmtB: different motifs mediate metal-induced protein-DNA dissociation. *Nucleic Acids Research.* 24, 3714-3721.
- Ulitzur, S., Lahav, T., Ulitzur, N., 2002. A novel and sensitive test for rapid determination of water toxicity. *Environ Toxicol.* 17, 291-296.
- van der Meer, J.R., Belkin, S., 2010. Where microbiology meets microengineering: design and applications of reporter bacteria. *Nat Rev Microbiol.* 8, 511-522.
- van Rossum, T., Muras, A., Baur, M.J.J., Creutzburg, S.C.A., van der Oost, J., Kengen, S.W.M., 2017. A growth- and bioluminescence-based bioreporter for the in vivo detection of novel biocatalysts. *Microbial Biotechnology.* 10, 625-641.
- Waldron, K.J., Rutherford, J.C., Ford, D., Robinson, N.J., 2009. Metalloproteins and metal sensing. *Nature.* 460, 823-830.

- Yagi, K., 2007. Applications of whole-cell bacterial sensors in biotechnology and environmental science. *Appl Microbiol Biotechnol.* 73, 1251-1258.
- Zhao, C.-M., Campbell, P.G.C., Wilkinson, K.J., 2016. When are metal complexes bioavailable? *Environmental Chemistry.*

**C
O
N
C
L
U
S
I
O
N
S**

CONCLUSIONS

1. A self-bioluminescent bioreporter strain based on the unicellular cyanobacterium *Synechococcus* sp. PCC 7942 was successfully constructed by fusing the promoter region of the *smt* locus (encoding a metallothionein, SmtA and its transcriptional repressor, SmtB) to *luxCDABE* genes from *Photobacterium luminescens*.
2. The constructed bioreporter was sensitive to six heavy metals: Hg, Cu, Ag, Co, Zn, and Cd. Zn was the maximum inducer. The broad specificity of the bioreporter makes impossible to discriminate between different heavy metals, but it might be useful as a first screening tool in environmental assessment.
3. The bioreporter performance was tested in medium and different real environmental samples. Chemical speciation modelling was used to link the response of the bioreporter with the free ion metal concentrations. The use of the chemical speciation model correlated quite accurately the response of the bioreporter with the free ion metal concentrations in different complex media.
4. The combination of analytical methods, chemical modelling, and bioanalytical strategies was very useful in determining the causes of the high antimicrobial activity towards photosynthetic organisms of Co, Zn and Ag-MOFs.
5. The proposed multivariate extension of Loewe additivity was successfully validated experimentally. Departures from additivity could be quantified based on the proposed bidirectional and weighted combination indices (CIs). The prediction of the bioreporter response to mixtures using single chemical experimental data only could be performed.
6. Freeze-drying has been shown to be a successful method to maintain the viability and sensitivity of turn-off cyanobacterial-based bioreporters up to 3 years of storage. In addition, its usefulness in the evaluation of real samples toxicity has been demonstrated.

CONCLUSIONES

1. Se construyó con éxito una cepa bioreporter auto-bioluminiscente basada en la cianobacteria unicelular *Synechococcus* sp. PCC 7942 fusionando la región promotora del locus *smt* (que codifica una metalotioneína, SmtA y su represor transcripcional, SmtB) a los genes *luxCDABE* de *Photorhabdus luminescens*.
2. El bioreporter construido fue sensible a seis metales pesados: Hg, Cu, Ag, Co, Zn y Cd. Zn fue el máximo inductor. La amplia especificidad del bioreporter hace imposible discriminar entre diferentes metales pesados, pero puede ser útil como primera herramienta de cribado en la evaluación ambiental.
3. La respuesta del bioreportador se evaluó en medio y en diferentes muestras ambientales. Un modelo de especiación química se utilizó para vincular la respuesta del bioreporter con las concentraciones de ion libre. El modelo de especiación química correlacionó de manera muy precisa la respuesta del bioreporter con las concentraciones de ion libre en diferentes medios complejos, confirmando su eficacia biosensora.
4. La combinación de métodos analíticos, modelización química y estrategias bioanalíticas fue muy útil para determinar las causas de la alta actividad antimicrobiana hacia organismos fotosintéticos presentadas por los MOFs de Co, Zn y Ag.
5. La extensión de la definición de aditividad (*Loewe additivity*) fue validada experimentalmente con éxito. Las desviaciones de la aditividad pudieron cuantificarse utilizando los CIs bidireccionales y ponderados. Por primera vez, se pudo llevar a cabo la predicción de la respuesta del bioreportador a mezclas usando datos experimentales de compuestos individuales.
6. Por primera vez, se ha demostrado que la liofilización es un método exitoso para mantener la viabilidad y la sensibilidad de los bioreporters cianobacterianos que hasta 3 años de almacenamiento. Además, se ha demostrado su utilidad en la evaluación de la toxicidad de las muestras reales.